NEW DEVELOPMENTS IN THE GENERATION OF CONTROLLED ATMOSPHERES FOR HIGH TEMPERATURE PROCESSING

Charles W. Sanzenbacher

Surface Combustion Division, Midland-Ross Corporation
Toledo, Ohio

This paper is concerned with recent developments in generating controlled atmospheres from gaseous hydrocarbon fuels by reaction with air. Atmospheres, their generation and control have become a very important consideration in many processes; such as ore benefication, metal treating and food and chemical applications. Developments in the generating of hydrogen are excluded, since these have been covered in detail in other papers presented at this symposium.

I. ADIABATIC (HIGH COMBUSTIBLES) GENERATOR

The increasing use of newly developed or improved ore reduction processes is creating requirements for large quantities of gaseous atmospheres for the reduction of metal oxides. In many cases, such as for copper and iron, a single pure reductant is not required and mixtures of CO and H_2 are suitable, providing the ratios of CO/CO_2 and H_2/H_2O are controlled. In these cases, one economical way to prepare such atmospheres in large quantities (100 M - 1 MM cfh) is by means of a fixed bed adiabatic catalytic reactor as shown in flow diagram in Figure 1.

The atmosphere produced consists of CO_2, CO, H_2, H_2O, N_2 and unreacted CH_4, and the process may be carried out in several ways depending on the relative concentrations of the oxidizing and reducing agents needed.

Figure 1 incorporates two basic flow schemes, one with a gas preheater and the other without a preheater. No preheat is required if the maximum combustibles content ($CO+H_2$) of the product gas is not required to exceed approximately 45%. If the product gas must contain 45 to 60% $CO+H_2$, some external energy is necessary to sustain the reaction. This energy is conveniently provided by preheating the gases ahead of the reactor. The product gas leaving the reactor may be discharged at reactor temperature, or superheated to a higher temperature, or it may be cooled. The several options are shown on the flow diagram.

The simplest process is the production of the 45% combustibles atmosphere for use at reactor discharge temperature.

To produce 45% combustibles atmosphere, the catalytic reactor is first brought to approximately 1200°F by passing hot air through the generator. The catalyst is then at a high enough temperature to start the reaction when the reactants are introduced. Heating is accomplished by means of a simple excess air burner and no indirect preheater is required.

After the reactor is hot, reaction air and desulphurized fuel gas are delivered to the generator at suitable pressure, very accurately proportioned and intimately mixed. When this mixture is introduced into the catalytic reactor, typical reforming reactions occur. The exothermic formation of CO_2 occurs near the reactor inlet and the endothermic reactions occur later so that a characteristic temperature gradient persists throughout the catalyst bed. The reactor temperatures rapidly attain equilibrium, and composition of the product atmosphere becomes stabilized quickly so that a constant analysis of product gas is attained within minutes after the reaction is started. In the same manner, the reactor responds rapidly to changes in air-gas ratios to produce the atmosphere desired.

The reactor is shut down by simply closing the gas and air valves and allowing the reactor to cool. Since it is heavily insulated, it will lose temperature slowly and may be restarted without preheating for a number of hours after shutdown. The length of time will depend on the size of the unit and its operating conditions. This is a very desirable feature for applications where gas demands are intermittent.

The production of atmospheres containing greater than 45% combustibles requires the use of a preheater. This is an indirect heater used to heat the reactants during normal operation and to heat the air to bring the reactor to its starting temperature. Other components of the system are identical to the 45% combustibles generator.

The temperature of the product gas leaving the reactor is dependent upon the type of fuel gas used, air-gas ratio and the degree of preheat employed. It has been found that the water gas shift reaction ($CO+H_2O \rightleftharpoons CO_2+H_2O$) stays in equilibrium with the discharge gas temperature over a wide range of space velocities. It has also been determined that the unreacted Methane content of the product gas varies in a predictable manner with the discharge gas temperature and the space velocity. Since system heat losses are calcuable and small, it is feasible to calculate accurately the air-gas ratio, space velocity, and preheat required to produce a specific analysis of product gas. This in turn permits the rapid attainment of equilibrium conditions after start-up. Figure 2 shows typical reactor operating data, using natural gas or commercial propane fuels with the generator operating at rated capacity. Adjustments can be made to operate anywhere within the limits of Tests 1 and 2 and also under somewhat leaner conditions than shown in Test 1. The relationship between Methane and reactor discharge temperature and space velocity is shown in Figure 3.

Major development considerations center around the proper design of the reactor catalyst bed, means for introducing the reactants into the bed, and the selection of suitable catalyst to make the process operate without exceeding the temperature it limits and without carbon deposition. The equipment which has been developed successfully meets the application requirements.

Approximate equipment and utilities costs for typical adiabatic reactors are shown on Figure 4. Equipment costs include air compressor and adequate instrumentation. Utilities are based on natural gas at 50¢/M scf, and electric power at 3/4¢/KWH. Product gas is at one atmosphere pressure and reactor temperature. A photograph of a high combustibles adiabatic reactor is shown in Figure 5.

II. NITROGEN GENERATOR

Nitrogen generators are widely used throughout industry for purging, blanketing, heat treating, and many other operations requiring so called inert atmospheres to insure safe operation and/or improved processing. The nitrogen for such applications can be provided by many methods. Small demands are satisfied by using cylinder gas; larger requirements by on-site production via a variety of methods. One inexpensive means is by removing CO_2 and H_2O from the products of combustion of hydrocarbon fuels. The nitrogen produced contains small concentrations of CO and H_2 which are generally controlled between 0.5% and 4.0%, making the nitrogen sufficiently pure for the majority of applications.

At the present time numerous purification systems and generators have been developed and are being used for this purpose. The majority of such generators use an adsorption system to remove CO_2 and refrigeration and/or adsorption systems for dehydration. Typically the CO_2 absorption system is a closed Monoethanolamine (MEA) solution which absorbs CO_2 from the process gas and in turn is regenerated by utilizing the exothermic heat of combustion released in the preparation of the process gas. The adsorption dryers are normally of the thermally reactivated alumina type. These generators are highly developed, reliable and efficient machines, but are subject to corrosion problems. Over the years, considerable work has been done to circumvent this problem by many means, especially using dry adsorbent systems to remove both CO_2 and H_2O. This developmental activity has increased with the advent of higher

capacity adsorbents such as the Molecular Sieves.

Many systems have been devised to apply these new adsorbents to the manufacture of simple, reliable, and economical nitrogen gas generators. One method is shown diagrammatically in Figure 6. Operation is generally as follows:

Air and fuel gas are proportioned by suitable flow rationing means and burned in an exothermic gas generator wherein the products of combustion are cooled either directly or indirectly with cooling water. The cooled gas contains nitrogen, generally with approximately 11% CO_2 and 1.0 to 4.0% combustibles. It is saturated with water at approximately cooling water temperature. The cooled gas enters the right hand adsorbing bed at a pressure slightly above one atmosphere. Both CO_2 and H_2O are adsorbed from the gas stream by the adsorbent in the tower, and thus dry nitrogen containing essentially 1/2% to 2% CO and 1/2% to 2% H_2 is produced.

While the right hand bed is purifying the process gas stream, the left hand bed is being reactivated. This is accomplished without heat by maintaining the desorbing bed under a vacuum during the desorption cycle and utilizing some of the product nitrogen as a purge gas to sweep the desorbed CO_2 and H_2O from the reactivating bed. Reactivation is accomplished without additional heat and at essentially ambient temperature. After reactivation the left tower is repressurized. The towers are cycled alternately so that one is adsorbing CO_2 and H_2O at all times, and the other desorbing or reactivating. A continuous flow of nitrogen is maintained from the system.

Cycle times are less than 10 minutes to maintain essentially adiabatic conditions in the towers and to minimize the quantity of dessicant required. Cycle time is determined by the economics of nitrogen loss for purging and repressurizing, and pump down desorption times.

The pressure swing system is automatic, simple, and has few components. Equipment costs are comparable to MEA systems and utility costs are approximately 13¢ per MCF nitrogen.

Figure 7 is a photograph of a nitrogen generator of the type described.

III. EXOTHERMIC GAS GENERATORS

Because of their simplicity and economy, exothermic generators continue to be used for processes and in applications in which nitrogen containing CO_2 and H_2O in relatively high concentrations and CO, CH_4 in small concentrations are not detrimental. Many heat treating processes in ferrous and non-ferrous metallurgy utilize exothermic generator atmospheres. For example, the annealing of sheet steel, aluminum sheet, coils and foil, copper alloy and also the calcining of charcoal, all represent uses of such atmospheres for high temperature processes. At lower temperatures exothermic generator atmospheres are used in grain storage and for safety applications. Figure 8 shows the compositions of several typical atmospheres which may be produced from exothermic generators. In many cases the generators are expected to operate over the entire range of air-gas ratios shown and they must be designed accordingly.

The simplicity of exothermic gas generating equipment may be seen in Figure 9. The air-gas proportioning system is identical to that used for the nitrogen generator.

Since the main attribute of this type of atmosphere is its low equipment cost and operating economy, emphasis has been and is on producing more gas in a single generator and at the same time decreasing the physical dimensions of generators.

The air-gas mixing and burner system is probably the major consideration in the designing of exothermic generators. Poor mixing will result in stratification of the

gases and non-uniform and incomplete combustion. Slightly rich or lean zones will develop at the mixer and burner and will persist throughout the combustion chamber. This will result in the production of exothermic gas containing some free oxygen in a rich gas atmosphere or some combustibles in a lean gas atmosphere. This problem becomes more difficult as generator capacities increase.

An ideal mixer and burner system will intimately mix and allow the air and fuel gas streams to react in as short a time as possible in order to keep premix and combustion volumes at a minimum. From a safety standpoint a nozzle mixing system is desirable since it eliminates hazardous premix volumes altogether and does not require fire checks. For large capacity generators this is especially desirable, since otherwise multiple fire check and burners are required, both of which increase the cost and operating complexity of the equipment.

The problem of developing a simple nozzle mixing burner system for large generators is difficult and becomes more so as generators increase in capacity. This is because of the longer mixing paths associated with larger equipment.

Many approaches to the problem have been used and much development work has been done. Hydraulic studies, cold gaseous models using various tracer techniques and special hot probe studies have been employed to evaluate the characteristics of various mixing and burner systems. As a result of such work, large nozzle mixing burners have been developed which mix well with a minimum expenditure of energy and promote complete combustion in a small volume. Figure 1 shows one such generator, 120,000 scfh capacity, using a single nozzle mixing burner. Development is continuing to insure improved performance as the demand for generators of increasing capacities continues.

The generator shown in Figure 10 also incorporates a gas cooling system which is an integral part of the unit. The purpose is, again, simplicity and saving of floor space. The cooler consists of an annular shaped packed tower surrounding the combustion chamber. Gas is passed upward through the cooler and is cooled by water flowing downward. Where it is necessary to employ indirect cooling, condensate from the products of combustion is cooled and recirculated through the cooler. This is one of several compact cooling systems which are being used successfully on exothermic generators at the present time.

The general trend of virtually all classes of generators is towards more accurate control of product gas composition, increasing emphasis on automatic and simplified operation, and the production of increasing quantities of gases in smaller floor spaces at a lower capital expenditure. Continually improving instrumentation for analysis and control and the development of analytical techniques aided by computers is permitting a better understanding of the important mechanisms of gas generator systems and the development of improved equipment to meet industrial demands. The development of the three generators described in this paper are a direct result of the modern technological advances of the last few years.

ADIABATIC CATALYTIC REACTOR FLOW SCHEME

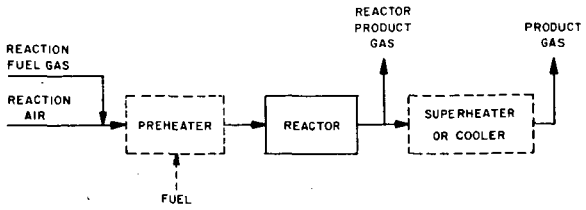

FIGURE 1

ADIABATIC REACTOR OPERATING DATA

	TEST-1	TEST-2	TEST-3
AIR/GAS RATIO	3.43	2.49	7.04
REACTANT PREHEAT	NO	YES	YES
MAXIMUM BED TEMPERATURE °F.	1970	1700	2000
PRODUCT TEMPERATURE °F.	1500	1550	1720
PRODUCT ANALYSIS - %			
CO_2	2.7	0.25	0.3
CO	16.0	20.1	23.7
H_2	28.9	38.3	30.6
CH_4	0.9	0.5	0.3
N_2	51.5	40.3	44.6
H_2O	-	0.55	0.5

FUEL: TESTS 1 AND 2 - TOLEDO NATURAL GAS
TEST 3 - COMMERCIAL PROPANE

OPERATING PRESSURE - 1 ATMOSPHERE

FIGURE 2

EFFECT OF SPACE VELOCITY & TEMPERATURE ON RESIDUAL METHANE

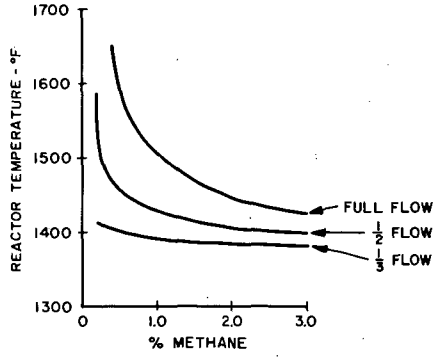

FIGURE 3

ADIABATIC REACTOR EQUIPMENT AND UTILITY COSTS

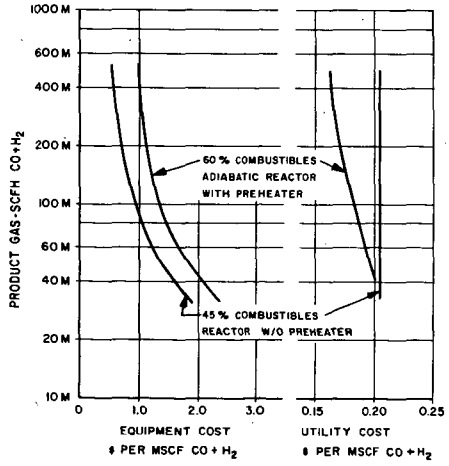

FIGURE 4

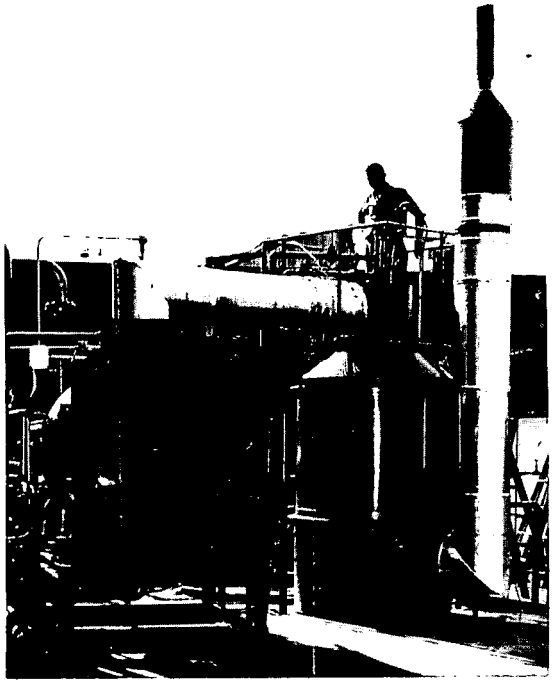

ADIABATIC REACTOR
FIGURE 5

NITROGEN GENERATOR FLOW SCHEME

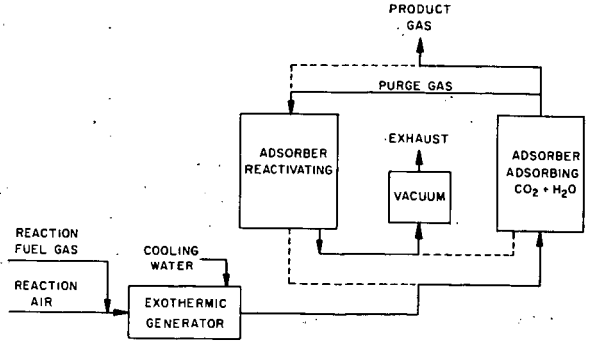

FIGURE 6

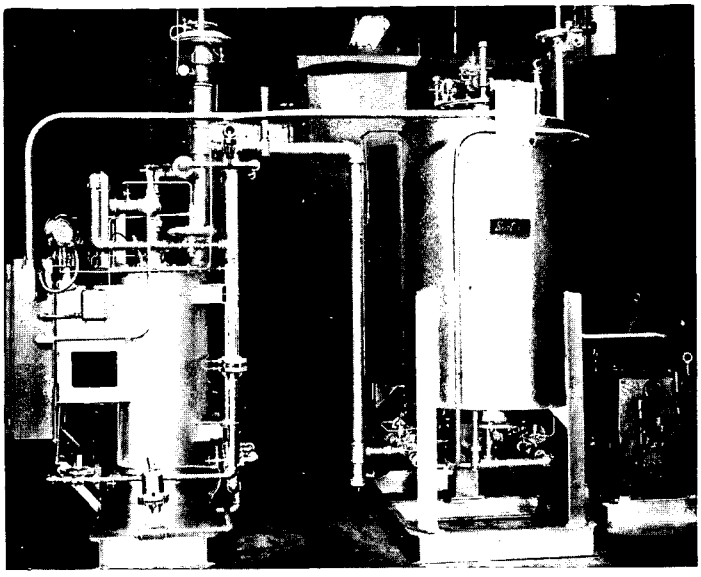

NITROGEN GENERATOR
FIGURE 7

EXOTHERMIC GAS GENERATOR
TYPICAL GAS COMPOSITIONS

AIR/GAS RATIO	6.2	9.0	10.0
DRY ANALYSIS - MOL %			
CO_2	5.3	11.0	11.0
CO	9.8	1.3	0.0
H_2	10.4	0.7	0.0
CH_4	0.1	0.0	0.0
O_2	0.0	0.0	1.3
NO	0.0	0.0	0.1

BASIS: TOLEDO NATURAL GAS, PRODUCTS AT ONE ATM.

FIGURE 8

EXOTHERMIC GAS GENERATOR FLOW SCHEME

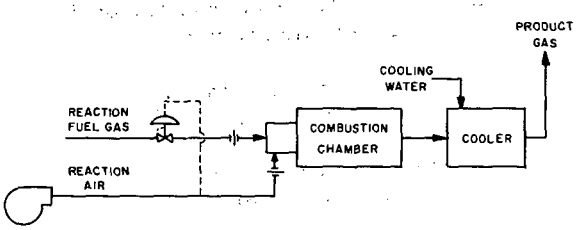

FIGURE 9

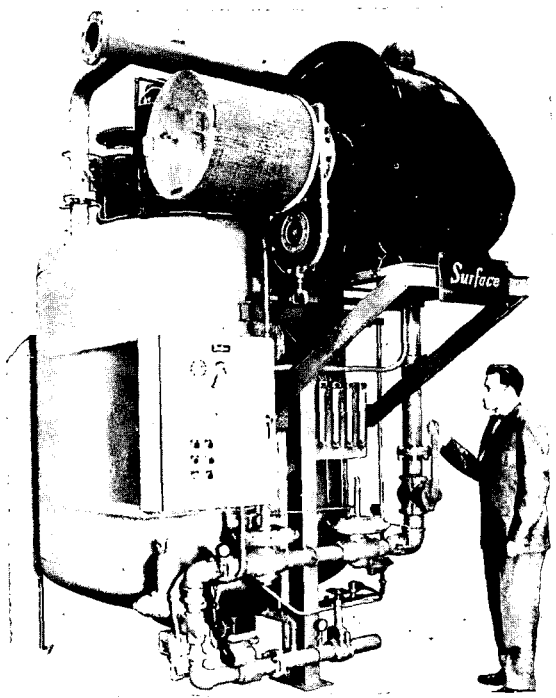

FIGURE 10

Low Temperature Carbon Monoxide Conversion Catalysts

Robert Habermehl
Kenton Atwood

Catalysts and Chemicals Inc.
Louisville, Kentucky

The purpose of this paper is to report on the initial commercial operation of a low-temperature carbon monoxide conversion catalyst and to show some of the economic advantages of using such a catalyst in the production of hydrogen and ammonia synthesis gas.

HISTORICAL: The production of hydrogen for making ammonia synthesis gas has reached major proportions. The quantity of hydrogen used in ammonia synthesis in the U.S. last year exceeded 540 billion cubic feet, more than 1.5 billion cubic feet per day. The consumption of hydrogen for ammonia synthesis world-wide now exceeds 1500 billion cubic feet per year and is growing at the rate of somewhere between seven and ten per cent per year. In addition, the production of hydrogen for chemical hydrogenations and for hydrotreating and hydrocracking is becoming an increasingly important factor in the consumption of hydrogen. Hydrocracking along with increased ammonia production portends a continued increase in the requirements for more hydrogen production.

Most of the hydrogen being consumed is produced by the reaction of steam with a hydrocarbon

$$C_xH_y + xH_2O = xCO + \left(x + \frac{y}{2}\right) H_2$$

and is commonly referred to as "reforming." Smaller quantities of hydrogen are produced by the partial oxidation of hydrocarbons by the reaction

$$C_xH_y + \frac{x}{2} O_2 = xCO + \frac{y}{2} H_2$$

In order to maximize the quantity of hydrogen produced in these processes, it is essential to convert the carbon monoxide to carbon dioxide and additional hydrogen by reacting it with steam

$$CO + H_2O = CO_2 + H_2$$

This reaction is in equilibrium and tends to go to completion towards the right as the temperature is decreased. Pressure has no effect on the equilibrium. It, therefore, becomes desirable to promote this reaction at the lowest possible temperature. In order to increase the reaction rate at which equilibrium

conditions are approached, it has been necessary to carry out the reaction in the presence of a catalyst. The catalyst used almost exclusively for this reaction for the last 40 to 50 years has been an iron oxide-chrome oxide promoted catalyst. This catalyst caused the reaction to proceed at commercially feasible rates at temperatures as low as 650°F, and it had a useful life of three to over ten years, depending on the conservatism of the design. Although other catalysts have been investigated and reported [1] [2] for promoting the reaction between carbon monoxide and steam at temperatures lower than 650°F, none have found commercial acceptance, due principally to an impractically short life when used at near atmospheric pressure. One low-temperature conversion catalyst, however, found limited commercial acceptance when used at relatively high pressures.

It was not until 1953 that a commercial plant was constructed for the production of hydrogen for the manufacture of ammonia synthesis gas by steam-hydrocarbon reforming at pressures appreciably higher than atmospheric, approximately 90 psig. Since that time most of the plants constructed operate at pressures ranging from 75 to 300 psig. The plants formerly constructed to operate at near atmospheric pressure are now being replaced or converted into plants operating at the higher pressures.

In 1931 Larson [3] was granted a patent on a catalyst for promoting the reaction between carbon monoxide and steam at temperatures as low as 540°F. A commercial plant was constructed early in the period of 1940-1950 for the production of hydrogen from water-gas for the manufacture of ammonia synthesis gas. The conversion of carbon monoxide to carbon dioxide and hydrogen was carried out over a catalyst apparently based on the Larson patent at approximately 450 psig. Although exact operating temperatures and rates have never been published, they are known to be in the range of 350° to 650°F, and space velocities of 400 to 1000 SCF per cubic foot of catalyst. Even though the catalyst had a relatively short life, it continued to be used even to the present time. This catalyst never found commercial acceptance for low pressure operation, presumably because of an impractically short life.

Catalysts and Chemicals Inc., soon after its formation in 1957, started successful development work on the adaptation of a catalyst, in general similar to the Larson catalyst, for promoting the conversion of carbon monoxide in the temperature range of 350°to 650°F. Over eight commercial charges of this catalyst, designated as C18[4], are in operation or soon to go in operation at pressures ranging from near atmospheric to 350 psig; however, most of these plants will operate at over 100 psig. Pilot plant and commercial experience show that the catalyst will operate at rates appreciably in excess of those for the conventional iron oxide-chrome oxide type catalyst. With reasonable extrapolation of the available commercial experience, a practical life of at least one and one-half to three years can be expected.

PRINCIPAL ADVANTAGES OF C18 TYPE LOW-TEMPERATURE CONVERSION CATALYST: The advantages of a low-temperature carbon monoxide conversion catalyst in hydrogen production are obvious from a study of the equilibrium reaction

$$CO + H_2O = CO_2 + H_2$$

The equilibrium constant for the reaction has a value of 22 at 650°F, which is the generally accepted minimum effective temperature for the use of the iron oxide-chrome oxide catalyst. The equilibrium constant is 207 at 400°F, which is a reasonable temperature for the C18 type low-temperature conversion catalyst. The practical significance of this is that at the same steam concentration, the use of the C18 catalyst will result in over 99 per cent conversion of the carbon monoxide, whereas the iron oxide-chrome oxide catalyst will give only 90 to 95 per cent conversion at its lowest effective temperature.

If it is assumed that the processing scheme for hydrogen production for the manufacture of ammonia synthesis gas is the conventional steam-hydrocarbon reforming--consisting of a primary and secondary reformer followed by carbon monoxide conversion, carbon dioxide removal and then methanation of the residual carbon monoxide--and that the acceptable level of residual carbon monoxide to be methanated is not more than 0.3 mol per cent, the steam requirement for achieving this degree of conversion in a single stage of carbon monoxide conversion with the usual interstage cooling is 3.5 mols of steam per mol of dry feed gas when an iron oxide-chrome oxide catalyst is used. When the C18 low-temperature conversion catalyst is used, the steam requirement is 0.7 mol per mol of dry feed gas, a reduction of 80 per cent. The greater quantity of steam required with the iron oxide-chrome oxide catalyst, however, is considered impractical and either a lower quantity of steam is used with a single stage of conversion, followed by carbon dioxide removal and methanation, or two stages of carbon monoxide conversion are used with carbon dioxide removal after each stage, followed by methanation. In the first case, the carbon monoxide to be methanated ranges from 0.6 to 1.0 mol per cent. This greater quantity of carbon monoxide not only increases the quantity of inerts in the synthesis gas, thus making the synthesis of ammonia less efficient, but for each mol of carbon monoxide methanated, 3 mols of hydrogen are consumed, requiring a larger plant to produce the expected quantity of ammonia. In the second case where two stages of conversion are used, the carbon monoxide to be methanated does not exceed 0.3 mol per cent; however, considerably more equipment is required, consisting of a stage of carbon dioxide removal, heaters, saturators, exchangers, coolers, etc., which not only increase the capital cost of the plant, but also the operating cost.

The additional steam that must be added to the gas for the second stage conversion reaction brings the over-all steam requirements to 1.4 mols of steam per mol of dry gas exit the secondary reformer. This is still twice the quantity of steam required for achieving the same degree of conversion in a single stage conversion system using the low-temperature shift catalyst.

These steam requirements for the three basic carbon monoxide conversion systems are summarized in Figure 1. Additional significance to the potential advantage of the low-temperature shift catalyst can be seen by observing on the graph that the steam level in the gas required to achieve a methane leakage of 0.2 mol per cent from a secondary reformer is 0.5 mol per mol of dry gas at 150 psig and 0.7 mol per mol of dry gas at 300 psig. It has already been indicated that the 0.7 steam to dry gas ratio is the required steam level to reach the 0.3 per cent carbon monoxide level in the feed to the methanator. Further, the practical steam levels required in the gas to supply the energy requirements of regenerating the carbon dioxide removal solution are shown for an amine system and for one of the newer carbon dioxide removal systems. These steam to gas ratios are 1.40 and 0.70, respectively.

Once again, the 0.70 value appears and shows that the C18-1 development is an important contributor to the advancing technology in ammonia synthesis gas production.

Figure 1 also shows the relative physical size of the shift converters for the three basic conversion systems. If the size requirement of the single-stage system using the C18-1 catalyst in conjunction with pre-conversion over a conventional catalyst is considered as 1, the size of the two-stage conventional catalyst system is 1.4 and for the single-stage conventional catalyst system is 6.0.

The potential advantages of the low-temperature shift catalyst in ammonia synthesis gas production are further shown in Table I, wherein a comparison is made in some of the critical conditions and requirements for a hypothetical 300 ton per day ammonia plant for the following three alternate processing schemes. The reformer pressure level in all cases is 300 psig exit the reformer tubes.

Case 1 — A single-stage conversion system employing conventional catalyst in series with low-temperature shift catalyst and using one of the newer "lower energy" carbon dioxide removal processes.

Case 2 — The same as Case 1 except employing conventional catalyst throughout the single-stage converter and operating with higher inerts in the synthesis gas loop.

Case 3 — The same as Case 2 except using amine as the carbon dioxide removal system and obtaining a greater conversion of the carbon monoxide due to the higher steam requirements of the amine system.

Comparison of the hydrocarbon requirements in the above systems in Table I indicates that the use of low-temperature shift catalyst permits the synthesis gas section of the plant to be reduced in size by approximately 12 per cent. The increased cost of the catalyst required to give this advantage is approximately $50,000, including the use of a primary reforming catalyst with the best known activity and heat transfer characteristics such that full advantage can be taken in reducing the physical size of the plant.

Figure 2 shows the relative hydrocarbon requirements for the process, including fuel and steam production, for these three systems of synthesis gas production.

The production of large quantities of relatively high-purity hydrogen, such as are necessary for the new hydrocracking of hydrocarbons processes, is gaining rapidly in industrial importance. The typical plant involves high pressure reforming, single-stage conversion, carbon dioxide removal, and methanation of residual carbon oxides. The degree of conversion of the carbon monoxide exit the reformer influences the ultimate cost of these plants since unconverted carbon monoxide ends up as a methane impurity in the product and affects the degree of reforming to reach a given product purity. The greater conversion of carbon monoxide is made possible through the use of low-temperature shift catalyst and, therefore, permits a substantial reduction in the physical size of the reformer with attendant lower steam and fuel requirements, or alternatively, permits reforming at a higher

pressure level with a subsequent reduction in compression costs.

Figure 3 shows a comparison of a reformer design when using conventional catalyst versus the use of low-temperature carbon monoxide conversion catalyst and the best reforming catalyst available. The size of the reformer in terms of catalyst volume required and the maximum tube wall temperature in the reforming furnace are plotted against hydrogen purities of 95 to 98 per cent for a production capacity of 50 MMSCFD of net hydrogen delivered at 150 psig. It is shown that the use of the low-temperature conversion catalyst permits a 25 to 30 per cent reduction in the size of the reformer.

For example, in the case of 95 per cent hydrogen purity, it is observed that approximately 740 cubic feet of catalyst are required in the reformer when using the conventional catalyst, whereas approximately 550 cubic feet are required when using the low-temperature shift catalyst and the best reforming catalyst available. The maximum tube wall temperature in both cases is 1670°F assuming the same physical size of the tubes in terms of inside diameter and length in the fired zone of the reformer. For 97 per cent hydrogen purity, when using the conventional catalyst, the reformer must contain about 785 cubic feet of catalyst and the maximum tube wall temperature required is 1720°F. With C18 catalyst in the shift converter, the reformer size may be reduced to contain 665 cubic feet of catalyst and the tube wall temperature required is now 1700°F.

LABORATORY DEVELOPMENT AND COMMERCIAL DEMONSTRATION OF THE EFFECTIVENESS OF C18 LOW-TEMPERATURE CARBON MONOXIDE CONVERSION CATALYST: Bench scale and pilot plant work have been conducted in the laboratories of Catalysts and Chemicals Inc. to establish the preferred catalyst composition, the best method of preparation of the catalyst, the method of reduction giving a catalyst of the highest activity, the optimum operating conditions, the effect of poisons, and the decline of activity with time on stream versus operating temperature. Specific studies were made on the effect of total pressure, the partial pressure of carbon dioxide, and the partial pressure of steam on the kinetics of the reaction.

It is not to be implied that the laboratory studies have resulted in complete answers to the quantitative effect of all the variables involved; however, it is believed that sufficient information is known upon which to base workable designs at the usual processing conditions.

Life tests in excess of 13 months' duration were conducted at typical operating conditions.

The first commercial charge of C18 was placed on stream on January 1, 1963 in a 210 ton per day ammonia plant at about 120 psig. An operating mishap during reduction of the catalyst and adverse conditions during the initial stages of operation resulted in below-normal initial activity of the catalyst. Despite these factors, however, the catalyst had sufficient activity to show a distinct advantage over the previous conventional catalyst, and operation has continued to the date of this writing with no more than the anticipated decline in activity. The initial activity and the rate of decline in activity are shown in Figure 4. This charge of catalyst has been on stream for 12-1/2 months as of this date.

The second commercial charge of C18 catalyst was placed on stream on May 11, 1963 in a 260 ton per day ammonia plant on the West Coast. In contrast to the first charge of catalyst, the conditions of reduction and initial operation were in accordance with the recommended procedures, and this charge of catalyst is continuing to operate at an inlet temperature of 400°F, which was the initial inlet temperature. The relative activity level and decline in activity of this charge of catalyst are shown in Figure 4, and specific data are presented in Table II. The performance of this charge of catalyst has thus far exceeded the anticipated performance based on the pilot plant life tests.

A third charge of C18 catalyst was placed in operation on July 24, 1963, operating on a slip stream of a reformer effluent at 2 psig. It continues to perform satisfactorily, and the relative activity and decline in activity are shown in Figure 4. The design level of this operation, however, which was deduced from experiments at low pressure, may prove to be uneconomical in many applications. Further operating experience is required before the use of the catalyst can be encouraged at low pressures.

As stated, Figure 4 shows the performance of the C18 catalyst in these three commercial units. The relative activity with time on stream is shown in relation to the performance of the catalyst throughout the 13-month life test in CCI's pilot plant.

A projection of these curves indicates an anticipated life of the catalyst of one and one-half to three years in commercial operation. A significant factor shown in Figure 4 is the commercial verification of the importance of reduction conditions on the activity of low-temperature conversion catalysts when the performance in Plants 1 and 2 is compared.

As of this writing, five more commercial charges of C18 catalyst have been sold for startup in early 1964.

SUMMARY: The C18 low-temperature carbon monoxide conversion catalyst has been demonstrated commercially to offer a proven economical life in hydrogen and ammonia synthesis gas manufacture. The catalyst is, in general, more sensitive to both catalyst poisons and abnormal operating conditions than is the conventional iron oxide-chrome oxide catalyst and, therefore, requires more careful operation and greater attention to detail in process design. Specifically, the catalyst activity is severely affected by even trace quantities of sulfur in the feed gas. The activity is appreciably affected by the subjection of the catalyst to temperatures in excess of the normal operating level.

The C18 catalyst must be reduced under special conditions and with great care in order to obtain maximum activity and long life.[5]

Application of the catalyst in low pressure operations has not been shown to be practical, and more operating experience will be required before this can be determined.

The catalyst has been proven to offer an attractive payout factor in terms of initial plant investment and operating economy. The ultimate life of the catalyst could well exceed the projected minimum of one and one-half to three years based on the commercial operation to date.

References:

(1) Storch, H. H. and Pinkel, I. I., Industrial and Engineering Chemistry, 29, 715; 1937.

(2) White, E. C. and Schultz, J. F., Industrial and Engineering Chemistry, 26, 95-7; 1934.

(3) U. S. Patent 1,797,426, March 24, 1931.

(4) Patent application pending.

(5) Patent application pending (on reduction procedure).

TABLE I

Comparison of Process Design Features of Ammonia Synthesis Gas Manufacture Using Low-Temperature Carbon Monoxide Conversion Catalyst

Process Scheme: Steam-Hydrocarbon Reforming, Primary and Secondary; 300 psig; Carbon Monoxide Conversion; Carbon Dioxide Removal; Methanation of Carbon Oxides.

Basis: 300 Tons Per Day Ammonia

Case *	1	2	3
CO in Shift Converter Effluent**	0.2 mol per cent, dry basis	1.1 mol per cent, dry basis	0.5 mol per cent, dry basis
Inerts (CH_4 + A) Exit Methanator, mols/hr	29.89 (0.96 mol per cent)	70.85 (2.1 mol per cent)	38.30 (1.21 mol per cent)
Synthesis Gas Required for 300 TPD NH_3			
mols/hr	3114.98	3361.01	3165.46
Relative Amount	100%	107.9%	101.6%
Hydrocarbon, mols/hr			
Process Requirements	702.44	788.11	720.68
Fuel Requirements	295.63	331.68	451.77
Total Requirements	998.07	1119.79	1172.45
Relative Amount	100%	112.2%	117.47%
Air, mols/hr			
Process Requirements	988.47	1054.25	1001.99
Fuel Requirements	2957.70	3318.42	4519.74
Total Requirements	3946.17	4372.67	5521.73
Relative Amount	100%	110.81%	139.93%
Steam Requirements			
Total Lbs/Hr	69,570	75,200	114,350
Relative Amount	100%	108.1%	164.4%
Relative Reformer Size	100%	112.9%	103.0%
Relative Shift Converter Size	100%	125.1%	194.6%

* Cases are defined in text.

** Practical level of carbon monoxide in shift converter effluent using the steam requirements of the carbon dioxide regeneration system to full effectiveness in the shift converter.

Table II Plant Operating Data; C18 Low-Temperature Carbon Monoxide Conversion Catalyst (260 Tons/Day Ammonia Plant, 120 PSIG)

Date	Days on Stream	Dry Gas S. V. SCFH/ V/Hr.	Inlet Temp. °F	Outlet Temp. °F	Inlet S/G Ratio	Gas Analyses, Mol Per Cent				
							CO_2	CO	H_2	CH_4	N_2 + A
5-24-63	13	1925	410	445	0.336	In	4.2	3.0	71.4	0.2	21.2*
						Out	7.0	0.02	72.4	0.2	20.38*
6-27-63	47	1980	400	450	0.42	In	0.8	3.0	74.0	0.3	21.9
						Out	3.8	0.06	74.0	0.3	21.8
9-4-63	116	1800	402	453	0.38	In	0.11	3.16	71.76	0.27	24.70
						Out	2.91	0.06	72.97	0.27	23.80
12-4-63	207	1840	405	456	0.388	In	0.23	3.10	75.69	0.28	20.70
						Out	3.18	0.05	76.40	0.27	20.10

*Analyses by customer's laboratory. Nitrogen and argon by difference. All other analyses by CCI chromatograph and were essentially confirmed by customer analyses.

Figure 1 - Low Temperature CO Conversion Catalyst (C18)

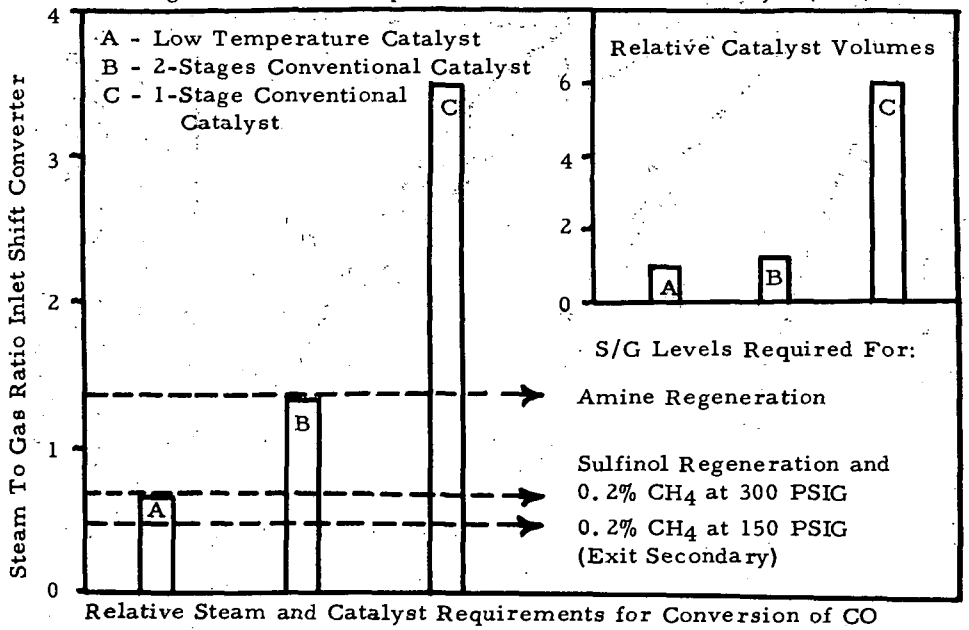

Figure 2 - Low Temperature CO Conversion Catalyst (C18)

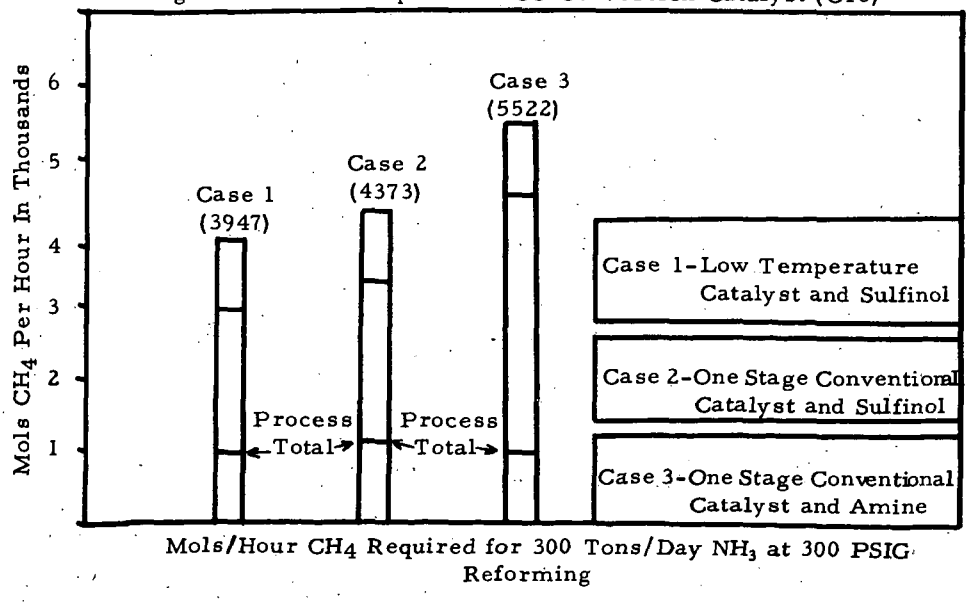

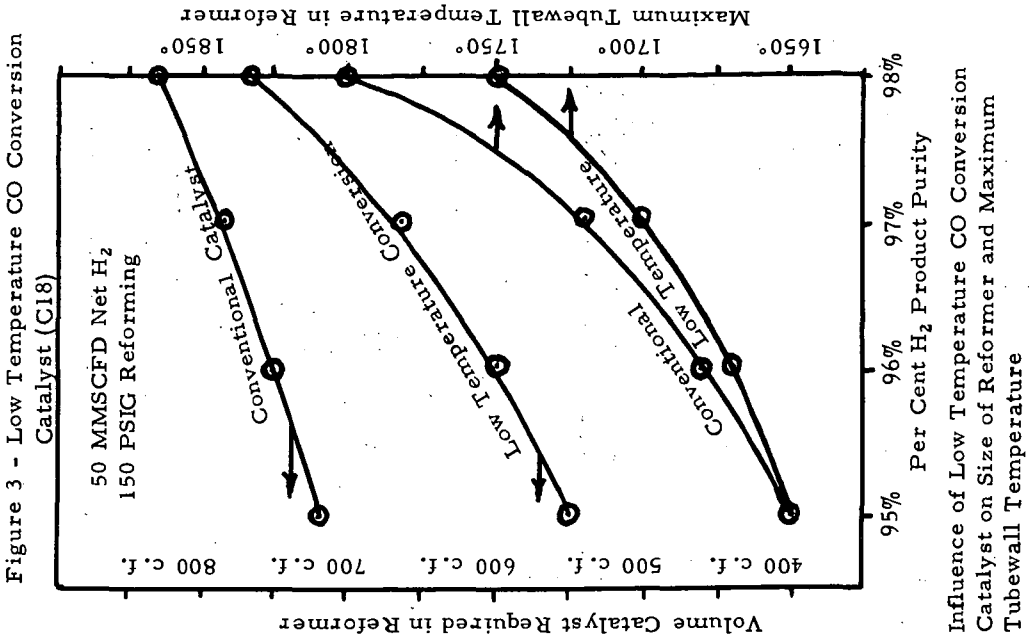

Figure 3 - Low Temperature CO Conversion Catalyst (C18)

Influence of Low Temperature CO Conversion Catalyst on Size of Reformer and Maximum Tubewall Temperature

Figure 4 - Low Temperature CO Conversion Catalyst

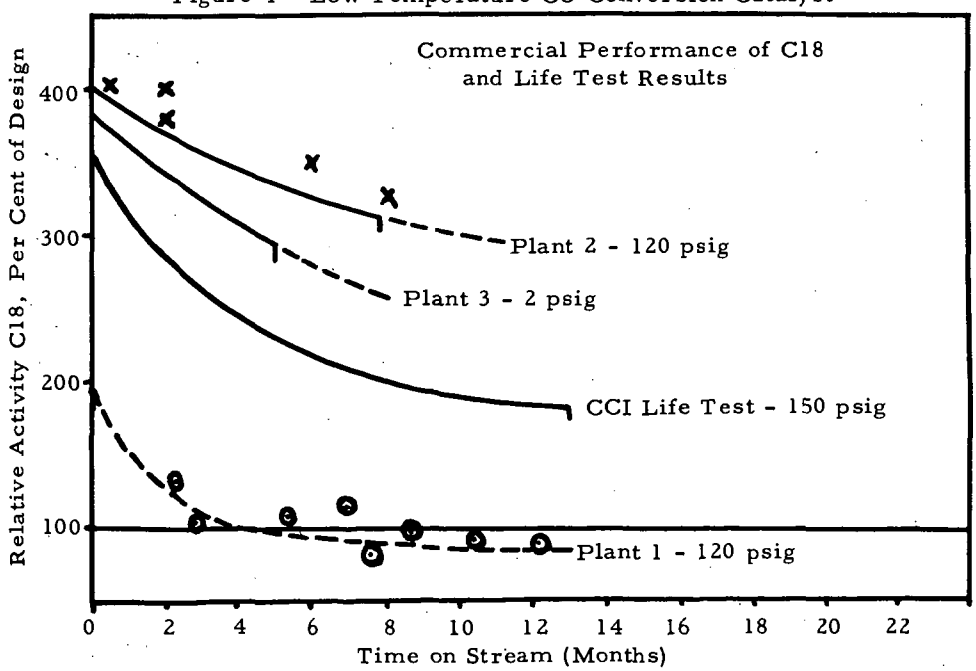

Ultra Pure Hydrogen for Fuel Cell Operation

H. H. Geissler

Engelhard Industries, Inc.
Process Equipment Division

The first practical fuel cells to be developed used pure oxygen and hydrogen. It has proven to be quite feasible to adopt certain of these cells to use air at the oxygen electrode, that is, the cathode.[1] An intensive effort is underway to develop cells which can use a more convenient fuel at the anode.[2] However, it appears unlikely that such cells will be available for practical application in the near future.

One alternate approach is to separate a conversion function from the cell and modify the anode to use an impure hydrogen-rich gas. It is relatively simple, for example, to dissociate ammonia[3] and it would appear to be easier to modify the anode to handle the resulting 75% hydrogen in nitrogen mixture than it was to modify the cathode to handle the 21% oxygen in nitrogen mixture which is air. Residual fuel gas from the anode can then be burned to supply the energy requirements of the dissociation reaction. This method of operation has recently been described by ASEA.[4]

Producing a hydrogen-rich gas from hydrocarbons (or from oxygenated hydrocarbon derivatives such as alcohols) requires appreciably more elaborate conversion equipment and the product gas stream will contain a variety of impurities. Methane, carbon monoxide, carbon dioxide, nitrogen and water vapor may all be in the hydrogen-rich stream. The presence of these impurities introduces a large number of problems with respect to the development of anodes and to the design of the fuel cell battery system. The conditions for efficient operation of gas diffusion electrodes with gases containing inerts have been developed by Baucke and Winsel.[5] In the case of gases containing potential catalyst poisons, however, it may well be much more desirable to combine hydrogen purification with the fuel conversion function so that only pure hydrogen need enter the cell.

The production of hydrogen for fuel cell applications has been explored for a considerable time. A number of reports prepared recently indicate the difficulties which arise in scaling down conventional processes for manufacturing hydrogen.[6,7,8] Conventional processing schemes are as shown in Figure 1.

- The primary reaction may be steam reforming or partial combustion or a combination of the two. In any event it involves a high temperature endothermic reaction to which heat energy must be supplied.

- Carbon monoxide removal is generally accomplished by the catalysed water gas shift reaction wherein carbon monoxide reacts with water vapor to form carbon dioxide plus hydrogen. Recent advances in catalyst composition permit this reaction to proceed at commercially operable rates at moderate temperatures.[9,10] The advantage is that the equilibrium is sufficiently favorable so as to require only a single stage of shift reaction in a plant producing about 99% purity hydrogen. Formerly several stages with intermediate carbon dioxide removal were required. While the shift reaction is exothermic the temperature level is such that the heat is not generally usefully recoverable.

- Carbon dioxide removal is done at near ambient temperatures by scrubbing the gas with suitable regenerable basic reagents. A variety of reagents and processes are available.[11,12,13]

- Final purification is often accomplished by catalytically hydrogenating the residual oxides of carbon to the much less objectionable impurity methane, followed by drying the product hydrogen stream. Alternately cold box processing, generally involving a liquid nitrogen wash, can be used.

It is evident that scaling down conventional equipment without significantly altering the process steps cannot result in any appreciable reduction of equipment components in small hydrogen generators for fuel cell use.

The Engelhard Hydrogen Process provides a new improved approach for solving these problems by combining three basic concepts:

- a hydrogen producing reaction

- the removal of pure product hydrogen

- the utilization of the residue as fuel to supply the energy requirements of the process.

This makes it possible to design and construct compact hydrogen generators. The process is schematically indicated in Figure 2.

The dissociation of ammonia is a suitable hydrogen producing reaction. An earlier paper[14] describes the design, construction and performance of a miniature generator delivering 4 SCFH of hydrogen to serve a 200 watt fuel cell. This unit was developed for the Electronics Research and Development Laboratories of the United States Army.

Hydrogen generators based on hydrocarbons are of much greater general interest. Engelhard is currently engaged in constructing a number of liquid hydrocarbon fueled hydrogen generators having hydrogen output capacities in the range of 4 to 600 SCFH.

Steam reforming of hydrocarbons lends itself well to the Engelhard Hydrogen Process because the energy required for the process is liberated outside of the reaction zone rather than within it as in the case of partial combustion. Thus the residual fuel gas can be used to operate the process.

While various hydrogen removal methods may be considered, diffusion through a material permeable only to hydrogen accomplishes the objectives in one simple step and can be readily adapted for use in small hydrogen generators such as we are discussing here. Palladium and palladium alloys are well known for their ability to diffuse hydrogen. Several reviews of the hydrogen permeation process have recently been presented.[15,16,17] The process is unique in that it supplies the purest grade of hydrogen available: ultra-pure hydrogen containing no impurities measurable by presently available techniques. Use of ultra-pure hydrogen greatly simplifies fuel cell battery design. With no impurities contamination of the electrolyte does not occur, nor do inert gases accummulate. The requirement of venting such gases which would complicate the mechanical design of a fuel cell battery can be eliminated with ultra-pure hydrogen.

The Engelhard Hydrogen Process is a highly efficient way of producing hydrogen. This becomes particularly important if it is to be considered as a component of a fuel cell power source package. Now consider the energy balance of a hydrogen generator as shown in Figure 2, for the steam reforming version with liquid water and liquid hydrocarbon feed streams. In principle the energy content of the product hydrogen would be the same as the gross heating value of the hydrocarbon feed and the generator would have an energy conversion efficiency of 100%. For this the following conditions would have to be met: The product hydrogen and the flue gas leave the apparatus at the same temperature as the incoming streams. The water contained in the flue gas is discharged as a liquid. No radiation and convection heat losses occur. In practice these idealized conditions cannot be realized.

The temperatures of the output streams can be brought to relatively low levels by heat exchange, output hydrogen against incoming combustion air, flue gas against fuel and water feed streams. It is not feasible, however, to usefully recover the latent heat of the water vapor in the flue gas, and this may represent a sizeable loss.

Radiation and convection losses depend upon the size and arrangement of the apparatus, and vary from very small relative to the gross heating value of the fuel fed, in large generators, to as much as 20% in very miniaturized generators.

The energy loss represented by any excess water fed as a liquid but discharged as a vapor in the flue gas is one reason for operating at the lowest possible molal water to carbon ratios. Another reason is to reduce the water vapor content of the reformed gas stream and hence to increase the partial pressure of hydrogen in the diffusion zone. This reduces the amount of palladium alloy required and the overall size and weight of the apparatus. A third reason is that if the ratio is sufficiently low a combined hydrogen generator-fuel cell power source could operate with no external water supply if the fuel cell can be engineered so that the water produced from the hydrogen consumed is returned to the steam reforming hydrogen generator.

There is currently a great interest in developing improved catalysts for the steam reforming of normally liquid hydrocarbons.[18,19] Moreover, for universally useable hydrogen generator-fuel cell power sources a catalyst is required capable of steam reforming any type of currently available hydrocarbon fuel, in particular gasoline, jet fuel, and diesel fuel meeting present military specifications. Such catalysts do not appear to be available at the present.

In the Engelhard hydrogen generators now being built proprietary catalysts are being used which have demonstrated the ability to steam reform a wide variety of hydrocarbon structures, i.e. paraffins, naphthenes, olefins, aromatics. Commercial fuels such as BTX raffinates (essentially C_6-C_9 paraffins), light naphthas, and jet fuels such as JP-4 have been steam reformed with these catalysts at molar water to carbon atom ratios of three or lower, with runs of over 1000 hours, provided the sulfur content was below 40 ppm. In tests with other commercial fuels having higher sulfur contents, excessively rapid catalyst deterioration was observed, which we have ascribed to sulfur poisoning.

The maximum sulfur content permitted by military specifications for JP-4 is 4000 parts per million;[20] we have found it interesting that batch after batch of JP-4, from at least one refiner, has consistently analysed under 50 ppm. We believe this reflects how overly liberal sulfur specifications are in this day of modern refineries. Nowadays sulfur removal often occurs incidentally to other processing and is frequently done to protect the process equipment and catalysts used by the refiner. When and if direct conversion of hydrocarbons in fuel cells becomes a reality a sulfur problem is likely to arise there also. It would appear reasonable and desirable that any new fuel specifications be written with low sulfur limits.

Returning to the mechanical aspects, it must be remembered that although the Engelhard Hydrogen Unit is appreciably simpler

than other hydrogen manufacturing processes it still requires a number of components and controls. There are ways of designing certain very small generators to operate without any auxiliary electric power, but in general pumps and blowers and controllers are necessary, all of which require power.

One version is illustrated in a simplified schematic flow diagram, Figure 3. Fuel and water are metered to the system in fixed ratio by controlling the speeds of positive displacement pumps to supply adequate feed for the hydrogen demand at any instant. The feed stream is heated in a flue gas exchanger, it is then reformed and product hydrogen removed in the reactor/diffusor. The hydrogen stream is cooled against incoming combustion air, which is metered by a speed controlled positive displacement blower. The residual fuel gas from the reactor/diffusor passes through a high temperature back pressure control valve, on to the furnace burner where it is burned with the controlled combustion air. The flow rates of the fuel/water feed and the combustion air must be closely controlled to maintain high efficiency. Feed, air, and product hydrogen flows are not linearly related, which complicates the control system.

The interplay between generator size and weight, efficiency, and power requirement is complex. Optimization is particularly difficult and critical in generators for mobile fuel cell power systems. There is need for more efficient auxiliary equipment than now available. For example, in one 140 SCFH unit under construction, theoretical feed pump power is 2 watts, air blower power 50 watts, while actual available equipment requires 200 watts and 400 watts respectively.

REFERENCES

(1) Yeager, E., Science 134 1178 Oct. 20, 1961

(2) "Fuel Cells, Volume Two" edited by G. J. Jung, Reinhold, New York, 1963

(3) Rosenblatt, E. F. and Cohn, J. G., U.S. 2,601,221 (1952)

(4) Allmanna Svenska Elektriska A.B., Swedish Patent 5589/62.

(5) Baucke, W. and Winsel, A., Advanced Energy Conversion 1 (1963)

(6) AD 292 134. "Design Study of a Hydrogen-Generating Plant for Submarine Use Based on the Steam Reforming of Methanol," for Bureau of Ships Contract NObs 86744, The M. W. Kellogg Co., N. Y., September 30, 1962.

(7) AD 292 252. "Design Study Hydrogen Generation from Light Petroleum Distillate," for Bureau of Ships Contract NObs 86747, Chemical Construction Corp., N. Y., September 28, 1962.

(8) AD 292 273. "Design Study on The Generation of Hydrogen from Methanol For Fuel Cell Systems on Board Submarines," for Bureau of Ships Contract NObs 86743, Girdler Corp., Louisville, October 12, 1962.

(9) Moe, J. M., Division of Petroleum Chemistry, A.C.S., Preprints 8, No. 4, B-29 (1963).

(10) Habermehl, R., "Low Temperature Carbon Monoxide Shift Catalyst." (Paper to be presented at 147th National Meeting, American Chemical Society, Philadelphia, April 5-10, 1964.)

(11) Stotler, H. H., "Acetone Process for Removal of Carbon Dioxide from Hydrogen", paper presented at 49th National A.I.Ch. E. Meeting, New Orleans, La. (March 14, 1963).

(12) Deal, C. H., Dunn, C. L., Hill, E. S., Papadopoulos, M. N., and Zarker, K. E., "Sulfinol - A New Process for Gas Purification", paper presented at 6th World Petroleum Congress, June, 1963.

(13) Kohl, A. L. and Riesenfeld, F. C., "Gas Purification", McGraw-Hill, New York, 1960.

(14) Geissler, H. H., Proceedings - 17th Annual Power Sources Conference, May, 1963.

(15) Cohn, G. and Straschel, H. K., Division of Petroleum Chemistry, A.C.S., Preprints 8, No. 4, B-43 (1963).

(16) Hunter, J. B., ibid, page B-49.

(17) Rubin, L. R., Engelhard Industries Technical Bulletin 2 No. 1, 8 (1961).

(18) Fox, J. M. and Yarze, J. C., Division of Petroleum Chemistry, A. C. S., Preprints 8, No. 4, B-21 (1963).

(19) Voogd, J., and Tielrooy, J., Hydrocarbon Processing & Petroleum Refiner 42 No. 3, 144 (1963).

(20) Specification MIL-J-5624D, JP-4.

FIGURE 1
HYDROGEN MANUFACTURING PROCEDURES

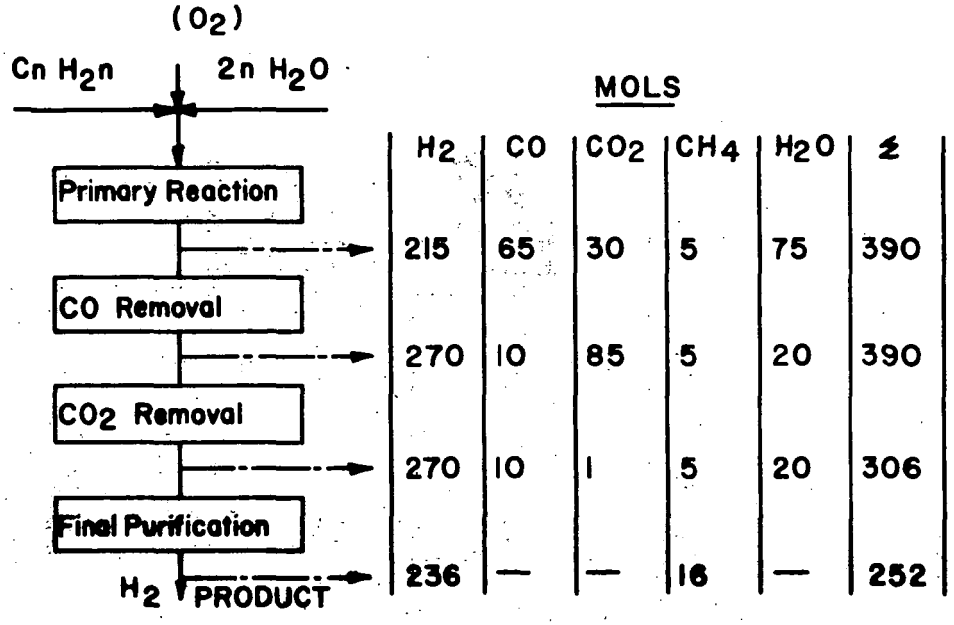

MOLS

	H_2	CO	CO_2	CH_4	H_2O	Σ
	215	65	30	5	75	390
	270	10	85	5	20	390
	270	10	1	5	20	306
	236	—	—	16	—	252

FIGURE 2
ENGELHARD HYDROGEN PROCESS

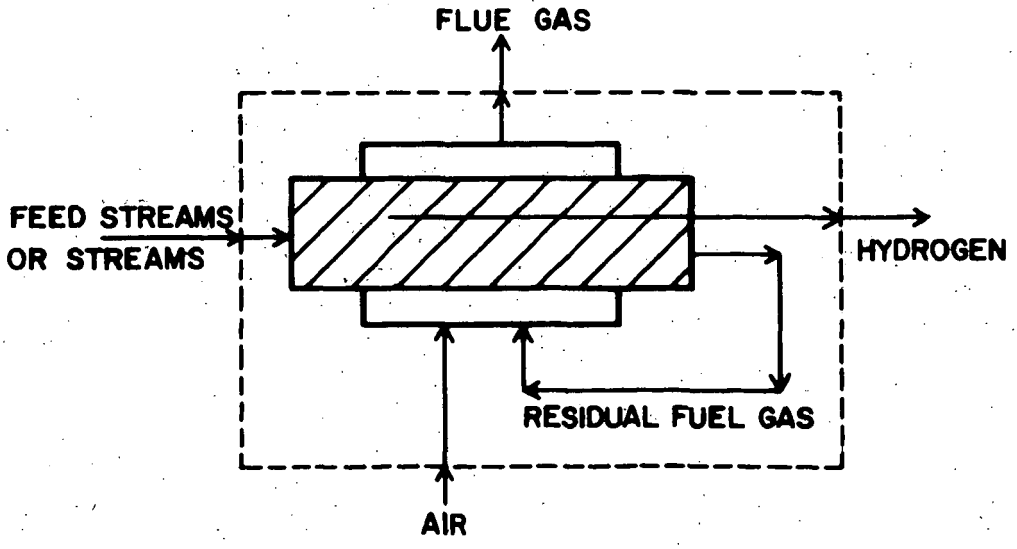

FIGURE 3
EHP SCHEMATIC FLOW DIAGRAM

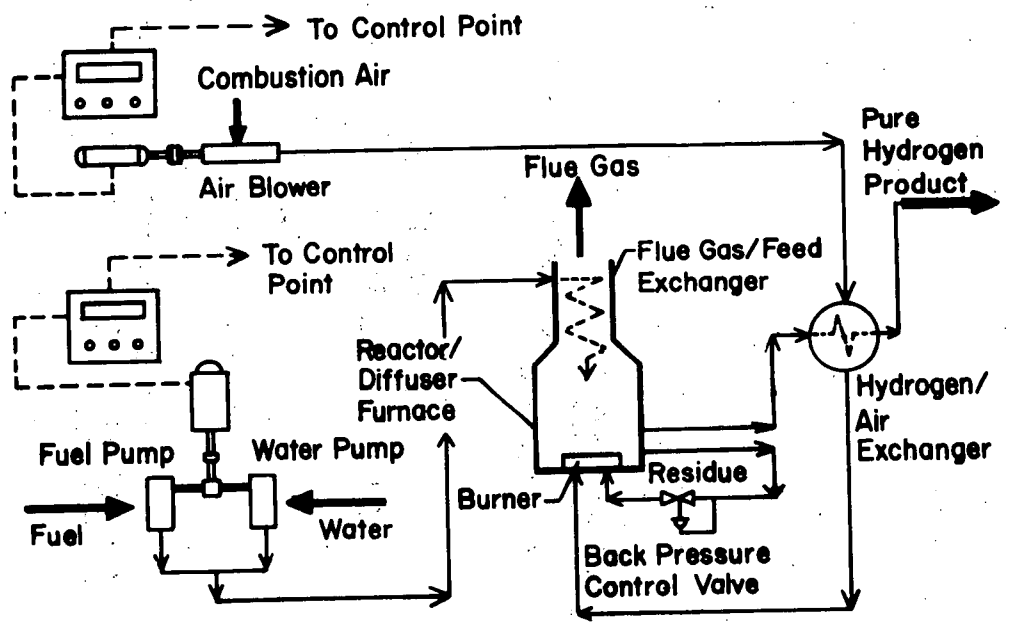

A Hydrogen-Generating Plant for Submarine Fuel-Cell Use Based on Methanol Decomposition

W. H. Heffner, A. C. Veverka and G. T. Skaperdas
M. W. Kellogg Company
New York 17, New York

ABSTRACT

A design study of a hydrogen-generating plant based on the decomposition of methanol and intended as a source of hydrogen for fuel cells to be used in submarine propulsion is reported. The plant is designed to supply 20 pounds per hour of ultrapure hydrogen normally (70 pounds per hour maximum) and is optimized on the basis of minimum volume and weight, minimum oxygen consumption, maximum efficiency, maximum simplicity and reliability, minimum hazard, minimum maintenance, and minimum cost. For ten days of continuous operation at normal capacity, the hydrogen-generating equipment and fuels (methanol and oxygen for combustion) represent a combined specific weight of about 1.0 lb./kwh and a specific volume of 0.018 cu. ft./kwh.

HYDROGEN FROM NATURAL GAS FOR FUEL CELLS

John Meek and B. S. Baker

Institute of Gas Technology
Chicago 16, Illinois

INTRODUCTION

To be practical, any commercial fuel cell system for use with natural gas must be competitive with existing power generation schemes. Under this stringent economic limitation, many potential fuel cell systems are eliminated. A review of the more common fuel cells (Table 1) summarizes the authors' estimate of these systems, based only on the criterion of economic feasibility for use in the gas industry.

At the beginning of 1963, a low-temperature fuel cell program was initiated at the Institute of Gas Technology to study the use of reformed natural gas and air in acid fuel cells. This system, based on the use of impure hydrogen, does not appear to have been extensively studied elsewhere. The following considerations motivated this course of study:

1. Natural gas (methane) is difficult to react directly at low temperatures in fuel cells.
2. Hydrogen is known to be a good fuel cell fuel at low temperatures.
3. Natural gas is an easily reformed hydrocarbon fuel.
4. Reformed natural gas will contain about 80 mole percent hydrogen.
5. An acid cell, in principle, does not require a high-purity hydrogen feed.

The present paper is concerned with that portion of the IGT program devoted to the production from natural gas of a hydrogen-rich feed which is compatible with economic fuel cell operation.

The objectives set forth for the hydrogen generation system were dictated by economic as well as practical feasibility. The project was guided by the following goals:

1. Low-cost components.
2. Maximum methane conversion.
3. Minimum carbon monoxide content.
4. No moving parts.
5. Low system pressure drop.

The need for low-cost components with low pressure drop eliminated conventional palladium diffuser purification schemes. The impracticability of having moving parts in small generators (delivering 2- to 100-kilowatt fuel cells) eliminated scrubbing towers, often used in larger hydrogen purification processes. Maximum methane conversion is essential to obtain high efficiency. The desirability of a low carbon monoxide concentration resulted from information derived from the fuel cell portion of the program. All of the above goals are based on the needs of on-site generation systems for use in the gas industry.

THE HYDROGEN GENERATION SYSTEM

To achieve the design goals outlined above, a multi-stage process was necessary. The scheme studied was a three-stage process made up of the following steps:

$$\text{Reforming: } CH_4 + H_2O \rightarrow 3H_2 + CO \quad (1)$$

$$\text{Shifting: } CO + H_2O \rightarrow CO_2 + H_2 \quad (2)$$

$$\text{Methanation: } CO + 3H_2 \rightarrow CH_4 + H_2O \quad (3)$$

The overall process is shown schematically in Figure 1.

Methane Reforming

Reaction (1) being well-known, it was the intent of this study to establish operating parameters which might be useful in the construction of small hydrogen generators. Experiments were conducted in reactors capable of providing power for a fuel cell system of a few hundred watts. Since most experience with these reactions is with larger systems, it was felt that scaleup in this instance would be relatively straightforward.

A steel reactor 1 inch in diameter and 18 inches long was filled to a 4-inch bed height with Girdler G-56B catalyst, which was reduced in size to give a reactor diameter-to-particle size ratio of about 10:1. The total pressure drop through the reactor at a space velocity of 1000 SCF per cu. ft. of catalyst per hour was only 1 inch of water. A steam-to-methane mole ratio of 3:1 was chosen, and studies were made at space velocities of 500 and 1000 SCF per cu. ft. of catalyst per hour at a variety of temperatures. Effluent gas was analyzed chromatographically for carbon monoxide and methane with a Fisher-Gulf partitioner using a charcoal column. The only other detectable carbon-containing species present, carbon dioxide, was determined from a mass balance.

The results of these experiments (Figure 2) show that methane conversion was a strong function of space velocity with respect to the temperature required to achieve complete conversion, higher temperature being required for higher space velocities. For the space velocities studied, complete conversion was obtained at 800°C. and above. The exit gas carbon monoxide content was not a strong function of space velocity, and the effluent carbon monoxide concentration at 800°C. was about 15 mole %. At the lower space velocity, experiments conducted at temperatures up to 1000°C. resulted in a further increase in carbon monoxide concentration. Since the ultimate goal is a low carbon monoxide content in the fuel cell feed gas, operating at this high temperature is undesirable. Also, from a thermal efficiency standpoint the lowest possible reforming temperature is most desirable. Having established reasonable operating limits for the reforming stage, the effluent from the reformer was used as the input to the shift reactor.

Carbon Monoxide Shift

Conventional shift processes operating between 300° and 500°C. require, to achieve a low carbon monoxide content (3000 parts per million or less), the use of a carbon dioxide absorption stage, which is unwieldy for use in small systems. Recently work done by Moe (1) indicated that reformed and shifted gases containing 2000 to 3000 parts per million carbon monoxide could be achieved without carbon dioxide removal if a low-temperature (175° to 300°C.) shift catalyst was used. This relatively new catalyst, Girdler G-66, was placed in a reactor of 1-inch diameter and 18-inch length, filled to a bed height of 8 inches, and the shift reaction was studied with respect to temperature, space velocity, and

steam-to-gas ratio. As in the study of the reforming reaction, the carbon monoxide and methane contents of the effluent gas stream were analyzed chromatographically.

The results of this study are shown in Figures 3 and 4. In Figure 3, the effects of space velocity and temperature on the carbon monoxide content of the effluent gas are indicated. At the higher space velocity, 1000 SCF per cu. ft. of catalyst per hour, the desired reduction in the carbon monoxide content of the effluent gas could not be obtained. Experiments at still higher space velocities, 2000 SCF per cu. ft. of catalyst per hour, yielded much poorer results, not reported here. However, at a space velocity of 500 SCF per cu. ft. of catalyst per hour, a minimum in the carbon monoxide concentration is seen to occur at about 267°C. In Figure 4, the strong effect of the steam content of the reacting mixture on the effluent carbon monoxide concentration is indicated. At 250°C., a continuous reduction in the carbon monoxide content is obtained as the steam-to-methane ratio is increased. The maximum ratio tested was 7.3:1, as this ratio readily yielded a carbon monoxide content which was known to be further reducible by methanation. Whether additional steam is desirable will be decided later on the basis of the cost of the steam, as well as the fuel cell performance on impure hydrogen feed.

Carbon Monoxide Methanation

Reaction 3, methanation, posed the greatest challenge in the overall carbon manoxide reduction process. The first attempts at achieving an effective reduction in the carbon monoxide content of a synthetic gas containing 80 mole % hydrogen, 19.7 mole % carbon dioxide, and 0.3 mole % carbon monoxide, using conventional methanation catalysis, were unsuccessful. Either of two events occurred. At very low temperatures no reactions occurred, while at higher temperatures the water gas shift was promoted along with methanation and at best only a slight decrease, and in some cases an actual increase, in carbon monoxide was observed.

The problem was to find a catalyst which would permit selective methanation of carbon monoxide in the presence of carbon dioxide, under conditions in which the latter is present in concentrations two orders of magnitude greater than the former. The need for selective methanation is twofold. If appreciable amounts of the carbon dioxide react, the exothermic nature of the reaction almost ensures a complete loss of temperature control in the system. As the temperature rises, more carbon dioxide is methanated and large amounts of hydrogen are consumed. In the limiting case, all of the hydrogen and carbon dioxide could react to form methane. Equilibrium calculations clearly indicated the desirability of low-temperature operation, although even under these conditions the sought-after reduction did not appear achievable.

Using the above-mentioned gas composition, experiments were conducted with a ruthenium-on-alumina catalyst obtained from Englehard Industries, Inc. The effluent gas composition was analyzed with the afore-mentioned chromatograph and a Mine Safety Appliances Co. Lira infrared analyzer. With the infrared analyzer, carbon monoxide was determined with an accuracy of about 10 parts per million. Again, a variety of parameters were studied, including excess water, and the results are shown in Figures 5 and 6. The excess water tests were made to ascertain at what stage in the hydrogen generation system it would be most favorable to remove water.

In Figure 5, the carbon monoxide content of the exit gas is seen as a function of temperature for the case of 2 mole % water vapor in the feed. Distinct minimums in carbon monoxide content – about 100 parts per million, dependent on space velocity and temperature – are seen. It is interesting that, for increasing space velocity, the same minimum carbon monoxide content is obtained, but at higher temperatures. In Figure 6, the same parameters are studied with a feed gas containing 15% water vapor. Again, the same minimum carbon monoxide concentration is obtained, but at slightly higher temperatures. It was also observed that, in the range of minimum carbon monoxide content, no appreciable conversion of carbon dioxide to methane occurred; hence, the reaction can be considered highly selective. The carbon manoxide reduction process is summarized in Figure 7.

Complete Hydrogen Generation System

After completing the experimental work on the reactions described above, reforming, shift, and methanation reactors were connected in series, and the complete system was analyzed. A natural gas containing about 95% methane and 5% higher hydrocarbons was passed through a sulfur removal cartridge and fed to the first reactor stage, where it was reformed in the presence of excess steam (steam-to-gas mole ratio of 7.3:1) at a space velocity of 250 SCF per cu. ft. of catalyst per hour at 800°C. The effluent from this reactor was fed to the shift reactor operating at a space velocity of 500 SCF per cu. ft. of catalyst per hour at 270°C. The effluent from this stage was fed to a condenser where a portion of the excess water was removed, and the remaining gas mixture was fed to the methanation reactor operated at a space velocity of 1000 SCF per cu. ft. of catalyst per hour and at a temperature of 190°C. The total system pressure drop was 4 inches of water column. The product gas was analyzed to be 78 mole % hydrogen, 19.7 mole % carbon dioxide, 0.3 mole % methane, 2 mole % water, and 8 parts per million carbon monoxide. The carbon monoxide was analyzed on a special MSA Lira infrared analyzer with a sensitivity of 2 parts per million.

The tenfold improvement in performance compared with the previous experiment is not readily explainable. Some improvement had been anticipated on the basis that the original methanation experiments were performed with a feed gas containing about 3400 parts per million carbon monoxide, while the actual shift reaction reduced that concentration by almost a factor of 2. Experiments are being continued to study further the effects of steam-to-methane ratio, space velocity, and catalyst life. Experimental evidence from the fuel cell portion of the program indicates that the above-mentioned carbon monoxide content can be readily tolerated by the hydrogen electrode.

EFFICIENCY AND ECONOMICS

One of the most attractive features of fuel cells is their potentially high efficiency. When an additional processing stage, such as the one just described, is added to the fuel cell system, a reduction in overall efficiency may be anticipated. To place the external reformer-fuel cell system in the proper perspective, estimates of the overall system efficiencies have been made, based on several fuel cell and reforming parameters.

Two models have been chosen for evaluation, and these are shown schematically in Figure 8. In both schemes, it is assumed that the heat required to sustain the reforming reaction is supplied from an external burner (i.e., there is no partial combustion in the reformer). Also, both schemes assume single-pass conversion in the fuel cell.

The two schemes chosen for analysis differ only in the effect of recovery of the heat value of recycled spent fuel from the fuel cell. The following parameters have been defined:

η_O - overall efficiency, electrical energy output based on the heat of combustion of the total amount of methane consumed

η_V - voltage efficiency, fraction of the theoretical fuel cell potential actually obtained

η_C - conversion efficiency, fraction of the fuel converted in the fuel cell

η_R - reactor thermal efficiency, total reformer heat requirement, based on the assumption of nonideal insulation

η_E - heat exchanger efficiency, fraction of heat recovered in heat exchangers

A partial summary of the results of these calculations is shown in Figures 9 and 10. In Figure 9, a case where reactor thermal efficiency is 80% was analyzed for the no-recycle system. A number of arbitrary conversions and voltage efficiencies were chosen as parameters, and the overall system efficiency was calculated as a function of heat exchanger efficiency. A typical 1-kilowatt fuel cell system using impure hydrogen feed might be expected to operate in the grey zone shown in Figure 9. An overall system efficiency range of from 21.5% to 32.5% can be realistically anticipated. For the case of a pure hydrogen cell, a somewhat higher conversion efficiency and voltage efficiency might be

anticipated, and a total system efficiency of 40% is most likely. In Figure 10, using the same parameters for the recycle schemes two characteristics are seen. First, the overall system efficiency is less dependent on conversion efficiency because of the utilization of the heating value of the spent fuel. Second, a cutoff point is seen at high heat exchange efficiency and the lowest chosen conversion efficiency. This point indicates the case where the hydrogen generation system can be operated solely on the spent fuel from the fuel cell. With the same range of heat exchanger efficiency as in the no-recycle case, an overall efficiency between 26.5% and 35.5% appears likely.

A more complete analysis of low-temperature fuel cell systems with external reforming places the parameters studied in the following order of importance with respect to overall efficiency in a recycle system operating below the cutoff point: 1) voltage efficiency, 2) reactor thermal efficiency, 3) heat exchange efficiency, and 4) conversion efficiency.

The complete economics of the present hydrogen generation system will not be known until more hardware is developed. Present estimates, based on the fuel requirements of the fuel cells under study and the catalysts and conditions described in this paper, indicate the cost of catalysts in the IGT hydrogen generation system would be less than 5 cents per watt.

REFERENCE

1. Moe, J. M., Paper presented at 145th National Meeting, Division of Petroleum Chemistry, American Chemical Society, New York, N.Y., September 8-13, 1963, Preprint No. 4-B, Vol. 8, B-29.

ACKNOWLEDGMENT

The authors wish to thank the Southern California Gas Co., the Southern Counties Gas Co., and Con-Gas Service Corp., who are sponsoring the low-temperature fuel cell project for which this investigation was made. Also, the authors wish to thank Henry Linden of IGT for his helpful suggestions with respect to the conception of the overall process and Jack Huebler of IGT for his suggestions with respect to the choice of catalysts to be used in these studies.

Table I.-STATUS OF FUEL CELLS FOR USE IN GAS INDUSTRY APPLICATIONS

Type of Fuel Cell	Present Principal Drawback	Potential Gas Industry Applications
Low-Temperature Alkaline Direct (25°-250°C.)	Electrolyte Incompatible with Methane	Poor
Low-Temperature Alkaline Indirect (25°-250°C.)	Cost and Technical Drawbacks of Ultra-Pure Hydrogen Production	Fair
Low-Temperature Acid Direct (25°-200°C.)	Very High Cost of Fuel Cell Catalysts and Components	Fair
Low-Temperature Acid Indirect (25°-90°C.)	High Cost of Fuel Cell Components	Good
High-Temperature Molten Salt (450°-800°C.)	Operating Lifetime	Good
High-Temperature Solid Oxide (1000°-1200°C.)	Operating Lifetime	Good

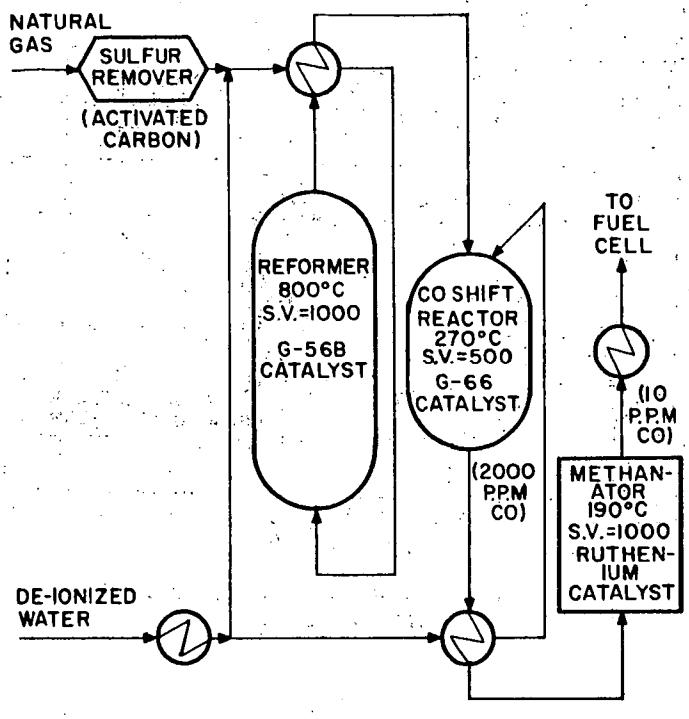

Fig. 1.-IGT HYDROGEN-GENERATION PROCESS

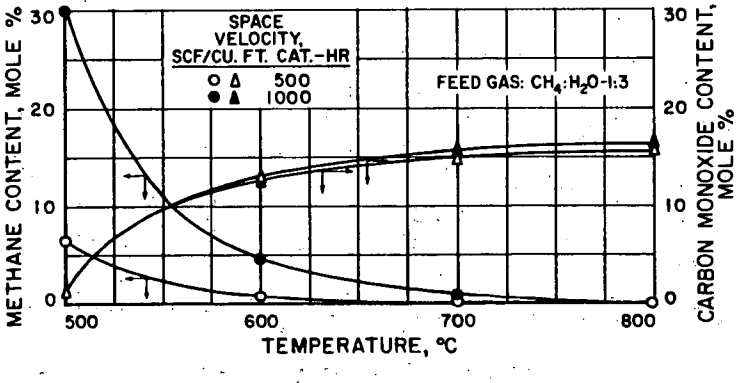

Fig. 2.-METHANE CONVERSION AND CARBON MONOXIDE COMPOSITION IN REFORMER

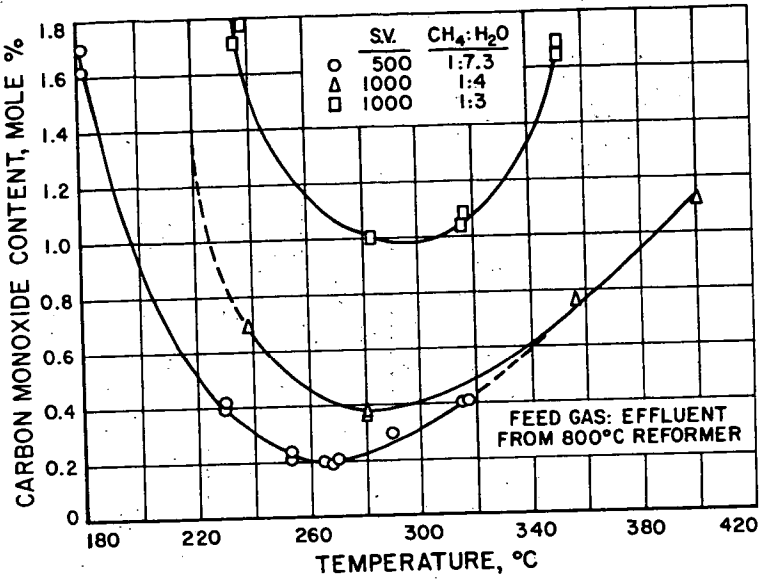

Fig. 3.-CARBON MONOXIDE CONVERSION IN SHIFT REACTOR

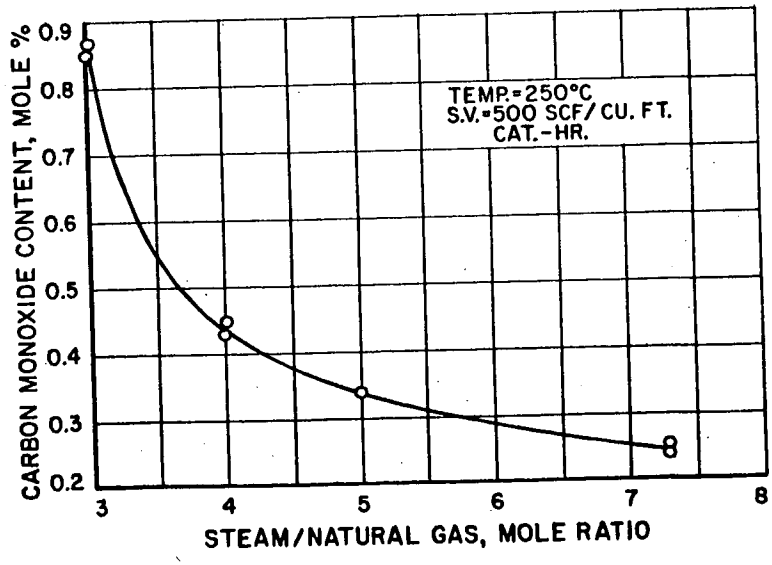

Fig. 4.-EFFECT OF STEAM-NATURAL GAS RATIO ON THE SHIFT REACTION

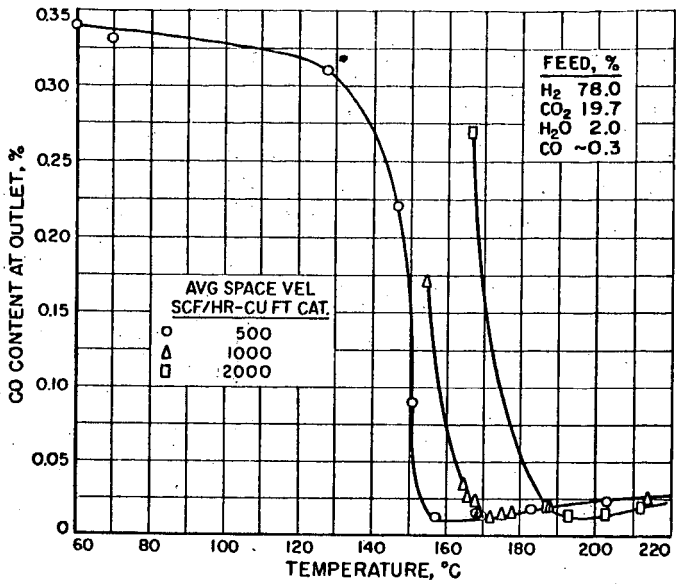

Fig. 5.-SELECTIVE METHANATION OF CARBON MONOXIDE AT LOW WATER CONTENT

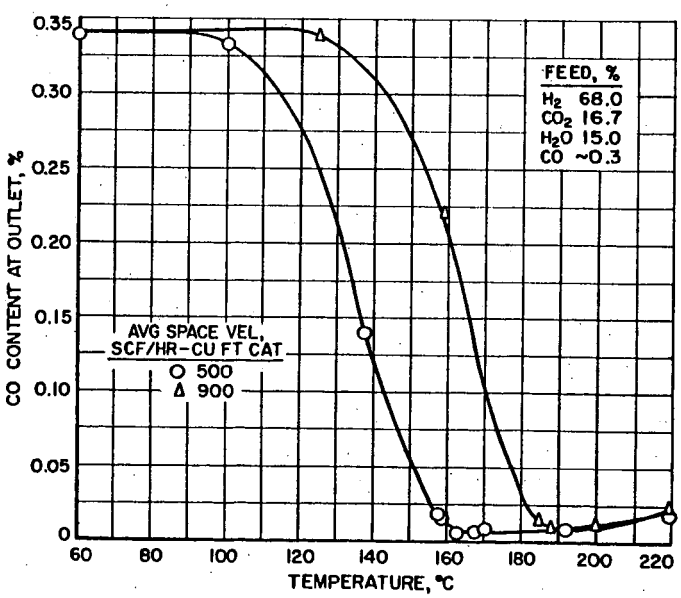

Fig. 6.-SELECTIVE METHANATION OF CARBON MONOXIDE AT HIGH WATER CONTENT

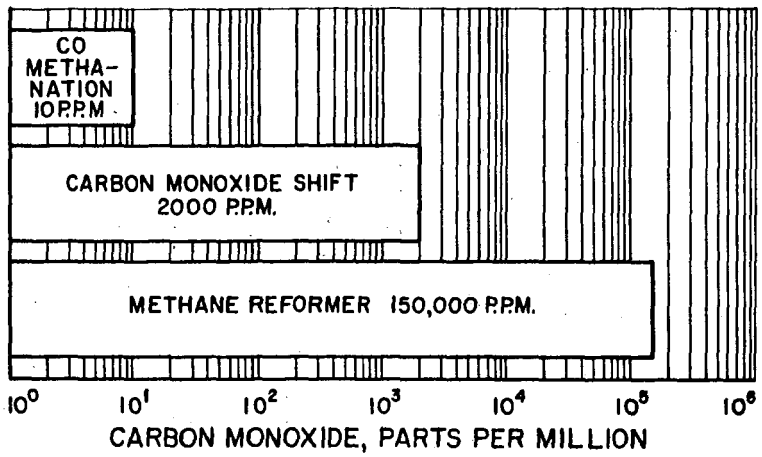

Fig. 7.-CARBON MONOXIDE REDUCTION IN IGT HYDROGEN GENERATION PROCESS

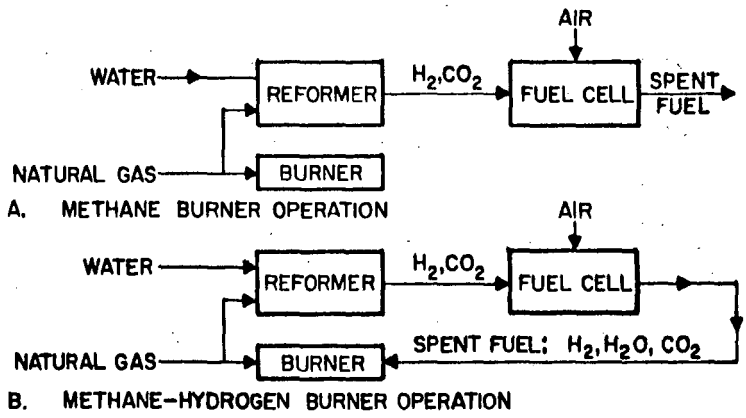

Fig. 8.-OPERATIONAL MODES FOR REFORMER-FUEL CELL-BURNER SYSTEM

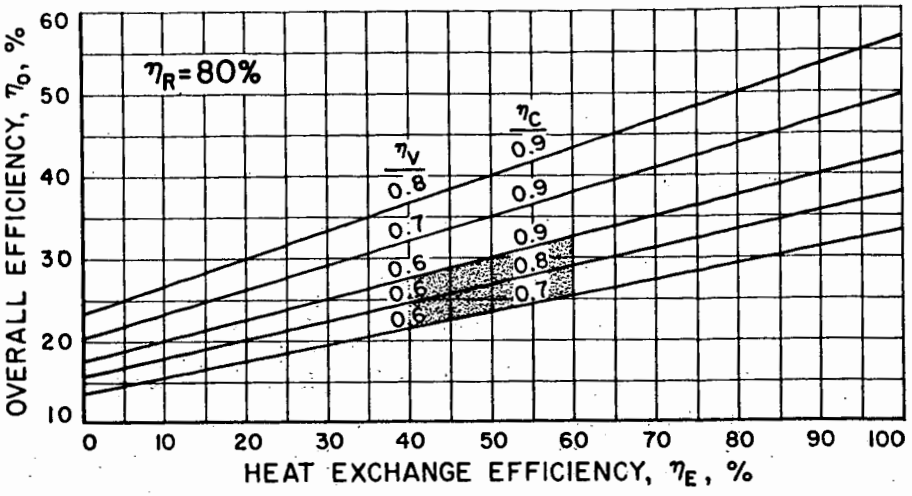

Fig. 9.-EFFECT OF FUEL CELL AND HYDROGEN GENERATOR PARAMETERS ON SYSTEM EFFICIENCY
CASE I - NO RECYCLE

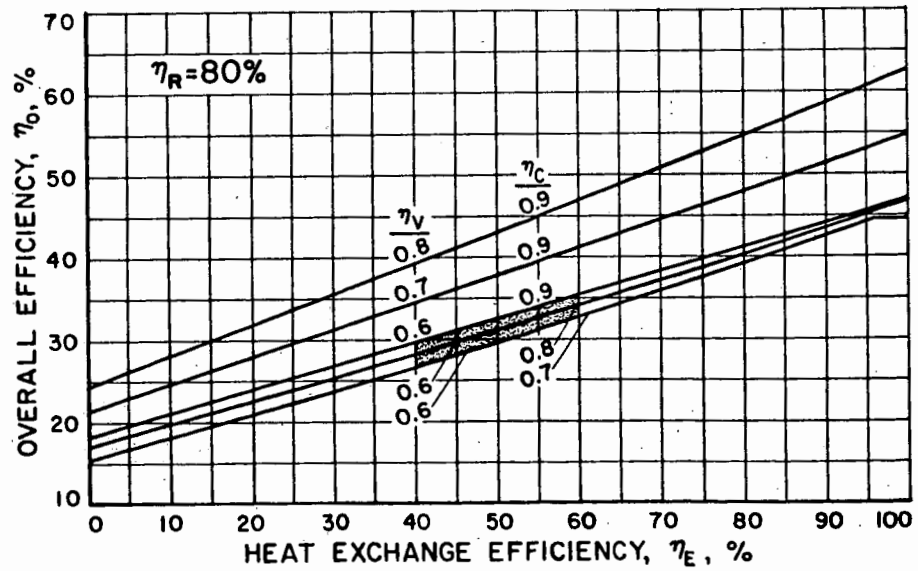

Fig. 10.-EFFECT OF FUEL CELL AND HYDROGEN GENERATOR PARAMETERS ON SYSTEM EFFICIENCY
CASE II - RECYCLE

Steam Naphtha Reforming By The Imperial Chemical Industries Process

Raymond J. Kenard, Jr.

Joseph C. Maginn

Selas Corporation of America

Dresher, Pennsylvania

In 1803 Thomas Robert Malthus published his "Essay on Population" which culminated a five year study of population growth in all the countries of the world. Malthus concluded that population tends to grow at a rate faster than the rate of growth of food producing resources and that therefore famines, wars and pestilence were an unavoidable means of checking this growth. Malthus' pessimistic view of the future was bourne out in the 1800's by the Napoleanic wars followed by food shortages in Europe and the Irish famine of the 1840's.

Some 70 to 80 years later Sir William Crooks, the eminent English chemist who discovered the element thallium, predicted that the entire world faced a wheat famine in 25 years because existing supplies of nitrogenous fertilizers (Chilean saltpeter) would be exhausted by that time. Sir Crooks stated: "The fixation of atmospheric nitrogen is one of the greatest discoveries awaiting the ingenuity of chemists". (1)

Now, after another period of some 70 to 80 years, attention is again being directed to the age old problem of producing enough food to support the world's growing population. The emphasis has passed, however, from the prevention of starvation to maintaining and, hopefully, to improving the diet of undernourished millions, and as well as to planning the use of raw material resources to feed the burgeoning population of the world. (2)

That the emphasis has shifted reflects with credit upon advances in science. The use of manures and composts for improving the yield of farm products dates from the earliest days of civilization. In the second century before Christ, Cato, in his book De re Rustica, detailed the benefits to be derived from organic fertilizers. Arab scholars in the 10th Century noted the value of blood as manure - suggesting that human blood was the best kind. American Indians placed fish in their corn hills.

Lacking, however, was the scientific approach that would lead to recognition of the value of inorganic sources of soil nutrients. Obviously, organic material was limited in availability. The first scientific efforts were undertaken by John Bennett Lawes at his estate, Rothamsted.

Lawes studied chemistry at Oxford and was well versed in the theoretical discussions of contemporary chemists on the subject of soil management. He determined to perform practical application work on his estate, tackling as his first problem the making of water soluble soil nutrients.

By extensive experimentation in pots and then in the open soil of the fields, Lawes found that bones needed a preliminary treatment with acid to consistantly achieve

their maximum effectiveness. In 1842 he patented a process for treating bones and rock phosphate with sulfuric acid to make soluble phosphates.

By about 1880, application of Chilean nitrates to the soil was accepted, and shipment of nitrates expanded 10 fold in the subsequent 30 years. (3) With this as the background, the stage was set for some scientist to synthesize ammonia.

One likes to think that the ability to synthesize ammonia opened a new era of well being for mankind. Unfortunately, nitrogenous compounds were as vitally important to the waging of war, at least before the atom bomb, as they were to the growing of food. Within 4 years after successful laboratory synthesis of ammonia by Fritz Haber, World War I was declared.

The production of nitrogen from various sources before and after World War I is shown in Table I.

In 1913, production of nitrogen totalled 851 thousand tons. In 1918, production had increased 38% to 1160 thousand tons. In the same 5 year interval of time, production of synthetic nitrogen increased 700% from 3% to 16% of the total production.

Germany was the only nation to achieve self-sufficiency in nitrogen required for both explosives and fertilizers. The United States did not have an ammonia synthesis plant in production until 1921.

With the importance of fertilizers now scientifically demonstrated, and with techniques available to synthesize ammonia from the plentiful supplies of nitrogen in the atmosphere, attention was directed to alternate sources of, and economic means for recovering, hydrogen.

In these early years, the various sources of hydrogen were limited to byproduct gas from the electrolysis of brine, byproduct gas from the conversion of coal to coke and "producer gas" from the reaction of incandescent coke with steam.

Considerable work was being done on the reforming of gaseous hydrocarbons by the I. G. Farben interests. (4) Basic patents were issued in 1913 and 1927. Following an exchange of information with Standard Oil Development Company (now Esso Research & Engineering Co.), Standard Oil brought the process to commercial realization in 1930 with an installation of three reformers at their Bayway, New Jersey Refinery. Three more installations were made soon thereafter at their Baton Rouge, Louisiana Refinery. Standard Oil's installations were for the purpose of producing hydrogen to hydrogenate low quality gasolines, kerosenes and diesel fuels. It appeared that hydrogenation of distillate oil stocks would be a major process for all refiners because of the relatively poor quality crude oils available at the time.

Concurrent with Standard's interest, Imperial Chemical Industries in 1928 undertook pilot plant studies of steam reforming of gaseous hydrocarbons. These studies led to a commercial installation in 1936.

In the latter part of the Thirties, Standard Oil's interest in the process waned as the need for oil hydrogenation processes failed to materialize. However, ICI continued their intensive pilot plant work, as their prime interest was ammonia production and they recognized the importance of steam reforming in the preparation of ammonia synthesis gas.

The United States chemical companies were not unaware of the potential for steam reforming. Both Hercules Powder Company and Atlas Powder Company approached I. G.

Farben in the latter part of the 1930's for knowhow and rights to build reforming furnaces. Both companies were rejected (3). Hercules proceeded to develop its own reforming catalyst and furnace, starting up a small plant in 1940.

At the outbreak of World War II, the United States ammonia industry was ill-equipped to handle the quantity of nitrogen required to support the war effort, since the major producers of ammonia, DuPont at Belle, West Virginia and Allied Chemical at Hopewell, Virginia were still dependent upon coke for hydrogen. There were seven other plants--all quite small. Five used electrolytic hydrogen, one cracked refinery gases and one reformed natural gas. Consequently, the U. S. government had constructed ten new ammonia plants with an estimated annual productive capacity of 800,000 to 900,000 tons per year of nitrogen--more than twice the productive capacity of the plants then in operation (3).

Of the ten new plants built by the Government, six were based on steam methane reforming. ICI loaned a team of engineers to cooperate in the construction of three of the reforming plants, and undoubtedly the ICI knowhow was of influence on the design of the other three reforming plants.

ICI's interest in reforming of hydrocarbons was not limited to gaseous hydrocarbons. As early as 1938, ICI had demonstrated the ability to reform sulfur-free distillate hydrocarbons. This technique was not commercially applied until 1954 when a plant at Heysham, England was adapted to reform a sulfur-free synthetic hydrogenated gasoline with a 192°C end point. After development of a sulfur removal process, this plant was converted to reform straight run distillate fractions with the same end point.

The early naphtha reforming plants operated at low pressure, but further development work led to a pressure process which permitted reforming up to 400 pounds pressure at steam to carbon (mol) ratios comparable to those used in steam methane reforming.

The success of the ICI Steam Naphtha Reforming Process is being demonstrated today by ICI's own construction program. Practically all ICI's capacity to produce ammonia and methanol synthesis gas is already converted from coke to naphtha reforming. Additional ammonia plants based on naphtha reforming are planned or under construction.

Furthermore 13 towns gas plants producing a 400-500 Btu per cubic foot gas from naphtha are operating or under construction in Great Britain.

Reforming Reactions

The reactions occurring in steam naphtha reforming are basically the same as those in steam methane reforming, with the addition of a series of reactions, extremely complex due to the length and configuration of the carbon chain of the heavy hydrocarbons making up the naphtha fraction.

The pertinent reactions are shown in Table II. In reaction 1, substitution of methane (CH_4) for C_nH_m yields a statement of the overall reaction for steam methane reforming. In all probability the actual reaction mechanism consists of a cracking-dehydrogenation reaction, which produces carbon, and a concurrent and competing reaction of carbon with steam to yield hydrogen and the carbon oxides.

In the case of a naphtha containing various paraffinic, aromatic and naphthenic compounds having a boiling range encompassing C_4 to C_{10} fractions, the complexity of the reaction mechanism increases greatly.

The ability of the reforming process to operate successfully depends upon the avoidance of carbon laydown. Two mechanisms for carbon laydown can be identified: one based on the equilibrium relations expressed by equations (2.), (3.) and (4.) in Table II, and the other based on the cracking-hydrogenation-polymerization reactions of the hydrocarbon.

In the case of the first mechanism, based on the reaction of an average light distillate hydrocarbon with steam, ICI has computed a tendency to form carbon in the range of 1000 to 1200°F. This carbon forming reaction takes place very rapidly in the presence of nickel catalyst. In this temperature range, should the steam rate be reduced below a certain minimum, carbon forms instantaneously throughout each catalyst pellet causing the pellet to disintegrate.

The second carbon forming mechanism is believed to occur as a result of a cracking-dehydrogenation reaction, followed by polymerization to tarry substances which, in turn, carbonize to a soft sooty carbon. This carbon forms on the exterior of the catalyst not within the intersecticies. No damage to the catalyst results from this carbon deposition. The active surface of the catalyst is blanketed, thereby reducing its activity and also building up pressure drop through the catalyst bed. This type of carbon can be removed by oxidation (i.e. regeneration with steam and air) without impairment of catalyst activity or physical strength. Prevention of carbon is a matter of maintaining suitable steam ratios and keeping the reactants in contact with the catalyst. Care must be exercised in loading the catalyst so that bridging is avoided.

Reaction 1, in Table II is a highly endothermic reaction. Reaction 3, which is the well known water-gas shift reaction, is exothermic. This, coupled with the complexity of the feed analysis and the potential for carbon deposition, makes necessary the selective use of a catalyst which promotes the desired reactions while also inhibiting the reactions leading to carbon deposition. It also necessitates precise control of the heat input profile to the tubes of the reformer.

Reformed gas from the naphtha reformer consists of hydrogen, carbon dioxide, carbon monoxide, methane and traces of heavier gaseous hydrocarbons. Feed naphtha is completely converted. The presence of methane in the gas results from either, or both, the initial cracking reaction of the naphtha or reaction 2 (shown in Table II) which is the reverse of the steam methane reforming reaction.

The ICI Process

The ICI process consists of sulfur removal and steam reforming over a special ICI catalyst, followed by conventional processing techniques to make hydrogen synthesis gas for ammonia or methanol and towns gas.

Sulfur removal is fundamental to the successful performance of the ICI reforming catalyst, as the catalyst is sulfur sensitive. A three-bed desulfurization process is usually required. The first bed is a bed of zinc oxide; the second bed a cobalt molybdate catalyst; the third bed another bed of zinc oxide.

Elemental sulfur and hydrogen sulfide are absorbed by the zinc oxide. Mercaptan and disulfide sulfur, in the presence of hydrocarbons and zinc oxide, are converted to hydrogen sulfide, which is then absorbed by the zinc oxide. Thioethers are also hydrogenated to hydrogen sulfide and similarly removed. Other sulfur compounds are non-reactive in the presence of zinc oxide and are hydrogenated over cobalt molybdate catalyst to hydrogen sulfide, which is removed in the final zinc oxide bed. The sulfur concentration in the feed to the reformer is reduced to between 3 and 5 parts per million.

The zinc sulfide formed in the above process must be periodically replaced. In the case of naphthas with high sulfur content, it may be economic to use preliminary electrostatic acid treatment to remove most of the sulfur before the three-bed treatment.

After desulfurization, the vaporized naphtha passes to the steam reformer where it is admixed with steam and converted to a hydrogen-rich gas. The steam reformer is the heart of the process. Suspended in the center of its firebox are vertical tubes packed with catalyst. These suspended tubes are heated externally by a large number of burners. Advancement in furnace design and tube metallurgy have gone hand in hand with advancements in catalyst technology. Reformers today not only can reform liquid fractions but also produce at higher space velocities, with higher flux densities and higher tube wall temperatures than have been considered for methane reforming.

A simple outline drawing of a typical steam reformer is shown in Figure I. Desulfurized, vaporized naphtha flows down through a bed of catalyst contained in a multitude of tubes. Because the reactions occurring at the top of the tube are highly endothermic, a large quantity of heat must be contributed to the reaction to prevent carbon laydown. Various furnace designs accomplish this in different ways. (4) In the furnace design shown (Selas Corporation of America), the variable heat input down the length of the tube is accomplished through the use of a multiple number of radiant cup burners arranged in horizontal rows which can be independently fired to give the optimum heat profile.

The tube wall temperatures of a naphtha reformer will operate in the range of 1700 to 1750°F. The generally accepted technique for manufacture of the catalyst tubes is permanent-mold centrifugal casting of a Type 310 stainless steel (ASTM 297-55 HK). The grain formation is such that the tubes have higher stress values than the extruded tubes.

Despite the greater carbon laydown potential of naphthas relative to gaseous hydrocarbons, the ICI catalyst is able to operate continuously without carbon laydown or loss of activity, even at operating conditions more severe than those of conventional steam methane reforming. Current designs are based on a 3 to 1 steam to carbon mol ratio and 400 pounds pressure. Outlet temperatures, determined by the desired effluent gas composition, range from 1200 to 1500°F. Straight-run naphthas with end points as high as 400°F can be reformed. There is no restriction on the degree of aromaticity.

Application Of The ICI Process

The applications of the ICI Steam Naphtha Reforming Process are the same as those of the conventional steam methane reforming process. The process produces a hydrogen-rich stream containing, as impurities, carbon dioxide, carbon monoxide, methane and traces of heavier gaseous hydrocarbons. This stream is subsequently processed by conventional techniques to give either a relatively pure hydrogen, a hydrogen-nitrogen mixture for ammonia synthesis, hydrogen-methane mixture for towns gas, or a hydrogen-carbon oxide mixture for methanol or oxo chemicals manufacture.

Block-flow diagrams are shown in Figure II to delineate the fundamental differences of processing schemes for hydrogen, ammonia synthesis gas and towns gas manufacture.

The scheme for hydrogen generation includes sulfur removal, the primary reforming reaction, shift conversion (where the carbon monoxide is reacted with steam to produce more hydrogen and carbon dioxide), and purification to remove carbon dioxide and to methanate the residual quantities of the carbon oxides back to methane by

reaction with hydrogen (a reversal of the reforming reaction). The resultant final product has only parts per million of the carbon oxides which are catalyst poisons in most processes that require hydrogen. The reforming operation will be at temperatures sufficiently severe to minimize the methane in the outlet of the reforming process. The concentration of methane will usually be of the order of 1 to 4% depending upon the ultimate use of the hydrogen.

The scheme for ammonia synthesis differs from the hydrogen generating scheme by the addition of a secondary reformer which combusts part of the product stream with air. The secondary reformer introduces the nitrogen required to yield a 3 to 1 hydrogen-nitrogen mixture which, after purification, goes to an ammonia synthesis converter.

It is obviously not necessary to reform the naphtha as severely in this scheme, since a certain amount of residual hydrocarbon can be used to combust with air. Under the less severe operating conditions, the methane content in the product from the reformer will be in the range of 7 to 10%. It is interesting to note that, even in cases where the reforming is not done under severe conditions, naphtha does not show up in the product from the reforming step.

In the secondary reformer, after combustion, the gases pass through a catalyst bed that further reduces the methane content. The secondary reformer is a refractory-lined vessel which operates at a temperature higher than the outlet temperature of the primary reformer, thereby making it possible to achieve concentrations of methane in the product as low as one-quarter of one percent.

The balance of the processing steps are similar to hydrogen manufacture, i.e. shift conversion and purification.

In the production of towns gas, the process scheme varies greatly with the final specifications of the towns gas. In prinicple however, as shown in Figure II, a low-severity reforming and shift conversion step is required. Addition of an enrichment gas is also required, and some balance must be struck between carbon dioxide removal and inert gas makeup.

Naphtha Reforming Vs. Steam Reforming

At the present time, the determinant for using Naphtha Reforming instead of Steam Reforming is more one of raw material availability than one of economics. In major market areas of the world, natural gas either does not occur or has not been discovered and developed. In these areas natural gas can only be made available by liquification and tanker shipment. The economies of these areas are therefore oriented around oils for heating and, to an ever decreasing extent, around coal. Naphthas are usually in long supply, as the gasoline consumption is not great enough to absorb them. Here the ICI Steam Naphtha Reforming process has its broadest application.

On the other hand in an economy built around natural gas as a fuel, and with a large automobile population as is the case in the United States, naphthas as a raw material for reforming are too expensive relative to natural gas.

To demonstrate the relative values of naphtha and natural gas as raw materials for reforming data have been developed from a recently published paper on the economics of reforming (5). By comparing the relative requirement of feed and fuel for naphtha reforming and methane reforming a breakeven curve has been plotted as shown in Figure III.

46

In Great Britain, which conforms to the condition of an oil-based or coal-based economy, lacking natural gas resources, naphthas in large quantities can be contracted for at a price of about 0.8 cents per pound. The breakeven value of natural gas is 47-48 cents per million Btu--not an unusually high price in terms of the U. S. economy, but without significance in Great Britain where the gas is not naturally available.

However, in the case of the United States which is the largest natural-gas-fuel-based economy having a large automobile population, naphthas on the East Coast sell in the range 1.5 cents per pound. The natural gas breakeven is about 90 cents per million Btu, or just about double the going market price for natural gas.

The United States economy, with respect to sources and uses of natural gas, automobile population, and refining capacity is a mature enough economy that no unusual dislocation of this price structure is anticipated. Such is not the case in many of the major market areas such as Great Britain. Extensive discoveries of natural gas in Holland and the North Sea could have a significant bearing on the future economics of the entire European area.

To the extent that natural gas replaced fuel oil for heating purposes, crude oil runs would be reduced, thus reducing the surplus of naphtha. The expanding automobile population of Europe would absorb more of the naphthas. The net result would be firming of the price for naphtha.

In view of the potentially unstable fuel economy in Europe, many naphtha reforming projects under bid require rating of the naphtha reforming equipment on natural gas. The ICI process is readily converted to methane reforming.

Basic to naphtha reforming are the following processing steps not required by methane reforming:

1. Desulfurization. Either a fixed bed or combination of electrostatic acid treating and a fixed bed.

2. Vaporization facilities for naphtha.

3. Imperial Chemical Industries naptha reforming catalyst.

4. Larger capacity facilities for carbon dioxide removal.

Were a naphtha reforming plant to be converted to methane reforming, the acid-treating sulfur removal step and the naphtha vaporizer could be dispensed with. The fixed-bed desulfurizer could be used for removal of sulfur from the natural gas, although the desulfurizer would be grossly oversized. The ICI catalyst will reform methane equally well as naphtha. Carbon Dioxide removal facilities would be over-sized, since the less favorable carbon-to-hydrogen ratio of naphtha, relative to methane, result in the production of more carbon dioxide per unit of product. (See Table III)

In the case of capital investment, it has been shown (5) that the battery limits cost for an ammonia plant based on naphtha reforming is about 18% greater than for one based on methane reforming. For a plant to produce 97% purity hydrogen, the naphtha reforming plant investment is about 30% greater than that of one based on methane reforming. It should be noted that although the two percentage figures are different by a large degree, nevertheless the order-of-magnitude differences of the absolute values are roughly comparable, since the ammonia plant cost includes the cost of the

ammonia synthesis loop. Technological advances in the ICI process during the past year have resulted in pressing the technological frontier back faster than methane reforming, and the spread between the costs for naphtha reforming and methane reforming are probably somewhat diminished today.

Conclusion

Science has demonstrated over the years the ability to develop new technologies to meet the ever increasing demands of population for food.

What once was a problem of elimination of starvation has now become a problem of maintenance, and improvement, of a minimum diet.

Technologies have been developed which free the world from the uneconomic restrictions on the use of raw materials to manufacture fertilizers. Development of oil resources, shipping facilities and technologies, such as the Imperial Chemical Industries Steam Naphtha Reforming Process, permit the construction of economic facilities for ammonia manufacture anywhere in the world.

The problem of carbon deposition when reforming liquid fractions has been solved by the development of the ICI catalyst. Continued development work on naphtha reforming has pushed naphtha reforming technology beyond methane reforming technology, and furnaces are now being designed at higher space velocities, higher pressures, high tube wall temperatures and high heat flux densities.

REFERENCES

1. "Chemistry in The Service of Man" by Alexander Findlay, Longmans, London, 1916

2. "World Fertilizer Requirements", Coleman, Chemical & Engineering News, December 2, 1963, p. 84

3. "Cartels in Action", Stocking & Watkins, The Twentieth Century Fund, 1946

4. "Steam Methane Reforming For Hydrogen Production", R. J. Kenard, Jr., World Petroleum, March & April 1962

5. "Make Hydrogen by Naphtha Reforming", J. Voogd & J. Tielrooy, Hydrocarbon Processing & Petroleum Refiner, March 1963.

TABLE I

Production of Nitrogen From Various Sources Before And After World War I

	Thousands of tons of nitrogen	
	1913	1919
Chilean Nitrate	473	487
By Product Nitrogen	313	402
Cyanamide Nitrogen	42	98
Synthetic Nitrogen	24	172
	852	1159

TABLE II

Reactions

1. $C_nH_m + nH_2O = n\,CO + \frac{2n + m}{2} H_2$

2. $CO + 3H_2 = CH_4 + H_2O$

3. $CO + H_2O = CO_2 + H_2$

4. $2CO = CO_2 + C$

TABLE III

Carbon Dioxide Produced By Reforming Reactions

Hydrogen Production - 97%	tons CO_2/ M SCF H_2
Steam Methane Reforming	14.51
Steam Naphtha Reforming	17.90
Ammonia Synthesis Gas Production	**tons CO_2/ton ammonia**
Steam Methane Reforming	1.22
Steam Naphtha Reforming	1.58

Figure I

Design of Selas Corporation of America Steam Reformer

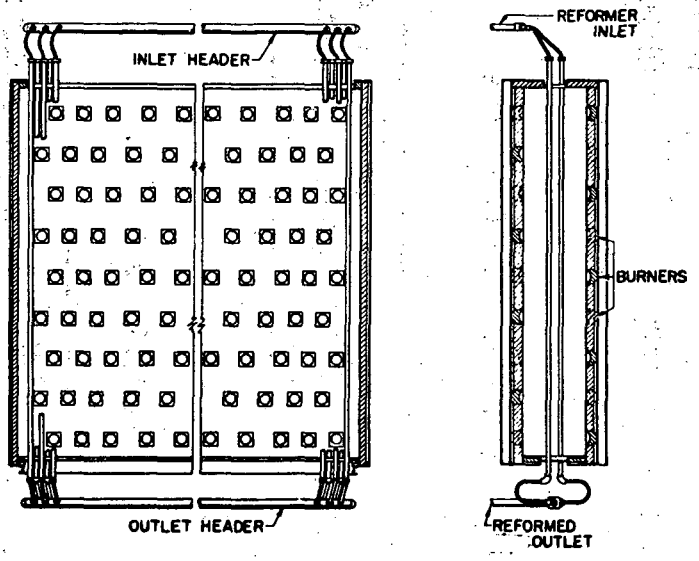

HYDROGEN PRODUCTION

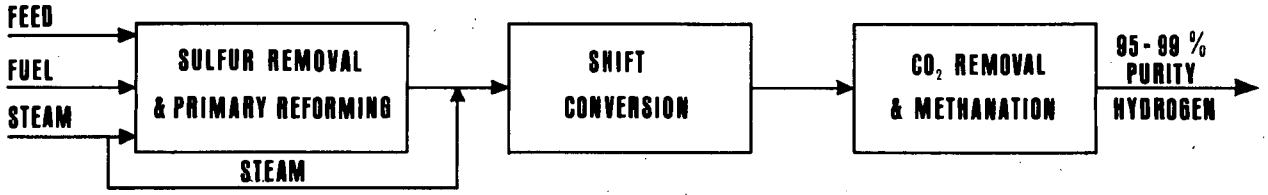

AMMONIA SYNTHESIS GAS GENERATION

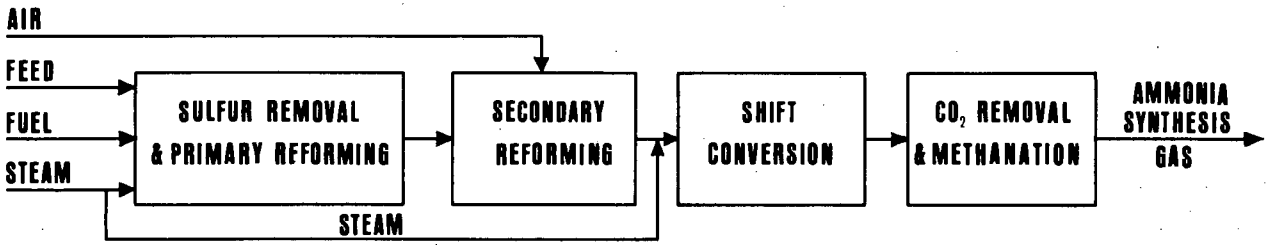

TOWNS GAS GENERATION

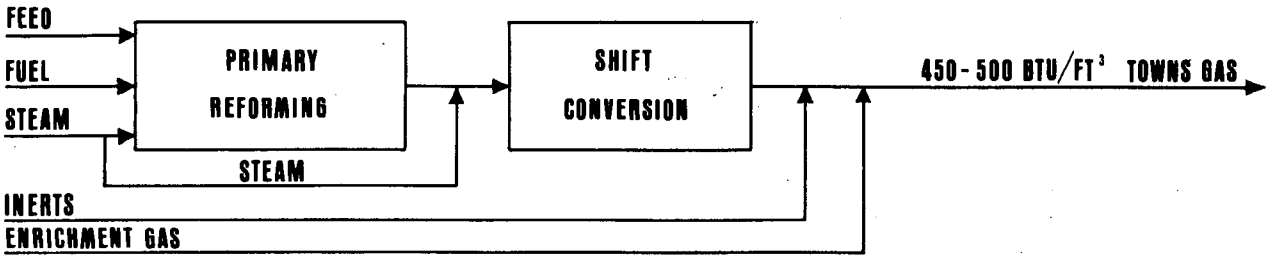

FIGURE 2

FIGURE 3

Breakeven costs of feed & fuel: naphtha reforming vs. methane reforming

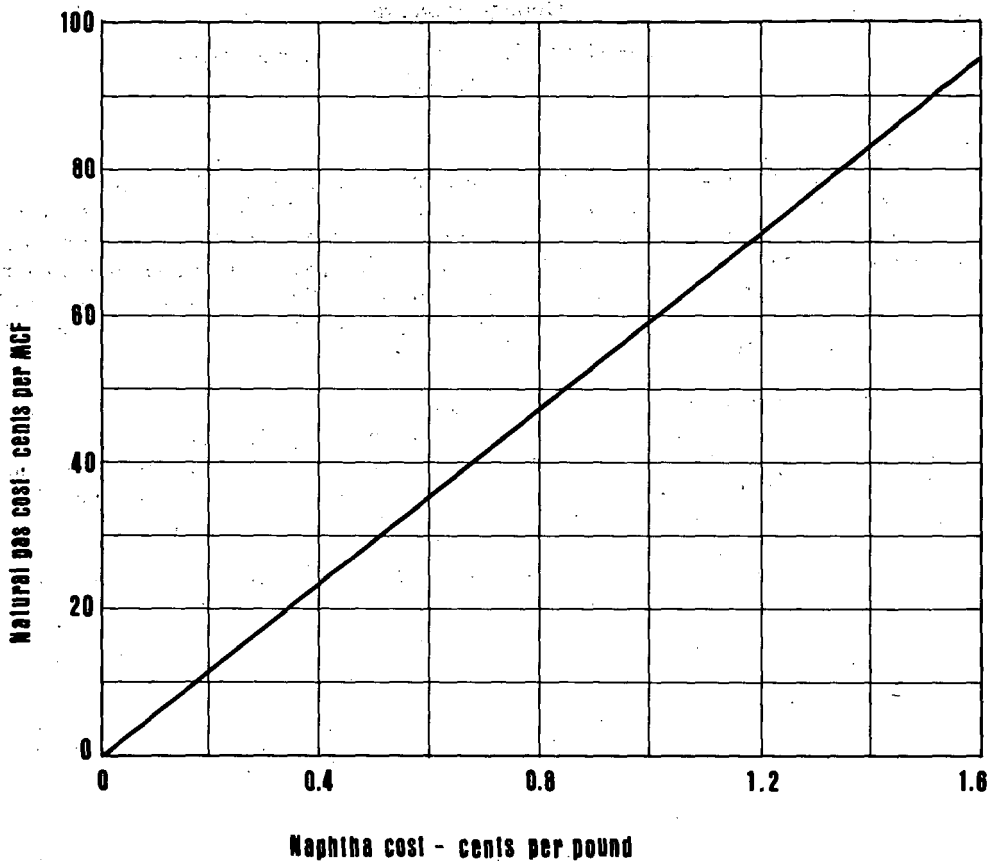

The Production of High B.t.u. Gas from Light Petroleum Distillate by Low Temperature Catalytic Steam Reforming

Robert G. Cockerham
George Percival

Gas Council, Midlands Research Station
Solihull, U.K.

Summary

This paper describes processes for the production of high calorific value gas by the steam reforming of light petroleum distillate under pressure at low temperature. The distillate is first purified and then gasified to a methane-rich gas over a catalyst at 500°-550°C. At this temperature carbon deposition is avoided and steam-distillate ratios approaching the theoretical minimum can be employed. After carbon dioxide removal, the product gas would have a calorific value of 800-850 B.t.u./cu.ft.

The methane-rich gas which is non-toxic and free of sulphur may be methanated at about 350°C. The re-establishment of equilibrium at this lower temperature produces a gas, which after the removal of carbon dioxide, contains over 95 per cent of methane. The calorific value of this gas would be 950 B.t.u/cu.ft. With butane, high calorific value gas can be produced in one stage.

Results are given for experimental work in the laboratory and on a pilot plant in which the feedstock varied from butane to distillates boiling up to 170°C.

I Introduction

Work on the catalytic gasification of light distillate began at the Midlands Research Station of the Gas Council in 1956[1]. The investigation was designed to develop a process for the manufacture of a gas with a calorific value of 500 Btu per cu.ft. for peak load use alongside coal gasification plant operating at pressure. A primary consideration was plant cost and therefore an autothermic system was chosen which required the introduction of air for internal combustion.

The early laboratory work indicated that steam economy and a high thermal efficiency would be more readily achieved if the transition from distillate to town gas were made in two principal stages. In the first, steam and distillate reacted at about 500°C over a highly active catalyst to give a gas rich in methane and, in the second, a reforming reaction reduced the methane content of the gas to the level required for town gas. The temperature of the first stage was maintained by the exothermic formation of methane whilst the combustion of air supplied to the second satisfied the thermal requirement of the reaction between the methane and steam.

It is the gasification of the distillate in the first stage which provides the substance of this paper, however, since gas of up to 650 Btu/cu.ft. calorific value can be prepared by it. Still higher calorific values can be achieved by methanating the gas obtained.

II The Catalytic Gasification of Distillate at Pressure

(a) Laboratory Experiments on Process Design

When hydrocarbons are gasified with steam in the presence of a catalyst the gas produced consists of methane, hydrogen, carbon monoxide and carbon dioxide. Provided that the catalyst is sufficiently active the following reactions are brought to equilibrium:

$$CO + 3H_2 \rightleftharpoons CH_4 + H_2O \quad .... \quad (i)$$
$$CO + H_2O \rightleftharpoons CO_2 + H_2 \quad .... \quad (ii)$$

At equilibrium, the gas composition is determined by the reaction conditions, so that for a given ratio of steam to hydrocarbon the gas becomes richer in methane as the working pressure is raised and the reaction temperature is lowered. As the system moves towards methane the steam requirement falls and the overall reaction becomes exothermic. Conditions may be chosen, therefore in which it is possible to convert a hydrocarbon feedstock to a methane rich gas continuously, the heat of reaction being sufficient to provide for heat losses from the system.

Laboratory experiments showed that a temperature within the range 400-550°C eliminated the danger of depositing carbon by the thermal decomposition of the hydrocarbon before reaction with steam. In order to establish equilibrium at these temperatures it was necessary to use a very active catalyst and to free the feedstock from sulphur compounds to avoid poisoning it. The composition of the gas produced when distillate was gasified with twice its weight of steam at 500°C. and under a pressure of 25 atmospheres is given in Table 1.

A process was envisaged, therefore, in which vaporized hydrocarbon in the form of liquified petroleum gas or light distillate was freed from sulphur compounds, mixed with steam, preheated and supplied under pressure to a suitable catalyst. The removal of sulphur from the feedstock eliminates the need for gas purification and safeguards catalysts that are used in subsequent reactions. The low temperature employed allows the steam requirement to be reduced to the minimum and increases the thermal efficiency of the process. Approximately 1.05 therms of methane-rich gas are produced per therm of light distillate supplied and, if heat recovery is practised, an overall thermal efficiency of 95% can be achieved. The flow diagram of the process shown in Fig.1. includes the purification of the feedstock, gasification and the removal of carbon dioxide. A small proportion of the scrubbed gas is recycled to provide hydrogenating gas for the purification section.

Table 1 The Composition of Gas Produced at 500°C and 25 Atmospheres

	Wet	Dry	Calculated to CO_2 = 1%
Gas Composition, per cent by volume.			
CO_2	10.4	20.6	1.0
CO	0.35	0.7	0.85
H_2	8.45	16.8	20.95
CH_4	31.2	61.9	77.2
H_2O	49.6	-	-
Calorific Value, Btu. per cu.ft.		671	836
Equivalent Temperatures for the equilibria, °C.			
$CO + 3H_2 \rightleftharpoons CH_4 + H_2O$	496		
$CO + H_2O \rightleftharpoons CO_2 + H_2$	500		

(b) The Purification of the Feedstock

The amount of sulphur in light distillates available in the U.K. is within the range 100-500 p.p.m. by weight. In low boiling fractions mercaptans and disulphides are present, but in the higher boiling materials heterocyclic sulphur compounds may be found.

Early experiments showed that the removal of sulphur compounds from distillate in the liquid phase was unlikely to be successful and that a chemical method, applicable to all types of sulphur compound was essential to achieve a satisfactory degree of purity.

Absorption of sulphur from distillate in the vapour phase, at pressure, was therefore attempted, using alkaline iron oxide in the manner in which it has been used for synthesis gas. This reagent operates by a mechanism which involves conversion of sulphur compounds to hydrogen sulphide, and the presence of a trace of oxygen in the gas facilitates absorption as sulphur oxides in the alkali. Oxygen could not be used with distillate with which it reacts preferentially although, when hydrogen was added to the distillate vapour, iron oxide had an adequate capacity to absorb the sulphur as hydrogen sulphide without oxidation. It was found that the sulphur compounds could be more effectively hydrogenated by treatment separately over a molybdenum based catalyst at 350 - 400°C. The process thus developed as the vaporization of the distillate, admixture of hydrogenating gas, the conversion of sulphur compounds over a molybdenum catalyst and the absorption of the hydrogen sulphide formed in iron oxide.

Commercial molybdenum catalysts supported on alumina were found to be suitable for the conversion step, when about half a cubic foot of hydrogen was

used per pound of distillate. Luxmasse, widely used for synthesis gas purification was retained as it is a powerful absorber of hydrogen sulphide at elevated temperature; it is porous and there is rapid diffusion into the interior of granules. Prepared forms are of necessity of lower porosity, but this is of little account since absorber vessels are designed for relatively long periods of operation. The crude material contains approximately 6% of alkali and approximately 50% by weight of iron oxide as ferric oxide. There is evidence however that under working conditions conversion to hydrated magnetic oxide of iron occurs and sulphur absorption proceeds according to the equation:-

$$Fe_3O_4 + 3\,H_2S + H_2 \rightarrow 3\,FeS + 4\,H_2O$$

After treatment, the amount of sulphur in distillate was very small, in all cases less than one part per million, and a special analytical technique was required to measure it accurately. A combustion procedure described by Wickbold[2] proved satisfactory, the sulphur being finally estimated by nephelometric titration with 0.0025M. barium chloride.

The amount of hydrogen added is many times the quantity theoretically required for reaction with the sulphur compounds in order to displace the equilibrium towards hydrogen sulphide. In some cases even more would be required, because it was found that if olefins were present in the distillate they were hydrogenated, although aromatics in the distillate were unchanged after processing. The quantity of olefins in the distillates available was insufficient to show this directly, but distillates from olefinic crudes were simulated by the addition of n-hexene and n-heptene, and styrene was employed to represent the effect of blending in fractions from cracked stocks.

The process described has been applied to a number of distillates ranging from butane, containing 0.6 per cent of butenes and 8 parts per million of sulphur, up to kerosene, containing 3 per cent of olefins and 1000 parts per million of sulphur. With the higher gravity distillates, it was necessary to increase the hydrogen supply and temperature.

In reforming processes, make gas is usually used as the hydrogenating gas for purification and this practice can be followed when making rich gas, if the volume recycled is increased to compensate for its low concentration of hydrogen. Carbon dioxide should be removed to below 5 per cent since it interferes with the purification.

(c) Further Laboratory Experiments on the Gasification Reaction

After purification, the gasification process outlined operated satisfactorily in the laboratory with butane and low- boiling types of distillate using in the gasification stage a co-precipitated nickel-alumina catalyst formulated for methane synthesis.[3] Further development of the catalyst has since been necessary, however, since with distillates of higher specific gravity and boiling point, it was found that there was a tendency for the catalyst to lose activity. The reaction zone would increase in length during an experiment until it extended to the full depth of the catalyst bed and

undecomposed distillate would then appear in the product gas.

Considerable evidence has now been collected which indicates that the deactivation with higher boiling distillates is due to the formation of a polymer which reduces the accessibility of the reacting molecules to the surface of the catalyst. The work of Kemball[4] throws light on a possible mechanism involving the production of radicals on the catalyst surface which may either react with steam or link together to form polymer. There is a difference between this polymerisation and the deposition of carbon, however. The latter depends upon the complete breakdown of distillate molecules to carbon atoms which appear to enter the catalyst structure and crystallize from there leaving the surface active. This process can continue until there is a blockage, whereas no increase in back pressure is observed during the deactivation of catalyst by polymer.

The regeneration of deactivated catalysts has been only partly successful. Oxidation processes which will remove the polymer also damage the catalyst and the original level of activity cannot be restored. Treatment with hydrogen at the working temperature will re-activate a recently poisoned surface. The object of the experimental work, however, has been to minimise polymer formation and the stage has now been reached where the loss of catalyst activity has been reduced to negligible proportions with the distillates available.

This has been achieved by modifying the catalyst composition, using an optimum preheat temperature for the distillate and paying attention to the rates of supply of feedstock and steam to the catalyst bed. Distillate having a boiling point of 170°C. can be gasified satisfactorily and it is estimated that the life of the catalyst in a commercial plant will be at least one year and possibly up to five years.

Experiments are continuing with feedstocks of higher boiling point and in the laboratory it has been found possible to gasify kerosene.

(d) The Steam Requirement

Since the amount of steam used in all reforming processes is an item which affects both the thermal efficiency and the operating costs, it has been the practice during the present investigations to keep the amount near the theoretical minimum. The minimum is governed by the fact that catalysts not only establish the methane-steam and water gas equilibria but also promote the Boudouard reaction:

$$2\ CO \rightleftharpoons CO_2 + C$$

Carbon will tend to be deposited by this reaction if the concentration of carbon monoxide in the gases exceeds the value corresponding to the equilibrium. Control can be exercised by allowing an excess of steam to limit the carbon monoxide/dioxide ratio according to the water gas reaction. The minimum amount of process steam required to prevent carbon deposition by this reaction can therefore be calculated from the equilibrium constants.

Fig. 2 shows the curves for the minimum steam requirement for hexane when reformed at various pressures. Although the curves pass through a maximum and then fall again at the highest temperatures, the latter values are not attainable

in practice since the system would inevitably have been taken through the lower temperatures. The curves indicate that at a temperature of 530°C for example, and under a pressure of 20 atmospheres the minimum steam-hexane ratio is 1.0 parts by weight. These are similar to the conditions which are employed in the gasification stage of the process but allowance must be made for the composition of distillate feedstocks and a margin provided against accidental fluctuations. A steam-distillate ratio of 1.2 has been satisfactory in the laboratory but, for the commercial production of rich gas under pressure, a ratio of 1.5 would be regarded as the minimum for distillates boiling up to 170°C. It will be noted that steam ratios of 1.6 and 2.0 have been used on the pilot plant but this is because in the U.K. the rich gas has subsequently to be reformed at a higher temperature in order to reduce its calorific value to 500 Btu/cu.ft. The effect of varying the proportion of steam supplied on the composition of the gas produced is given in Table 2.

TABLE 2

The Effect of Varying the Proportion of Steam on the Composition of the Gas Produced at 540°C and 25 atmospheres

Steam supplied, lbs/lb distillate	1.2	1.6	2.0
Gas Composition, dry, per cent by volume			
CO_2	22.55	22.85	22.95
CO	2.0	1.75	1.55
H_2	12.5	16.15	19.25
CH_4	62.95	59.25	56.25
Gas Composition, dry, calculated to 1.0% carbon dioxide, per cent by volume.			
CO_2	1.0	1.0	1.0
CO	2.55	2.25	2.0
H_2	16.0	20.7	24.75
CH_4	80.45	76.05	72.25
Calorific Value, Btu/cu.ft.	859	829	803

(e) Pilot Plant

The pilot plant in operation at Solihull is shown in Fig. 3. It has an output of 1/5 million cu.ft. of town gas per day. From the left, the three short vessels constitute the distillate purification section followed by the catalytic gasifier, second reforming stage for town gas, carbon monoxide converter and final cooler, in that order. No provision was made for removing carbon dioxide from the gas since this was regarded as an established operation and gas compositions can be readily adjusted.

The pilot plant was designed to have catalyst beds of a similar depth

to those of a commercial plant and, therefore, at a given space velocity, the linear velocity of the reactants through the beds is full scale. Scaling up then involves an increase in reactor diameter only and it is believed that large units can be designed from test results with confidence. For this reason the pilot reactors are long, of small diameter and liable to heat loss from the walls. This was prevented by the use of electrically heated lagging. No heat exchangers were used on the pilot plant, the preheating of the distillate vapour prior to purification and of the process steam being carried out in gas fired equipment.

The control of the plant during tests involved maintaining constant preheat temperatures to both the purification and the gasification sections and adjusting the steam supply to give the appropriate ratio. The preheat temperature to the gasification catalyst was 440°C when butane was used and varied from 460° to 535°C in the case of distillate feedstocks. The tests have normally lasted at least a month in order to obtain an indication of the life of the gasification catalyst. Observations of the movement of the reaction zone are made with a system of thermocouples.

Table 3 gives a selection of results covering different feedstocks, steam ratios and pressures.

TABLE 3

The Results of Pilot Plant Tests

Test No.	1		2		3	
Type of Distillate, F.B.P., °C.	170		115		Butane	
Pressure, atmospheres	20		20		25	
Process Steam, lb. per lb of feedstock	1.6		1.6		2.0	
Temperatures, °C Inlet catalyst	515		515		440	
Outlet catalyst	553		550		487	
Gas Composition, per cent by volume	Wet	Dry	Wet	Dry	Wet	Dry
CO_2	14.4	21.9	13.0	20.5	9.2	18.5
CO	1.0	1.5	1.0	1.55	0.3	0.6
H_2	12.6	19.15	12.0	18.95	7.5	15.1
CH_4	37.8	57.45	37.4	59.0	32.7	65.8
H_2O	34.2	-	36.6	-	50.3	-
Calorific Value, Btu. per cu.ft.	637		652		704	
Gas Composition, dry, calculated to 1.0% carbon dioxide, per cent by volume						
CO_2	1.0		1.0		1.0	
CO	1.9		1.95		0.7	
H_2	24.25		23.6		18.35	
CH_4	72.85		73.45		79.95	
Calorific Value, Btu per cu.ft.	807		811		855	
Specific Gravity (Air = 1.0)	0.454		0.457		0.462	
Gas Yield (CO_2=1%)s.cu.ft. per lb feedstock	26.6		26.7		25.7	
$\frac{\text{Therms in gas}}{\text{Therms in feedstock}}$	1.06		1.06		1.0	

The effect of changing the feedstock can be seen by comparing Tests 1 and 2 in which distillates boiling up to 170°C and 115°C respectively were used under identical conditions of pressure, preheat temperature and steam ratio. The concentration of carbon dioxide is lower in the gas produced from the lighter distillate whilst the methane content of the scrubbed gas is higher at 59.0 per cent. Test 3 was carried out using butane at 25 atmospheres pressure and with a steam ratio of 2.0. The low preheat temperature of 440°C gives rise to a high concentration of methane in the product gas.

Calculated gas compositions are given in which carbon dioxide has been removed to one per cent. It will be seen that the calorific values of the resultant gases would lie in the range 807 to 855 Btu per cubic foot.

A commercial plant is being built for the production of 25,000 therms per day of methane-rich gas at 17 atm. pressure from a distillate feedstock.

(f) The Production of Gas Interchangeable with Natural Gas

Although the process so far described is capable of producing a gas having a calorific value of up to 850 Btu per cu.ft., the presence of hydrogen raises the flame speed above the level of certain natural gases. In order to be interchangeable with natural gas, therefore, the equilibrium needs to be established at as low a temperature as possible. When liquefied petroleum gases are used as the feedstock the reaction with steam may be carried out at a temperature between 300°C and 400°C. Gas of the following composition was produced when butane was gasified at 25 atmospheres pressure using a steam-butane ratio of 1.3 by weight :-

CO_2 17.75, CO 0.05, H_2 1.8, CH_4 80.45 per cent by volume.

After the removal of carbon dioxide this gas would contain 96.55 per cent of methane and have a calorific value of 970 Btu/cu.ft. With high boiling distillate, however, the temperature of the gasification stage cannot be reduced to this low level without causing deterioration of the catalyst, but a subsequent methanation stage can be used.

The pilot plant was equipped with an auxiliary methanation tube through which gas from the gasification catalyst was passed at 360°C and 25 atmospheres pressure. If carbon dioxide had been removed, the dry gas produced would have had the following composition, per cent by volume :-

CO_2 1.0, CO 0.3, H_2 0.7, CH_4 98.0, Calorific Value = 977 Btu per cu.ft.

When two stages are used it is convenient to condense some of the undecomposed steam as an intermediate step in order to raise the concentration of carbon oxides in the reaction zone. The scale of the experiment was not large enough for the problem of heat removal from the catalyst bed during methanation to be encountered. There are a number of ways in which this may be done, but a discussion of these techniques is outside the scope of this paper. When operating at 25 atm. pressure, 1 therm of methane can be produced from 0.98 therms of distillate at a thermal efficiency of 95%.

Acknowledgments

This paper is published by permission of The Gas Council, and the work described in it was carried out under the direction of Dr. F.J. Dent. The Authors thank their colleagues who were responsible for the experimental work.

Literature References

1. Cockerham, R.G. and Percival, G. "Experiments on the Production of Peak Load Gas from Methanol and Light Distillate". Gas Council Research Communication G.C.41, 1957, 36 pp; Trans. Inst. Gas Engrs., 107 pp. 390-424, 1957-58.

2. Wickbold, R "Bestimmung von Schwefel-und-Chlor-Spuren in organischen Substanzen" Angew. Chem., 69, pp. 530-533, 1957.

3. Dent, F.J., Moignard, L.A., Eastwood, A.H. Blackburn, W.H. and Hebden, D. "An Investigation into the Catalytic Synthesis of Methane for Town Gas Manufacture" 49th Report, Joint Research Committee, Gas Research Board and the University of Leeds; Trans. Inst. Gas Engrs., 95, pp. 602-704, 1945-6.

4. (i) Kemball, C. and Rooney, J.J. "The Cracking of cyclopentene on a Silica-Alumina Catalyst". Proc. Roy.Soc., A 257, pp. 132-145, 1960; (ii) Kemball, C and Rooney, J.J. "The Cracking of cyclopentane and n-pentane on a Silica-Alumina Catalyst". Proc. Roy.Soc., A.263, pp. 567-577, 1961.

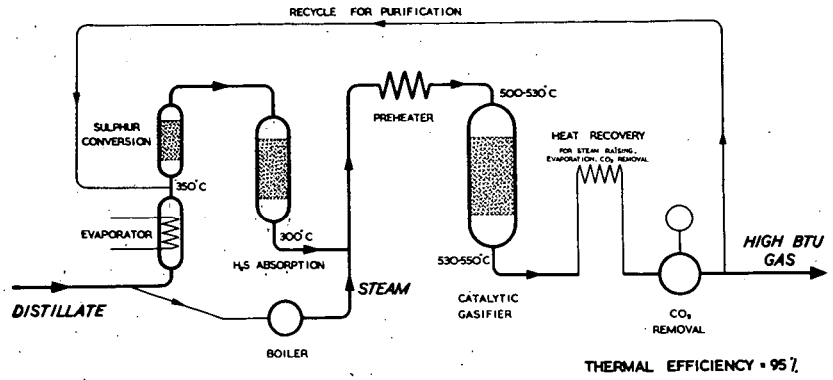

Fig.1. Flow Diagram of the Gasification Process

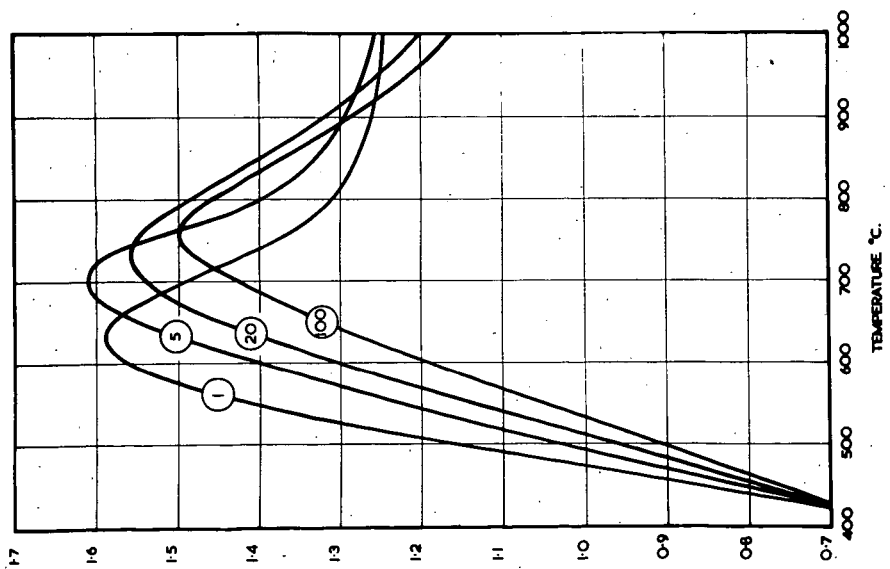

Fig.2. Minimum Steam Requirement for the Gasification of Hexane at Various Temperatures (Pressures in atmospheres are shown on the curves)

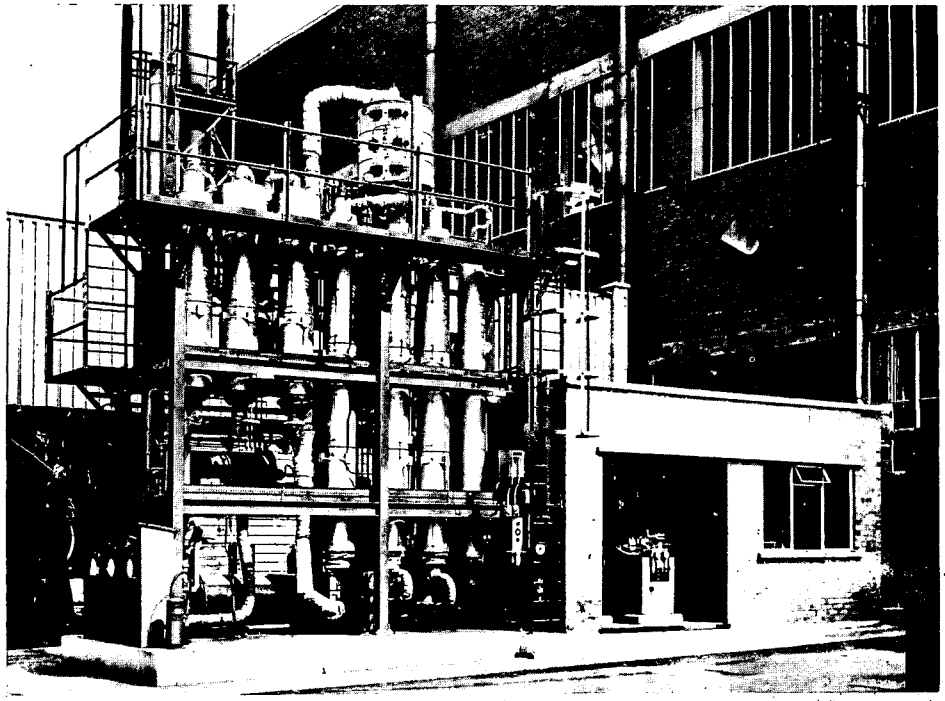

Fig. 3. The Pilot Plant for the Gasification Process

The Production of High B.t.u. Gas From Light Distillate By Continuous Pressure Hydrogenation

Binay B. Majumdar and Brian H. Thompson

Gas Council, Midlands Research Station
Solihull, U.K.

Summary

This paper describes the use of light petroleum distillates for the production of gas of high calorific value. In the process the distillate is converted to methane and ethane by reaction with gas rich in hydrogen. An aromatic condensate is obtained as a by-product.

Two methods of carrying out the operation have been used. In the first, a hydrogenator of simple design incorporates temperature control by recycling the reacting gases. The second uses a fluidised bed of coke for the same purpose and can be operated to give an increased yield of liquid products.

I. Introduction

The hydrogenation of oils was developed initially[1] for the enrichment of lean gas produced by the total gasification of coal with steam and oxygen, for example, by the Lurgi Process. In recent years hydrocarbon reformers operating at high pressures have been developed which are capable of gasifying distillate to produce a comparatively lean gas. It is in association with such plants that hydrogenation units are being extensively introduced. The hydrogenation stage is capable of producing gases of high calorific value which can be used as a satisfactory substitute for natural gas.

II. The Hydrogenation Process

When a mixture of distillate vapour and lean gas are exposed to a temperature of 700 - 750°C the hydrogen in the lean gas reacts with the distillate to produce gaseous hydrocarbons, mainly methane and ethane. Little change in gas volume occurs.

$$(- CH_2) + H_2 \longrightarrow CH_4$$

1 vol. 1 vol.

$$2(- CH_2) + H_2 \longrightarrow C_2H_6$$

1 vol. 1 vol.

The methane and ethane arise from the breakdown of the aliphatic constituents of the distillate which usually form the bulk of the feedstock. Further quantities arise from the hydrogenation of the side-chains from aromatic constituents in the distillate. Under the operating conditions normally used the aromatic nuclei themselves survive to give a condensate, free of paraffins, from which high purity benzene can readily be obtained.

The reaction is exothermic and being non-catalytic the distillate need not necessarily be purified before hydrogenation. The degree of preheat required for the reactants can be obtained by heat exchange with the products.

It is necessary to be able to control reaction conditions in order that the exothermicity of the reaction does not lead to hot zones where excessive temperatures cause carbon deposition. Process design has been directed so that this problem does not arise. Initially a fluidized bed was used to maintain uniform temperatures within a reactor but recently the process has been simplified. Rapid recirculation of the reacting gases within the hydrogenator is now used to maintain strict temperature control.

III. The Gas Recycle Hydrogenator

The Hydrogenator is shown diagramatically in Fig. 1[2]. It consists of a cylindrical vessel with a coaxial tube inside it enclosed within a pressure vessel of sufficient diameter to allow 9" of heat insulation. The mixture of distillate and hydrogen are introduced through a jet at high velocity and directed down the inner tube. The momentum of the jet causes the gaseous reactants to circulate down the tube and up the annulus. The recirculation results in the mixing of the inlet reactants with a relatively large volume of hot gases already at reaction temperature. In the pilot plant, a recirculation ratio, i.e. the number of volumes of recirculating gas per volume of reactants, of 10 : 1 or more has been readily achieved.

The recirculation of gases gives precise control of reaction temperature and the temperature distribution within the reactor is remarkably even. Except in the vicinity of the inlet jet the temperature variation in the reactor is within 3 - 4°C. It is merely necessary to control the preheat temperature to maintain the required temperature. When making gases of high calorific value the preheat temperature required is usually within the range 400 - 450°C whilst maintaining a reaction temperature of 700 - 750°C.

The distillate is converted to hydrocarbon gases, mainly ethane and methane with small quantities of olefines. The proportion of ethane increases as the reaction temperature is lowered. The output of a reactor of a given size varies directly as the pressure. At a given pressure, however, a plant is extremely flexible and output can be controlled over wide limits.

In trouble free operation over long periods carbon deposition must be avoided. This governs the choice of operating conditions especially if the operating pressure is comparatively low. Operation at 350 p.s.i.g. enables a calorific value of 800 Btus/s.c.f. to be readily attained with an operating temperature of 750°C. At lower pressures or when attaining higher calorific values it is necessary to lower the temperature. Below about 675°C however the reaction is slow and operation becomes unstable, 700°C is, therefore, considered to be a safe minimum operating temperature. The presence of 5 - 10% of steam in the hydrogenating gas is usually

sufficient to overcome any remaining tendency for carbon deposition. If a hot potassium carbonate scrubber is used to remove carbon dioxide from the lean gas, there is sufficient steam left in the gases for this purpose.

Fig. 2 shows the flow diagram of the pilot plant. The hydrogen was made by the steam reforming of commercial butane followed by carbon monoxide conversion, carbon dioxide removal and compression, approximately 0.9 million s.c.f./ day of gas containing about 93% hydrogen being available. The distillate, which was not purified, was pumped into the hydrogenating gas stream and the mixture preheated so as to maintain the required temperature in the hydrogenator using gas-fired preheaters which would be replaced on a commercial unit by heat exchangers between product gases and reactants. The product gases removed from inside the top of the reactor were water quenched followed by indirect cooling. Samples for analysis were taken from the hot gases before the quench.

The plant was started up using hydrogenating gas, preheated to about 650°C, to raise the temperature in the hydrogenator to 575 - 600°C. Distillate was then introduced into the hydrogenating gas stream at a low rate and as the heat of reaction raised the hydrogenator temperature the distillate rate was increased and the preheat temperature reduced until over a period of about ½ hour the final reaction conditions were attained.

IV. Tests in the Gas Recycle Hydrogenator

The results of some three days tests are given in Table 1.

Test 1 represents a run at 350 p.s.i.g. using an hydrogenating gas containing 92.4% hydrogen, obtained by reforming commercial butane followed by carbon monoxide conversion and carbon dioxide removal. A calorific value of 804 Btus/s.c.f. was obtained without difficulty using a comparatively high specific gravity distillate with a final boiling point of approx. 170°C. Analysis of the feedstock gave an aromatic content of 8.1% by volume and on hydrogenation 11.1% of the carbon in the oil appeared as condensate and 88.9% as hydrocarbon gas. There was no trace of unreacted paraffins in the condensate. The gas contained a considerable concentration of ethane, but no trace of higher paraffinic hydrocarbons showing the relatively slow rate of ethane decomposition compared with higher hydrocarbons under these conditions. A small amount of unsaturated hydrocarbons also survived.

A preliminary test showed that at a pressure of 450 p.s.i.g. and a reaction temperature of 725°C a calorific value of 960 Btus/ scf. using a similar distillate and a dry hydrogenating gas could not be obtained without an appreciable amount of carbon deposition. Tests 2 and 3 were therefore carried out to make calorific values of 900 Btus/s.c.f. and 1,000 Btus/s.c.f. respectively using an hydrogenating gas to which 9 - 10% steam was added, carbon deposition troubles being then eliminated.

As the calorific value of the gas was increased from 900 - 1,000 Btus/ s.c.f. the yield of aromatic condensate increased so that in the latter case 15.1% of the carbon in the oil appeared as condensate and only 84.9% as hydrocarbon gas. With the reduced operating temperature and the low partial pressure of hydrogen in the final gas traces of paraffins appeared in the condensate.

Table 1 - Tests in the Gas Recycle Hydrogenator.

Test No.	1	2	3	4	5
Hydrogenation Pressure, p.s.i.g.	350	450	450	180	180
Inlet Gas Rate, s.c.f.h.	30,790	18,230	18,400	13,855	14,090
Dry Inlet Gas Composition, % by volume:					
CO_2	0.3	1.0	0.8	12.7	12.8
CO	3.7	3.7	3.7	2.5	2.4
H_2	92.4	93.6	92.4	83.3	83.9
CH_4	3.0	1.2	2.4	0.6	0.1
N_2	0.6	0.5	0.7	0.9	0.8
	100.0	100.0	100.0	100.0	100.0
Steam content of hydrogenating gas vols/100 vols dry inlet gas	Nil	10.2	9.2	7.3	7.2
Distillate Type:	170	170	170	170	115
Specific Gravity	0.71	0.71	0.72	0.71	0.66
Aromatic Hydrocarbon, % by volume	8.1	7.2	6.5	7.4	1.6
Carbon/Hydrogen, w/w	5.7	5.7	5.8	5.7	5.4
Imp. Gals. of distillate per 1000 cu.ft. of dry inlet gas	4.27	5.39	6.87	3.98	3.99
Preheat temperature, °C	441	403	425	503	530
Hydrogenation temperature, °C	750	715	715	715	715
Product Gas Rate, s.c.f.h.	33,600	20,480	21,400	15,330	15,575
Product Gas Composition, % by volume:					
CO_2	0.4	0.7	0.7	11.35	10.9
C_xH_y	1.1	1.1	2.4	1.4	2.1
CO	3.3	3.8	3.3	2.9	2.8
H_2	44.6	34.8	23.8	43.1	44.6
CH_4	32.6	36.8	43.95	23.35	21.3
C_2H_6	17.5	22.1	25.15	16.8	17.5
N_2	0.5	0.7	0.7	1.1	0.8
	100.0	100.0	100.0	100.0	100.0
Calorific Value, Btu/s.c.f.	804	896	1008	704	713
Calorific Value, Btu/s.c.f. (inert free)	810	909	1022	804	808
Carbon Balance					
Percentage of carbon supplied in distillate appearing as:					
Hydrocarbon Gas	88.9	88.8	84.9	87.3	96.0
Benzene	8.8	7.9	7.9	7.8	3.2
Toluene	1.1	1.5	2.7	2.3	0.3
Xylene and Higher Monocyclics	0.6	0.7	1.7	1.5	0.2
Naphthalene	0.3	0.6	1.2	0.5	0.1
Higher Aromatics	0.3	0.4	1.5	0.4	0.0
Unreacted Paraffins	0.0	0.1	0.1	0.2	0.2
Carbon Deposited	0.0	0.0	0.0	0.0	0.0
Gases Produced and absorbed s.c.f./imp. gallon of distillate:					
CH_4 produced	76.4	74.4	71.0	63.4	58.7
C_2H_6 "	44.8	46.0	42.6	46.7	48.5
C_xH_y "	2.8	2.3	4.1	3.9	5.8
H_2 absorbed	102.5	100.9	94.2	89.5	86.8

The use of steam to avoid carbon deposition difficulties enabled the use of lower operating pressures and Tests 4 and 5 were comparative tests at 180 p.s.i.g. Gas with an inert free calorific value of 800 Btus/s.c.f. was made using an initial gas containing about 13% of carbon dioxide. The hydrogen partial pressure was only 135 p.s.i.g. Two types of distillate were used, one the comparatively high gravity distillate used for the previous tests and the other of lesser gravity with a final boiling point of about 108°C containing only 1.6% aromatics. The main feature of the results is the increased yield of hydrocarbon gases with the lighter feedstock, 96% of the carbon in the distillate being converted to gas. A second feature is that taking the increase in volume into account the product gas contains almost as much carbon dioxide as present in the inlet gas. There is no marked tendency for the carbon dioxide to react with hydrogen to give carbon monoxide.

A typical potential heat balance when making a gas of 900 Btus/s.c.f. from 170 distillate is given in Table 2. The efficiency of the process is seen to be high with 88.4% of the potential heat in the distillate appearing in the gas and 9.2% in the condensate, the combined yield being 97.6%.

TABLE 2

Typical Potential Heat Balance when making 900 C.V. gas in Gas Recycle Hydrogenator

Type of Distillate	L.D.F. 170
Potential Heat in Products as percentage of Potential Heat in Distillate:	
Hydrocarbon Gas	88.4
Benzene	6.5
Toluene	1.3
Xylene and other Monocyclics	.6
Naphthalene	.4
Higher Aromatics	.3
Unreacted Paraffins	.1
Heat of reaction by difference	2.4
	100.0

V. The Fluidized Bed Pilot Plant

The use of a gas recycle simplified the design of a hydrogenator for use with distillate under conditions when carbon deposition is avoided. The fluidized hydrogenator developed for crude and heavy oil, is an alternative and can be used when carbon is deposited. In this process a fluidized bed of coke serves to take up any carbon and also serves to establish the uniform temperature requirement. The large heat capacity of the fluidized bed compared with that of the inlet reactants serves to bring them rapidly to reaction temperature and by absorbing reaction heat prevents excessive temperatures in the bed.

The hydrogenator design is shown in Fig. 3. The reaction vessel consists of a thin walled cylinder 22¾" dia. and 16 ft. deep terminating at the lower end in an inverted cone. It contained a fluidized bed of coke particles (size range 0.017" - 0.002") and to prevent agglomeration when using heavy feedstocks the bed could be recirculated through a lower fluidized bed via a downcomer and riser about 15 ft. long. The main stream of hydrogenating gas was introduced just below the bottom of the riser. Subsidiary streams of hydrogenating gas were used to maintain fluidization in the lower bed and at the bottom of the downcomer. When using distillate the solid recycle system was not necessary but was retained as part of the development programme of the reactor for use with heavier feedstocks. The latter were introduced through an atomiser located below the riser and coaxial with it. When using distillate it was merely evaporated into the main hydrogenating gas stream fed in below the riser.

Simplification of the plant for use solely with distillate would leave a single fluidized bed with only the one inlet gas stream containing the preheated mixture of distillate and hydrogenating gas. A system of horizontal and vertical baffles was included in the main fluidized bed to improve the fluidization characteristics. The whole internal assembly of the pilot plant was surrounded by 10 ins. of heat insulation and enclosed in a mild steel pressure vessel.

The flow diagram for the plant is shown in Fig. 4. The hydrogenating gas was produced as for the Gas Recycle Plant by reforming of butane followed by carbon monoxide conversion and carbon dioxide removal. It was then preheated in gas fired preheaters but on a commercial unit heat exchange with the product gases would be utilised. The reaction products were water quenched to about 200°C and then cooled further by direct scrubbing with recycled condensate in a tower packed with raschig rings. Final cooling to 30°C was by an indirect cooler. Gas samples for analysis were taken before the water quench.

The plant was started up with the full flow of preheated hydrogenating gas but at a reduced pressure to give the required fluidizing velocity in the reactor. The coke was then carried in with a subsidiary stream of gas and the plant warmed up further with gas preheated to 650°C. When the reactor temperature reached 350°C air was admitted to accelerate the heating. At 650°C distillate was introduced at a low rate and as the heat of reaction raised temperatures the air rate was reduced to zero followed by a reduction of the preheat temperature of the reactants. As temperatures rose the pressure was increased to maintain the desired fluidizing velocity.

VI. Tests in the Fluidized Hydrogenator

The results of tests carried out in the pilot plant are given in Table 3.

Test 1 gives the results of a run of 14 days duration operating at 25 atmospheres pressure and 750°C. The gas produced had a calorific value of 850 Btus/s.c.f. Operation of the plant was extremely steady and there was no measurable carbon deposition. The elutriation of coke from the bed amounted to less than 65 lbs./day. A comparatively low gravity distillate with a final boiling point of 130° was used.

Table 3 - Tests in the Fluidised Hydrogenator

Test No.	1	2	3
Hydrogenation Pressure, p.s.i.g.	350	350	720
Inlet Gas Rate, s.c.f.h.	33,240	32,369	32,052
Inlet Gas Composition, % by volume:			
CO_2	1.2	1.3	1.85
CO	2.6	2.3	3.6
H_2	93.5	92.0	91.3
CH_4	2.1	3.9	2.75
N_2	0.6	0.5	0.5
	100.0	100.0	100.0
Distillate Type:			
Specific Gravity	0.67	0.70	0.71
Aromatic Hydrocarbon Content, % by volume	3.6	6.3	7.44
Carbon/Hydrogen ratio, w/w	5.3	5.7	5.6
Imp. Gals. Distillate per 1000 cu.ft. of dry inlet gas	4.88	4.95	7.82
Time of residence, secs.	28	29	66
Preheat temperature, °C	455	454	379
Hydrogenation temperature, °C	755	755	722
Product Gas Rate, s.c.f.h.	37,767	36,343	40,348
Product Gas Composition, % by volume:			
CO_2	0.85	1.0	1.35
C_xH_y	1.00	1.3	1.05
CO	2.55	2.45	3.15
H_2	37.9	33.7	16.75
CH_4	39.1	45.3	54.05
C_2H_6	17.4	15.4	23.05
N_2	1.2	0.85	0.6
	100.0	100.0	100.0
Calorific Value Btus/s.c.f.	840	859	1024
Carbon Balance			
Percentage of carbon supplied in distillate appearing as:			
Hydrocarbon Gas	94.8	89.4	82.8
Benzene	4.5	8.7	11.2
Toluene	0.1	0.3	1.7
Xylene and higher monocyclics	0.1	0.2	0.6
Naphthalene	0.3	1.0	1.4
Higher Aromatics	0.2	0.4	1.7
Unreacted Paraffins	-	-	-
Carbon Deposited	-	-	0.6
Gases Produced and absorbed as ft.^{3}/ imp. gallon of distillate:			
CH_4 produced	86.8	94.3	83.5
C_2H_6 "	40.5	34.7	37.1
C_xH_y "			
H_2 absorbed	103.4	108.8	89.8

Test 2 was of similar duration and reaction conditions but a higher gravity distillate (S.G. 0.70 and final boiling point 165°C was used.) The performance of the plant was equally satisfactory the most significant difference being the increased condensate yield with the heavier feedstock. In test 1 94.8% of the carbon in the oil appeared in the gas and only 89.4% in test 2.

In comparison with the tests in the gas recycle hydrogenator using the heavier type of distillate the yield of naphthalene and higher aromatics is higher, possibly due to a more sudden heating on entry to the fluidised bed and the absence of dispersion of the reacting distillate in a large volume of reacted gas.

Test 3 shows the results of a run at 50 atmospheres pressure to produce a gas of 1,000 Btus/s.c.f., a calorific value which was reached without difficulty. With an operating temperature of 722°C 0.6% of the carbon in the oil was deposited on the particles in the fluidized bed. In comparison with tests 1 and 2 the effect of increased residence time due to the higher pressure was to reduce the ethane/methane ratio in the gas produced, despite the counteracting effect of a reduced operating temperature. The yield of condensible aromatic hydrocarbons was increased and only 82.8% of the carbon in the oil appeared in the gas.

VII. The Hydrogenation of Light Distillate with the production of Aromatic Hydrocarbons

In the tests described so far the aromatic condensate is mainly derived from that already in the distillate. The ring structure of these aromatics remains intact under the reaction conditions although the side-chains are removed increasing the yield of gaseous hydrocarbons.

However, it is evident that as the distillate/hydrogen ratio is increased in order to obtain a higher calorific value of product gas the yield of condensible aromatic hydrocarbons is increased. The synthesis of aromatics is believed to be due to the fact that, when present in greater concentration, radicals have an opportunity to cyclise before they are hydrogenated. It was considered, therefore, that if the distillate/hydrogen ratio were increased to an even larger extent the production of aromatic hydrocarbons could be very greatly increased, whilst still producing a very high calorific value of gas.

Laboratory experiments[3] showed that at an operating temperature of 750 - 775°C and with a distillate/hydrogen ratio of about 20 - 25 imp. gallons/1000 cu.ft. 20% or more of the carbon in the oil could be recovered as aromatic hydrocarbons even when there was virtually no aromatic content in the distillate. Pressure was found to have little effect on the reaction. With the limited partial pressure of hydrogen the condensate contained an appreciable proportion of alkylated aromatic compounds and the gaseous hydrocarbons contained a comparatively high proportion of unsaturated compounds. It was apparent that further hydrogenation was desirable in a second stage to de-alkylate the condensate and to convert olefinic hydrocarbons to methane and ethane.

TABLE 4

The Hydrogenation of Distillate with Aromatic Hydrocarbon Formation

Hydrogenation Pressure	365
Inlet Gas Rate, s.c.f.h. (90% H_2)	33,350
Distillate Type:	
Specific Gravity	0.682
Aromatic Hydrocarbon Content	3.0
Carbon/Hydrogen, w/w	5.4
Imp. Gals. of distillate /1000 cu.ft. of gas:	
a) synthesis stage	21.2
b) overall	7.5
Hydrogenation temperature, °C:	
a) synthesis	760 - 765°C
b) de-alkylation	790
Product Gas Rate, s.c.f.h.	45,080
Product Gas Composition, % by volume	
CO_2	2.9
C_xH_y	0.3
CO	3.4
H_2	30.0
CH_4	51.8
C_2H_6	11.0
N_2	0.6
Calorific Value, Btus/s.c.f.	821
Carbon Balance	
Percentage of carbon supplied in distillate appearing as:	
Hydrocarbon Gas	71.6
Benzene	17.2
Toluene and Higher monocyclics	1.5
Naphthalene	3.6
Higher Aromatics	5.2
Deposited Carbon	0.9

It was realised that the fluidized hydrogenator with the solids recycle suitable for carrying out this process with very little modification (Fig. 5). The lower fluidised bed was utilised for the 1st stage of the reaction and the 2nd stage was carried out in the main bed.

The whole of the distillate was mixed with the hydrogenating gas used to fluidize the lower bed which was deepened to 5 ft. to give adequate time for reaction. The hydrogenating gas for the second stage was introduced at the base of the riser. The first stage reaction was endothermic and the second stage exothermic. The solids recycle then served to transfer heat from the second stage to the first stage maintaining overall heat balance with a temperature differential between the two stages of 25 - 30°C.

The results of operating the process are given in Table 4 showing that for a distillate containing only 3% of aromatics the yield of aromatics accounted for 27.5% of the carbon in the distillate. The condensate itself was free of paraffins. Carbon deposition amounted to 0.9% of the carbon in the oil and this was deposited as a graphitic coating on the fluidised particles. The overall product gas had a calorific value of 821 Btus/ft.^{3}, a value which could be increased with a reduced supply of hydrogen to the second stage.

Acknowledgements

This paper is published by permission of the Gas Council, and the work described in it was carried out under the direction of Dr. F. J. Dent. The Authors thank their colleagues who were responsible for the experimental work.

Literature References

1. Dent, F.J., Edge, R.F., Hebden, D., Wood, F.C. and Yarwood, T.A. "Experiments on the Hydrogenation of Oils to Gaseous Hydrocarbons" Gas Council Research Communication, G.C. 37, 1956, 51 pp., Trans. Inst. Gas Engrs., 106, pp. 594-643, 1956-7.

2. Murthy, P.S. and Edge, R.F. "The Hydrogenation of Oils to Gaseous Hydrocarbons" Gas Council Research Communication G.C.88, 18 pp., 1962, J. Inst. Gas Engrs., 3, pp. 459-476, 1963.

3. Noignard, L.A. and Stewart, K.D. "The Hydrogenation of Light Distillate with reference to the Production of By-product Aromatic Hydrocarbons" Gas Council Research Communication G.C.51, 36 pp., 1958, Trans. Inst. Gas. Engrs., 108, pp. 528-562, 1958-9.

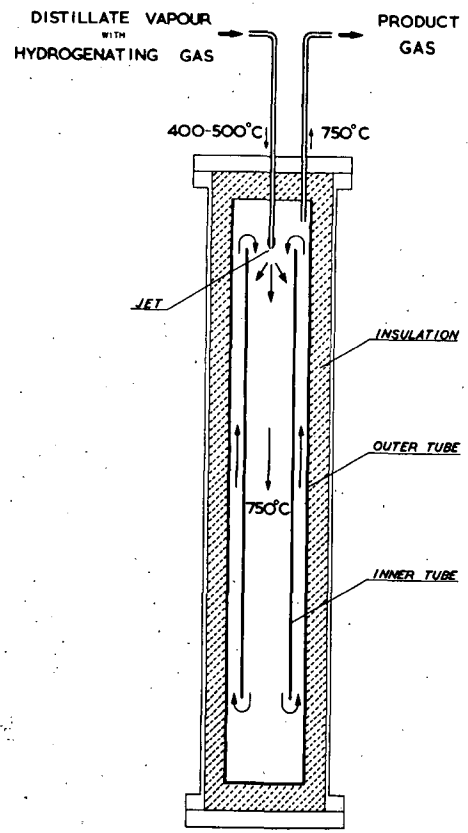

Fig. 1. The Gas Recycle Hydrogenator.

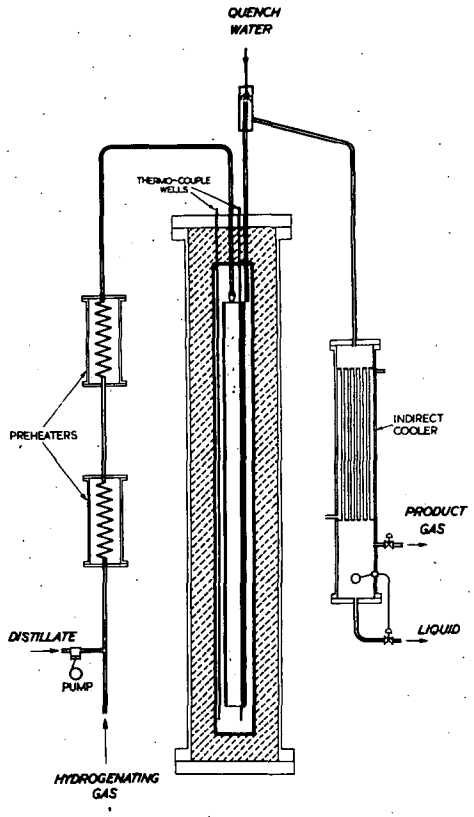

Fig. 2. Flow Diagram of the Gas Recycle Pilot Plant.

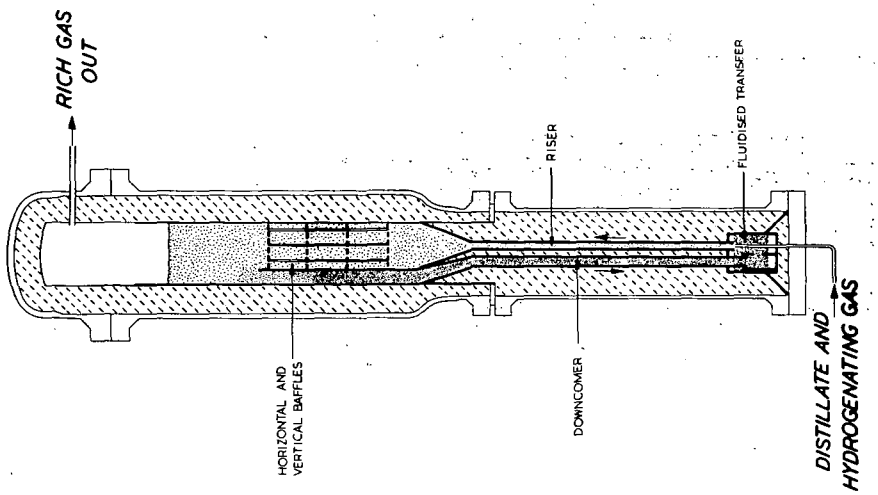

Fig. 3. The Fluidised Pilot Plant.

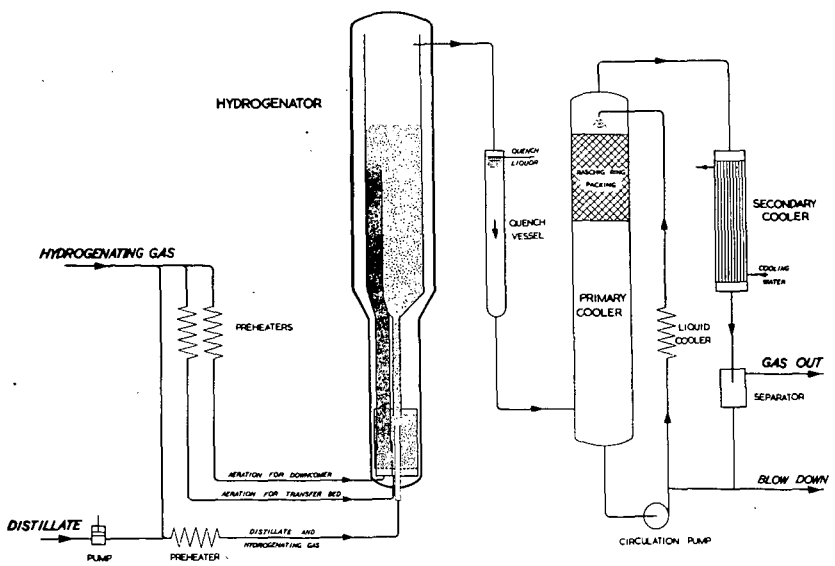

Fig. 4. Flow Diagram of the Fluidised Bed Pilot Plant.

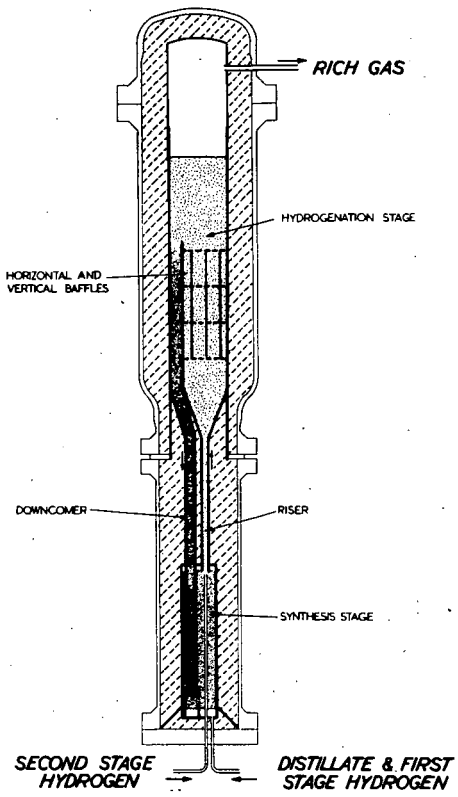

Fig. 5. The Fluidised Bed Hydrogenator used for the Production of By-Product Aromatic Hydrocarbons.

THEORETICAL ANALYSIS OF CYCLIC PROCESSES FOR PYROLYSIS OF PETROLEUM OILS

Alan Kardas, S. A. Weil, A. R. Khan, and Jack Huebler

Institute of Gas Technology
Chicago 16, Illinois

INTRODUCTION

The most severe problem which faces any utility is the ability to supply gas, water, or electricity during periods of peak demand. In the case of the natural gas industry, the gas comes from wells which are generally a great distance from the point of use. This requires the construction of very expensive transmission pipelines. To use these pipelines economically, it is necesary to run them at near their maximum capacity at all times. If this is to be done during periods of low consumption, the pipelines will be incapable of furnishing the required gas during periods of high consumption and means of supplementing gas will have to be found.

In practice, the gas industry meets this problem in a large variety of ways. For example, additional uses of gas during periods of low consumption are encouraged by selling the gas on an interruptible basis at a low cost. This means that when non-interruptible customers – principally residential – require gas the interruptible service can be shutoff. Gas is quite generally sold to industrial manufacturers on this basis. These concerns meet the problem which confronts them when their service is interrupted by putting in standby facilities such as combination burners which can burn oil as well as gas. A second method, very commonly used by the gas industry, is to store the gas near the point of consumption. This method has been used quite extensively where natural storage facilities exist. Such facilities might be depleted oil or gas wells, aquifers, or underground storage caverns which occur naturally and which are capable of containing gas at relatively high pressure. At the present time there is great interest in liquefying natural gas and storing it in various types of containers near the point of consumption.

While all of the above means are used to meet this problem there still remains, in many localities, a problem of meeting the high peaks of demand which occur during extremely cold weather. Commonly, such periods are only a few days in length and occupy only from ten to thirty days of the year. In the creation of facilities to handle such peaks it is apparent that investment cost is a paramount item. If, for example, the average annual usability of the facility is 15 days, the fixed charge on the investment must be carried by 15 days of operation rather than 365 days. Therefore the fixed charge must be multiplied by a factor of nearly 25 in arriving at the cost which must be added to the cost of the gas which is furnished during the peak period.

One of the methods used to meet the peak demands is storage of propane, which can be blended with air when needed and sent out with the natural gas which is arriving via the pipeline. As mentioned above, storage of natural gas either in underground facilities or as liquid natural gas can be used to meet the problem. In some sections of the United States, principally the northeastern sections, it is advantageous to store oil and to gasify the oil when the supplemental gas is required. The present paper is concerned with the oil gasification process.

A large number of processes have been developed to gasify oil. Among these are highly sophisticated processes such as hydrogasification (1,2,3) or thermofor pyrolytic cracking (4,15), which are both continuous processes capable of gasifying a wide range of feedstocks. They are found to be unsuitable, however, because of their high investment cost. The cyclic processes to be discussed here most nearly meet the requirements of the gas utility industry in the important aspect of having low investment cost.

GENERAL PROCESS CONSIDERATIONS

When petroleum oils are heated to about 1100°F. or higher, pyrolysis occurs, that is, the larger oil molecules undergo thermal cracking to form a wide variety of end products. The chemistry and the chemical kinetics of this process has been thoroughly studied and reported by Linden *et al* (6,7). During the thermal cracking process coke, tar, aromatic liquids, and butadienes are formed, as well as permanent gases such as methane, ethane, ethylene, hydrogen, etc., which can be used as substitutes for natural gas. The gas issuing from the thermal cracking device is, therefore, cooled to condense the tar and scrubbed with light oil to remove objectionable constituents such as benzene, toluene and the butadienes. After being properly blended with flue gas to adjust the heating value and density to make it substitutable for natural gas, the product gas is sent to the customer.

In spite of the highly involved chemistry, Linden *et al* (6,7) have shown that the gas resulting from the cracking operation can be characterized by a fairly simple expression; the heating value and products formed are a function of

$$t\,\theta^{0.06}$$

in which t is the temperature at which the cracking occurs in °F. and θ is the time in seconds. While Linden's work was conducted under essentially isothermal conditions one can derive from it the integrated effects of temperature and time at temperature in a non-isothermal heating process. These relationships will be discussed in a future paper. The present paper is concerned with the heat transfer aspects of an oil gas set (the cyclic heating apparatus) and not directly with the chemical kinetics.

The equipment used to carry out the oil gasification process can, in principle, be extremely simple. It may consist of an insulated shell into which refractory shapes are placed in such a fashion as to provide free access of flowing oil vapors to the surface of the refractory shapes and to allow the refractories to be heated up by a flow of hot flue products. For example, one might lay up conventional firebrick to form parallel walls with spaces between the walls for the passage of the gases. Heat is stored in the refractories by passing a combusted oil and air mixture through the passages. When the desired amount of heat has been stored in the refractory, a small amount of steam is passed through the passages to remove most of the flue products. Then oil mixed with steam is passed through the passages. The oil-steam mixture utilizes the stored heat to vaporize the oil, to heat it to cracking temperature, and to furnish the required heat of cracking. When the stored heat has been removed, a small amount of steam is again passed through the set to remove the last of the oil gas and the heating cycle is again initiated.

In principle, the oil gas set performs simply as a regenerative heat exchange device. A significant difference between the operation of the oil gas set and the regenerators in common industrial use arises from a fact which can be seen in Linden's correlation; i.e., the heating value of the gas product is extremely sensitive to temperature. In any regenerative process the temperature of the stream being heated will be hotter at the beginning of the cycle than it will be at the end. Since temperature has such a pronounced effect in the oil gas process it is necessary to use extremely short cycles to minimize this temperature difference.

THE HEAT EXCHANGE PROBLEM

The number of permutations and combinations of ways to accomplish the cyclic heat exchange required in an oil gas operation are limitless. One can chose from a large number of heat exchange materials and there are limitless variations in their size and shape. The process can be operated cocurrent flow (the heating stream and the make (oil) stream traveling in the same direction through the set) or countercurrently (the heating stream flowing through the set in one direction and the make stream in the reverse direction). The heat or make streams can be introduced into the set at a variety of points and the heating air can be preheated from the residual heat in the make stream before the air is combined with oil for combustion on the heating cycle. The problem can be further complicated by carbon deposition, which occurs during the cracking portion of the cycle and which is, of necessity, burned off during the heating cycle. Nearly all of these variations, as well as the chemical kinetics, have been built

into a digital computer program which is capable of describing the details of the process with sufficient accuracy that the computed heating value of the product gas is in very good agreement with actual operating results. A detailed description of this computer program is beyond the scope of the present paper. We will, however, show some very simplified expressions for the heat transfer problem which will give a clear indication as to the important variables in the heat transfer process together with some results of the computer program for a typical cocurrent-flow set.

Simplified Model

The simplest model of a regenerative heat exchanger is one in which the heating gas and the cooling gas flow through the set in the same direction (parallel flow), and having heat exchange material with an infinite heat capacity. The heat exchange material will then adopt a constant temperature intermediate to the heat and make streams. Thus one can write

$$h_1 A\ (t_1 - t_i)\ T_1 = h_2 A\ (t_i - t_2)\ T_2 \qquad (1)$$

$$h_1 A\ (t_1 - t_i)\ T_1 = -w_1 c_1\ T_1\ \frac{dt_1}{dx} \qquad (2)$$

$$-w_1 c_1\ T_1\ \frac{dt_1}{dx} = w_2 c_2\ T_2\ \frac{dt_2}{dx} \qquad (3)$$

where

h = heat transfer coefficient - Btu/(hr x ft^2 x $^\circ$F.)

A = heat transfer area per unit length - ft^2/ft

t = temperature - $^\circ$F.

T = time of period - hr

w = mass flow rate of gas per unit open area, lb/(hr x ft^2)

c = specific heat of gas - Btu/(lb x $^\circ$F.)

x = length in direction of flow - ft

Subscripts

1 = heating gas

2 = cooling gas

i = heat transfer surface

Equation (1) equates the heat transfer rate multiplied by the period time of the two parts of the cycle, assuming no purge periods. Equation (2) equates the same to the heat given up by the heating gas as sensible heat of temperature change

per unit length along the regenerator. Equation (3) equates the heat lost by the heating stream to the heat gained by the cooling stream.

Equation (1) is used to solve for t_1 in terms of t_1 and t_2. This result is substituted into Equation (2). Equation (2), with the substitution, is differentiated with respect to x and the resulting term containing dt_2/dx is eliminated by using its value from Equation (3). Thus, a second order equation in t_1 is obtained as follows:

$$-a_1 \frac{d^2 t_1}{dx^2} = b \left(1 + \frac{a_1}{a_2}\right) \frac{dt_1}{dx} \qquad (4)$$

$$a_1 = w_1 c_1 T_1$$

$$a_2 = w_2 c_2 T_2$$

$$b = \frac{h_1 T_1 h_2 T_2 A}{h_1 T_1 + h_2 T_2}$$

Appropriate boundary conditions of

$$x = o, \; t_1 = t_1^o, \; t_2 = t_2^o$$

$$x = o, \; \frac{dt_2}{dx} = -\frac{b}{a_1} \left(t_1^o - t_2^o\right)$$

$$x = \infty, \; t_1 = t_2$$

can be applied to the integration of Equation (4) and the related expressions for t_2, and the final result is

$$\frac{t_1^o - t_1}{t_1^o - t_2^o} = \frac{a_2}{a_1 + a_2} \left\{1 - \exp\left[-\frac{(a_1 + a_2)\, b}{a_1 a_2} x\right]\right\} \qquad (5)$$

$$\frac{t_2 - t_2^o}{t_1^o - t_2^o} = \frac{a_1}{a_1 + a_2} \left\{1 - \exp\left[-\frac{(a_1 + a_2)\, b}{a_1 a_2} x\right]\right\} \qquad (6)$$

To a fair degree of approximation, the temperature rise of the make stream (100° to ~ 1300°F.) and the temperature drop of the heating stream (3000° to ~ 1700°F.) are of the same order of magnitude. As a consequence, the values of a_1 and a_2 are also of the same order of magnitude. If the periods and the heat transfer coefficients are also equal, Equation (6) reduces to

$$\frac{t_2 - t_2^o}{t_1^o - t_2^o} = \frac{1}{2} \left\{1 - \exp\left[-\left(\frac{2}{WCT}\right)\left(\frac{hT}{2}\right) ax\right]\right\} \qquad (7)$$

which is trivial except to show that the period time will tend to cancel out under these operating conditions. In addition if T_2 is made lower but not T_1 or a_1, then w_2c_2 will have to go up or the set capacity will fall and if w_2c_2 goes up, h_2 will also rise and h_2T_2 will tend to stay the same. As a result the effect of the period is very small. The computer program bears this conclusion out as can be seen in Figs. 1, 2, and 3 where the make period has been varied from 43 to 86 seconds without appreciable change in the heating value of the oil gas produced. The heating value of the oil gas is very sensitively related to the temperature the oil reaches as described above.

Refined Heat Transfer Model

The above very simple treatment of the problem gives no information on the effect of the properties of the heat transfer medium. A better approximation to the actual problem can be obtained in the following way.

If a sine wave temperature variation having an amplitude equal to (t_1-t_o) is impressed upon a heat transfer material having real properties, c_1, ρ_1, k_1, α_1

where

ρ_1 = density - lb/ft^3

k_1 = conductivity - Btu/hr x ft x °F.

α_1 = diffusivity - ft^2/hr

and if h_1 is equal to h_2, it can be shown (8) that the surface temperature of the heat transfer medium will oscillate between $t_{i,1}$ and $t_{i,2}$ in such a way that

$$t_{i,1} - t_{i,2} = F\,(t_1 - t_2) \qquad (8)$$

where F is a constant and is given by

$$F = \left[1 + \frac{2k_i}{h}\sqrt{\frac{\pi}{2\alpha_i T}} + \frac{\pi k_i^2}{\alpha_i T h^2}\right]^{-1/2} \qquad (9)$$

Equations (1) and (2) may be revised to account for the fact that the heat exchange medium has an average surface temperature which is higher than t_1 during the heating cycle and cooler during the cooling cycle.

$$h_1A\,(t_1 - t_{i,1})\,T_1 = h_2A\,(t_{i,2} - t_2)\,T_2 \qquad (1a)$$

$$h_1A\,(t_1 - t_{i,1})\,T_1 = -w_1c_1T_1\,\frac{dt_1}{dx} \qquad (2a)$$

If Equation (8) is used in combination with (1a) and (2a) and the same procedure followed as shown above the resulting solutions will be exactly as in Equations (5) and (6) except for the definition of b which becomes b'.

Some values of F have been computed for reasonable values of the various parameters and using a fireclay and a silicon carbide refractory as the heat exchange medium. Table I shows the properties of these two refractories

Table I

Material	k	c	ρ	α
Fireclay	0.88	0.295	130	0.023
Silicon Carbide	9	0.289	160	0.195

Silicon carbide represents a nearly optimum material while fireclay represents about the least expensive material which has sufficient structural strength under the conditions of use. Table II shows the assumed values of T and h and the resulting values of (1-F).

Table II

Period Time, T, min.	Heat Exchange Medium	1-F	
		h = 5	h = 10
1.5	Fireclay	0.93	0.87
1.5	Silicon Carbide	0.98	0.96
2.5	Fireclay	0.90	0.84
2.5	Silicon Carbide	0.97	0.94

This table shows that the thermal properties of the heat exchange material are not an overriding consideration. The largest effect is at an h of 10 and a period of 2.5 minutes (5 minute cycle), where the silicon carbide shows a 12% higher value of (1-F). This would allow the use of 12% less surface area of silicon carbide (less refractory) or 12% more production of oil gas with the same surface and no change in h (same amount of refractory but rebricked to keep the gas velocities unchanged).

In an extensive monograph on regenerative heat transfer, Hausen (8) derives equations which are very similar to those given above but which cover long cycles as well as short ones. If the two are compared for the conditions of interest in oil gas sets the quantitative results are very close although the algebraic form of expressions showing the effect of the properties of the heat exchange medium are quite different. In place of F given above in Equation (9), Hausen has

$$1 - \frac{1}{1 + \frac{0.375\ h\delta}{k(0.3 + \frac{\delta^2}{\alpha T})}^{1/2}}$$

where

δ is the brick half thickness - ft

He also has the same harmonic form of combining the values of h_1T_1 and h_2T_2, T_1 and T_2 as well as a_1 and a_2.

The Computer Model

While the foregoing relationships are very useful to examine the effects of the variables they can not be used to predict actual operating results. Partly this is due to the fact that the results of the cracking reaction are dependent upon time as well as on temperature and in a very complex fashion. The capability of being able to consider the large number of possible ways to construct and operate a set is important.

In addition the heat transfer coefficient during the heating period varies by a substantial amount due to the intense gas radiation in the first several courses of brick and the effective heat capacity of the make stream varies considerably due to heat of vaporization in the first few courses and heat of cracking in the central sections.

Fig. 4 shows an example of a very common cocurrent set design. It is built with two vertical sections with an empty crossover section. This construction comes about because these sets are actually converted carburetted water gas sets. As mentioned earlier there are a large variety of shapes and sizes of this design and many other designs as well.

The open space at the top of the left hand section is required as a combustion section on the heating period. The refractory in the first few courses just below the combustion chamber is usually made of silicon carbide in order to withstand the extreme temperature fluctuations which occur in the switch from hot flue gas (3000°F.) to cold oil and steam (200°F.). The high thermal conductivity and diffusivity of this material greatly minimizes its temperature fluctuation as can be seen in Table II and Equation (9). Below the silicon carbide are courses of bricks which are usually fireclay and which are not always laid up in the same pattern as the silicon carbide.

The crossover section is usually left relatively open but it still provides heat transfer surface which must be included in the computer analysis. The right hand section, which is not necessarily of the same cross section of the left hand section, is partially filled with checkers; usually fireclay. Above this checkerwork there is an open space in which relatively little heat transfer is accomplished but which provides residence time for cracking to continue under nearly isothermal conditions. The exit oil gas is quenched and cleaned up as described earlier.

The computer program is confirmed so that each of the sections just described can be analyzed with the input data pertinent to it. Generally speaking each section can be subdivided into small layers in order to improve the accuracy of the computations. In each subdivision the surface area, the heat transfer coefficient and the thermal properties of the gases are computed for the particular conditions which exist at that position. The variation in time of both the refractory and the gases is computed at the subdivision with the refractory temperature being computed as a function of depth into it normal to the gas flow direction. In sections where thermal cracking occurs the heating value and yield of the oil gas are computed as a function of time over the period and time weighted average values calculated.

The cocurrent sets are relatively simple to compute compared to the countercurrent. This is because the temperature of each gas stream is known at their common inlet point to the set. This makes it possible to start at the front, solve the first subdivision and then proceed to the second, etc. It is not inferred that the solution itself is simple but only that the procedure is straightforward. In the countercurrent set this can not be done because the initial gas stream temperatures are known at opposite ends of the set. This makes it necessary to make an "educated guess" for the entire set, run through the solution, "guess again" and repeat until an acceptably close agreement is obtained. This iteration process is superimposed on the iterative processes used at each subdivision and the required computer time is considerably greater.

Typical computer results are shown in Figs. 5, 6, and 7. Fig. 5 shows the heating gas and oil gas temperatures at the beginning and end of each period. Fig. 6 shows the variation in heating value of the oil gas during the make period at various positions in the set. Fig. 7 shows the heating value and yield at the start and end of a period as well as the average values as a function of the length of the set. These results are for an idealized set and do not represent actual operation but actual results would not appear too different in principle.

CONCLUSION

A highly sophisticated computer program has been developed which is capable of handling both the complex heat exchange relationships and the chemical kinetics involved in cyclic oil gas sets. The program is being used to analyze existing sets and to enable recommendations for improving them to be made. It will also be used to design an optimum oil gas set in the near future.

Closed form solutions of the heat transfer problem have been obtained. These solutions can be used to show the general effects of the parameters and their interrelationships and to approximate the design of the optimum set.

ACKNOWLEDGMENT

This work was supported by the Gas Operations Research Committee of the American Gas Association under Project PB-42.

REFERENCES CITED

1. Linden, H. R., Guyer, J. J., Pettyjohn, E. S., Institute of Gas Technology Interim Report "Production of Natural Gas Substitutes by Pressure Hydrogasification of Oils," January (1954).

2. Reid, J. M., Bair, W. G., Linden, H. R., Institute of Gas Technology Research Bulletin 28, March (1960).

3. Bair, W. G., Linden, H. R., Institute of Gas Technology Research Bulletin 27, June (1960).

4. Chaney, N. K., Gas Operations Research Bulletin No. 7, American Gas Association, (1956).

5. Loughry, T. F., American Gas Association Proceedings, 924-28 (1953).

6. Linden, H. R., Peck, R. E., Ind. Eng. Chem. 47, 2470-74 (1955).

7. Shultz, E. B. Jr., Guyer, G. J., Linden, H. R., Ind. Eng. Chem. 47, 2479-82 (1955).

8. Hausen, H., Warmeubertragung im Gleichstrom, Gegenstrom und Kreuzstrom, Springer-Verlag, Berlin, 1950.

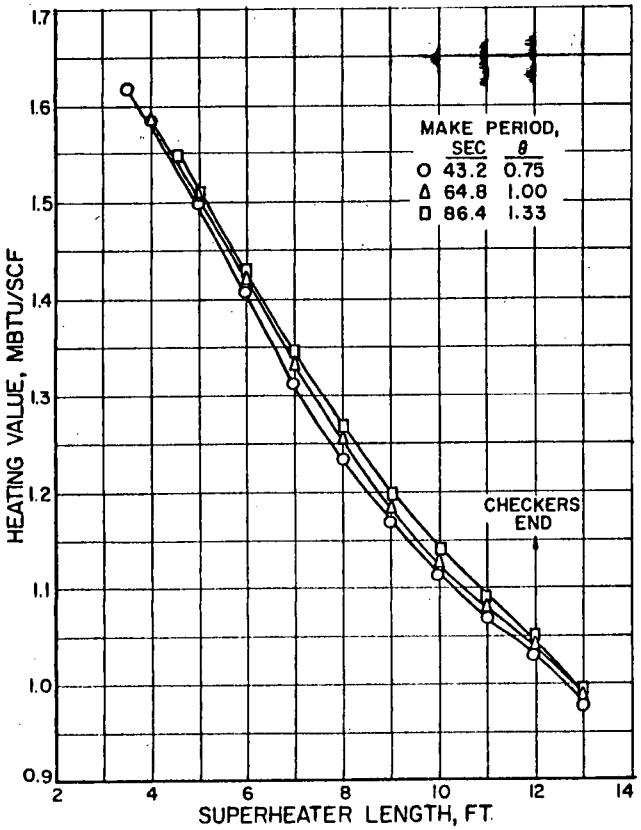

Fig. 1.-EFFECT OF SUPERHEATER LENGTH AND MAKE PERIOD DURATION ON MAKE GAS HEATING VALUE FOR A MAKE OIL RATE OF 852 POUNDS PER SQ. FOOT-HOUR

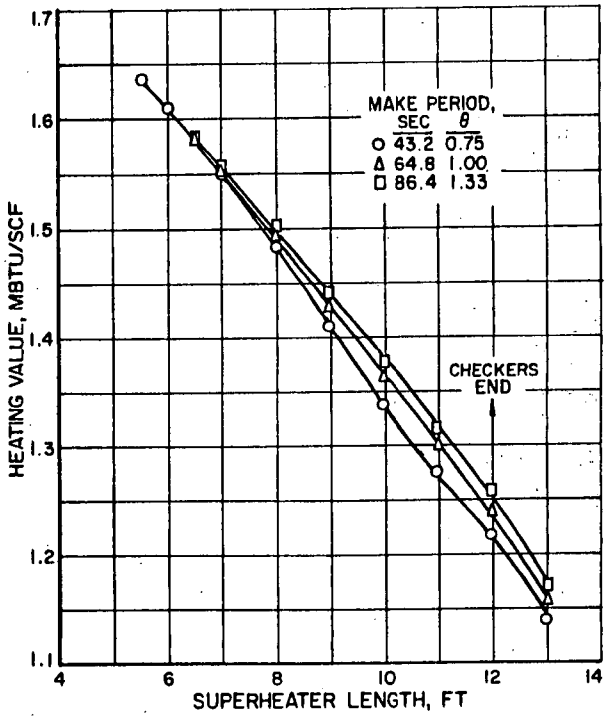

Fig. 2.-EFFECT OF SUPERHEATER LENGTH AND MAKE PERIOD DURATION ON MAKE GAS HEATING VALUE FOR A MAKE OIL RATE OF 1420 POUNDS PER SQ. FOOT-HOUR

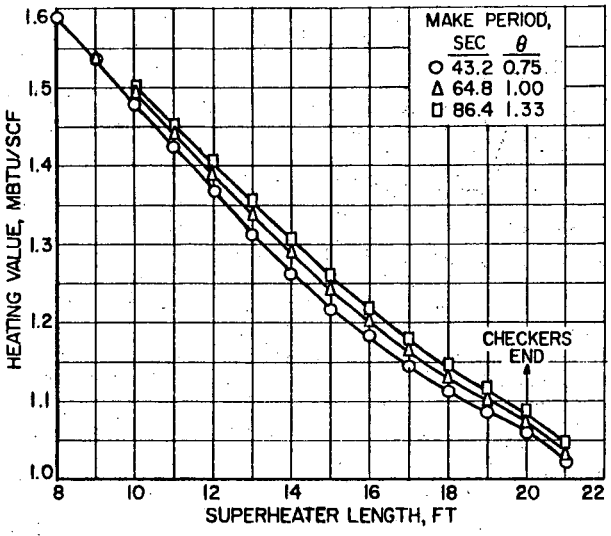

Fig. 3.- EFFECT OF SUPERHEATER LENGTH AND MAKE PERIOD DURATION ON MAKE GAS HEATING VALUE FOR A MAKE OIL RATE OF 1988 POUNDS PER SQ. FOOT-HOUR

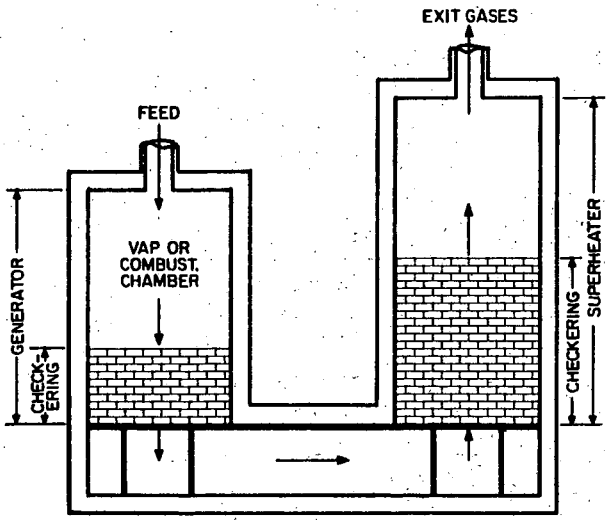

Fig. 4.- SCHEMATIC DIAGRAM OF TWO-SHELL COCURRENT OIL GAS SET

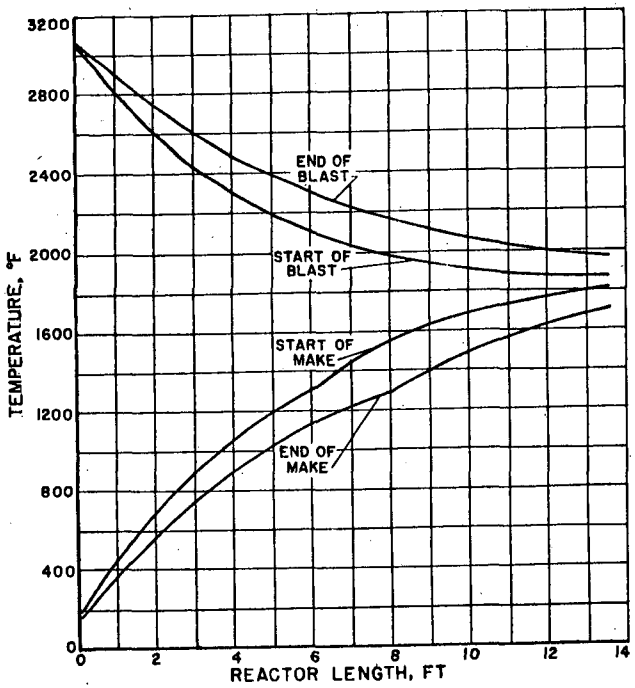

Fig. 5.-GAS TEMPERATURE PROFILES IN COCURRENT REACTOR

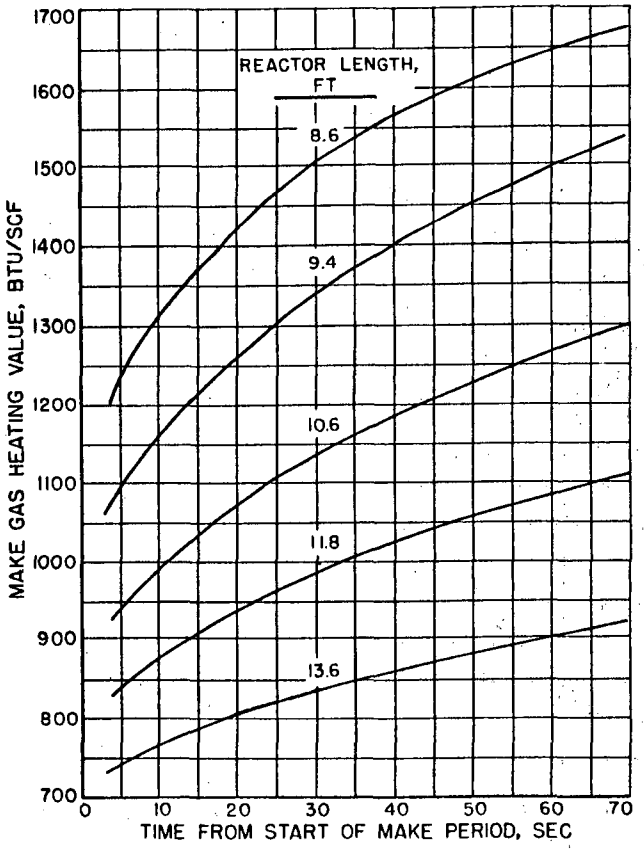

Fig. 6.-EFFECT OF MAKE TIME AND REACTOR LENGTH ON MAKE GAS HEATING VALUE

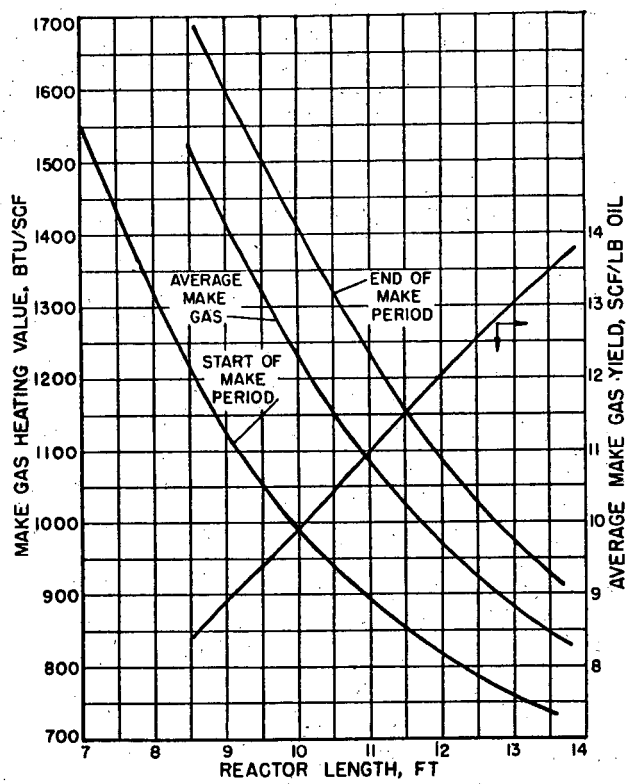

Fig. 7.-EFFECT OF REACTOR LENGTH ON MAKE GAS HEATING VALUE AND AVERAGE MAKE GAS YIELD

HYDROGASIFICATION OF OIL SHALE IN A CONTINUOUS FLOW REACTOR

Herman Feldmann and Jack Huebler

Institute of Gas Technology
Chicago 16, Illinois

INTRODUCTION

Satisfaction of the projected needs for pipeline gas from a domestic source will ultimately require supplementing the available natural gas with gas produced from the large reserves of solid fossil fuels, coal and oil shale. The time when natural gas will have to be supplemented by the gasification of solid fossil fuels depends on many factors. These factors, along with information on the potential reserves of solid fossil fuels and processes for the production of pipeline gas, have been discussed by Linden (4).

Oil shale is a carbonate mineral which rather tenaciously holds oil-yielding hydrocarbons called kerogen. The production of pipeline gas from this kerogen requires the addition of sufficient hydrogen (hydrogasification) or subtraction of enough carbon (pyrolysis) to convert it into methane or a mixture of methane, ethane and hydrogen having burning properties similar to methane. The most attractive present technique for producing pipeline gas from oil shale is by hydrogasification.

A major processing problem with oil shale arises from the fact that the pipeline gas forming reactions are accompanied by side reactions which occur at significant rates. The major side reactions are mineral carbonates (calcite and dolomite) decomposition, liquid formation, and carbon deposition. Maximum heat economy and kerogen utilization can be obtained if these side reactions are minimized to the greatest extent possible.

The objective of the present work was to develop sufficient information to allow design of a prototype plant for the economic production of pipeline gas from oil shale. Studies were carried out on a pilot plant scale in a continuous-flow tubular reactor. The study evaluated the effects of important process variables such as the hydrogen-to-shale feed ratio, feed gas composition, shale space velocity, pressure, temperature, gas-solid contacting scheme, and oil shale feed stock.

EXPERIMENTAL

Equipment

The hydrogasification unit used in this study consisted of an interconnected feed hopper, a screw feeder, a reactor tube, a discharge star gate, and a residue receiver. A drawing of the assembled unit, showing dimensions and relative positions of the vessels as well as working pressures and temperatures, is given in Figure 1. The flow and instrumentation diagram for the entire plant is shown in Figure 2.

The feed gas was fed into the top of the reactor cocurrently with the shale. The product gas was taken out at the top of the residue receiver, and was passed through porous stainless steel filters, a water-cooled condenser and cartridge filters filled with glasswool, for final cleanup. Pressure was maintained on the hydrogasification unit by an externally loaded back-pressure regulator. Feed gas flow was controlled manually by a needle valve and was metered by a plate orifice.

The shale bed level was controlled by means of a differential pressure measurement by probes set at the desired bed level and at the reactor top. A change in the differential pressure reading of 10 inches of water column (full scale) between the bed and the reactor top corresponded to a change in the bed level of about 4 inches. In moving-bed tests, the shale space velocity was set by setting the bed height and the shale feed rate.

The reactor was heated externally by an electric furnace having eight individually controlled heating zones. Reactor temperatures were measured by eleven Chromel-Alumel thermocouples placed in an interior thermowell. Reactor outside wall temperatures were measured at the center of each heating zone. Reactor pressure, reactor differential pressure, and the hydrogen orifice differential pressure were recorded. Product gas volume was measured with a tin case meter. The specific gravity and heating value of the product gas were measured and recorded continuously.

Procedure

Colorado shale was obtained from the Union Oil Co. mine at Grand Valley, Colorado. The material was selected because of its availability in amounts required for pilot plant testing (approximately 200 pounds per run) and because it is typical of shale from the Green River deposit. New Albany shale was selected as representing a promising Eastern shale. A typical Colorado oil shale ultimate analysis is shown below:

	Wt. % (dry basis)
Ash	59.21
Organic Carbon	18.05
Hydrogen	2.54
Sulfur	0.85
Oxygen (By difference)	13.87
Nitrogen	0.46
Mineral Carbon	5.02
TOTAL	100.00

Feed shale was prepared in batches by crushing the 6-inch chunks to -10 +55 or to -55 +200 U.S.S. sieve size and drying in a steam-heated oven.

Prior to beginning a test, the reactor tube was heated to the desired operating temperature, the feed hopper was filled with shale, and all vessels were purged with nitrogen, depressurized, and then repressurized to the desired operating pressure with feed gas. In moving-bed tests, the reactor tube was initially filled to the desired operating level with inert material prior to starting the run so that steady operating conditions could be obtained more quickly.

When the proper flow of feed gas had been established and was steady, the screw feeder was started. This feeder was calibrated so that the rate of flow of solids could be predicted from the feeder rate. Actual feed rates, however, were obtained by measurement of the weight of solids removed from the hopper divided by the elapsed time of the run. Simultaneously with the start of screw feeder, the discharge star feeder was set into rotation. The star was operated either at a rate just sufficient to hold the bed level at the predetermined position or, as in the free-fall tests, at a maximum rate so that no shale bed could be built up within the reactor tube.

With hydrogen feed, as a run progressed, the product gas would gradually increase in gravity and in heating value. Steady values were reached during the latter part of a run. All test results were based on the steady-state portion of the run. Gas samples taken directly from the reactor, however, were found to approach steady values much more quickly than those taken after the product gas passed through the residue receiver, which indicates that steady state conditions were achieved quite rapidly in the bed and that the approach of the product gas to steady state was slow because of back-mixing of the product gas in the residue receiver. In all runs there was an adequately long steady period. In a typical run, using a shale rate of 35 pounds per hour and a 4-foot deep bed, the material in the reactor was completely replaced approximately 20 times.

Liquid rates were measured during the run by means of high pressure Jerguson gages in the bayonet and condenser knockout pots. Liquid recoveries were usually incomplete, due in part to absorption of the liquids on the residue in the receiver hopper.

After completion of a test, the unit was depressurized, purged, and allowed to cool. Feed remaining in the feed hopper, the solid residue in the solids receiver and the liquid products were removed and weighed. Feed and residue solids were given complete chemical analyses and were screened to determine the degree of particle degradation. Residue solids were sampled from near the top of the receiver in order to obtain material representative of steady operation. Liquid products were analyzed for carbon and hydrogen and specific gravity. Product gases were analyzed with a mass spectrometer - except that carbon monoxide was determined by infrared analysis.

The residue rate was calculated from the feed rate and an ash balance between the feed and residue. Feed and product gas rates for the steady-state period were corrected for pressure and temperature and reported in standard cubic feet per hour (at 60° F. and 30.00 inches of mercury), on a dry basis. Gas heating value and specific gravity were computed from gas on a dry gas basis at standard conditions (5).

Process Variables Studied

The range of process variables studied are given below.

Hydrogen-to-shale feed ratio: 0 to 200 percent of the stoichiometric requirements for complete conversion of the organic carbon and hydrogen content of the shale to methane.

Temperature: 1150° to 1360°F.

Total Pressure: 400 to 1600 p.s.i.g.

Shale space velocity: 50 to 900 pounds per cu. foot-hour in moving bed tests (residence time 6 to 90 minutes, and in free-fall tests shale residence times approximately 3 seconds).

Feed gases: Hydrogen, synthesis gas, nitrogen-hydrogen mixtures, and nitrogen.

RESULTS

Hydrogasification with Hydrogen

The most important variable in determining the degree of conversion of the oil shale to gaseous hydrocarbons was shown to be the hydrogen-to-shale feed ratio. For the sake of consistency this parameter was defined as the actual hydrogen feed rate divided by the stoichiometric amount. This ratio is the percent of stoichiometric hydrogen and denoted by S.

Figure 3 shows how this stoichiometric ratio influences the conversion of organic carbon to gaseous hydrocarbons and residue, the remaining carbon being converted to liquid products. The scatter in the fraction of residual carbon formed is due to varying amounts of liquid absorbed by the spent shale and to experimental error. Selected residue samples were extracted with toluene to eliminate variation due to absorbed liquids. This lessens the scatter considerably as indicated by Figure 3.

As the hydrogen-to-shale stoichiometric feed ratio is increased, the conversion of organic carbon to gas increases, until the ratio is approximately 90 percent, at which point approximately 65 percent of the conversion is obtained. Increasing the amount of feed hydrogen beyond 90 percent of stoichiometric only results in dilution of the product gas with hydrogen and no further significant conversion of kerogen.

The decreasing fraction of hydrogen utilization with increasing stoichiometric hydrogen-to-shale feed ratio is also apparent from Figure 4 which shows the composition of the product gas as a function of the hydrogen-to-shale feed ratio.

Since the objective of this work is to develop a process for converting oil shale to high-B.t.u. gas suitable for pipeline transmission it is necessary to remove the carbon oxides and excess hydrogen. The preferred method of accomplishing this is by catalytic reaction of the carbon oxides with hydrogen to form methane. Since the

methanation reaction involves expensive equipment and lowers the overall process efficiency, it is desirable to minimize the amount of carbon oxides and hydrogen consumed in this reaction. Consequently, the use of excess hydrogen is not desirable and only a relatively limited number of experiments were conducted above 90 percent of the stoichiometric ratio.

Pressure

The only variations in gasification yields and product distributions noted with changes in total pressure between 400 and 1600 p.s.i.g. were the result of changes in the gas phase residence time. Even at the lowest pressures and highest gas rates studied with pure hydrogen, gas phase residence times were sufficiently long to convert the heavier aliphatic intermediates. Liquid products collected were mainly aromatic. These aromatics would be difficult to hydrogenate at even the longest gas phase residence times studied.

Temperature

The average bed temperature has a great effect on the paraffin distribution in the product gas as is shown in Figure 5. The methane-to-ethane molar ratio increases very rapidly at temperatures above 1250°F. Propane and butane increase and pentane appears as the temperature is reduced to 1150°F. Both propane and butane vanish as the temperature approaches 1350°F.

These changes in gas composition are due to the decrease in the rates of hydrogenolysis of the heavier gaseous constituents to methane with decreases in temperatures (8). This verifies the mechanism suggested by the earlier laboratory scale work (2) that the hydrogasification reactions proceed via the stepwise destructive hydrogenolysis reactions of oil vapor through successively lower molecular weight aliphatics and finally to ethane and methane.

There are indications that a maximum of organic carbon conversion for a given stoichiometric hydrogen ratio occurs between temperatures of 1200° to 1250°F. A corresponding increase in residual carbon occurs above 1250°F. while increased liquid formation occurs below 1200°F. These results indicate that there is no incentive in operating an oil shale hydrogasification reactor above 1250°F. because of the increased formation of residual carbon. In addition, there is a rapid increase in mineral carbonate decomposition at higher temperature as shown in Figure 6. A portion of the carbon oxides in the product gas has been suggested (6) to result from the decomposition of groups containing organic carbon-oxygen linkages such as carboxyl groups. Carbon oxides from the decomposition of these groups occurs at temperatures as low as 575°F.(1). However, mineral carbonates are the chief source of carbon oxides.

Shale Space Velocity and Free-Fall Tests

Shale residence time had virtually no effect on the conversion of kerogen in the shale to gaseous hydrocarbons and liquid products. Shale residence times were varied from approximately 3 seconds in free-fall operation to 90 minutes in moving-bed operation, with the majority of the tests being made at a shale residence time of approximately 10 minutes. A comparison of the results of a shale residence time of 90 minutes with the results obtained at 10 minutes, at 90 percent of the stoichiometric hydrogen, showed that the organic carbon conversion only increased from 65 to 72 percent. Extrapolation of these results indicates that a nearly tenfold increase in reactor volume would be necessary to achieve this additional 6 percent conversion. Under the conditions, carbonate decomposition was increased from 34 to 70 percent because of the longer residence time. The 6 percent increase in conversion is offset by the greatly increased reactor size necessary to achieve it and by the increased carbonate decomposition with its detrimental effects on process heat economy, hydrogen utilization and product gas cleanup costs.

Carbonate decomposition decreased with increasing shale space velocity from approximately 70 percent at a shale space velocity of 50 pounds per cu. foot-hour to 34 percent at 800. Further increases in shale space velocity in moving-bed operation were not effective in reducing carbonate decomposition because 34 percent of the carbonate is magnesium carbonate which decomposes at a very high rate (3). However, free fall operation reduced the carbonate decomposition to only 8 percent and made possible the direct production of a high-B.t.u. gas. The effect of this decrease is shown by the much higher hydrocarbon composition of the product gas in Figure 4.

The distribution of organic carbon between gaseous hydrocarbons, liquids, and residual carbon products remained unchanged in free-fall as compared to moving-bed operation. The reaction model described below attempts to rationalize this important fact as well as the observed effect of the hydrogen-to-shale stoichiometric ratio.

Reaction Model

It is known from retorting experience that when an oil shale is heated above 500 to 600°F., oil is evolved. Retorting is usually done at moderate temperatures of the order of 1000°F. and fairly complete evolution of the kerogen is attained.

In hydrogasification work conducted by Shultz and Linden (7), conversions of the organic material to gaseous hydrocarbons above 90 percent were obtained. This work was conducted in a batch system which was charged with hydrogen and heated from room temperature to a final temperature of 1300°F. at a heating rate of approximately 9°F. per minute. In marked contrast to this, the heating rate in the present reactor was on the order of 400°F. per second. It is believed that the rapid heating rate in the present work is responsible for the relatively low conversion to gas.

In the present system the shale particles heat so rapidly that a portion of the oil vapor is probably pyrolysed to relatively unreactive aromatics and coke before it can escape from the particle to the gas phase. The rate of evolution of oil vapor is so large that no hydrogen from the gas phase can enter the particle while the vaporization is occurring. This places an upper limit on the conversion to gaseous hydrocarbons, which is represented by the carbon lost to pyrolysis within the shale particle.

The oil vapor which reaches the particle surface without being pyrolysed can either react with hydrogen in the immediate vicinity of the surface of the particle or it can pyrolize. Thus, one would visualize a gas film surrounding the particle in which both pyrolysis and initial hydrogasification will occur. The extent to which hydrogasification can predominate would seem to be logically a direct function of the rate of mixing of the hydrogen with the oil vapor. It is assumed that the ability of the hydrogen to mix with the oil vapor is a function of the ratio of the hydrogen flow rate to the oil vapor flow rate. This ratio is proportional to the stoichiometric hydrogen to shale feed ratio S. In the lower limit, i.e., zero feed hydrogen, one would not expect zero conversion to gas since gaseous hydrocarbons are a direct product of the pyrolysis reaction.

As these results indicate, at the temperatures employed in these experiments the pyrolysis and hydrogasification reactions are quite rapid. Three seconds is sufficient time to heat the shale particle, evolve and partially pyrolize the oil. The oil evolved from the surface of the particle travels through the reactor at the gas phase velocity, typically on the order of 0.1 feet per second, which results in a total gas phase residence time of approximately 80 seconds. This residence time of the gas phase is essentially independent of either free-fall or moving-bed operation. Consequently, the gasification results should be, and were, independent of the method of handling the solids.

Following this initial reaction phase, further gasification would necessarily occur by hydrogenation of the residual coke formed by pyrolysis. This coke is apparently quite unreactive to the hydrogen-hydrocarbon gas mixture at the temperatures and residence time employed in these tests. This is due in part to equilibrium hindrance of the reaction

$$C + 2H_2 \rightleftarrows CH_4$$

due to the presence of CH_4.

This conceptual model of the hydrogasification reaction scheme, in addition to explaining the differences between the batch results reported by Shultz and Linden (7) and those reported here, allows an equation to be written which provides a satisfactory fit to the observed results.

The total organic carbon conversion of the shale may be written as,

(1) $$X_{Ri} + X_{Gi} + X_{Ro} + X_{Go} + X_L = 1$$

where

X_{Ri} is the fraction of the kerogen carbon cracked to residue inside the particle.

X_{Gi} is the fraction of the kerogen carbon converted to gas in the particle through the cracking reaction.

X_{Ro} is the fraction of the kerogen carbon cracked to residue outside the particle.

X_{Go} is the fraction of the kerogen converted to gas outside the particle.

X_L is the fraction of kerogen carbon which is converted to liquid products.

The conversion to gaseous hydrocarbons is, therefore,

(2) $$X_{Gi} + X_{Go} = 1 - X_{Ri} - X_{Ro} - X_L$$

On the basis of the model, X_{Ri} is a function of the heatup rate, X_{Ro} a function of both heating rate and the stoichiometric hydrogen feed ratio (a measure of the degree of mixing of the hydrogen with the oil vapor outside the particle) and X_L is also probably a function of heatup rate and the degree of hydrogen mixing. Because of the difficulty of measuring liquid rates in both the pilot plant and laboratory studies it is difficult to determine how X_L was affected by the various parameters. The liquid conversions in the pilot plant varied from 10 to 20 percent. In the batch tests (7) with hydrogen and slow heatup rates very little conversion to liquid products was observed.

A small increase in liquid product formation was noted with increasing hydrogen-to-shale feed ratio in the semiflow (2) tests. This was probably because gas phase residence time decreased in these tests with increasing hydrogen-to-shale feed ratio (hydrogen feed rate). Gas phase residence times were on the order of 10 seconds in these tests which is considerably shorter than the typical 80 second gas phase residence times in the pilot unit. Thus, the most important variable in the formation of liquid products is probably the particle heatup rate assuming sufficient gas phase residence times. This follows from the model since high heatup rates promote pyrolysis which in turn promotes formation of aromatic liquid products which are very difficult to hydrogenate.

Since all of the pilot plant tests were made at essentially the same heatup rates, the following expressions will be written for the various conversion parameters:

$$X_{Ro} = Ae^{-kS} \tag{3}$$

where

A is a function of the heatup rate. This function fulfills the boundary conditions that the $\lim_{S \to \infty} X_{Ro} = O$, i.e., perfect mixing, and $X_{Ro} = A$ when S = O, i.e., no hydrogen feed.

$$X_{Ri} = f(q) = B \tag{4}$$

A function only of the heatup rate, essentially constant for the pilot plant tests.

$$X_L = C \tag{5}$$

Assumed a constant for the pilot plant tests.

Substituting from (3), (4) and (5) into (2) gives,

$$X_{Gi} + X_{Go} = 1-B-C\,Ae^{-kS} \tag{6}$$

Determination of the constants gives the final equation,

$$X_{Gi} + X_{Go} = X_{Gt} = 0.68-0.30\,e^{-1.72S} \tag{7}$$

Equation (6) compared with the experimental data in Figure 3 and a reasonable fit is shown. Within the limits of the work done to date the model seems reasonable. It is hoped that future tests will further prove or modify the assumptions and allow a complete description of the process to be given.

Hydrogasification with Synthesis gas and Nitrogen-Hydrogen Mixtures

Operating the process with synthesis gas produced by partial oxidation of shale oil can provide a means of heating the oil shale to reaction temperature at sufficiently low hydrogen to shale ratios that hydrogen separation in the product gas will not be required. The presence of carbon dioxide in the synthesis gas also inhibits the decomposition of calcite ($CaCO_3$) thus improving hydrogen utilization and process heat efficiency. In an actual synthesis gas run, carbonate decomposition was reduced from 30-40 percent to approximately 20 percent.

Feed gas compositions for synthesis gas evaluation were chosen to be as close as possible to the reported values (10). Since synthesis gas was not available a gas was prepared whose composition at room temperature was the same as synthesis gas would be if cooled down to room temperature assuming water gas shift equilibrium were satisfied. The room temperature composition of this gas was:

Constituent	Mole, %
CO	36.0
CO_2	15.1
H_2	48.1
CH_4	0.6
C_2H_6	0.1
C_3H_8	0.1
TOTAL	100.0

In experimental runs the presence of gaseous constituents in the synthesis gas other than hydrogen did not have an effect on the hydrogasification results within the limits studied. The organic carbon conversion to gaseous hydrocarbons remained to be influenced by the hydrogen-to-shale ratio fed as shown by the general correlation for the conversion of organic carbon to gaseous hydrocarbons in Figure 3.

Alternate processing schemes include the use of steam, hydrogen-steam; or carbon dioxide-steam mixtures (flue gas) in a fluidized-bed reactor. External heat requirements, if necessary, would be furnished by heating coils. Since the process is to be operated at approximately 1200°F., steam and carbon dioxide are assumed to be essentially inert to the gaseous hydrocarbons. This was verified in the synthesis gas tests. Therefore, it was expedient to study the effect of diluents on hydrogasification by making tests with various nitrogen-hydrogen feed mixtures since nitrogen is certain to be inert. The intent was to determine if either the mole fraction hydrogen or the hydrogen partial pressure were important in effecting conversions to gaseous hydrocarbons. These tests employed nitrogen mole fractions from 100 percent to 0 percent. This series of tests correlate nicely with the results achieved with pure hydrogen as shown by Figure 3 indicating that the only important variable was the stoichiometric hydrogen ratio, and that neither the mole fraction or the partial pressure were important parameters.

Hydrogasification of New Albany Shale

New Albany shale was selected as being one of the more promising Eastern oil shales for the manufacture of pipeline gas. A complete survey of the important Eastern shale deposits has been reported by Shultz (9).

New Albany shale has a greater tendency to form carbonaceous residue than does Colorado shale. This is indicated by the table below where representative results with the New Albany shale are reported.

Run No.	57	59	68
Shale Particle Size, U.S.S.	-10 +55	-10 +55	-10 +55
Shale Space Velocity, lb./cu.ft.hr.	688	698	352
Average Bed Temperature, °F.	1219	1273	1261
Hydrogen-to-Shale Feed Ratio, % of Stoichiometric	43	42	205
Organic Carbon Conversion, Gaseous Hydrocarbons	36.3	40.6	53.2
Liquids	6.4	3.0	7.2
Residue	54.0	52.7	34.5
TOTAL	96.7	96.3	94.9

Also, with New Albany shale, the conversion to gaseous hydrocarbons is less dependent on the hydrogen-to-shale feed ratio than with Colorado shale. However, no difference was noted in the gasification behavior of these two materials in batch tests. The same model as presented for the Colorado shale, therefore, may also be valid for the New Albany shale, but insufficient data is available for the New Albany shale to determine the validity of this.

Qualitatively it appears that the Fisher assay oil yield is an important parameter in determining the reactivity of a shale to form gaseous hydrocarbons. For example, the Fisher assay oil yield for the New Albany shale was approximately 0.052 gallons per pound of organic material whereas the Colorado shale oil yield was approximately 0.088 gallons per pound of organic material. The carbon-hydrogen ratios were approximately 7.85 and 7.20 respectively. The lower oil yield with the New Albany material indicates an increased tendency to form residual carbon rather than oil vapor. This tendency of the kerogen to form carbonaceous residue appeared to have a similar effect on the hydrogasification yields.

SUMMARY AND CONCLUSIONS

The production of pipeline gas from oil shale is possible over a wide range of operating conditions. The conversion of the organic carbon in the shale was a function mainly of the hydrogen-to-shale feed ratio being independent of pressure and diluents in the feed gas. A slight effect of temperature was noted at the extremes of the temperature range studied, 1360° to 1150°F. The conversion of kerogen to gaseous hydrocarbons was reduced at the higher temperature level by increased residual carbon formation and at the lower temperature by increased liquid formation. Particle residence

time did not have an effect on product gas properties or conversion of organic carbon to gaseous hydrocarbons. A semi-empirical equation was developed, based on the rate of particle heatup and hydrogen-oil vapor mixing, which allowed the conversion of organic carbon to gaseous hydrocarbons to be predicted. The model indicates that the ideal hydrogasifier design should provide for slow solids heatup rates and rapid hydrogen-oil vapor mixing.

ACKNOWLEDGMENT

This work was supported by the Gas Operations Research Committee of the American Gas Association as part of the Promotion-Advertising-Research Plan of the Association. The work was guided by the Project PB-23b Supervising Committee under the chairmanship of C. F. Mengers. Thanks are due to E. J. Pyrcioch, W. G. Bair, H. L. Feldkirchner, S. Volchko, and H. A. Dirksen for their helpful suggestions in operation and design of the equipment. E. J. Pyrcioch, R. E. Cartier, E. C. Higgins, R. J. Hrozencik, J. C. Wolak, W. Podleckl, R. O. Buskey and C. Wuethrich assisted in conducting tests and performing calculations. A. Attari and J. E. Neuzil supervised the analytical work. Thanks are also due to the Indiana Geological Survey for their kind assistance in locating and obtaining the New Albany oil shale used in these studies.

REFERENCES CITED

1. Aarna, A. Ya., Trudy Tallinsk, Politekh Inst. Ser. A. 65-81 (1955) No. 63.

2. Feldkirchner, H. L., Linden, H. R., Paper presented at 143rd National Meeting, Division of Fuel Chemistry, American Chemical Society, Cincinnati, Ohio, January 13-18, 1963.

3. Jukkola, E. E., Denllauler, A. J., Jensen, H. B., Barnet, W. I., Murphy, W.I.R., Ind. Eng. Chem. 45, 2711-14 (1953).

4. Linden, H. R., Paper presented at 48th National Meeting, American Institute of Chemical Engineers, Denver, Colorado, August 26-29, 1962; Preprint No. 14, 17-52.

5. Mason, D. McA., Eakin, B. E., Institute of Gas Technology Research Bulletin 32, (1961) December.

6. Murphy, W. I. R., U. S. Bureau of Mines, Laramie, Wyoming. Personal Communication.

7. Shultz, E. B., Jr., Linden, H. R., Ind. Eng. Chem. 51, 573-76 (1959).

8. Shultz, E. B., Jr., Ind. Eng. Chem. Process Design Develop. 1, 111-16 (1962).

9. Shultz, E. B., Jr., Paper presented at 48th National Meeting, American Institute of Chemical Engineers, Denver, Colo., August 26-29, 1962; Preprint No. 9, 44-57.

10. Van Amstel, A. P., Petrol. Refiner 39, 151-52 (1960) March.

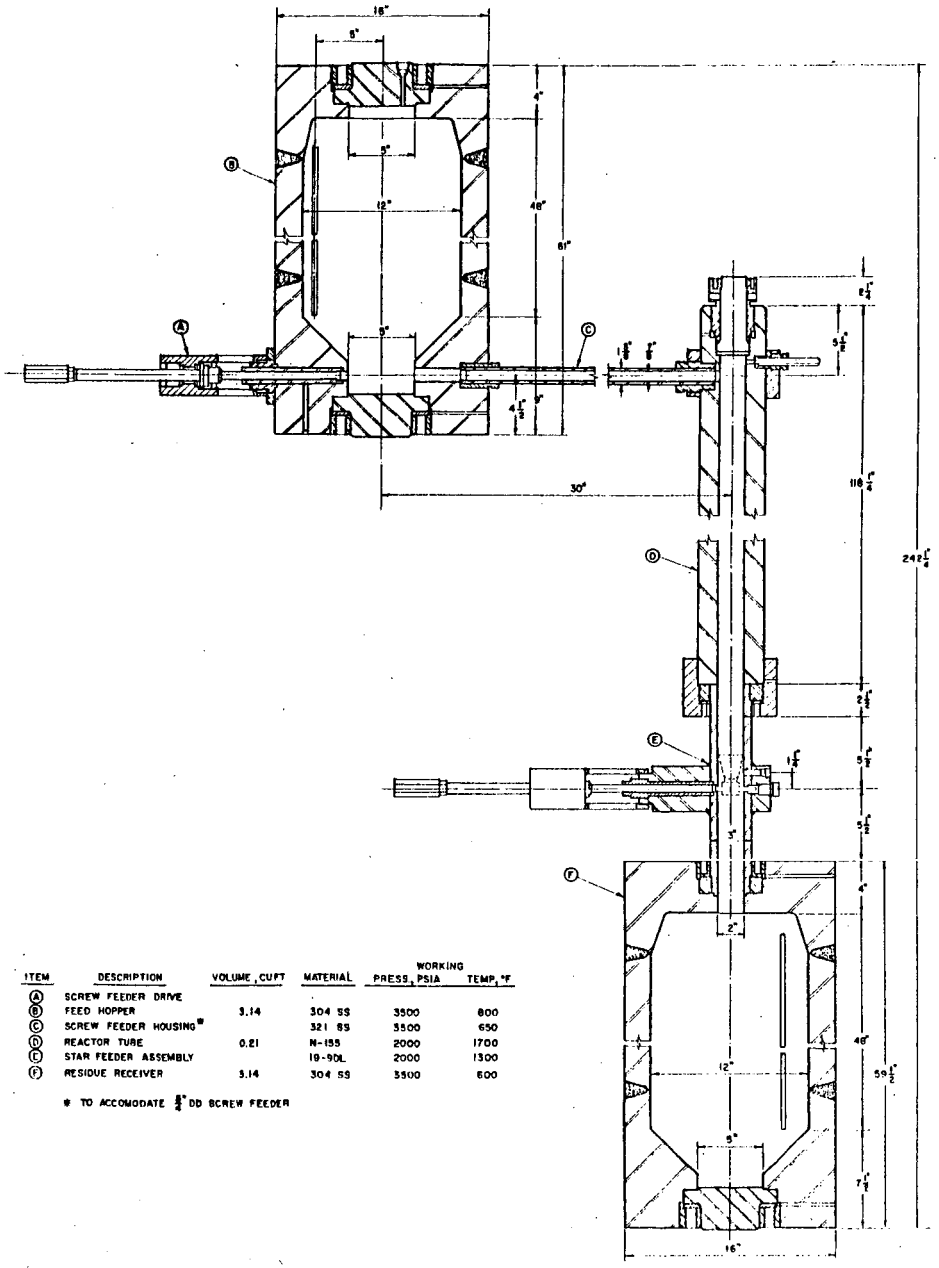

ITEM	DESCRIPTION	VOLUME, CU FT	MATERIAL	WORKING PRESS, PSIA	WORKING TEMP, °F
(A)	SCREW FEEDER DRIVE				
(B)	FEED HOPPER	3.14	304 SS	3500	800
(C)	SCREW FEEDER HOUSING*		321 SS	3500	650
(D)	REACTOR TUBE	0.21	N-155	2000	1700
(E)	STAR FEEDER ASSEMBLY		19-9DL	2000	1300
(F)	RESIDUE RECEIVER	3.14	304 SS	3500	800

* TO ACCOMODATE 3/4" DD SCREW FEEDER

Fig. 1.-OIL SHALE HYDROGASIFICATION PILOT UNIT

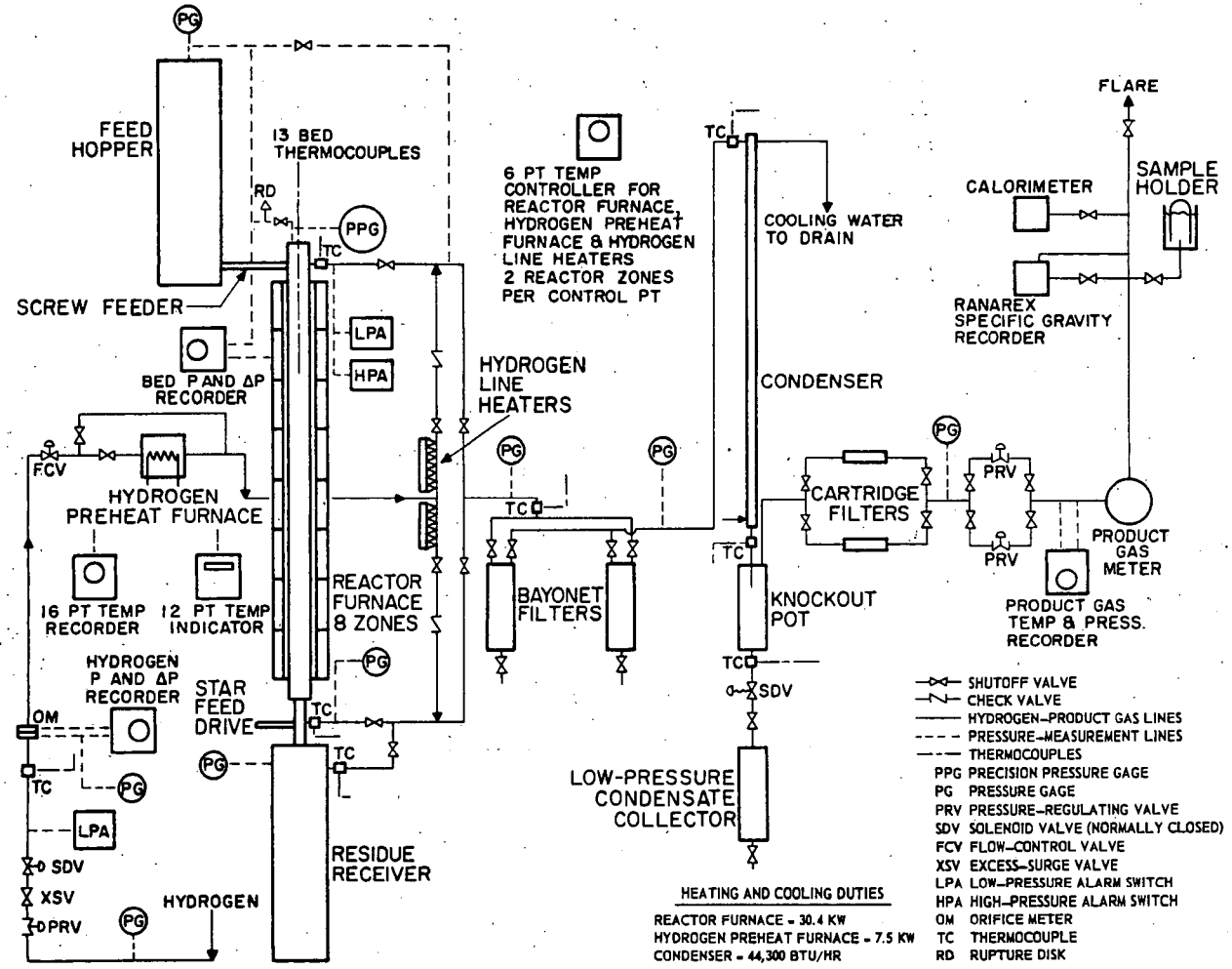

Fig. 2.- FLOW AND INSTRUMENTATION FOR HIGH-PRESSURE HIGH-TEMPERATURE SHALE HYDROGENATION PLANT

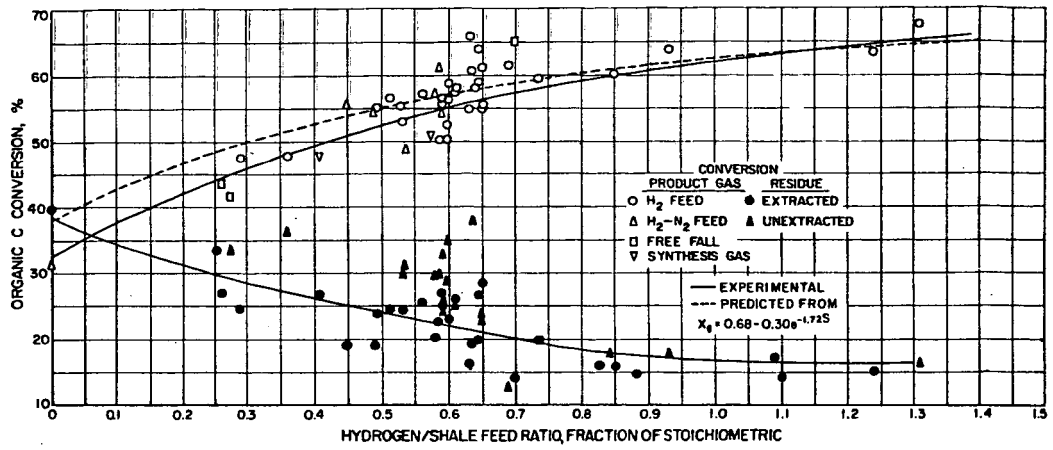

Fig. 3.- EFFECT OF HYDROGEN/SHALE FEED RATIO ON CONVERSION OF ORGANIC CARBON TO RESIDUE AND GASEOUS HYDROCARBONS

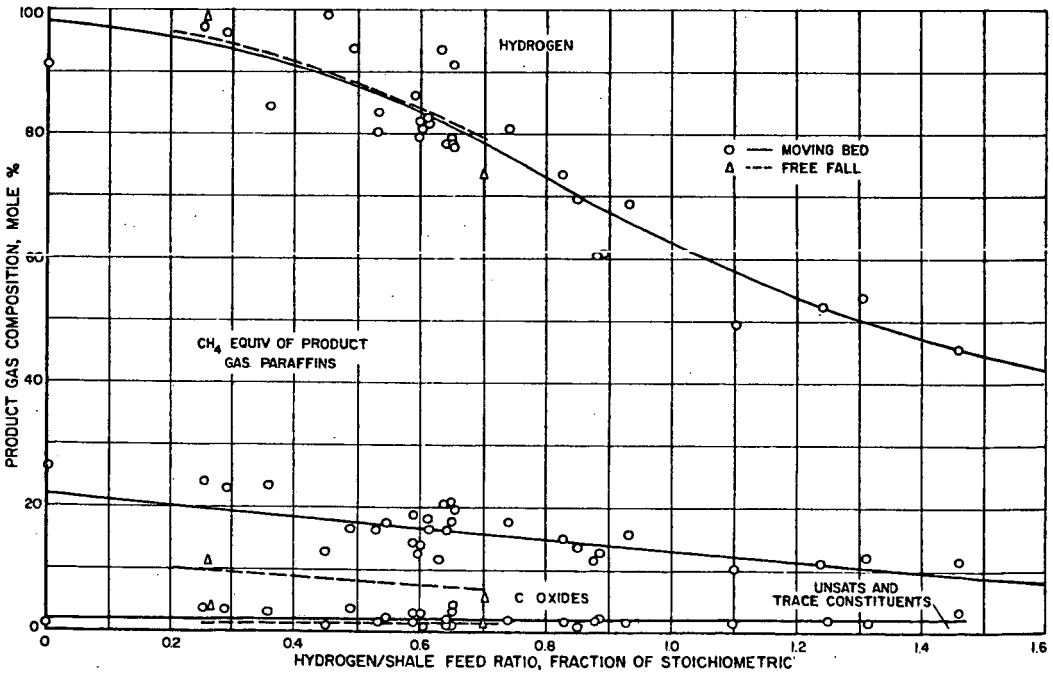

Fig. 4.- EFFECT OF HYDROGEN/SHALE FEED RATIO ON PRODUCT GAS COMPOSITION

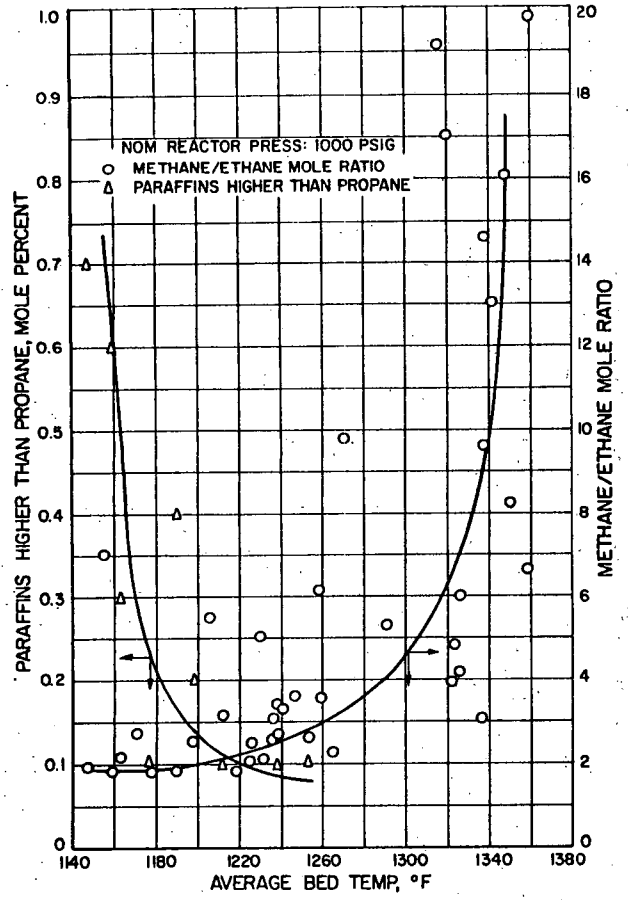

Fig. 5.-EFFECT OF AVERAGE BED TEMPERATURE ON GASEOUS HYDROCARBON DISTRIBUTION

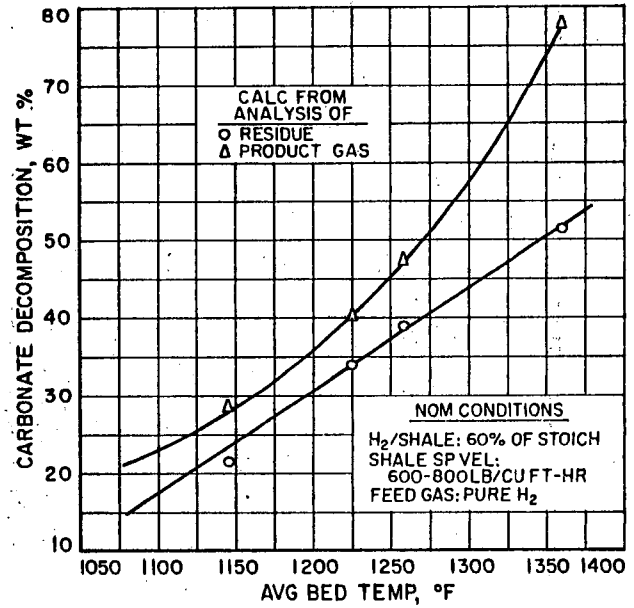

Fig. 6.-THE EFFECT OF AVERAGE BED TEMPERATURE ON CARBONATE DECOMPOSITION

Commercial and Industrial Fuel Gases from Coal

Neal P. Cochran
Office of Coal Research
Washington 25, D. C.

ABSTRACT

To produce fuel gases from coal at commercially attractive prices the Office of Coal Research has undertaken three projects. In one project low cost gasification equipment is under development while the other two seek to develop processes that will reduce capital and operating costs of synthetic gas plants. The projects are mutually supporting and directed toward OCR's over all objective of increasing the use of coal. Pipeline gas at 50 cents per 1000 cubic feet and hydrogen at 25 cents per 1000 cubic feet are the research targets.

A COAL-BURNING SOLID-ELECTROLYTE FUEL CELL POWER PLANT

by

R. L. Zahradnik
L. Fikan
D. H. Archer

ABSTRACT

A plant is proposed which combines a coal-gasification unit with a high-temperature solid-electrolyte fuel cell battery to produce an efficient power generation system. The special requirements imposed on the gasifier by its coupling with a fuel cell battery are discussed and two avenues of investigation - one experimental, one analytical - are proposed. The results of a computer simulation of the overall plant are presented and preliminary projections of plant economics and characteristics are reported. The many research and development problems, which must be solved before such plants are technically and economically feasible, are pointed out, and the progress made towards their solution is discussed.

This work was sponsored by the Office of Coal Research, Department of Interior under Contract 14-01-0001-303.

Introduction

The direct conversion of the energy of coal into useful electrical power has long commanded the serious attention of many investigators. This paper describes how in principle a coal gasification unit can be combined with a high temperature solid electrolyte fuel cell battery to produce just such a direct energy conversion system. Before the details of this system are discussed, however, it may be well to review some of the properties and characteristics of the solid-electrolyte fuel cell and to cite some of its operating characteristics for reference a little later on.

Solid Electrolyte Fuel Cell

The basic component of the Westinghouse solid electrolyte fuel cell is the zirconia-calcia or zirconia-yttria electrolyte. This material is an impervious ceramic which has the unique ability to conduct a current by the passage of $O^{=}$ ions through the crystal lattice. The ease with which these ions pass through the electrolyte is measured by the electrical resistivity of the electrolyte. Values of this resistivity for both types of electrolyte as functions of temperature have been published in several places.[9,5]

Fuel cells have been made by applying porous platinum electrodes to this material.[16] The operating principles of the resultant cells have been discussed[1], and optimized batteries constructed from such cells have been described.[4] In brief these batteries operate at about 1000°C and consist of short, cylindrical electrolyte segments of about 30 mils thickness shaped so that they can be fitted one into the other and connected into long tubes by bell-and-spigot joints, as shown in Figure 1. The overall length of an individual segment is 1.1 cm, with a mean diameter of 1.07 cm. The segment weighs 2 g and occupies a volume of 2.0 cm^3. Electrodes are applied to the inside and the outside of these segments which then have an overall resistance of about 0.2 - 0.3 Ω. The inner electrode of one segment is attached to the outer electrode of the adjacent

segment, in this way connecting the individual segments electrically in series. Gaseous fuel passes through the center of the resultant, segmented tube, and oxygen or air is supplied on the outside. Figure 2 shows two 15-cell batteries constructed on this principle.

The performance of this and similar batteries has been evaluated for a variety of fuels, using either air and pure oxygen as the oxidizing agent. With H_2 fuel and pure O_2, a three cell battery has produced an open circuit voltage of 2.9 volts. The current density at maximum power was 750 ma/cm^2. At the maximum power point the battery produced 2.1 watts; and each cell segment 0.7 watt - about the same as an ordinary flashlight battery.[2,3]

System Configuration

In order to utilize such batteries in the production of electrical power from coal, it is necessary to devise a reasonable overall system for the purpose. As fas as the present type cell is concerned, a gaseous fuel is required for cell operation. In order to provide such a fuel to the fuel cell batteries, the scheme shown in Figure 3 has been devised.

Essentially, coal (indicated as carbon on the figure) is introduced into a reactor, into which recirculating gases from cell bank 1 also enter. Cell bank 1 consists of a number of fuel cell batteries of the kind just described. The gases from this cell bank consist primarily of CO and CO_2 (along with H_2 and H_2O) in some definite ratio. In the reactor, some CO_2 and H_2O is reduced to H_2 and CO by reacting with the coal. This results in a gas composition leaving the reactor which has higher CO/CO_2 and H_2/H_2O ratios than that of the entering gas. The gas leaving the reactor is then cleaned and passed, without cooling, into the fuel cell bank 1. There it serves as fuel for the cell unit, combining with oxygen which has been ionically transported through the cell electrolyte, resulting in power generation. The gases leaving this cell bank are split into two streams. One stream is recirculated to the reactor at a given recycle rate, completing the major system loop. The second stream is sent to fuel cell bank 2, which completes the combustion of CO to CO_2 and H_2 to H_2O.

The reason for this system configuration is that it allows all of the oxygen which enters the system to react with the coal to pass through the electrolyte and thereby contribute to the electrical energy output of the system. In addition, by limiting the degree of oxidation in cell bank 1, the concentrations of CO_2 and H_2O entering the reactor are only slightly removed from their equilibrium values. This means the bed operates under more nearly reversible conditions, so that overall the maximum electrical energy output from the coal-oxygen reaction is recovered. In order to obtain such recovery, however, an over-size coal reactor, excessively large cell banks relative to the power produced and high recycle rates would have to be employed. A compromise must be effected between the desire to obtain high recovery and the desire to avoid large and expensive equipment. Much of the work to date on this system has been geared to locate those optimum conditions which best effect this compromise.

Reactor Considerations

Because the reactor must contribute to an overall system optimum, certain of its design features must be tailored specifically to the task of gasifying coal in a rather unusual way. In most conventional gasifiers, oxygen is introduced at some point directly into the reactor. The fuel-cell power plant has been so designed, however, that oxygen is introduced into the reactor only in the form of CO_2, H_2O, and CO. The coal may be considered to be gasified primarily by the two reactions:

Reaction 1 ... $C + CO_2 \longrightarrow 2CO$

Reaction 2 ... $C + H_2O \longrightarrow H_2 + CO$

which proceed at rather slow rates compared to the direct oxidation reaction:

Reaction 3 ... $C + O_2 \longrightarrow CO_2$

Moreover, reactions (1) and (2) are endothermic, as compared to reaction (3) which is quite exothermic, meaning that heat will have to be supplied to the reactor where (1) and (2) occur. The problem of supplying this heat considerably complicates the overall reactor design.

Because reactions (1) and (2) proceed at relatively slow rates, it is advantageous to take steps to increase the rate of these reactions. Two such steps which may be taken are the maintenance of a high reaction temperature or the use of a highly reactive fuel. The temperature level of the reactor is limited, however, due to the fact that the reactions which occur there are endothermic. This means that heat must be supplied to the reactor from an external source (e.g. the fuel-cell banks where exothermic oxidation reactions are taking place and internal battery heating due to I^2R losses is occurring). This transfer may be accomplished either directly through the walls of the gasifier or indirectly in the sensible heat of the recirculating gases. However; some finite temperature gradient will be required to transfer this heat, constraining the reaction temperature to be less than the source temperature. If the source is the cell banks, an upper temperature limit is imposed due to the mechanical and structural properties of the cells. This is reflected in an upper temperature limit on the reactor of about $1000^{o}C$.

At this temperature, many of the fuels, which appear attractive for fuel cell use because of the clean nature of their gasified products, become unusable because of their low reactivity. On the other hand, those fuels which are reactive at this temperature produce quantities of tars, pitches, and other impurities which may have a deleterious effect on cell operation. The presence of such undesirable gasification by-products is increased even further in the absence of a direct supply of oxygen in the reactor. The issue is complicated by the fact that cell performance is most efficient when the fuel contains high concentrations of either CO or H_2. In the reactor, however, large quantities of CO and H_2 inhibit reactions (1) and (2), retarding their reaction rate. This effect compounds the problem of striking an effective compromise between a reasonable reactor size and highly efficient cell operating conditions.

In order to study the effect of such factors as these on the overall system performance, two avenues of investigation have been pursued. A small test reactor has been built to which a stream of gases containing CO, CO_2, H_2 and H_2O can be added, simulating the recycle gases in the

proposed design. Secondly a systems study of the proposed plant has been undertaken, culminating in a computer simulation of both reactor and cell banks. The purpose of this study was to demonstrate the engineering feasibility of such a plant, to assess its economic desirability and to point out areas where further development effort would be most beneficial.

Test Reactor

The test reactor is shown in Figure 4. It consists of a 1-3/8" i.d. inconel tube located in a commercial four-zone furnace. This reactor itself is of conventional fixed bed design with the exception of two small fuel cells which are located near its inlet and outlet. (The inlet cell is barely visible in the figure.) The open circuit voltages of these cells are used to determine the compositions of the inlet and outlet streams, thereby providing a measure of the extent of gasification which occurs in the reactor. The use of the cells as measurement devices allows a rapid and convenient analysis of the gases to be obtained immediately upon their exit from the fuel bed, without cooling or tampering with the gas stream in any way. Initial runs using this setup have been entirely satisfactory, and a report from this laboratory on the observed gasification kinetics will be presented shortly.

In addition to providing kinetic data for the various coals of interest, the test reactor serves several other purposes. It is being used to study not only the inhibiting effect of high CO and H_2 concentrations on the gasification, but to examine the effects of operating very near to the equilibrium gas compositions, which yield the highest cell efficiency. The problems of cleaning and filtering the reactor output gases are being examined, and the effects of such materials as fly-ash, pitches, and tars on cell performance are being explored. Overall, the test reactor is used to supply necessary engineering information for the computer simulation in order that optimum system operating conditions and general feasibility can be determined.

System Simulation

Some preliminary results of this simulation may be of interest at this time. The simulation includes both fixed and fluidized bed conditions, operated either isothermally, or adiabatically. It includes both the reactor and cell banks 1 and 2. In the reactor the surface reactions between carbon and steam and CO_2 are assumed to be controlling. In the gas phase, the "water gas" equilibrium were assumed to hold. Rate expressions of the Langmuir-Hinshelwood type were adopted for the surface reactions, and published data for the specific constants were employed in the simulation.[7,10,11,14] In the cell banks equilibrium conditions were assumed to prevail as far as the gas composition was concerned, with the generated voltages modified to account for both the losses due to internal cell resistance and those which occur due to cell polarization.

Figure 5 illustrates how the gas composition varies in its passage through the main system loop, as predicted by the computer simulation. Note that as CO_2 and H_2O react with the carbon, their percentages decrease, while the percentage of CO and H_2 increase. In the gas space immediately adjacent to the coal bed provision has been made for some volatile material to enter the gas stream; this is indicated by the sharp change in composition indicated by the dotted lines. In the cell banks as oxidation occurs, the percentage CO and H_2 decrease while CO_2 and H_2O increase. In the example shown on Figure 5, the hydrogen (H) to carbon ratio, H/C, is 1.0. The oxygen (O) to carbon ratio at the inlet to the reactor is 1.67 and the system is considered to be isothermal at $1200^{o}K$.

In addition to predicting the change in gas composition as it moves through the system the simulation provides the size reactor needed to generate sufficient gaseous products to attain an assigned power level, if a particular fuel, an inlet O/C ratio, a recycle rate (moles of CO and CO_2 flowing through cell bank 1 per mole of carbon C, consumed in reactor), a percent fuel burnup, and a system temperature are specified.

Figure 6 shows how the reactor size required to gasify a g mole/sec varies with conversion, for an inlet n_o' value of 1.67 and a temperature

of 1200°K. Plotted on the same figure is a curve which represents the total theoretical power output of the system per g. mole / sec gasified - also as a function of conversion. Two cases are illustrated on the figure for reactor size: one corresponding to plug flow conditions in the reactor; the other corresponding to perfectly mixed conditions. The reactivity of the carbon in the bed itself was taken to be that for retort coke, and published rate data for this material was used in the construction of Figure 6[10,11].

Figure 7 shows how a normalized gasifier size depends upon degree of conversion. Here the size of the reactor in grams per 100 theoretical watts produced by the system is plotted vs the oxygen to carbon ratio, n'_o. This figure is obtained from the data on Figure 6 by dividing reactor size by power produced, each per g. mole gasified per second. The case presented in Figure 7 is for isothermal operation at 1200°K. Two inlet (n'_o) values, 1.25 and 1.67, are illustrated for both plug flow and perfectly mixed reactors. The gas flow in the cells is assumed to be plug flow in all cases. The size of a reactor for a particular configuration and inlet condition is obtained by locating the desired (n'_o), value on the abscissa and reading the ordinate for the appropriate curve. To demonstrate the effect of temperature on reactor size, Figure 8 shows a plot of reactor size vs. the reciprocal absolute temperature for an inlet (n'_o) of 1.67 and an outlet (n'_o) of 1.25.

In addition to such results obtained for isothermal operation, the simulation predicts system size and behavior under adiabatic conditions. In this case the net heat release by the exothermic reactions and I^2R losses in the cell banks contributes to increasing the sensible heat of the circulating gases. The heated gases then pass through the reactor, losing heat to the endothermic reactions which occur there. The simulation has shown that, depending on conversion and recycle rate, the temperature rise in the cells may exceed, balance, or be less than the temperature drop in the reactor, and careful design will be required to adjust effectively the various system parameters in order to attain a proper thermal balance.

Discussion

On the bases of the investigations both with present-day laboratory equipment and with the overall system simulation certain key problems have emerged which require solution before the proposed plant can be considered as a feasible power generation system. There is considerable incentive to seek out these solutions, however, because of the many desirable features such a plant would have, such as high overall efficiency, even for small sized plants, inherently simpler operation due to the lack of moving parts, and compact overall size.

Some of the problems connected with the suggested coal gasifier have been discussed briefly in a previous section. Essentially these problems center around the fact that heat will have to be supplied to the reactor and that the gasification temperature is not spectaculatly high. Both of these factors indicate that a rather large scale reactor may be required compared to the idealized size obtained from the iso-thermal simulation. However Jolley, Poll and Stantan reporting on the fluidized gasification of non-caking coals with steam in a small pilot plant have shown that reasonably good heat transfer through the walls of the gasification chamber can be attained with as little an overall temperature driving force as 100°C.[8] This is encouraging in that it means that much of the heat which is generated in the cell banks can be transferred directly to the reactor by conduction through separating walls. Moreover, the temperature gradient required to do this is not excessive.

In addition to this external heating of the gasifier, some measure of internal heating will be accomplished by means of the recycle stream, which serves as a heat-carrying fluid as well as a gasification agent. Preliminary indications are that the recycle molar flow rate will be three to six times larger than the amount of coal gasified per unit time. This means that a good portion of the endothermic heat of reaction can be provided by the recirculating gases.

The final solution to this problem remains still to be engineered, but for the reasons given above, there is some indication that a reasonable

answer may be found, resulting in a reactor size per theoretical watt approaching that given in Figure 7.

The fuel cell batteries themselves are not finished products to be sure, and still require considerable development effort. Essentially this effort is directed towards extending the life of the devices, minimizing associated electrode polarization losses, and reducing cell costs. Considerable progress has been made on these problems and reports concerning this progress have been published by this laboratory.[6]

If these and other problems can be solved, the overall plant described in this paper provides a very attractive method for the gasification and utilization of coal. Because it uses air as the oxidizing agent, this raw material cost is negligible. However, because only oxygen enters the major system process stream, the gasification step proceeds as if pure industrial oxygen had been used, with no nitrogen dilution of the gasified products. It is reported that the cost of oxygen represents about 40-60% of the raw material costs of gasification processes using industrial oxygen.[15] Thus, if viewed only as a gasification unit, the process offers the possibility of reducing a major portion of the raw material costs.

In addition to this savings, however, the attractiveness of the proposed scheme comes from the fact that the plant utilizes the gasified coal products in an extremely efficient manner. It has been estimated that the overall efficiency of the proposed plant in converting coal to electricity will be about 60%.[13] Present day stations operate at efficiencies of about 38-42%, with very large installations required to attain the higher figure.[12] Since fuel costs represent about 40-50% of the cost of generating electricity by present-day techniques, the improved efficiency of the proposed plant represents a highly desirable improvement.

In order to attain this efficiency however, certain demands on system performance will have to be met. Table I lists the projected system characteristics and operating conditions based on an economic optimization of the system as currently envisioned.[13] On the basis of this study, it has been suggested that: 1) if bell-and-spigot cells with

an internal resistance of 0.25 Ω can be made and fabricated into banks for \$0.10 a cell; and 2) if a minimum payout time of 5 years can be used to recover the investment, return a profit, pay taxes, and provide maintenance (the cell life must obviously exceed 5 years), then coal-burning solid-electrolyte fuel-cell power systems can produce electrical energy at 5 mils/kw-hr; the system efficiency will be 60%, and the current density in the cell banks, will be 700 milliamps/cm^2.

TABLE I

Projected System	Characteristics
Overall Efficiency	60-70%
Cell Banks	
Current Density	700 ma/cm^2
Cubic Feet per Kilowatt	0.3 ft^3/kw
Reactor	
Volume per Kilowatt	0.1-5.0 ft^3/kw
System	
Recycle Ratio (moles recirculated per mole gasified)	3-6
Percent Fuel Burnup	95-98%

Cells have already been built which have an internal resistance of 0.3 Ω. The cost of materials for these cells is about \$0.004 for zirconia and \$0.03 for platinum, and effort is being expended to find suitable replacements for platinum to further reduce this raw material cost. Cells have operated at 750 milliamps/cm^2 for short periods of time on H_2 fuel. These facts indicate that solutions to the cell problems may be in the making. If they can be attained, along with reasonable solutions to the coal reactor problems, the proposed plant offers much promise as a power generation station of the future.

References

1. Archer, D. H., and Sverdrup, E. F., "Solid Electrolyte Fuel Cells," 16th Annual Proceedings, Power Sources Conference, May 22-24, 1962.

2. Archer, D. H., et al, "Westinghouse Solid-electrolyte Fuel Cell," 145th Nat. Meeting, ACS Division of Fuel Chemistry, Sept. 8-13, 1963.

3. Archer, D. H., Sverdrup, E. F., and Zahradnik, R. L., "Coal Burning Fuel Cell Power System," 53rd National A. I. Ch. E. Meeting, Feb. 2-5, 1964.

4. Archer, D. H., et al, "An Investigation of Solid-electrolyte Fuel Cells," Technical Document Report No. ASD-TDR-63-448.

5. Archer, D. H., et al, "An Investigation of Solid-electrolyte Fuel Cells - Third Quarterly Progress Report," AF 33(657)-8251; BPS 2-3-3145-60813-17.

6. Archer, D. H., et al, "Application of the Westinghouse Solid Electrolyte Feul Cell to Use in Space," 17th Annual Proceedings, Power Sources Conference, May, 1963.

7. Gadsby, J., Hinshelwood, C. N., and Sykes, K. W., Proc. Roy. Soc. (London) A187, 129-51 (1946).

8. Jolley, L. J., Poll, A., and Stanton, J. E., "Fluidized Gasification on Noncaking Coals with Steam in a Small Pilot Plant," Gasification and Liquifaction of Coal, AIME Publication, New York (1953).

9. Kingery, W. D., et al, "Oxygen Ion Mobility in Cubic $Zr_{0.85}Ca_{0.15}O_{1.85}$," J. Am. Cer. Soc., 42, 394 (1959).

10. Lewis, W. K., Gilliland, E. R., and McBride, G. T., Jr., Ind. Eng. Chem., 41, 1213-26 (1949).

11. May, W. G., Mueller, R. H., and Sweetser, S. B., Ind. Eng. Chem., 50, 1289-96 (1958).

12. Olmstead, L. M., Elec. World, Oct. 7, 1963.

13. Sverdrup, E. F., Zahradnik R. L. and Archer, D. H., "Fuel Cell Power Generation Systems: An Appraisal," IEEE Winter Power Meeting, Feb. 3-7, 1964.

14. Von Fredersdorff, C. G., Inst. Gas. Technol. Research Bull, No. 19 (1955).

15. Von Fredersdorff, C. G., and Elliot, M. A., "Coal Gasification," Chemistry of Coal Utilization, John Wiley & Sons, New York (1963).

16. Weissbart, J. and Ruka, R., "Solid Oxide Electrolyte Fuel Cells," Fuel Cells Vol. 2, Reinhold Publishing Corp. (1963).

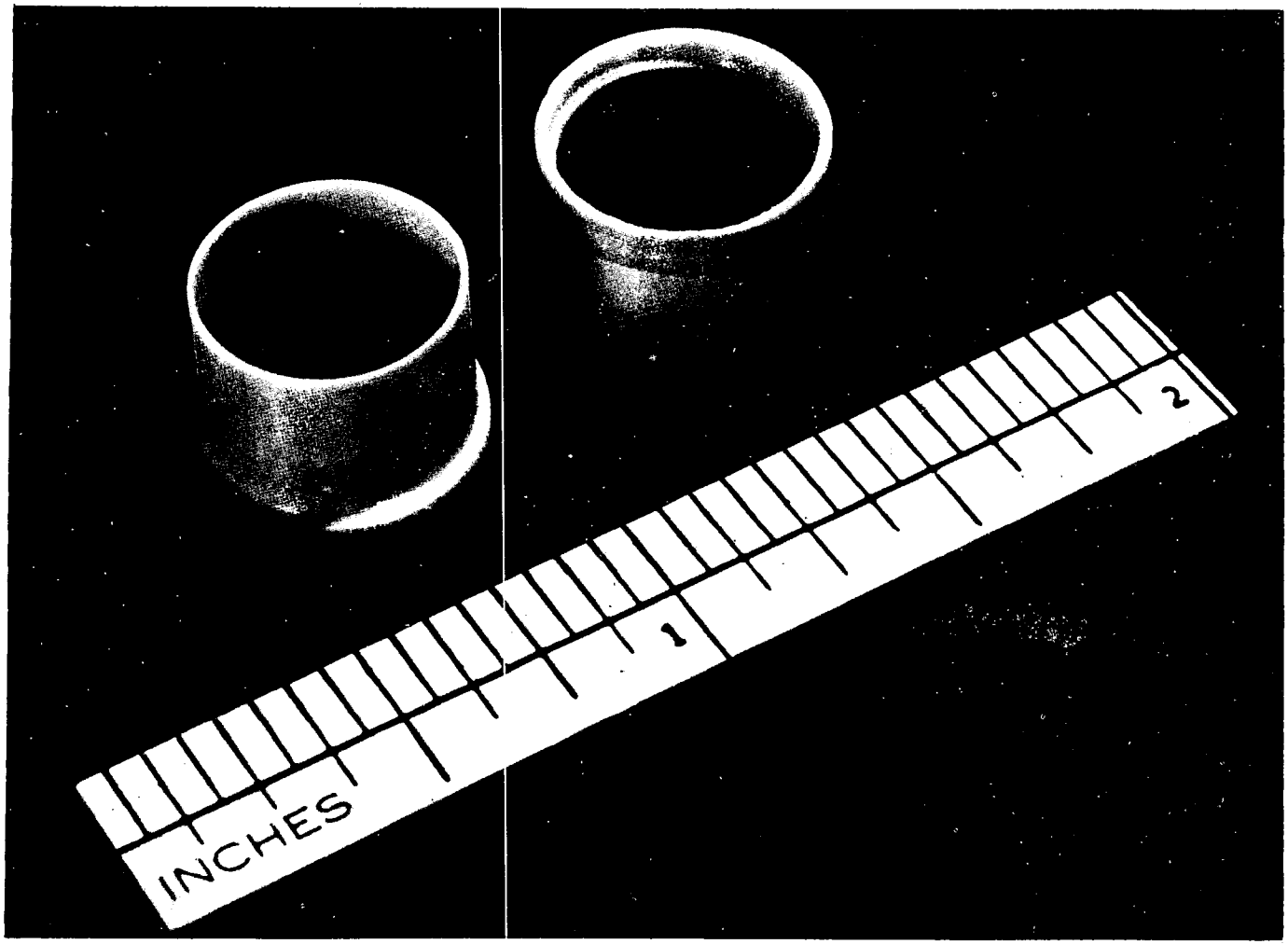

Figure 1 - Bell-and-Spigot Segments

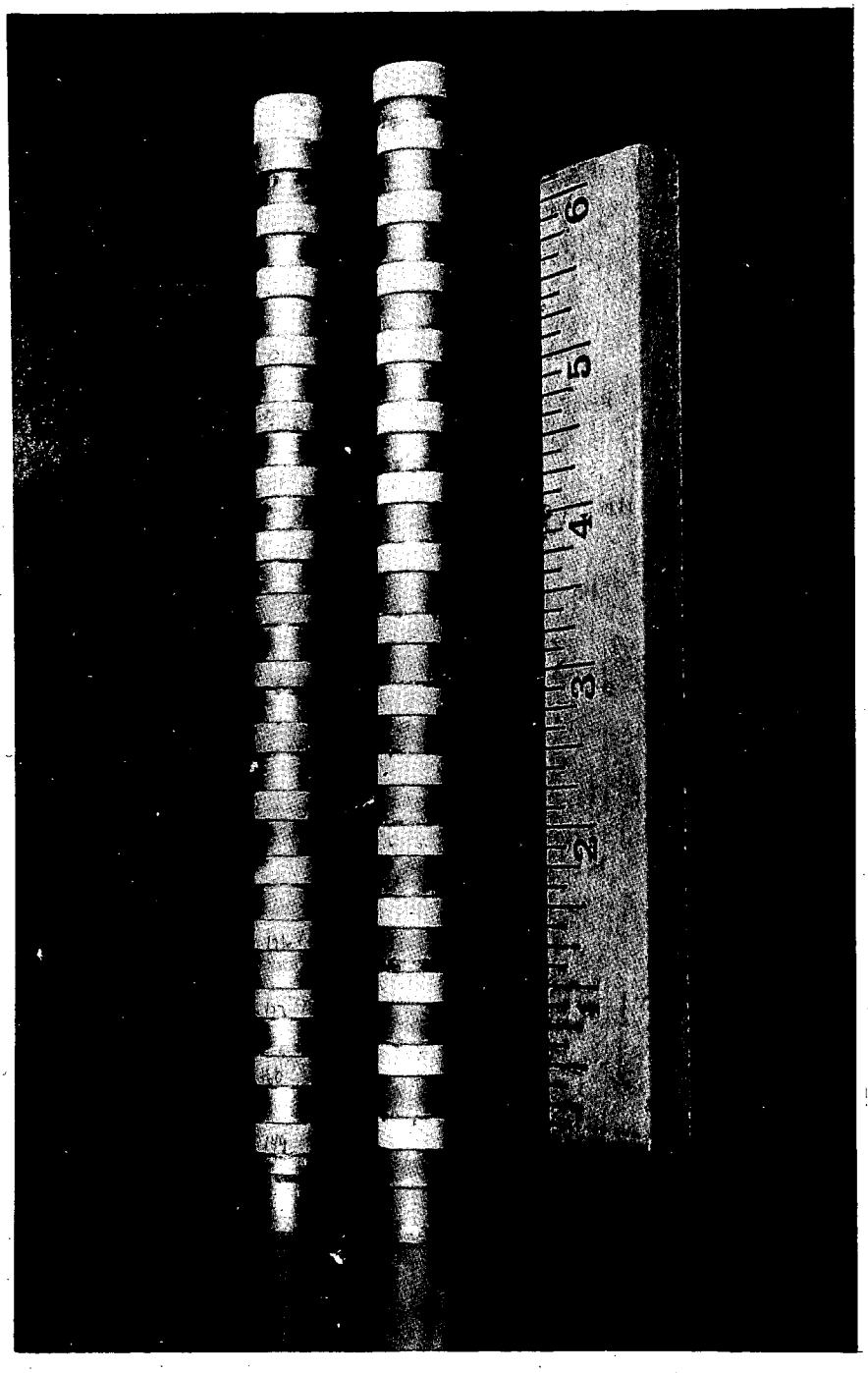

Figure 2 - Two 15 cell solid electrolyte fuel cell batteries without leads.

CLM 28480

DWG. 625A681

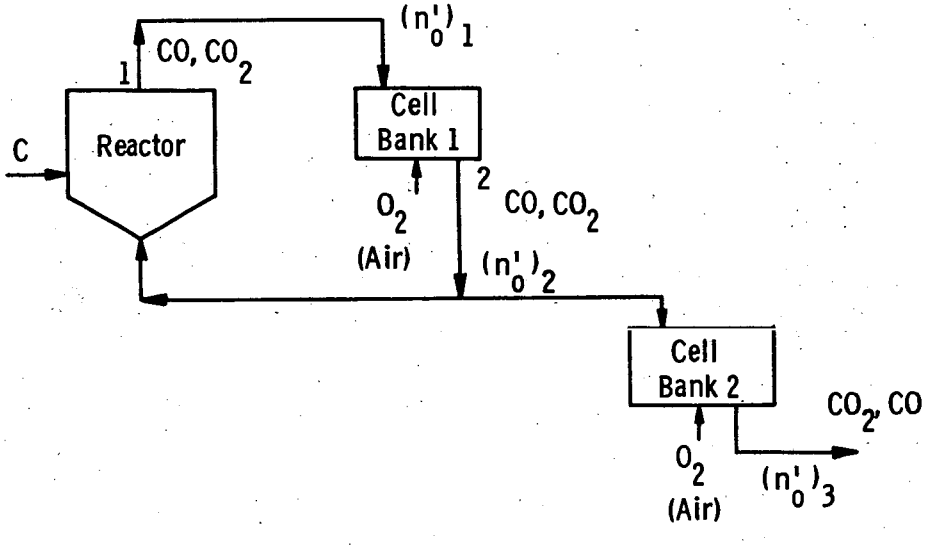

Fig. 3 — Simplified coal burning fuel cell system

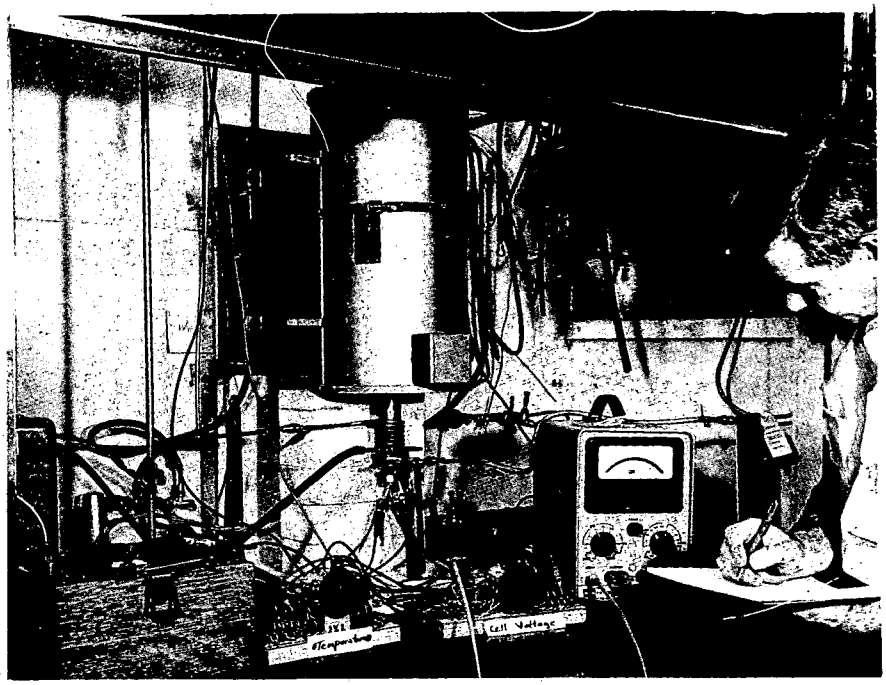

Figure 4 - Test Reactor

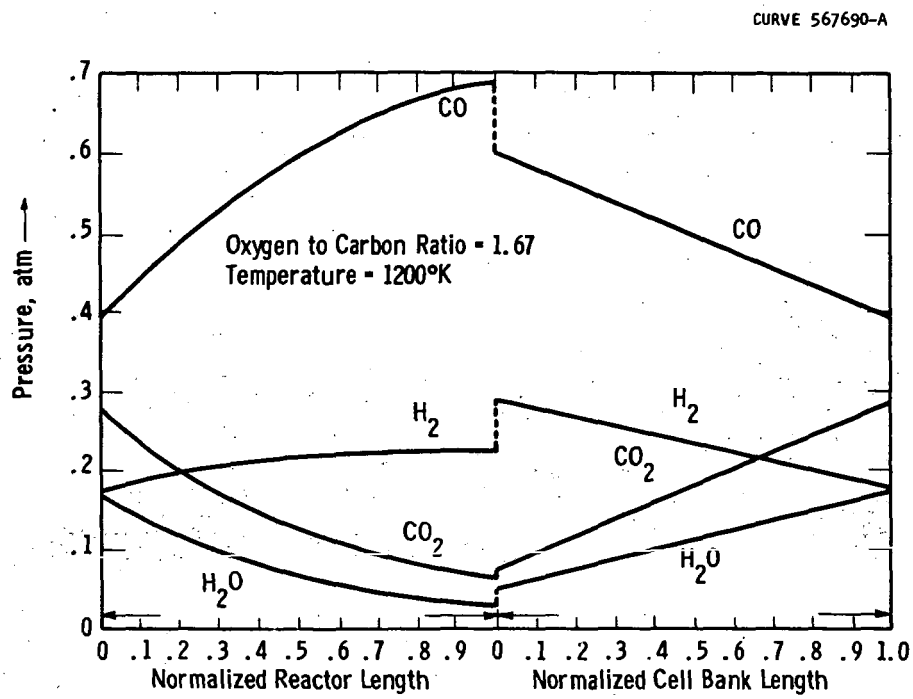

Fig. 5–Simulated reactor and cell bank concentration profiles

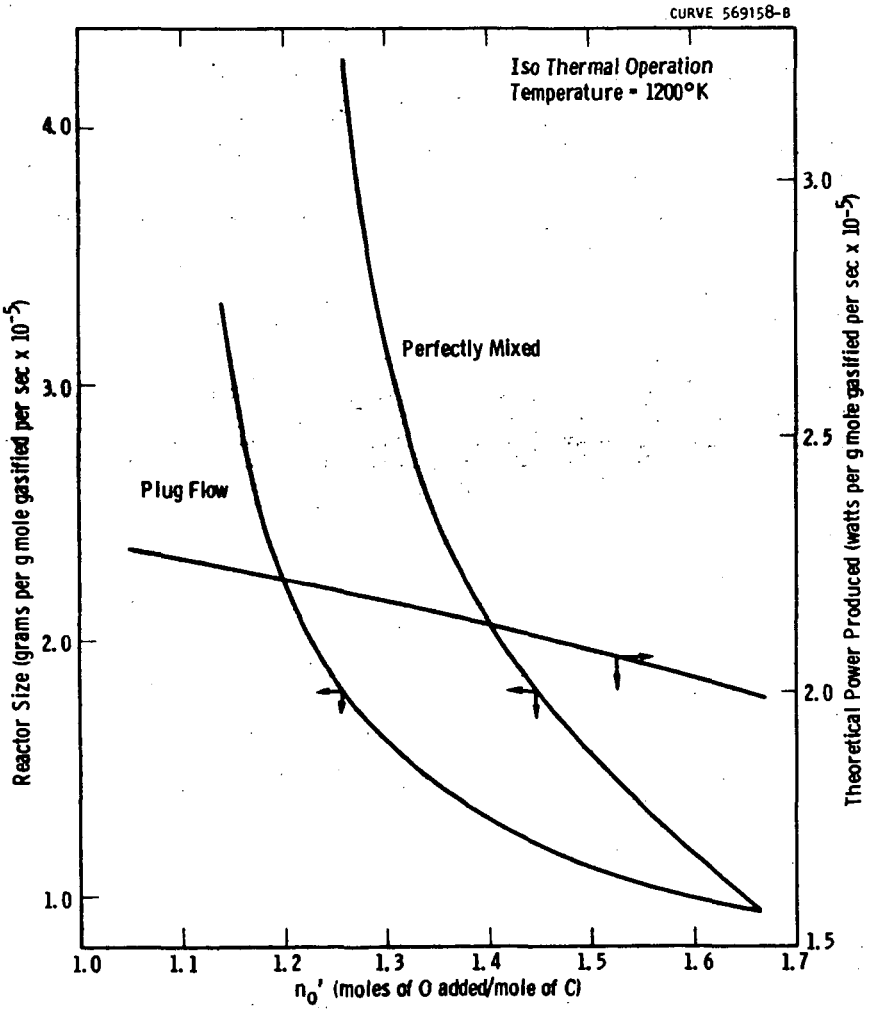

Fig. 6—Reactor size and system power vs conversion

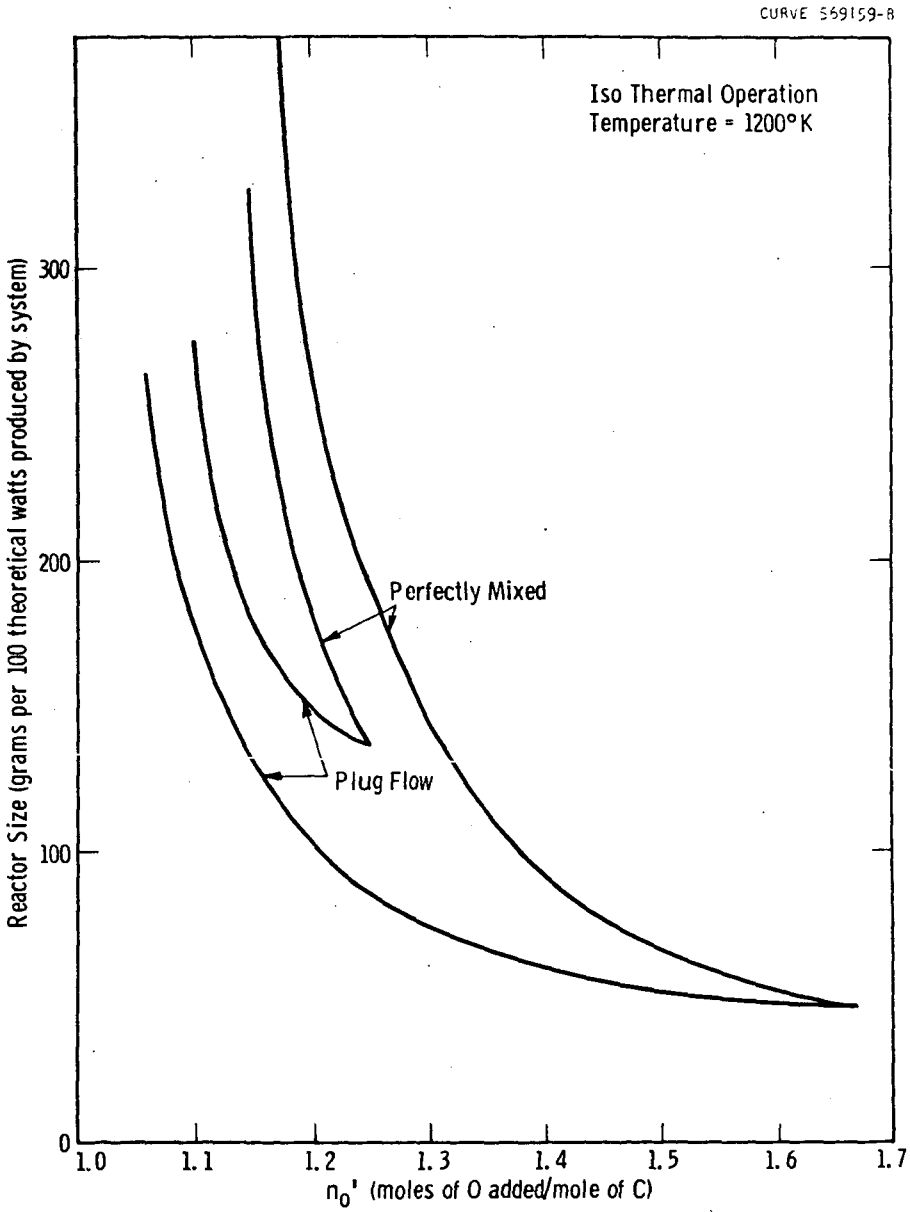

Fig. 7—Effect of conversion on normalized reactor size

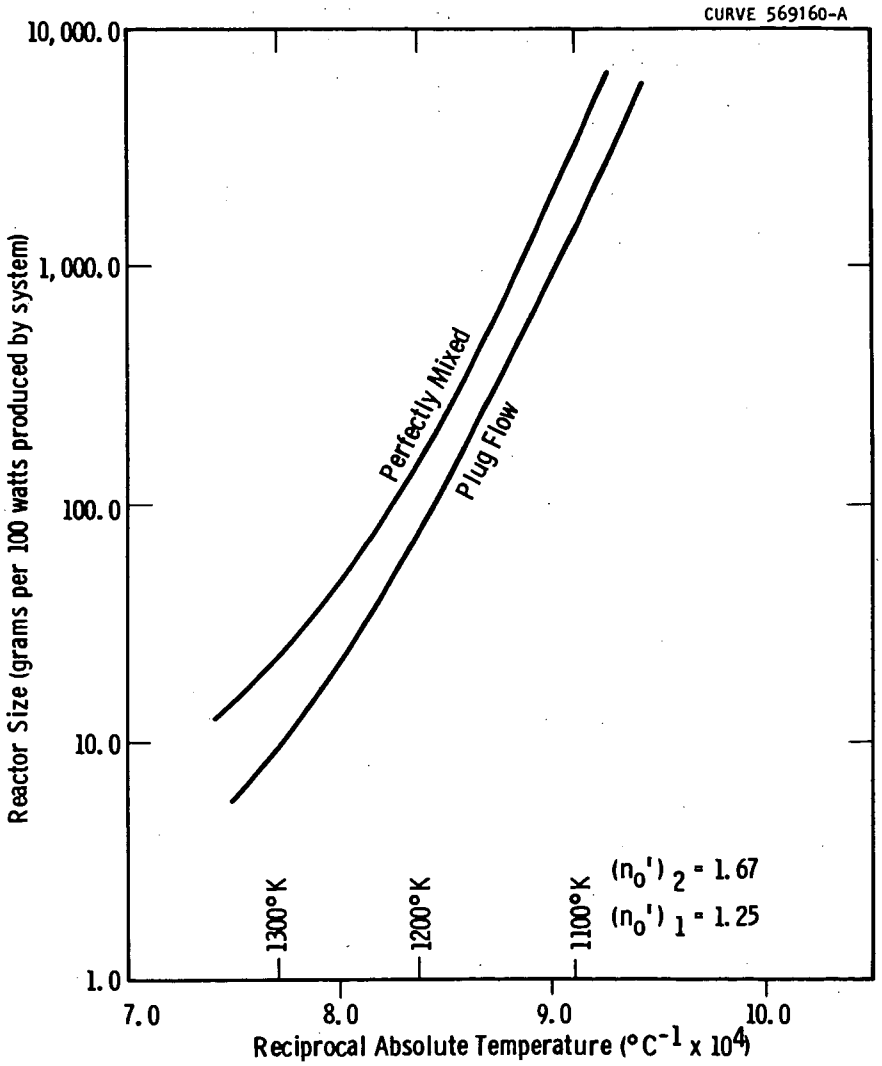

Fig. 8—Influence of temperature on reactor size

Carbon Dioxide Acceptor Gasification Process

By: G. P. Curran, C. H. Rice and E. Gorin

Research Division
Consolidation Coal Company
Library, Pennsylvania

- - - - - - - - - - - - - - -

Introduction

Production of both hydrogen rich and high BTU gas from coal has been under study in the Research Division of Consolidation Coal Company for several years. There are a number of partially or fully developed processes which are available for this purpose. These are all too expensive to be competitive with natural gas for the foreseeable future.

It is a feature of most of the available processes that oxygen is used to provide the endothermic heat of the gasification process. The high cost of oxygen is one of the more significant items which makes the conventional processes uneconomic.

It has thus become clear that elimination of oxygen is one of the prerequisites for the development of an improved process. The CO_2 acceptor process is one which satisfies this general objective. This paper describes some steps which have been taken in the development of the process. The emphasis is on a discussion of the properties of the acceptor as determined by the needs.

Process Description

The general principle of the CO_2 acceptor process is the use of a circulating lime-bearing acceptor.

The acceptor generates the heat required in the gasification step of the process by the reaction,

$$CaO + CO_2 = CaCO_3$$

The absorption of carbon dioxide serves also to enrich the gas in hydrogen. More heat is thus evolved by intensification of the two exothermic reactions,

$$CO + H_2O = CO_2 + H_2$$

$$C + 2\,H_2 = CH_4$$

It thus becomes possible to supply all the heat requirements of the gasification process by use of a suitable acceptor.

The acceptor is regenerated by calcining in a separate step the calcium carbonate at a higher temperature. The heat required is supplied by burning the residual char from the gasifier with air.

A number of variations in the acceptor process have been described in a series of U. S. patents[1]. A typical flowsheet of the process is illustrated in Figure 1. The char feed is passed sequentially through the series of process steps shown from the devolatilizer to the regenerator.

The elements of the process flowsheet have been studied individually. The product yields obtained in the devolatilization of low temperature chars produced from Pittsburgh Seam coals have been determined in a continuous 10 lb/hr[2] fluidized bed unit. Gasification of char with steam and oxygen has been studied in a 200 lb/hr fluidized pilot scale unit[6]. A detailed study has also been made of basic kinetics of the gasification reactions of char with pure hydrogen[8] and hydrogen-steam mixtures[4,5,9].

No operating data are available for the integrated process as shown in Figure 1. A detailed heat and material balance around the process is, however, given in Table I. These data represent reasonable projections of the operating conditions of the process based on available data on the kinetics and thermodynamics of the individual reactions involved.

The process conditions in the gasifier were determined from the kinetics data which show that the following approaches to equilibrium in the different reactions are reasonable.

	Percent Approach to Equilibrium
$C_{(graphite)} + 2\ H_2 = CH_4$	80
$CO + H_2O = CO_2 + H_2$	100
$C_{(graphite)} + H_2O = CO + H_2$	24.5

In Table I the CO_2 present in the gasifier is equivalent to the equilibrium CO_2 pressure for the acceptor reaction. Although our data show this reaction to be rapid, a small partial pressure driving force actually would be required.

The flowsheet and material balance serves largely as a framework for the discussion of required acceptor properties. Since the acceptor is the heart of the process, selection of a suitable material is the required first step in the process development.

The acceptor must be physically rugged, such that it resists excessive attrition and thus is separable in the regenerator from the finely-divided char ash. It must be resistant to chemical deactivation caused by repeated cycling through the conditions imposed in the process as well as by interaction with char ash. Finally, the conditions within the gasifier and

regenerator must be consistent with the thermodynamic properties of the acceptor.

One feature of the acceptor which will be discussed in more detail later is its tendency to melt at certain conditions. For the conditions listed in Table I, this property necessitates that the partial pressure of steam does not exceed about 13 atmospheres. In Figure 1, this is accomplished, as shown, by recycling about 45 percent of the gasifier effluent and mixing with the incoming steam.

Experimental Method

The initial exploratory studies were carried out in the 1-1/2" I.D. high pressure Uniloy reactor system used in the earlier kinetics studies of the H_2-H_2O-char system[4].

The studies on the properties of the acceptor were carried out in the equipment shown schematically in Figure 2. The acceptor solids, usually prescreened to a size of 24 x 28 mesh were treated in a 1" I.D. x 8" long fluidized bed reactor. The thin-walled, stainless steel reactor was contained along with its electrically heated furnace in a one-liter high pressure autoclave.

For atmospheric pressure work, a quartz reactor was used to replace the high pressure reactor. The process gas in both reactors is introduced axially down through a dip tube, reverses direction and fluidizes the acceptor. The quartz tube reactor was heated by immersion in a fluidized sand bed furnace.

The reactor was supplied either with metered dry gas (CO_2, N_2, and any desired premixed blend containing CO_2, N_2, SO_2, H_2S, and H_2) or with dry gas-steam mixtures. In the latter instance, the metered dry gas was passed through the steam generator. Steam partial pressure was determined by the water temperature in the generator which was controlled to $\pm$ 0.1°F.

The composition of the dry effluent gas was monitored continuously by a thermal conductivity cell. Dry feed gas was supplied continuously to the reference side of the cell.

Measurements of the equilibrium constants in several reactions of interest were made in the above equipment. A detailed description of the methods used and the results of this work will be published separately.

For study of deactivation at process conditions, the acceptor was put through a series of carbonation and calcination cycles which simulated the process conditions illustrated in Figure 1 and Table I. The charge to the reactor was 6 grams of 24 x 28 mesh acceptor and 60 grams of 100 x 150 mesh granular fused periclase which was used as an inert diluent. The diluent was used to minimize reaction heat effects and consequently to provide better temperature control in the carbonation and calcining steps. The total pressure

was adjusted to 8.87 atmospheres and the bed fluidized with a CO_2-N_2 mixture. The partial pressure of CO_2 was 5-8 atm. depending on the desired calcining temperature. The superficial gas velocity was held between 0.3-0.4 ft/sec at all times.

The bed was then heated rapidly to the calcining temperature which was held for different runs at 1900°F, 1950°F and 2000°F. The effluent gas analyzer monitored the course of the calcining. Upon completion of calcining, the inlet gas composition was adjusted to give 1.5 atm. CO_2 partial pressure and the bed was cooled rapidly to 1700°F when 7.0 atm. steam partial pressure was substituted for most of the nitrogen. The bed temperature was then decreased to 1650°F where it was held until recarbonation was essentially complete as shown by the effluent gas analyzer. Nitrogen was substituted at this point for steam and the cycle repeated for the desired number of times. The time required for a complete cycle was 20-25 minutes.

At the end of the prescribed number of cycles the acceptor was fluidized at 1650°F with an N_2-CO_2 gas mixture containing 1.5 atm. partial pressure of CO_2 and held under these conditions for 15 minutes. The acceptor was then cooled rapidly and tested for activity.

A Chevenard thermobalance modified by using a linear transducer to detect beam position and sample weight was used to arrive at a standard activity measurement.

The acceptor sample (about 200 milligrams) was placed in a monolayer between two stainless steel screens held by a ring which rested on the support rod. Gas flow downward through the particles maintained differential conditions with respect to the CO_2 partial pressure exterior to the particles.

The thermobalance was operated isothermally at 1525°F and at atmospheric pressure. Calcining and recarbonation were accomplished by changing the composition of the gas flowing through the sample holder. The gas inlet system provided practically instantaneous change from N_2 used for calcining to CO_2 used for recarbonation. The flow rates of each of the gases were chosen so that the combined effects of buoyancy and velocity head were the same.

The sample first was calcined and the weight loss recorded. It was then recarbonated for a standard time period of 7 minutes.

The standard activity value used in the discussion which follows is an average carbonation ratio, R, from the two above operations defined as follows:

$$R = \frac{(\text{Wt. Loss } CO_2 \text{ in gms} + \text{Wt. gain } CO_2 \text{ in gms})}{2\ (\text{gms Theoretical } CO_2 \text{ Content})} = \frac{\text{Average } CaCO_3}{CaCO_3 + CaO}$$

The study of potential activity loss due to repeated sulfiding of the acceptor and regeneration of the CaS formed was made in the quartz tube reactor. The acceptor was sulfided in an H_2S-H_2 mixture at 1650°F and was regenerated by fluidizing in air at 1950°F until SO_2 evolution ceased.

An accelerated test for potential deactivation due to interaction with ash was used. Acceptor sized to 20 x 24 mesh in either the carbonate or oxide form was briquetted using a Celvacene grease binder with -100 mesh ash in a weight ratio of 53 parts acceptor in oxide form to 30 parts of ash. The ash was derived by air combustion of char from Pittsburgh Seam coal in a fluidized bed. Ash was used in both oxidized and reduced forms. The briquets were calcined at 1500°F and crushed. The +8 mesh fragments were treated for 16 hours in a fixed bed at various temperatures and with several different types of atmospheres. In some cases after the initial treatment, the acceptor-ash fragments were subjected to the standard cycling between carbonation and calcination. A final activity test was then run in the thermobalance as described above after the acceptor had been cleaned of adhering ash.

Results and Discussion

a. Fixed Bed Experiments

The initial experiments using a fixed bed of char and lime demonstrated the basic feasibility of the process from the chemical point of view. Comparative results from a pair of fixed bed runs with and without lime present are shown in Table II. The char used here is the same devolatilized "Disco" char earlier employed in the kinetics studies. Sand was used in the blank experiment to give the same volumetric ratio of char to inorganic material.

The data of Table II are without a great deal of quantitative significance due to uncontrolled temperature gradients in the bed and variation of carbon burnoff with time. They do illustrate, however, the principle of the CO_2 acceptor method in providing for removal of carbon dioxide from the gas with simultaneous enrichment of the product gas in hydrogen and methane.

b. Study of Melt Formation

In the fixed bed run, the acceptor melted at the conditions used. Subsequent investigations showed that neither melting or agglomeration occurs in a fluidized bed of acceptor at 1650°F and 11 atm. steam partial pressure, over the entire range of carbonation ratios. A detailed investigation of melt formation is now underway. Results so far show that the steam partial pressure may be as high as 13 atm. at 1650°F without forming the melt, and that the melt is a ternary liquid composed of $Ca(OH)_2$, $CaCO_3$, and CaO. Phase equilibria behavior of this interesting system will be published when the work is completed.

c. Thermodynamic Limitations

Equilibria in the reactions given below are the most pertinent to the process:

$$CaO + H_2S = CaS + H_2O \qquad (1)$$

$$1/4\ CaS + 3/4\ CaSO_4 = CaO + SO_2 \qquad (2)$$

$$CaCO_3 = CaO + CO_2 \qquad (3)$$

The experimentally determined values for reaction (1) are given in Table III. No reliable values for this equilibrium have been available in the literature previously.

The experimentally determined values for reaction (2) are shown in Figure 6. The values check well with those previously determined by Zawadski[7].

The data in reaction (3) are shown in Figure 5. Some of the literature data imply that the equilibrium CO_2 pressure depends on the origin of the calcium carbonate. Our measurements on stones ranging in composition from pure limestone to impure dolomite, and having widely different geologic origins, have shown that the equilibrium CO_2 pressure is independent of all conditions except temperature. Figure 5 shows that our data agree very well with those of Smyth and Adams[3], who used pure calcite as the source of $CaCO_3$. These data must now be accepted as providing the correct values.

Experimentally, all three reactions have been shown to be rapid and equilibrium should be closely approached in actual operation of the process. The high values for the equilibrium constants in reaction (1) mean that substantially all the sulfur released from the char in the gasifier will be absorbed by the acceptor as CaS. This sulfur must be rejected as SO_2 in the regenerator. The regenerator must be operated with a slight deficiency of oxygen such that there is no oxygen breakthrough. Under these conditions the equilibrium for reaction (2) is controlling.

Reaction (3) determines the minimum temperature for operation of the regenerator to provide a driving force for calcination of the acceptor. The required temperature is higher, of course, the higher the operating pressure of the system. The operating pressure is thus set by steam pressure limitation in the gasifier, i.e., less than 13 atmospheres and by the limitation set on regeneration temperature by the equilibrium in reaction (3). It is on this basis that the operating pressure of 300 psia used in the illustrative example in Figure 1 and Table I was arrived at. Further calculations show that the driving force for the calcining reaction goes to zero at 1935°F and a pressure of 300 psia.

The sulfur rejection reaction (2) is not controlling since as the data in Table IV show the relative driving force is much greater than for the calcining reaction. The sulfur rejection problem would become limiting only for coals whose sulfur content is well beyond that of most steam coals.

d. Acceptor Selection

The choice of acceptor solids is determined by the factors of physical strength, high reactivity in carbonation and calcination reactions and resistance to deactivation upon exposure to process conditions.

A number of limestones and dolomites satisfactorily met the first two conditions. The reactivity for calcining and recarbonation reactions are also suitably high. Examples of the reactivity of a typical dolomite both in fresh and thermally treated conditions are given in Figures 3 and 4.

The data in Figures 3 and 4 show the rate of the calcining and recarbonation reactions as measured on the thermobalance at 1525°F in a nitrogen and CO_2 atmosphere, respectively. It is noted that in either case the reaction is nearly complete after 2 minutes exposure time. A more detailed kinetic study is now in progress.

None of the limestones or impure dolomites, however, showed sufficient resistance to deactivation under process conditions to be useful in the process. A dolomite from Western Ohio (Greenfield formation) had excellent resistance to deactivation and was selected for further detailed study.

The reserves of the Greenfield dolomite are sufficiently large so that it would be a logical choice for a future gasification plant located in either Illinois or the Ohio River Valley.

Analysis of the Greenfield stone is given below:

	Wt. %
$CaCO_3$	52.28
$MgCO_3$	44.61
$Al_2O_3 + SiO_2 + Fe_2O_3$	2.24
$FeCO_3$	0.20
Unaccounted for	0.67

At process conditions and at all experimental conditions used in this work, the $MgCO_3$ component of dolomite is unstable and decomposes to form MgO which is completely inert at these conditions.

e. Deactivation Under Process Conditions

The effect of cycling the 24 x 28 mesh Greenfield dolomite through simulated process conditions is shown in Table V. In no case did the activity decrease significantly below 0.80 Standard Carbonation ratio. Since some fresh acceptor make up inevitably will be required because of incomplete separation of the acceptor and spent char in the regenerator, the equilibrium activity of the recirculating acceptor will be at a level somewhat above 0.80.

The physical strength of the stone is remarkably high. At least 98 percent and usually at least 99 percent of the original acceptor was recovered as +48 mesh material after each one of the above tests.

The makeup requirements for the process in Table I were based on 94 percent recovery of the regenerated acceptor from the spent char in the regenerator which is adequately conservative.

A similar series of runs were carried out in which the Greenfield dolomite was converted to CaS followed by regeneration of the CaO by oxidative decomposition of the CaS at 1950°F. No deactivation of the stone due to the sulfur cycle was noted.

The stone is also highly resistant to deactivation by interaction with char ash as the results in Table VI show. The activity of the acceptor on exposure to ash does not depend upon the oxidation states of the ash that can exist at process conditions, nor on the extent of carbonation of the lime.

BIBLIOGRAPHY

(1) Consol CO_2 Acceptor Patents

E. Gorin	U.S. 2,654,661	Oct. 6, 1953
E. Gorin	U.S. 2,654,662	Oct. 6, 1953
E. Gorin	U.S. 2,654,663	Oct. 6, 1953
E. Gorin	U.S. 2,682,455	June 29, 1954
E. Gorin	U.S. 2,682,456	June 29, 1954
E. Gorin	U.S. 2,682,457	June 29, 1954
E. Gorin	U.S. 2,705,672	April 5, 1955
R. P. Tarbox	U.S. 2,807,529	Sept. 24, 1957
E. Gorin and W. B. Retallick	U.S. 3,108,857	Oct. 29, 1963
E. Gorin and C. H. Rice	U.S. 3,115,394	Dec. 24, 1963

(2) Batchelor, J. D., Gorin, Everett, and Zielke, C. W., Ind. Eng. Chem., 52, 161 (1960).

(3) Smyth, F. H. and Adams, L. H., JACS, 45, 1167 (1923).

(4) Goring, G. E., Curran, G. P., Tarbox, R. P., and Gorin, Everett, Ind. Eng. Chem., 44, 1057 (1952).

(5) Goring, G. E., Curran, G. P., Zielke, C. W., and Gorin, Everett, ibid, 45, 2586 (1953).

(6) Unpublished Data, Consolidation Coal Company.

(7) Zawadski, J., Z. Anorg. Chem., 205, 180 (1932).

(8) Zielke, C. W. and Gorin, Everett, Ind. Eng. Chem., 47, 820 (1955).

(9) Zielke, C. W. and Gorin, Everett, ibid 49, 396 (1957).

TABLE I

Material Balance in CO_2 Acceptor Process

Basis: 100 lbs MAF Char Feed, Pressure - 300 psia

Unit Operation	Devolatilizer				Gasifier				Regenerator			
	Input		Output		Input		Output		Input		Output	
	Temp., °F	Mols	Temp., °F	Mols	Temp., °F	Mols	Temp., °F	Mols	Temp., °F	Mols	Temp., °F	Mols
MAF Char (lbs)	800	100	1470	80.12	1470	80.12	1650	22.27	1650	22.27	--	--
Char Ash (lbs)	800	13.3	1470	13.3	1470	13.3		13.3		13.3	--	--
MgO·CaO	--	--	--	--	1950	2.338		0.442		0.442	1950	2.338
$MgO \cdot CaCO_3$	800	0.138	1470	0.138	--	--		1.872	1637	2.010	--	--
MgO·CaS	--	--	--	--	--	--		0.024	1650	0.024	--	--
H_2	1650	4.835	1390	4.971	--	--	1650	4.835	--	--	--	0.001
CH_4		0.789		1.481	--	--		0.789	--	--	--	--
CO		1.466		1.396	--	--		1.466	--	--	1950	0.075
CO_2		0.481		0.740	--	--		0.481	--	--		3.448
$H_2O(g)$		2.106		1.926	1450	8.214		2.106	--	--		0.113
N_2		0.025		0.057	--	--		0.025	--	--		5.834
H_2S		0.004		0.045	--	--		0.004	--	--		--
SO_2	--	--	--	--	--	--	--	--	--	--		0.031
Air	--	--	--	--	--	--	--	--	320	7.361		
Reject Stream												
Char MAF (lbs)											1950	3.17
Ash (lbs)												13.15
CaO·MgO (mols)												0.138

Feed Char - Pgh. Seam, LTC Char (900°F)

	H	C	N	O	Org. S
Ultimate Analysis (MAF)	3.72	87.25	1.84	5.24	1.94
Heating Value, Btu/MAF lb			14,480		

Ash (lbs/100 lbs MAF Char)

Total	13.29
Inorganic Sulfur	0.48

TABLE II

Comparative Fixed Bed Runs in the Presence and Absence of Lime

Steam Feed Rate, 8.8×10^{-3} mols/hr. Total Pressure, 30 atm.

Run	Wt. Solids Charged lbs	Average Dry Make Gas Composition				Steam Conversion %	Median Bed Temp. °F
		CO_2	H_2	CH_4	CO		
Blank	(Char - 0.5 (Sand - 1.87	23	48	9	20	*	1620
Lime	(Char - 0.5 (Lime - 0.87	0.5	79.5	17	3	70	1640

* Not determined.

TABLE III

Equilibrium Data in Reaction

$CaO + H_2S = CaS + H_2O$

°F	$K = H_2O/H_2S$
1310	2030
1420	1320
1550	837
1660	587

TABLE IV

Thermodynamic Driving Force in
Regenerator at 1950°F and 300 psia

P_{CO_2} Driving Force Atm.	0.55
P_{CO_2}/Equil. P_{CO_2}	0.93
P_{CO_2}/Equil. P_{CO_2}	0.37

Regenerator Effluent Gas, Mol %

H_2	0.01
CO_2	36.29
N_2	61.39
H_2O	1.19
CO	0.79
SO_2	0.33

TABLE V

Effect of Cycling Greenfield Dolomite (24 x 28M)
Thru Simulated Process Conditions

Recarbonation Conditions - 1650°F - 1.5 atm. CO_2 - 7.0 atm. H_2O

Calciner Temp.	Total Time at Process Conditions, hrs.	No. of Cycles	Std. Carb. Ratio
1900°F	2.9	2	0.87
↓	2.2	5	0.77
	7.4	5	0.80
	8.0	20	0.80
1950°F	2.3	5	0.81
↓	5.5	12	0.81
	8.5	20	0.76
2000°F	2.5	5	0.81
↓	6.0	12	0.77

TABLE VI

Effect of Ash

The acceptor was briquetted with ash and held for 16 hours at the conditions listed.

Run	Form of Acceptor	Form of Ash	°F	No. of Cycles	Ambient Gas	Std. Carb. Ratio
Q22	oxide	oxidized	1650	1	air	.81
Q19	↓	reduced(1)	1650	1	H_2	.90
Q20	↓	reduced	1900	1	H_2	.76
Q24	↓	oxidized	1900	1	(2)	.76
H76	carbonate	↓	1900	0	(2)	.80
Q33	oxide	↓	1950	5	(2)	.76

(1) Ash in form of 70% burnoff char.
(2) Inlet gas was 90% CO_2-10% H_2 which was converted by the water gas shift reaction at run conditions to the following composition: CO_2 80.5 mol %, H_2 0.5%, H_2O 9.5%, CO 9.5%.

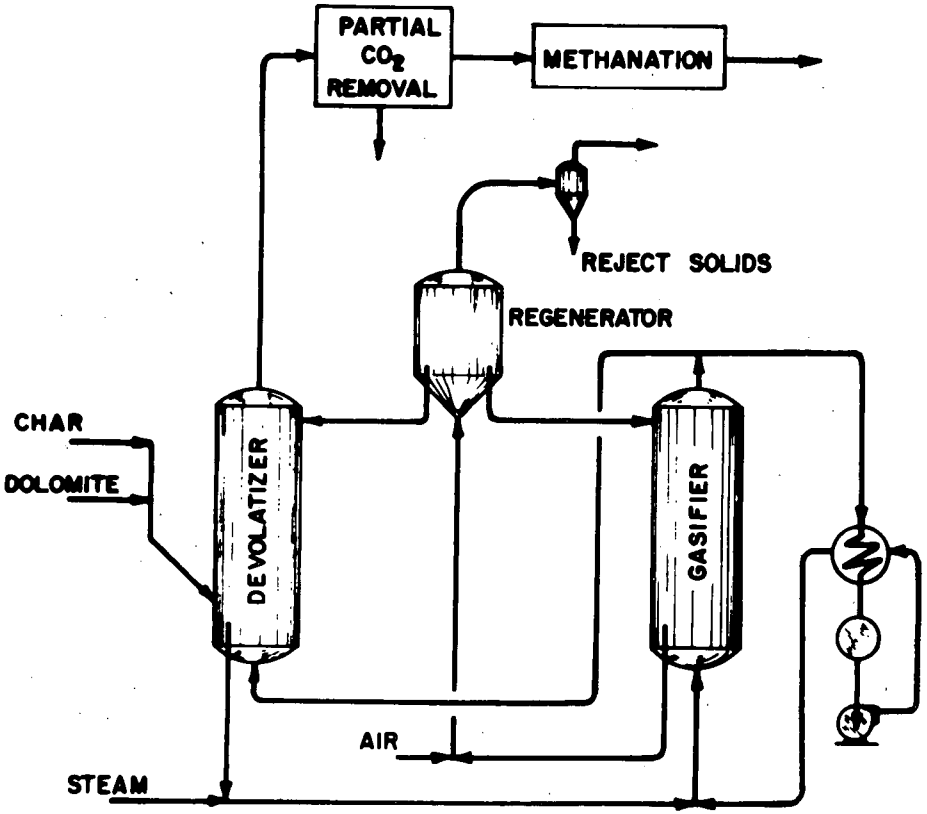

FIGURE 1

FLOW DIAGRAM
CO_2 ACCEPTOR PROCESS

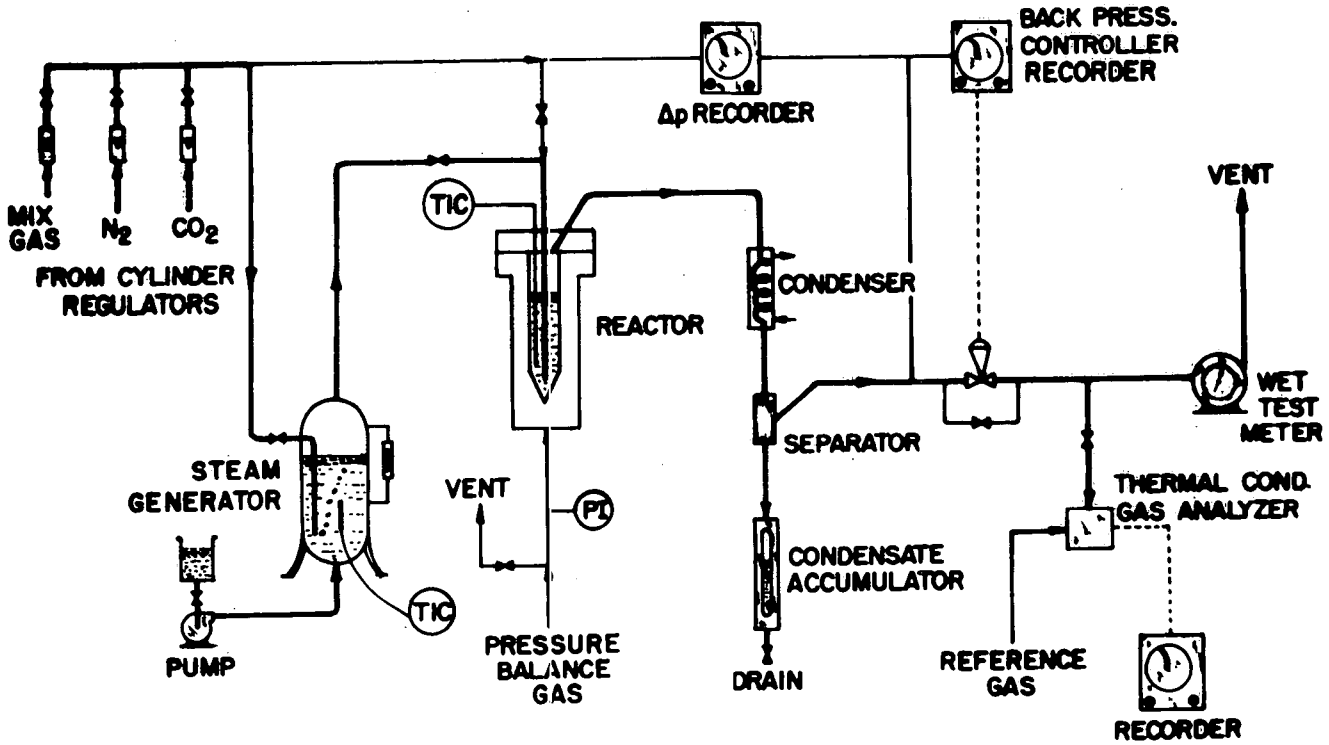

FIGURE 2

FLOW DIAGRAM
GASIFICATION BENCH UNIT

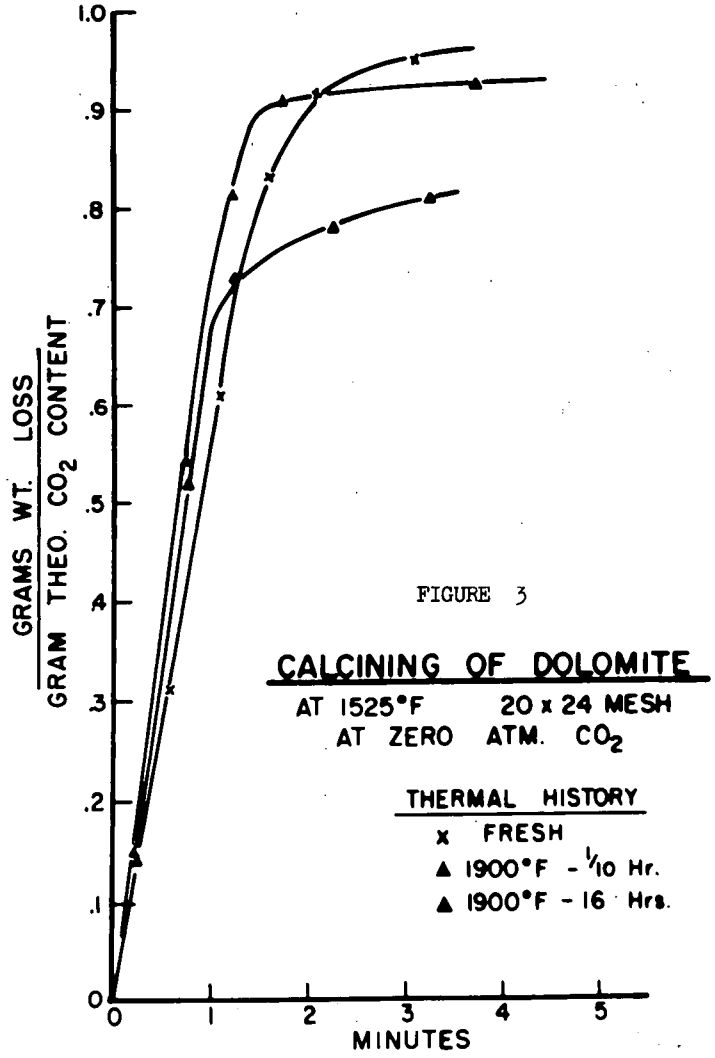
1.0
.9
.8
.7
.6
.5
.4
.3
.2
.1
0
GRAMS WT. LOSS / GRAM THEO. CO_2 CONTENT
0
1
2
3
4
5
MINUTES
CALCINING OF DOLOMITE
AT 1525°F 20 x 24 MESH
AT ZERO ATM. CO_2
THERMAL HISTORY
x FRESH
▲ 1900°F - 1/10 Hr.
▲ 1900°F - 16 Hrs.

FIGURE 3

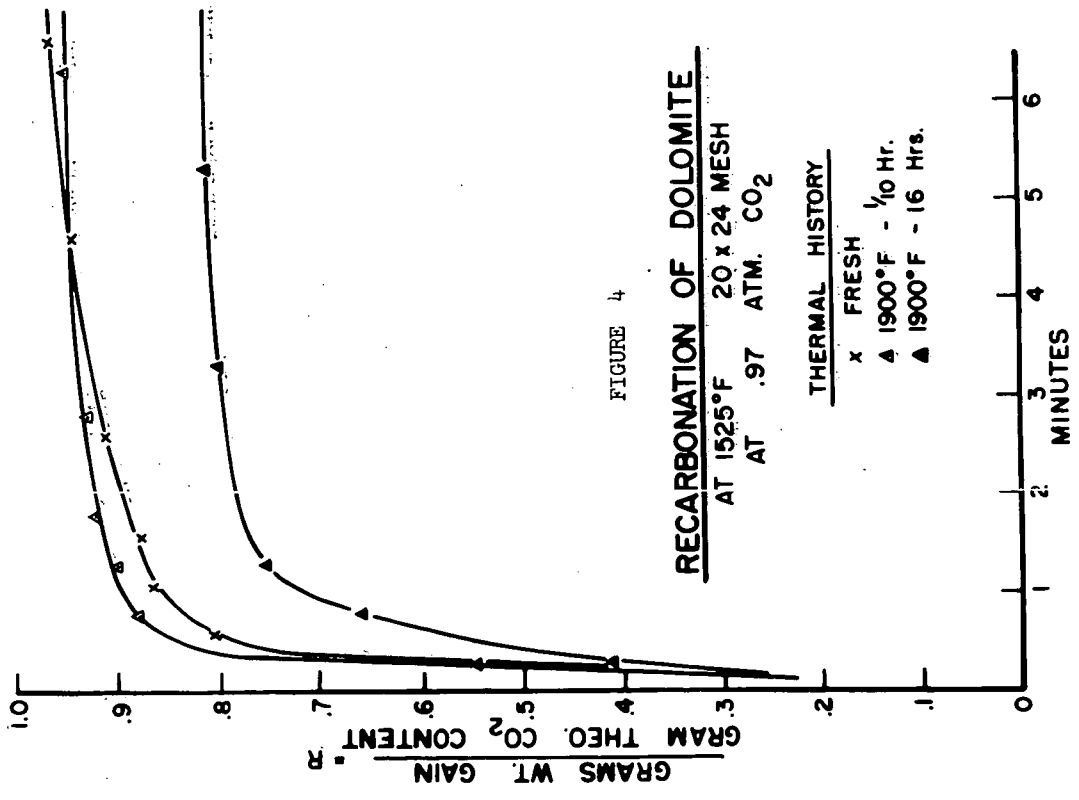
RECARBONATION OF DOLOMITE
AT 1525°F 20 x 24 MESH
AT .97 ATM. CO_2
THERMAL HISTORY
x FRESH
▲ 1900°F - 1/10 Hr.
▲ 1900°F - 16 Hrs.
GRAMS WT GAIN / GRAM THEO. CO_2 CONTENT = R
MINUTES
0
1
2
3
4
5
6
.1
.2
.3
.4
.5
.6
.7
.8
.9
1.0

FIGURE 4

FIGURE 5

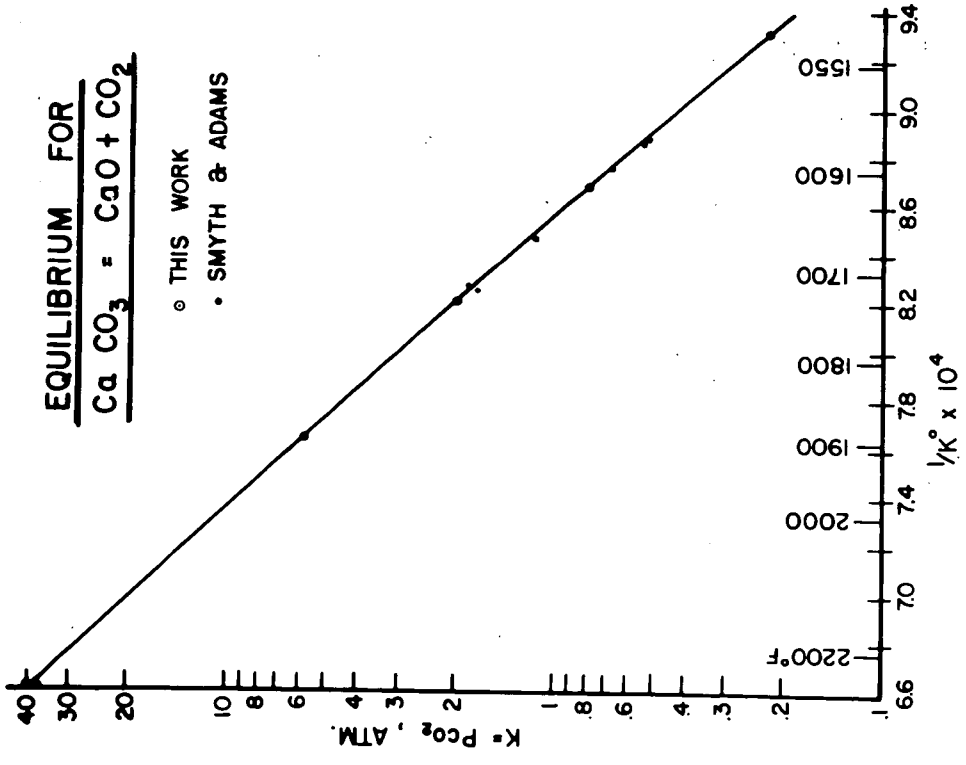
EQUILIBRIUM FOR
Ca CO3 = CaO + CO2
⊙ THIS WORK
• SMYTH & ADAMS
K = PCO2 , ATM.
40
30
20
10
8
6
4
3
2
1
.8
.6
.4
.3
.2
.1
2200°F
2000
1900
1800
1700
1600
1550
6.6
7.0
7.4
7.8
8.2
8.6
9.0
9.4
1/K° x 10⁴

FIGURE 6

EQUILIBRIUM FOR

$\frac{1}{4}$ CaS + $\frac{3}{4}$ $CaSO_4$ = CaO + SO_2

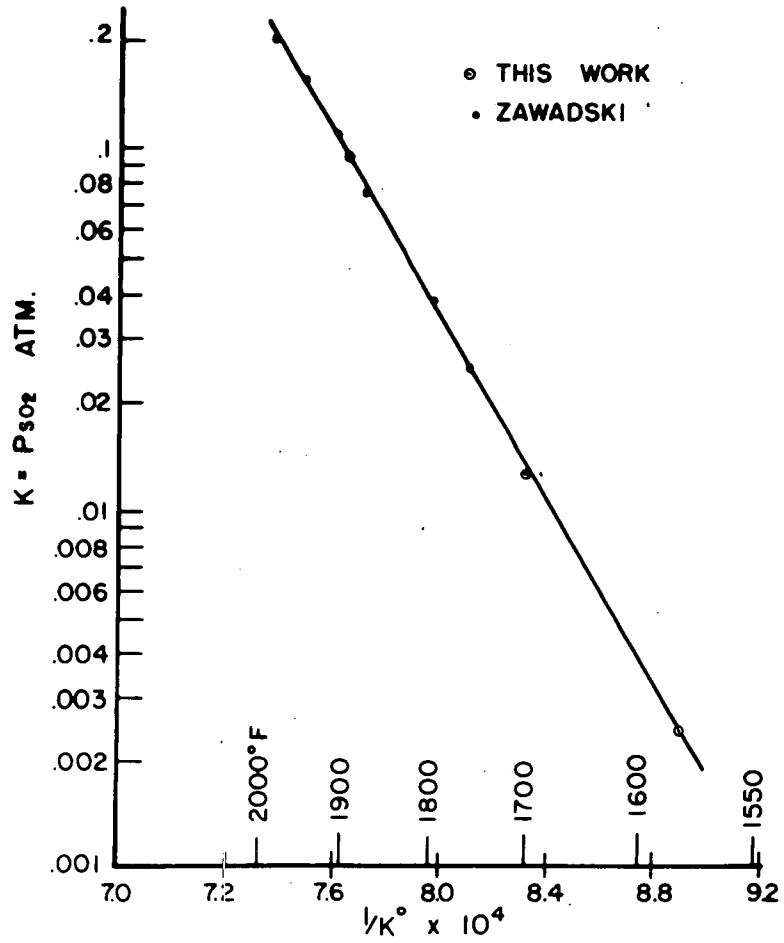

A KINETIC STUDY OF COAL HYDROGASIFICATION— THE RAPID INITIAL REACTION

C. Y. Wen

Institute of Gas Technology
Chicago 16, Illinois

INTRODUCTION

The production of synthetic methane from coal by hydrogasification has considerable economic potentiality. A number of experimental studies of coal hydrogasification have been reported during the last few years. Only a few studies were concerned with reaction kinetics. A thorough literature survey has been presented elsewhere. (3)

There are many problems associated with coal hydrogasification which must be solved before the process can become economically feasible. One of the important problems is concerned with the properties of coal which affect hydrogasification. From a reaction-kinetic point of view, carbon in coal consists roughly of two types differing greatly in reactivity – the portion associated with the volatile matter and the remainder corresponding to the residual carbonaceous matter, coke.

Under the high temperatures and pressures required for hydrogasification, coals tend to soften and agglomerate, thus preventing free flow through the reactor. Pretreatment of coal, therefore, has been required in moving-bed or fluidized-bed reactor operation. Roughly, 30 percent of the carbon in coal is in the form of volatile matter which reacts rapidly with hydrogen to form methane at temperatures ranging from 1300° to 1800°F. and pressures ranging from 50 to 200 atmospheres. The remainder of the carbon reacts very slowly and the reaction rate is subject to more severe equilibrium hindrance. (3) During the pretreatment of coal, which usually involves oxidation or charring of the coal surface by air or other gases to produce a protective film, a great portion of the reactive volatile matter is lost. In most cases, approximately one half of the volatile matter carbon content is lost in pretreatment.

It is quite appropriate, therefore, to search for means of utilizing unpretreated coals in order to fully utilize the highly reactive portion of coal. One such process is to conduct the hydrogasification of coal in a so called "free-fall" reactor. Coal particles pass through the top of the reactor in a dilute suspension and hydrogen gas is passed either counter-currently or co-currently. In such a process the contact time between the coal particle and the gas must be, by necessity, much shorter than in a moving-bed or fluid-bed operation. It is the purpose of this paper to present a kinetic study of the rapid reaction during the initial contacting of coal and hydrogen.

RESULTS

Mechanism of the Hydrogasification Reaction

It has been postulated that, in the initial period of hydrogasification, pyrolysis of the char occurs, involving devolatilization of light components which is then followed by their hydrogenolysis. The devolatilization produces reaction intermediates that are derived from aliphatic hydrocarbon side chains and oxygenated functional groups. (2) The remainder of the organic matter in the coal is converted more slowly to methane, apparently almost according to the carbon-hydrogen reaction. The rate-controlling steps of this reaction in moving and fluid beds have been studied. (3)

For convenience, the following two abbreviated simultaneous reactions will be employed to represent the mechanism of hydrogasification of different reactive coal components.

First-Phase Reaction:

$$C_n H_m O_i + qH_2 \rightleftarrows aCH_4 + dC_2H_6 + eH_2O + bCO_2$$

Second-Phase Reaction:

$$C + 2H_2 \rightleftarrows CH_4$$

Of course, the actual reactions are much more complex than indicated by the above simple schemes. However, these two reactions are believed to be sufficient to characterize the two greatly different rate periods observed in coal hydrogasification.

If X, x_1, and x_2 are respectively the total carbon gasified, the fraction of reactive carbon gasified in the first-phase reaction and the residual carbon gasified in the second-phase reaction, then:

$$X = fx_1 + (1 - f)\, x_2 \qquad (1)$$

where f is the fraction of carbon in coal which reacts according to the first phase reaction. For short reaction times, θ, the first phase reaction prevails, and;

$$X \cong fx_1$$

Coal char hydrogasification data, obtained in a semiflow system by Feldkirchner and Linden (1), indicate that the rate of carbon conversion in the first-phase reaction is proportional to the amount of unreacted carbon

and to the effective hydrogen partial pressure. Accordingly,

$$dx_1/d\theta = k_1 (1-x_1) (P_{H_2} - P_{H_2}^*) \quad (2)$$

where P_{H_2} and $P_{H_2}^*$ are the partial pressures of hydrogen in the system, and the partial pressure of hydrogen at equilibrium, respectively, and k_1 is the proportionality constant for the first-phase reaction expression. Combining Equations 1 and 2:

$$dX/d\theta = k_1 (f-X) (p_{H_2} - p_{H_2}^*) = k_1 P_t (f-X) (y - y^*) \quad (3)$$

where P_t is the total pressure of the system and y and y* are the mole fractions of hydrogen in the system and at equilibrium, respectively. Integration of Equation 3 between the initial and final conditions for media of constant hydrogen concentration gives,

$$\ln (1-X/f) = -k_1 P_t (y - y^*)\theta \quad (4)$$

when $y >> y^*$ (for pure hydrogen feed and small conversion),

$$\ln (1-X/f) = -k_1 P_t y \theta \quad (5)$$

A plot of ln (1-X/f) vs. $P_t y\theta$ can be made from the experimental data and the slope of the line, k_1, may be evaluated.

Analysis of Semiflow Tests

Feldkirchner and Linden (1) measured coal char hydrogasification rates by dropping char particles into a heated reactor, with gas passing through it. Their semiflow study covers the pressure range up to 2500 p.s.i.g. and the temperature range up to 1700°F. They carried out their experiments in such a way that both char heatup and product gas residence times were very short. This enabled them to follow directly the course of the reactions during the initial high rate period. Their data were examined in light of the mechanism presented. Figure 1 is a plot of ln (1-X/f) vs. θ for Montour No. 10 char and North Dakota lignite. Since the feeds were nearly pure hydrogen and the change in composition of the gas was small, $P_t y$ was approximately constant throughout the run. As is seen in Figure 1, the initial portion of the data for lignite and bituminous coal char can be represented by straight lines. From the slopes of these lines, k_1 is calculated to be 2.0 $(\text{atmosphere-hour})^{-1}$. The displacement of the intercept at θ = 0 from unity is due to the initial heatup of the particle to the reaction temperature. The higher the volatile matter content, the larger the value of f (the fraction of carbon which reacts by the first-phase reaction) must become if a straight line is to obtained.

Thus, the value of f for Montour No. 10 char is 0.25 at 1700° F. and that of lignite is 0.48 at 1700° F.

A slight effect of particle size may be seen in Figure 1, but the slope of the line is independent of the particle size, which indicates that a definite time is required to heat the particle which in turn, affects the position of the lines.

Figure 2 shows the linear relation of the data from two tests at different total gas pressures. The displacement at $\theta = 0$ is again due to particle heatup time. The slope of the lines is 2.0 (atmosphere-hour)$^{-1}$. A detailed comparison of results of tests with different feed gas compositions is given in Figure 3 and Figure 4.

Instead of θ, $P_t y\theta$ was plotted on semilogarithmic coordinates according to Equation 1 (Figure 3). Feeds include pure hydrogen, hydrogen-nitrogen mixtures, and hydrogen-methane mixtures. The data points indicate almost a linear relationship, but deviate somewhat from each other. However, if $P_t(y-y^*)\theta$ is used instead of $P_t\, y\theta$, a better agreement is obtained as is shown in Figure 4. y^* is the equilibrium composition of hydrogen obtained from Figure 5 and the temperature-correction equation:

$$(K_p)_T = [1/34713]\ (K_p)_{1300°F.}\ \exp\,(18400/T). \qquad (6)$$

T is the temperature, in °R.

Therefore, a slight equilibrium hindrance of the reaction exists even during the rapid, initial reactions, but the effect may be so small under most of the experimental conditions, particularly when pure hydrogen feed is employed, that this can be neglected.

Figure 6 shows the effect of temperature on the rate constant, k_1, and f. For relatively small temperature changes, the value of k_1 may be kept constant with a small adjustment of the value of f. The increase of the value of f as temperature is increased may be explained as follows. As the temperature of reaction is increased, the rate of devolatilization of reactive carbon becomes larger; consequently, the recondensation of the reactive carbon during pyrolysis to form stable ring compounds (as residual carbon) becomes less. In terms of the amount of carbon available for the first-phase reaction, this means the value of f increases as temperature increases. This relation is shown in Figure 7. However, the rates of pyrolysis should also increase as the temperature is increased. Therefore, the extrapolation of Figure 7 to the higher temperature range beyond the experimental points should be avoided.

Analysis of Continuous Free-Fall Reactor Test Results

To apply the above analysis of semiflow test results to continuous flow reactors, a material balance between the carbon in the solid phase and carbon in the gaseous phase must be made:

F = pounds of coal fed per hour.

G = moles of inlet gas per hour.

ψ = fraction of carbon in coal fed.

y_0 = mole fraction of hydrogen in inlet gas.

α = q/n = stoichiometric ratio of hydrogen and carbon for first-phase reaction.

Accordingly, for plug-flow of both gas and solids:

$$-(\alpha F\psi/12)\, dX = d(Gy) \equiv G\,dy \qquad (7)$$

Integrating Equation 7 between the limits of the conditions at the reactor inlet and exit,

$$X(\alpha F\psi/12) = G(y_0 - y) \qquad (8)$$

or $y = y_0 - (\alpha\,\psi/12)(F/G)\,X = y_0 - mX$

where $m = (\alpha\,\psi/12)(F/G)$

Substituting y into Equation 3,

$$dX/d\theta = k_1 P_t (f-X)(y_0 - mX - y^*) \qquad (9)$$

Since y^* may be taken to be nearly constant for a small conversion taking place in the first-phase reaction, Equation 9 can be integrated between the inlet and exit of the reactor. Hence:

$$k_1 \theta P_t (y_0 - y^* - mf) = \ln[f(y_0 - y^* - mX) / (y_0 - y^*)(f-X)] \qquad (10)$$

or $$k_1 = [1/P_t \theta (y_0 - y^* - \alpha\,\psi F f/12G)] \ln[f(y_0 - y^* - \alpha\,\psi X F/12G) / (y_0 - y^*)(f-X)] \qquad (11)$$

The results of several continuous pilot plant free-fall tests conducted at the Institute of Gas Technology were used to verify the above analysis.

The values of $\alpha = q/n$, computed from inlet and exit gas analysis of the tests, seem to be affected only slightly by conversion as is shown in Figure 8. Since residence times could not be readily calculated from the data given in the report, experiments were conducted. Terminal velocities of Montour No. 10 particles char were found by dropping the char from a hopper through a 2-inch inside diameter pipe approximately 10 feet long. The gas medium was air at 70°F. and 1 atmosphere.

The holdup of particles in the pipe was measured by simultaneously closing plug valves at the inlet and exit. The terminal velocities of the particles were calculated from the solids holdups and solids flow rates. If W is the weight of solid particles trapped in the pipe and L is the length of

the pipe through which the particles fall, then the average solid terminal velocity, U_t, is:

$$U_t = FL/W \qquad (12)$$

Terminal velocities of the solids at the reactor conditions were calculated from those at ambient conditions in air by use of Stokes Law. Both the terminal velocity in air and that calculated at reactor condition are shown as a function of solids feed rate in Figure 8. The residence time is,

$$\theta = \frac{L}{U_t - U_g} \qquad (13)$$

where U_g is gas velocity. The results of three countercurrent free-fall reactor tests were used to compute the values of k_1 and are listed in Table 1.

Table 1.

Results of Countercurrent Free-Fall Reactor Runs

Run No.	T, °F.	P_t, atm.	F, lb./hr.	G, SCF/hr.	f, %	ψ	L, ft.	θ, sec.	k_1, $(atm.-hr.)^{-1}$
SD56	1270	139.8	4.53	46.53	21.7	0.78	9	8.57	3.10
SD57	1245	137.6	7.68	50.21	21.5	0.782	9	6.67	2.10
SD58	1240	137.0	11.75	105.24	21.4	0.783	7	4.12	1.8

In view of some uncertainties involved in calculating the values of particle residence times, the agreement of the k_1 values from continuous reactor tests with those obtained from semiflow tests [$k_1 = 2.0\ (atm./hr.)^{-1}$ is good. Because of the high rate of the first-phase reaction, the particles must undergo deformation, reduction in size, and reduction in density during free-fall. The actual particle residence times must be affected by these changes, which did not exist in the residence-time measurement tests described previously.

Because of the assumptions and uncertainties introduced for such a complex system, instead of using Equation 11, simplified equations may be employed for practical application without introducing additional errors. This involves the use of some average driving force such as $(y - y^*)_{av.}$. From Equation 4:

$$k_1 = -\ln (1 - X/f) \,/\, P_t (y - y^*)_{av.} \theta \qquad (14)$$

$$\text{and } X = f\left\{1 - \exp[-k_1 P_t (y - y^*)_{av.} \theta]\right\} \qquad (15)$$

CONCLUSION

It has been shown that the initial rate of coal hydrogasification can be assumed to be proportional to the amount of reactive carbon left in the particles and to the effective hydrogen partial pressure. The rate constant, k_1, was found to be 2.0 (atmosphere-hour)$^{-1}$ and the reaction model, used in the analysis of semiflow tests was found to be applicable to continuous free-fall reactors. Product gas compositions for continuous reactors may be computed by the empirical relationships developed elsewhere for the partial pressures of CO, CO_2, C_2H_6 and H_2O. (3)

ACKNOWLEDGMENT

This study was sponsored by the Gas Operations Research Committee of the American Gas Association as part of the associations Promotion-Advertising-Research Plan. The work was guided by the Project PB-23a Supervising Committee under the chairmanship of B. J. Clarke, and by the Research Department of the Consolidated Natural Gas System (now Con-Gas Service Corporation) under the guidance of H. E. Benson and F. E. Vandaveer.

Notation:

D_p = Particle diameter, ft. or in.

F = Char feed rate, lb. per hr.

f = Fraction of carbon that reacts according to the first-phase reaction.

G = Gas feed rate, SCF per hr. or moles per hr.

k_1 = Reaction rate constant in the first phase reaction (hr.-atm.)$^{-1}$

K_p = Thermodynamic equilibrium constant = $P^*_{CH_4}/(P^*_{H_2})^2$

L = Length of the reactor, ft.

P_t = Total pressure, atm.

P = Partial pressure, atm.

P^* = Equilibrium partial pressure, atm.

T = Absolute temperature, °R.

U_g = Gas velocity, ft. per sec.

U_t = Terminal velocity of particles, ft. per sec.

W = Weight of bed, lb.

X = Overall fractional conversion of carbon.

x_1 = Fraction of carbon converted in the first-phase reaction.

x_2 = Fraction of carbon converted in the second-phase reaction.

y = Mole fraction of hydrogen.

y^* = Mole fraction of hydrogen at equilibrium

θ = Time, sec. or hr.

ψ = Fraction of carbon in coal

α = q/n, ratio of the hydrogen to carbon stoichiometric coefficiency for for the first-phase reaction.

References Cited:

1. Feldkirchner, H. L., Linden, H. R., Ind. Eng. Chem. Process Design and Develop. 2, 153-62 (1963).

2. Pyrcioch, E. J., Institute of Gas Technology Monthly Work Report PB-23a.

3. Wen, C. Y., Huebler, J., Paper presented at the 56th National Meeting American Institute of Chemical Engineers, Houston, Texas Dec. 1-5, 1963.

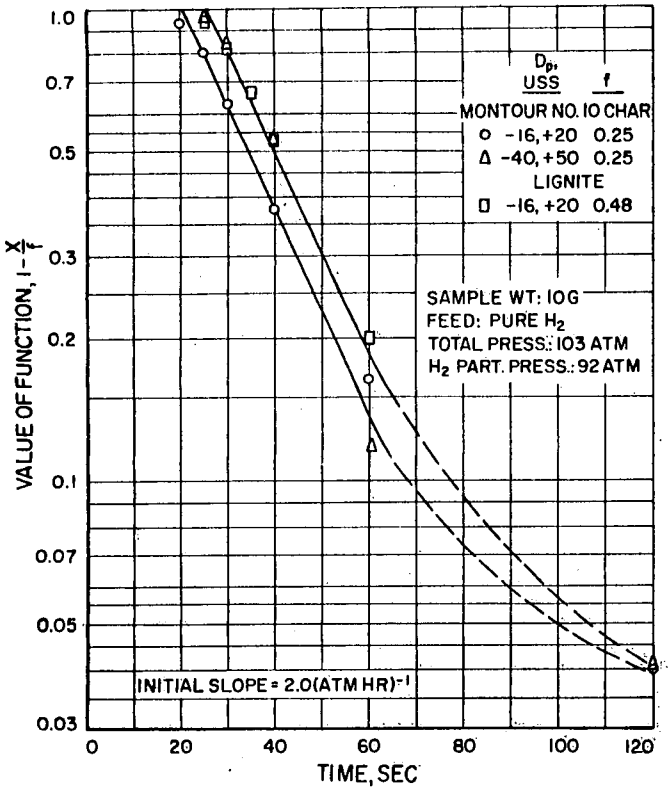

Fig. 1.-LINEAR RELATIONSHIP OF THE LOGARITHM OF THE FIRST-PHASE CONVERSION FUNCTION WITH TIME

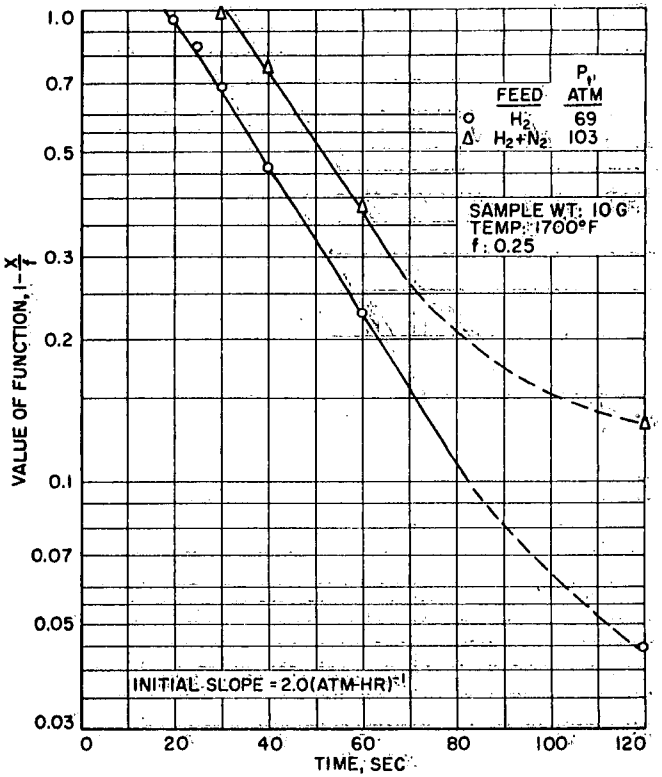

Fig. 2.-LINEAR RELATIONSHIP OF THE LOGARITHM OF THE FIRST-PHASE CONVERSION FUNCTION WITH TIME AT TWO DIFFERENT PRESSURES

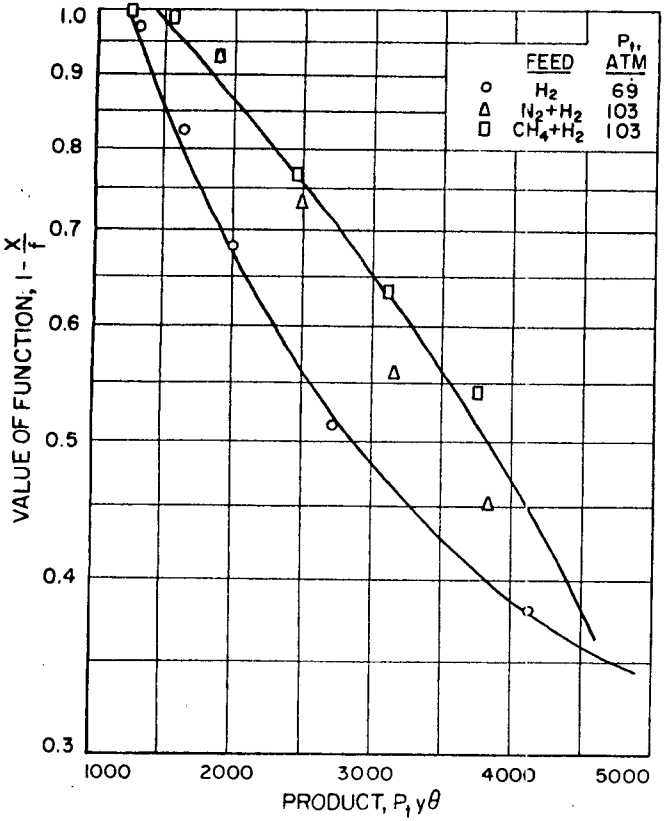

Fig. 3.- EFFECT OF HYDROGEN PARTIAL PRESSURE AND PRODUCT $P_t Y\theta$ ON THE LOGARITHM OF THE FIRST-PHASE CONVERSION FUNCTION

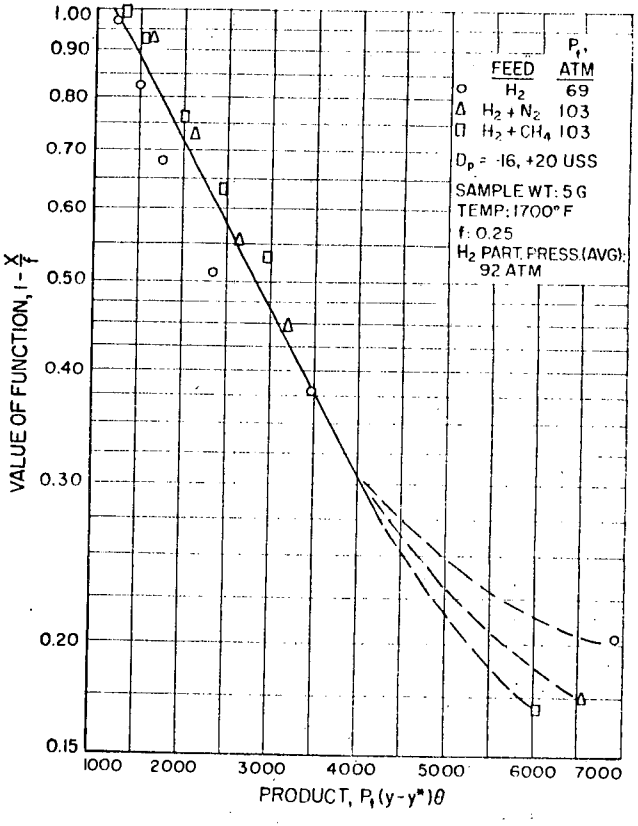

Fig. 4.- EFFECT OF HYDROGEN PARTIAL PRESSURE AND PRODUCT $P_t(Y-Y^*)\theta$ ON THE LOGARITHM OF THE FIRST-PHASE FUNCTION

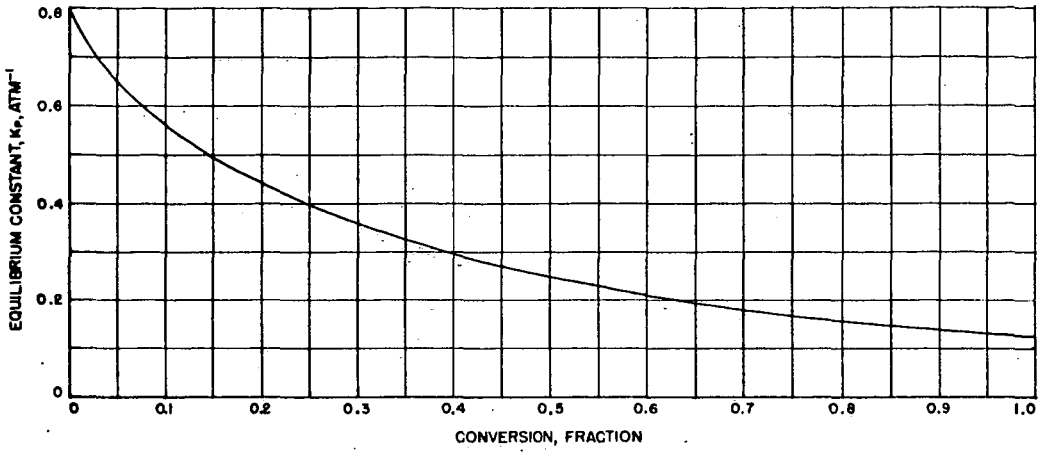

Fig. 5.- APPROXIMATE TREND OF THE EQUILIBRIUM CONSTANT AS A FUNCTION OF CONVERSION FOR THE HYDROGEN-CHAR REACTION AT 1300°F AND 2000 P.S.I.G. TOTAL PRESSURE

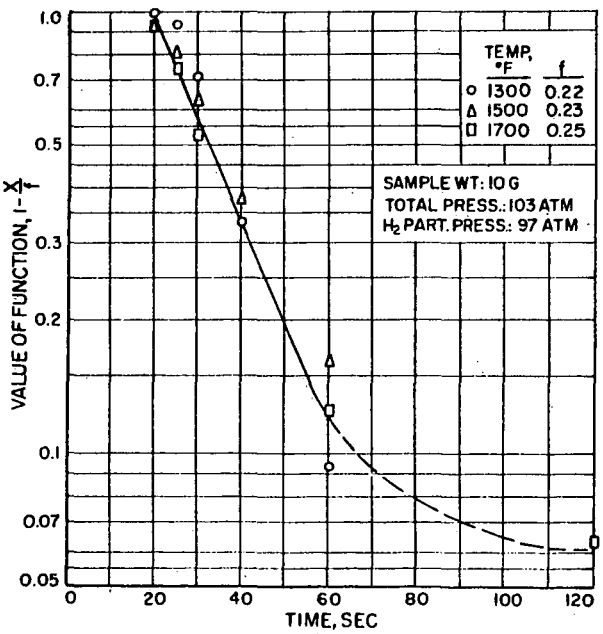

Fig. 6.-EFFECT OF TEMPERATURE AND TIME ON THE LOGARITHM OF THE FIRST-PHASE CONVERSION FUNCTION

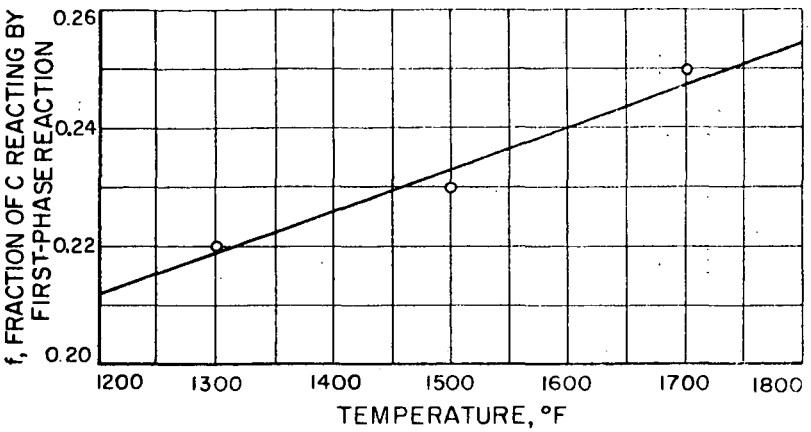

Fig. 7.-EFFECT OF TEMPERATURE ON THE FRACTION OF CARBON REACTING BY FIRST-PHASE REACTION

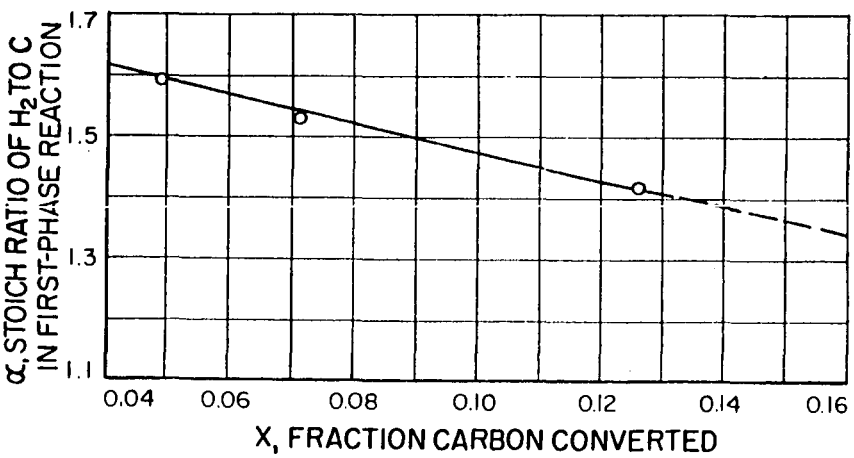

Fig. 8.-EFFECT OF CARBON CONVERSION ON α, THE STOICHIOMETRIC RATIO OF HYDROGEN TO CARBON IN THE FIRST-PHASE REACTION

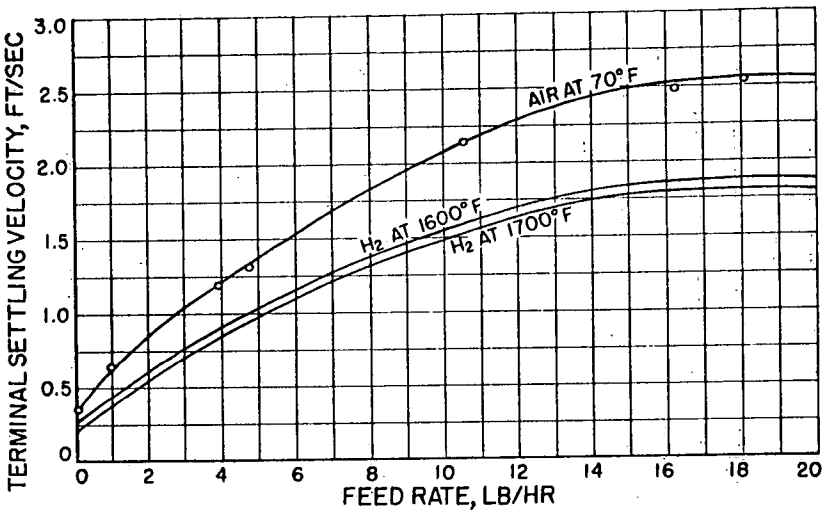

Fig. 9.-EFFECT OF CHAR FEED RATE OF TERMINAL SETTLING VELOCITY OF MONTOUR NO. 10 CHAR IN A TWO INCH I.D. TUBE

16c

REACTION OF COAL WITH STEAM-HYDROGEN MIXTURES AT HIGH TEMPERATURES AND PRESSURES

H. L. Feldkirchner and J. Huebler

Institute of Gas Technology
Chicago 16, Illinois

INTRODUCTION

Three basic problems have been encountered in the development of processes for the conversion of coals to pipeline gas by destructive hydrogenation at high pressures:

1. At 1300° to 1500°F., the temperature range which permits the direct production of a high-heating-value gas, the rate of coal conversion is relatively low.

2. An external source of hydrogen is required.

3. The high heat release of the hydrogenation reactions cannot be utilized to the fullest advantage; this creates a serious problem in the design of a reactor in which adequate temperature control and optimum process heat economy can be achieved.

The first limitation has been partially overcome by using countercurrent reactor operation with a steep temperature gradient. The use of this operating scheme has been found to be effective for producing a high-heating-value gas in a single step by destructive hydrogenation at 2000 p.s.i.g. and 1300° to 1700°F. (11). Several combined factors cause this countercurrent scheme to be preferred. First, it is known that, at high levels of gasification, the hydrogasification rates of coals increase rapidly with increases in temperature; but at low levels of gasification, in the temperature range of 1300° to 1700°F., the hydrogasification rates are nearly independent of temperature (1,2,5,15). Second, at all gasification levels, gasification rates are roughly proportional to the hydrogen partial pressure. Third, the equilibrium methane content of the product gas decreases with increases in temperature. For example, at 1700°F. and 1500 p.s.i.a., the maximum product gas methane concentration which can be obtained in the reaction of carbon with hydrogen is 47 mole %, while at 2000°F., this value is only 28 mole %.

In countercurrent operation, as now contemplated, a large excess of hydrogen contacts the relatively unreactive residue at the high-temperature end of the reactor. At the low-temperature end of the reactor, highly reactive feed char comes in contact with the product gas. It has been shown that methane concentrations in excess of those predicted for the carbon-hydrogen reaction can be produced when the gas is in contact with slightly gasified coal char (14). Thus, the contacting of fresh char and product gas at low temperatures

and spent char and feed hydrogen at high temperatures minimizes equilibrium limitations. Since the rate of gasification is roughly proportional to the difference between the hydrogen partial pressure in the gas and the hydrogen partial pressure in equilibrium with the char, countercurrent operation also provides a maximum average hydrogen partial pressure and thus a maximum average gasification rate.

Other variations of this basic countercurrent operating scheme might allow further increases in gas heating value or reductions in reactor size. For example, a reduction in the residence time of the residual char, and thus a reduction in hydrogasifier size, might be achieved by using an even higher temperature in the high-temperature end of the reactor.

Increase of the reaction temperature also offers an opportunity for reducing external hydrogen requirements. At temperatures of 1700°F. and above, it should be possible to supply part of the hydrogen requirements by steam decomposition reactions taking place simultaneously with the hydrogasification reactions. In addition to providing a source of "free" hydrogen, the endothermic steam reaction has the advantage of providing a means for temperature control by utilization of the exothermic heat of the hydrogenation reaction.

On the basis of the above considerations, it appeared that pilot plant studies of the production of methane from solid fossil fuels should not be limited to the low temperature range previously investigated, but should be extended into the temperature range above 1700°F., where very rapid gasification rates can be achieved. However, before prototype pilot plant equipment could be designed to investigate such high temperature processes, it was necessary to obtain basic data on the gasification characteristics of the various solid fossil fuels under these extreme conditions. No data of this type were available because of the great difficulty of constructing high temperature apparatus and devising experimental techniques capable of achieving the following three objectives:

1. Attainment of temperatures in excess of 2000°F., at pressures up to 3000 p.s.i.g.

2. Temperature control in spite of the considerable exothermicity or endothermicity of the reactions of interest.

3. Control and reliable measurement of reaction time.

In the course of the studies conducted by the Institute of Gas Technology in its Basic Research Program and in other studies, techniques had been developed which appeared to give an acceptable solution to these problems on a laboratory scale (4,5). These techniques minimized uncertainties resulting from the gasification of a batch fuel charge during heatup, as well as the uncertain solids residence times encountered in entrained-flow systems where the actual rate of flow of the solid fuel through the heated zone cannot be measured directly.

A study of available equipment indicated that the above-listed techniques could be applied to a reactor capable of operating at the extreme conditions desired. A suitable reactor was designed and built consisting of an external pressure vessel operating at low temperature, an electrical resistance heating system insulated from this outer shell, and a thin-walled, high-temperature, alloy steel reactor tube with means provided for balanced-pressure operation and fitted with a bellows to compensate for thermal expansion of the reactor tube.

EXPERIMENTAL

Apparatus

Figure 1 is a flow diagram of the system showing all major pieces of equipment and part of the control instrumentation. Coal char was fed in single batches from a feed hopper. This hopper was connected to the reactor by an air-operated, quick-opening ball valve. A pressure equalization line was used to keep the hopper pressure equal to the reactor pressure. A second hopper was also constructed which contained a rotating drum-type feeder for continuous coal char feeding.

Hydrogen was fed from a high pressure gas storage system and was metered by an orifice meter. Hydrogen flow rates were controlled manually. Orifice differential pressures were sensed and converted to a 3- to 15-p.s.i.g. air signal by a differential pressure transmitter. This air signal was then recorded, along with the orifice and reactor pressures, by conventional pneumatic recorders.

Controlled rates of steam feed were obtained by pumping water from a weigh tank through a steam generator by a positive-displacement, adjustable-stroke, metering pump. The steam generator consisted of a coil of 3/8-inch outside diameter by 1/8-inch inside diameter stainless steel tubing contained in an electric furnace. The temperature of the steam from the steam generator was controlled manually. Superheated steam and hydrogen were preheated to reaction

temperature in passing through the upper heating zone of the reactor.

Exit gases from the bottom of the reactor were cooled by being passed through a water-cooled stainless steel coil. Condensed steam was collected in a high pressure sight glass. To minimize loss of carbon dioxide or other dissolved gases in the condensed steam, the water was drained from the high pressure sight glass first into a low pressure flash chamber which was vented into the low pressure exit gas system, before water was drained from the unit.

Exit gases were metered continuously by wet test meter. A small portion of this stream was passed through a recording densitometer (to aid in selection of sampling times) and metered with a smaller wet test meter. To avoid distortion of the reaction rate-time relationship because of backmixing and gas holdup, which would occur if gas samples were taken after gas metering, the gas sampling manifold was installed in the exit gas line immediately after the pressure-reducing, back-pressure regulator, which was used to control the reactor pressure.

The reactor, shown in detail in Figure 2, was internally insulated and contained a stainless steel reactor tube which consisted of a length of 1 1/4-inch I.P.S., schedule 40, type 310 stainless steel pipe which was attached to two adapter fittings by pipe threads. This tube was heated electrically by a 2 3/8-inch inside diameter heater, containing three 8-inch long zones. The heater was fabricated from a single length of heating wire which was tapped for three-zone operation. A balanced pressure was maintained on the reactor tube by means of an on-off type pressure-balancing system. Full details of the design and operation of this reactor have been described elsewhere (6). Design of this reactor followed closely that of reactors described by Wasilewski (13) and Hodge and others (9).

Satisfactory operation was achieved at pressures up to 1000 p.s.i.g. and reaction zone temperatures up to 2100°F. Higher-temperature operation should be possible by use of higher temperature heaters, such as silicon carbide, and refractory metal reactor tubes. Insulation having a higher operating temperature limit than that of the insulation used here would also be required in the vicinity of the electric heater.

An insert, fabricated from a length of 1-inch I.P.S., schedule 40, type 310 stainless steel pipe, was installed within the reactor tube to provide for containment and complete recovery of the coal char charge. An integral thermowell,

fabricated from 1/8-inch I.P.S., schedule 40, type 310 stainless steel pipe, was located axially within the insert and contained three Chromel-Alumel, magnesium oxide-insulated, o.062-inch outside diameter, Inconel-sheated thermocouples. The temperatures sensed by these thermocouples were recorded at approximately one-second intervals by a high speed potentiometric-type temperature recorder.

Reactor temperatures were controlled by three on-off, indicating temperature controllers and three thermocouples located within the centers of the heating elements. Satisfactory operation was obtained with this type of thermocouple mounted in the electric heaters as well as in the insert at reactor temperatures up to 2100°F. Electric heater temperatures were kept below 2300°F. to ensure as long a heater life as possible.

Materials

In tests with hydrogen feed gas and hydrogen-steam feed gas mixtures, the hydrogen contained a small, accurately measured, amount of helium or argon (usually about 1 mole %) as a tracer for exit gas flow rate measurement. The hydrogen-inert gas mixtures were mixed during compression and stored in a central gas storage system at pressures up to 3600 p.s.i.g. Commercially available grades of hydrogen (99.987% pure), helium (99.99% pure), and argon (99.998% pure) were used.

The coal char was separated by screening from that used in pilot plant tests to ensure that the results obtained in these tests would be applicable to work to be done in the larger, pilot plant reactor system. This coal char was prepared by the Consolidation Coal Co. from Pittsburgh Seam bituminous coal from the Montour No. 10 mine by a low-temperature fluidized-bed pretreatment process. The analysis of the feed char is shown in Table I.

Procedure

In all of the tests, a semiflow technique employing a flowing gas and single, static coal char charge was used. It was essentially the same as that used in other studies conducted recently on the hydrogasification of solid fossil fuels (4,5). Test periods averaged about 1000 seconds in length.

Because heat losses by free convection from internally insulated reactors increase greatly when operating at high pressures, it was expedient to bring the reactor to operating temperature before pressurizing it to avoid long

Table I.-ANALYSIS OF COAL CHAR

Sample Designation	5851
Type	Low-Temperature, Bituminous Coal Char
Source	Consolidation Coal Co.
Particle Size	
U.S. standard sieve	-16,+20
Ultimate Analysis, wt.% (dry basis)	
Carbon	76.6
Hydrogen	3.25
Nitrogen	1.76
Oxygen	10.07
Sulfur	0.86
Ash	7.46
Total	100.00
Proximate Analysis, wt. %	
Moisture	0.9
Volatile Matter	18.1
Fixed Carbon	73.6
Ash	7.4
Total	100.0

heatup times. When the reactor had reached the run temperature, the reactor pressure was brought to the desired level by increasing pressure inside the reactor tube. As pressure was increased, the pressure-balancing system maintained a balanced pressure on the reactor tube by admitting pressurized nitrogen to the insulated area surrounding the reactor tube. About 15 minutes was required to bring the pressure to 1000 p.s.i.g.

After the desired pressure was attained, the flow of reactant gas through the reactor tube was initiated. In tests with steam feeds, the reactor tube was first pressurized with nitrogen and then, when the steam generator pressure had been increased to slightly more than the reactor pressure, the steam was admitted to the reactor and the nitrogen was shut off. This procedure was necessary to avoid introduction of large quantities of steam condensate into the instrument lines. In addition, since non-condensable exit gas flow rates were very small when using pure steam feed gases, the exit gas system was purged at a controlled flow rate of 25 SCF per hour with helium to avoid any distortion of the rate-time relationship because of backmixing or holdup in the exit gas system.

When feed gas flow rates, temperatures, and pressures had become completely stabilized, the feed gas was sampled. One minute later, the tests were initiated by opening the quick-opening ball valve between the hopper and the reactor. Single charges of either 2.5 grams or 5 grams of coal char were fed and reactant gas flow rates of 50 SCF per hour were employed in all tests. The coal charge was supported on a stainless steel screen on top of approximately 19 inches of high purity alumina inerts in the form of cylinders, 1/8-inch long and 1/8-inch in diameter. Temperatures of the bottom of the coal char charge and of the centers of the top and bottom heating zones were recorded. Exit gas samples were taken, in the early stages of a test at frequent intervals (as small as 10 seconds) and later as required, to delineate the entire course of the reaction.

The first reaction products appeared in the exit gas sampling system in about 15 to 35 seconds. This holdup time depended on the feed gas used, with holdup times being the shortest in tests with pure hydrogen feeds and holdup times being the longest in tests with pure steam feeds. In tests with steam-containing feed gases, a constant liquid level was maintained in the sight glass, so that gas holdup times in the exit system would not vary. This was necessary because a sizeable variation in gas holdup times could distort the gasification rate-time relationship. When the reaction rate had reached a value too small to be measured accurately, the run was stopped. The feed gas flow was stopped, the reactor heaters were turned off, and the unit was de-pressurized to minimize further reaction of the coal charge after the run.

The feed gas and helium-purge-gas orifice calibrations were performed before each run with the exit gas wet test meter. Exit gas flow measurements were also made during each run by wet test meter to provide a check on the flow rates calculated with the helium or argon tracers. Gas analyses were performed by mass spectrometer at high sensitivity. Carbon monoxide was determined by infrared spectrophotometer, since it was not possible to measure the relative amounts of carbon monoxide and nitrogen with sufficient accuracy in the presence of methane with the mass spectrometer.

RESULTS

Hydrogen-Coal Char Reaction

Initial testing was done at 1000 p.s.i.g. and 1700° to 2100°F., with hydrogen feed gas, 5-gram coal char samples, and feed gas flow rates of 50 SCF per hour. At temperatures of 1800°F. and above, no consistent effect of temperature on rate of gasification could be observed. In addition, during the tests at 1800°F. and above, stainless steel screens which

had been used to support the coal char charges were found to have melted, which indicated that very large temperature rises had occurred at some time during the course of these tests. Heat balance calculations were then made using finite difference techniques. A heat of reaction equal to that for hydrogenation of beta graphite to methane was assumed. These calculations showed that, at the high rates of reaction obtained with this highly reactive feedstock, sample temperatures could easily rise to over 2500°F. from a starting temperature of 2000°F., even with the high gas flow rates and small sample sizes used. Further tests were conducted with 2.5-gram samples at 1700° to 2100°F. A 2.5-gram sample size was deemed the smallest which would give sufficient methane in the product gas for accurate measurement. However, even with such small sample sizes, it was found that sample temperatures increased greatly. For example, pieces of -16, +20 U.S.S. sieve size temperature-indicating pellets having fusion temperatures of 1700°, 1900°, 2100°, 2250°, and 2500°F. were mixed with the feed char in one check run made at 1700°F. Here both the 1700° and 1900°F. pellets melted.

Therefore, three more tests were conducted with 2.5 grams of coal char mixed with 30 grams of alumina inerts to act as a heat sink. The results of these tests at 1800° and 2000°F. are shown graphically in Figure 3 along with results of tests conducted without inerts at 1800° and 2000°F. This dilution technique was used in all further tests with hydrogen feed gas and all further results presented for hydrogen feed gas were obtained by this method. It should be pointed out that in tests where char and inerts were fed, the indicated bed temperature first dropped rapidly several hundred degrees but by the time about 40 percent of the carbon was gasified, the indicated bed temperature had returned to the nominal run temperature. As can be seen, there is a gradual decrease in gasification rate with increasing carbon gasification which indicates a decrease in char reactivity. The degree of reproducibility of these tests can be seen by the close agreement of the two tests conducted at 1800°F. The finding that initial rates of gasification observed in these tests were almost as high as those in tests conducted without inerts is further evidence that initial rates are essentially independent of temperature at temperatures above 1300°F. (5).

Other investigators, for example Hunt and others (10) and von Fredersdorff (12), found diffusional limitations were present with the carbon-steam reaction. Therefore several tests were conducted at 1800°F. with hydrogen feed gas to show whether diffusional effects may have been present in the char-hydrogen system. The results of the tests using char samples having different particle sizes are shown in Figure 4. It can be seen that at carbon gasifications above

about 50 percent, there are no differences in the rates of gasification of -16, +20 and -30, +40 U.S.S. sieve-size particles. Because of the temperature upsets which occurred when inerts were fed with the char no reliable information can be obtained on this system for low carbon gasification levels. The results of tests conducted at different feed hydrogen flow rates are shown in Figure 5. Again, at carbon gasifications above about 50 percent, there is apparently no effect of hydrogen flow rate on gasification rate.

Steam-Hydrogen Coal Char Reaction

The next set of tests was conducted with equimolar steam-hydrogen mixtures, at 1700° to 2100°F., with 50-SCF per hour feed gas flow rates, and with 2.5-gram coal char samples. The results of these tests are shown graphically in Figure 6. Temperature-indicating pellets, which were mixed with the coal char in these tests, did not indicate the presence of large heat effects which were found in tests with hydrogen feed gas. Heat-balance calculations indicated that temperature changes during the course of these tests would be less than 100°F. In general, the rate of gasification increased with increases in temperature. These results also indicate that greater structural changes resulting in lost reactivity may occur after prolonged exposures of the char to steam-hydrogen mixtures at 2100°F. than at lower temperatures, or in gasification with pure hydrogen.

The effect of temperature on the relative rates of formation of carbon oxides and methane, shown graphically in Figure 7, is more pronounced than the effect of temperature on the total gasification rate. Since some carbon oxides are evolved during the early stages of gasification with hydrogen, these data are also included for comparison. At higher temperatures, the char is apparently more reactive toward steam than toward hydrogen. However, it was not possible to quantitatively measure the rates of the steam-char and hydrogen-char reactions here, since it is possible for some of the methane formed by the char-hydrogen reaction to undergo reforming to carbon monoxide and hydrogen in the gas phase or by secondary reaction catalyzed by the coal surface. Further work, using isotope- or radioactive-tracer techniques to measure these primary reactions, would be desirable.

Several conclusions can be drawn from these results about operation of high-temperature hydrogasification reactors with steam-hydrogen feeds. First, since the rate of carbon oxides formation is greater than that of methane formation above 1900°F. and is less below 1900°F., temperature control should not be a severe problem in steam-hydrogen coal gasifiers. For example, if bed temperatures began to increase, carbon oxide-forming reactions, which are endothermic, should eventually predominate and provide an

upper limit on the bed temperature. If, on the other hand, the temperature began to decrease, exothermic methane-forming reactions should eventually predominate and provide a lower limit on the bed temperature. Second, the reactivity of the char for carbon oxide-forming reactions and for methane-forming reactions depends strongly on the carbon gasification level. Thus, selection of operating conditions for process design will also depend on the carbon gasification level in the reactor.

The equilibrium relationships for the steam-hydrogen-carbon system also indicate that temperature control should not be a severe problem in steam-hydrogen coal gasifiers. Figure 8 shows the effects of temperature, for three pressure levels, on the equilibrium gas composition for steam-hydrogen gasification of carbon. In calculating these equilibrium compositions, ideal gas behavior and a unit activity for carbon were assumed. It can be seen that as temperature increases, the yield of methane and carbon dioxide decreases and the yield of carbon monoxide increases. Thus chemical equilibrium limitations will exert a temperature-moderating influence on the reactions.

It should be pointed out that, since the concentration of reaction products in the exit gas was very small in all tests, the relative rates of the various gasification reactions would probably be somewhat different under actual operating conditions than is shown in Figure 7. However, the approximate trends shown should still be valid.

Calculations were also performed to show the degree of approach to the carbon monoxide shift reaction equilibrium in these tests. Although the concentration of reaction products in the exit gas was too small at high carbon gasification levels for making these calculations accurately, it was possible to make calculations for carbon gasifications below about 50 percent. At temperatures of 2000° and 2100°F., the equilibrium was approached quite closely, but below 2000°F. the approach to equilibrium became progressively less with decreases in temperature. At 1700°F. the experimentally determined value for the ratio: $(CO_2)(H_2)/(CO)(H_2O)$ averaged approximately 0.55 times the equilibrium value calculated from thermodynamic data.

Steam-Coal Char Reaction

The final set of tests was conducted with pure steam feeds, at 1700° to 2050°F., with 50-SCF per hour steam rates. Because of the generally lower gasification rates measured with steam feed gas, it was necessary to use larger, 5-gram coal char samples so that the concentration of gaseous products in the exit gas would be large enough for measurement

by existing techniques. The concentration of products could also have been increased by using a lower helium sweep gas flow rate, but this would have resulted in longer holdup times in the exit gas system, which could cause distortion of the rate-time relationship by backmixing. Proportionately greater losses of dissolved carbon dioxide in the condensed steam with smaller sample sizes would be a further reason for using larger coal char sample sizes. The results of these tests are shown graphically in Figure 9.

The carbon gasification-gasification rate relationship is somewhat different from that with steam-hydrogen mixtures or hydrogen. Here, the rate of gasification is strongly influenced by temperature at all levels of carbon gasification, and the char reactivity decreases with increases in carbon gasification. The reactivity begins to drop very rapidly for all temperatures after about 100 to 150 seconds from the start of the run. A similar, but less pronounced behavior was observed in a test at 2100°F. with steam-hydrogen feed gas, which was discussed earlier. These results would indicate that, at higher temperatures, the reactivity of the char may be affected by its previous gas environment. This loss in reactivity with steam-containing feed gases may apparently be counteracted by operation at higher temperatures, however, so that this should not be a serious limitation.

The combined results of tests conducted with -16, +20 U.S.S. sieve size char and at a 50-SCF per hour feed gas flow rate are presented graphically in Figure 10 and Figure 11. It can be seen that at lower temperatures, the rate of gasification with hydrogen is many times that with steam, but as temperature is increased, the rate of steam gasification approaches that for hydrogen.

The results of these tests do differ from those conducted at lower temperatures and pressures with less reactive feedstocks. Previous investigators have found that, at hydrogen partial pressures below 30 atmospheres and at 1300° to 1700°F., the addition of steam caused an increase in the methane formation rate, (3,7,8,16), but no such "activating" effect was found here. This result is in agreement with previous work conducted at the Institute (5). From Figure 11, it can be seen that the methane content of the product gas varies almost inversely with the feed gas steam content, at higher carbon gasification levels. This decrease in methane yield with increases in feed gas steam content may, of course, be partially due to increased steam reforming of product methane with increases in steam partial pressure, which was discussed earlier. In addition, the high yields of carbon oxides at low carbon gasification levels and at low feed gas steam concentrations are partly due to devolatilization reactions which occur during the early phases of gasification. The relatively high oxygen content of this

coal char (10.07 wt. %), along with the fact that these carbon oxide-forming reactions occur very rapidly and in the very early stages of gasification (5) would cause the effects of these reactions to be accentuated.

Other investigators have observed an inhibition of the steam-char reactions by hydrogen when working with highly devolatilized chars (3,8,16). In work done recently with low-temperature bituminous coal chars at 1700°F., this inhibiting effect was also observed during initial stages of gasification (5). The results shown in Figures 10 and 11 were studied, therefore, to see whether there was evidence of hydrogen inhibition of the steam-char reactions. If a first order rate relationship for the formation of carbon oxides by steam is assumed, (i.e., the rate of formation of carbon oxides proportional to the steam partial pressure), the carbon oxide-formation rates per unit steam partial pressure were apparently no less in the tests with steam-hydrogen mixtures than in the tests with pure steam. This result may be due to experimental conditions being somewhat different in these tests from previous work (5). In the previous work with coal char the residence times of the exit gas in the heated portion of the reactor were only about one-quarter as large as those in this work. Therefore, since there may have been more steam reforming of exit methane in these tests, inhibition by hydrogen may have been obscured.

ACKNOWLEDGMENT

This work was supported by the Gas Operations Research Committee of the American Gas Association as part of the Promotion-Advertising-Research Plan of the Association. The work was guided by the Project PB-23a Supervising Committee under the chairmanship of B. J. Clarke. Thanks are due to H. A. Dirksen, W. G. Bair, and S. Volchko for their helpful suggestions in operation and design of the equipment. E. J. Pyrcioch, F. C. Rac, A. E. Richter, and R. F. Johnson assisted in conducting tests. A. Attari and J. E. Neuzil supervised the analytical work.

REFERENCES CITED

1. Birch, T. J., Hall, K. R., Urie, R. W., J. Inst. Fuel 33, 422-35 (1960).

2. Blackwood, J. D., Australian J. Chem. 12, 14-28 (1959).

3. Blackwood, J. D., McGrory, F., Australian J. Chem. 11, 16-33 (1958).

4. Feldkirchner, H. L., Linden, H. R., Paper presented at 143rd National Meeting, Division of Fuel Chemistry, American Chemical Society, Cincinnati, Ohio, Jan. 13-18, 1963.

5. Feldkirchner, H. L., Linden, H. R., Ind. Eng. Chem. Proc. Design Develop. 2, 153-62 (1963).

6. Feldkirchner, H. L., Lee, A. L., Johnson, J. L., Eakin, B. E., Paper presented at 52nd National Meeting, American Institute of Chemical Engineers, Memphis, Tennessee, Feb. 3-5, 1964.

7. Goring, G. E.,Curran, G. P., Tarbox, R. P., Gorin, E., Ind. Eng. Chem. 44, 1051-65 (1952).

8. Goring, G. E., Curran, G. P., Zielke, C. W., Gorin, E., Ind. Eng. Chem. 45, 2586-91 (1953).

9. Hodge, E. S., Boyer, C. B., Orcutt, F. D., Ind. Eng. Chem. 54, 31-35 (1962).

10. Hunt, E. B., Mori, S., Katz, S., Peck, R. E., Ind. Eng. Chem. 45, 677-80 (1953).

11. Linden, H. R., Paper presented at 48th National Meeting, American Institute of Chemical Engineers, Denver, Colorado, Aug. 26-29, 1962; Preprint No. 14, 17-52.

12. von Fredersdorff, C. G., Institute of Gas Technology Research Bulletin 19, May (1955).

13. Wasilewski, J. C., Ind. Eng. Chem. 52, 61A-64A (1960).

14. Wen, C. Y., Huebler, J., Paper presented at 56th National Meeting, American Institute of Chemical Engineers, Houston, Texas, Dec. 1-5, 1963.

15. Zielke, C. W., Gorin, E., Ind. Eng. Chem. 47, 820-5 (1955).

16. Zielke, C. W., Gorin, E., Ind. Eng. Chem. 49, 396-403 (1957).

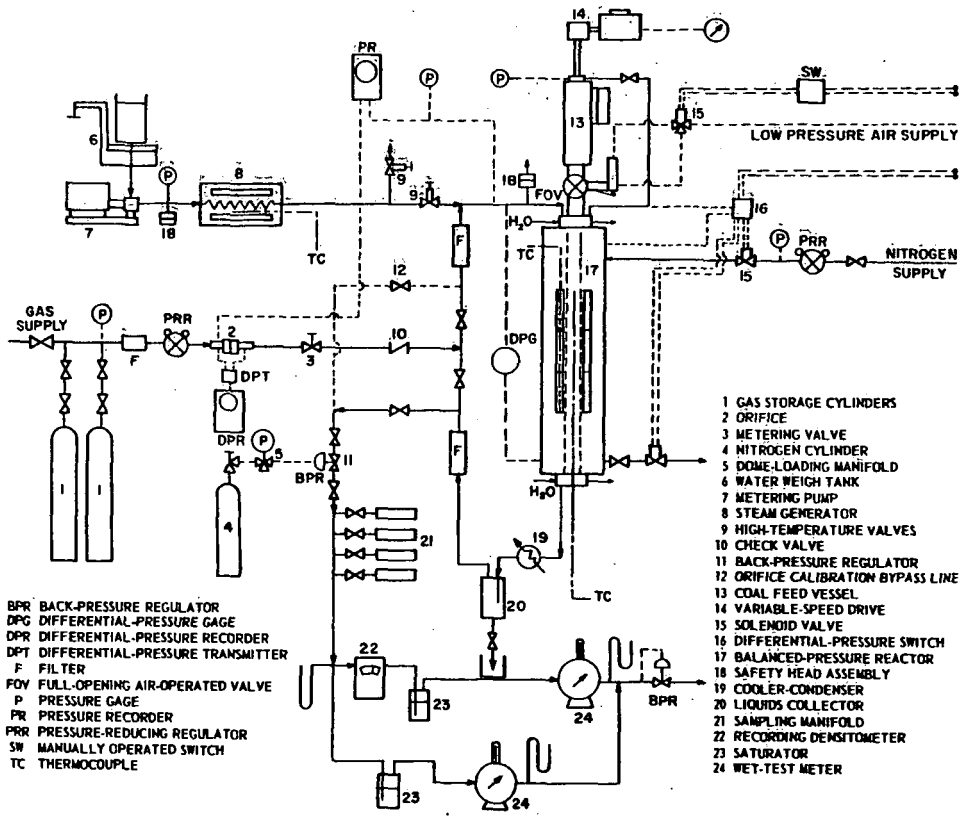

Fig. 1.-SEMIFLOW REACTOR SYSTEM

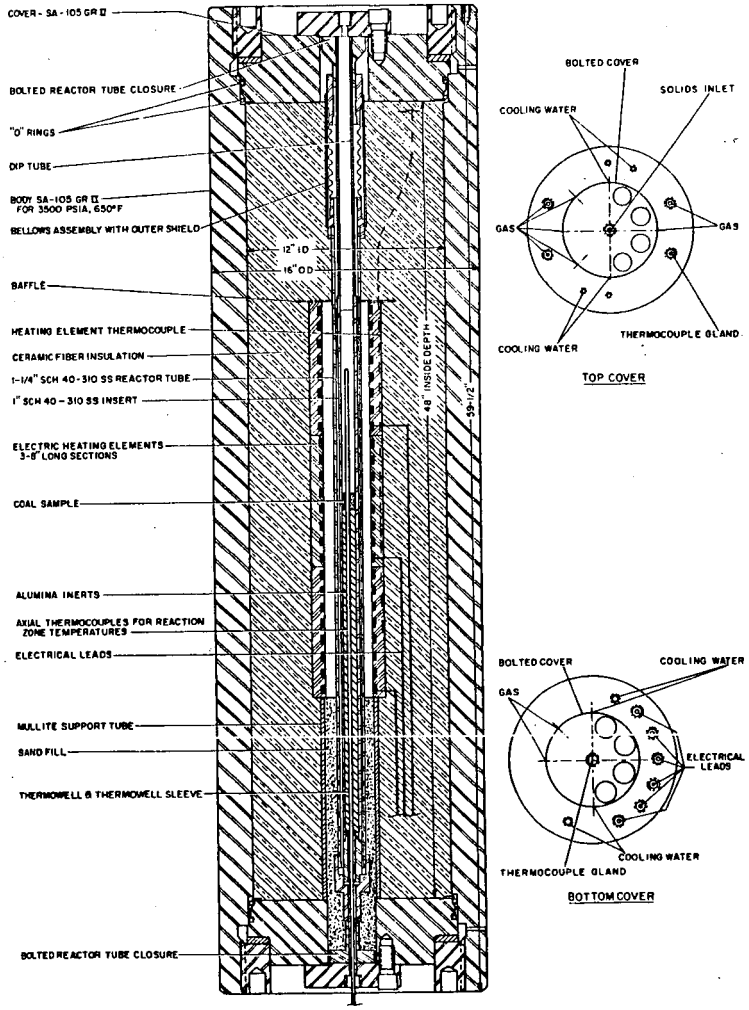

Fig. 2. - BALANCED PRESSURE REACTOR

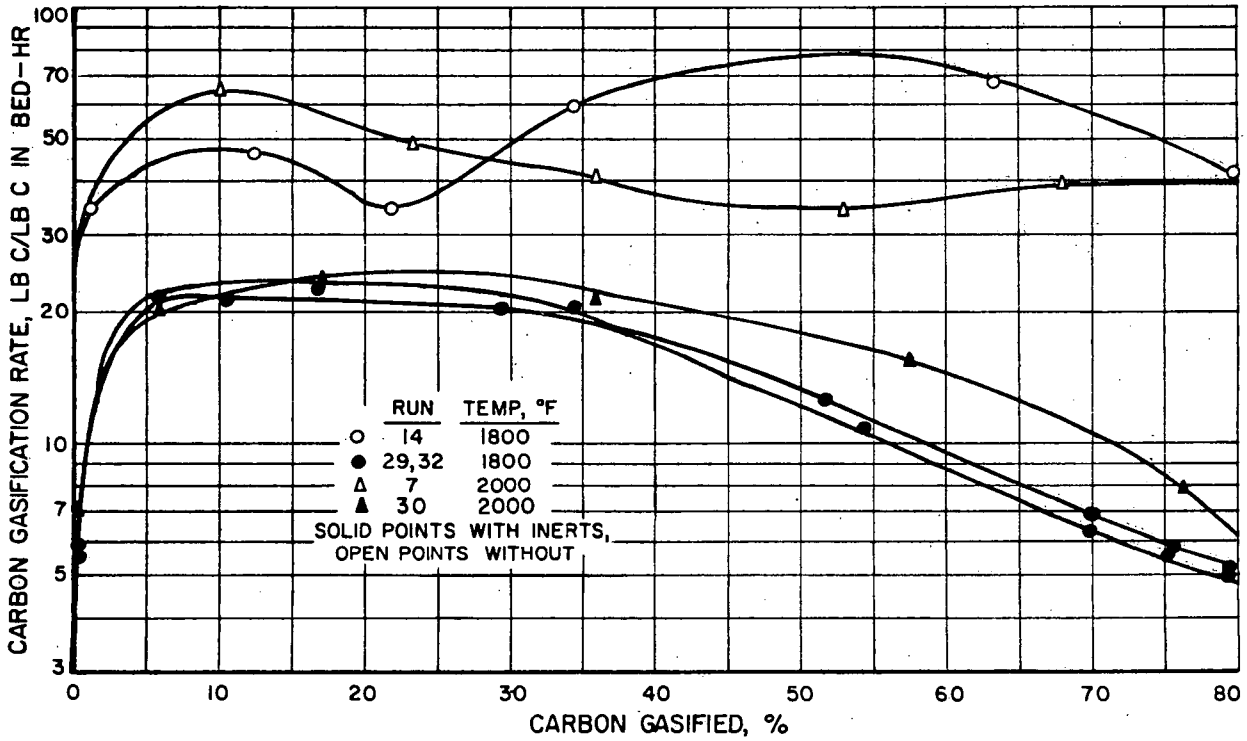

Fig. 3.-COMPARISON OF RESULTS UNDER CONDITIONS APPROACHING ADIABATIC WITH RESULTS UNDER CONDITIONS APPROACHING ISOTHERMAL

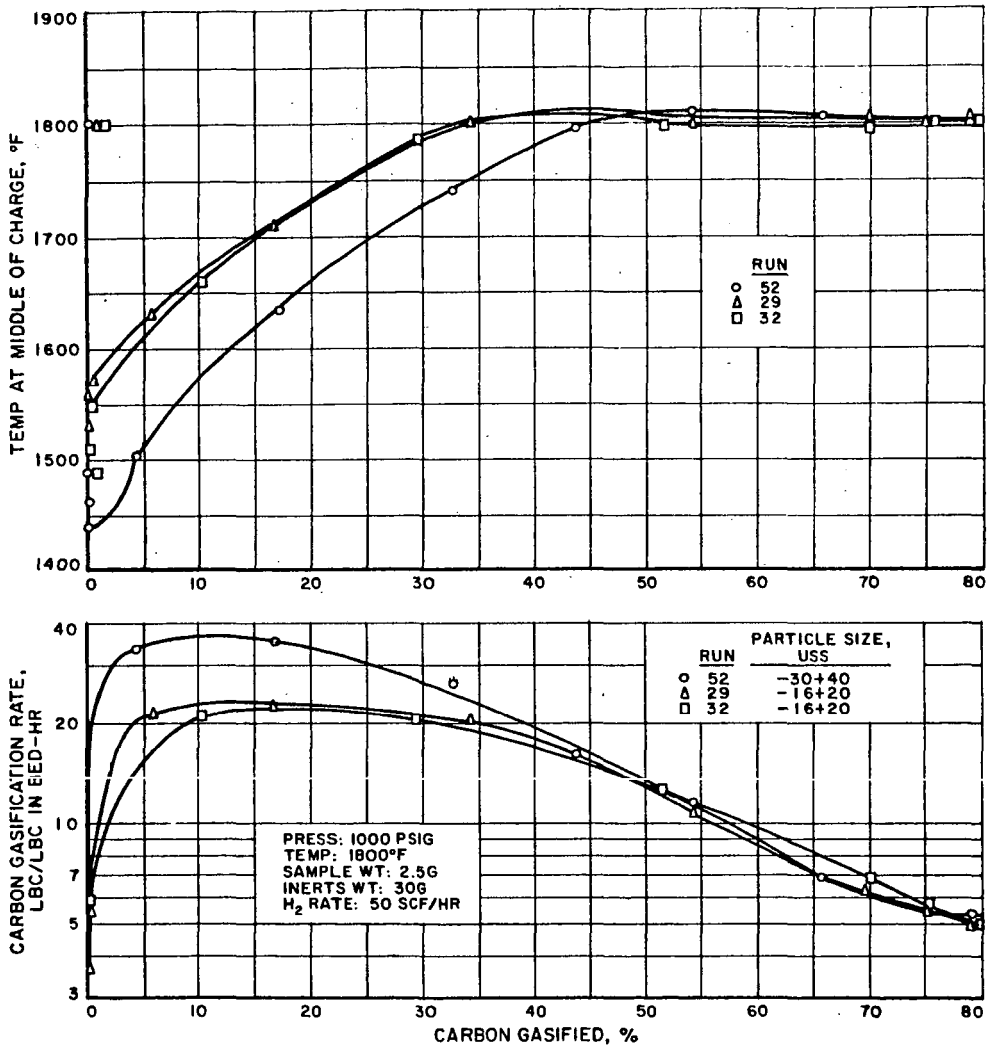

Fig. 4. EFFECT OF PARTICLE SIZE ON RATE OF HYDROGASIFICATION OF BITUMINOUS COAL CHAR AT 1800 F

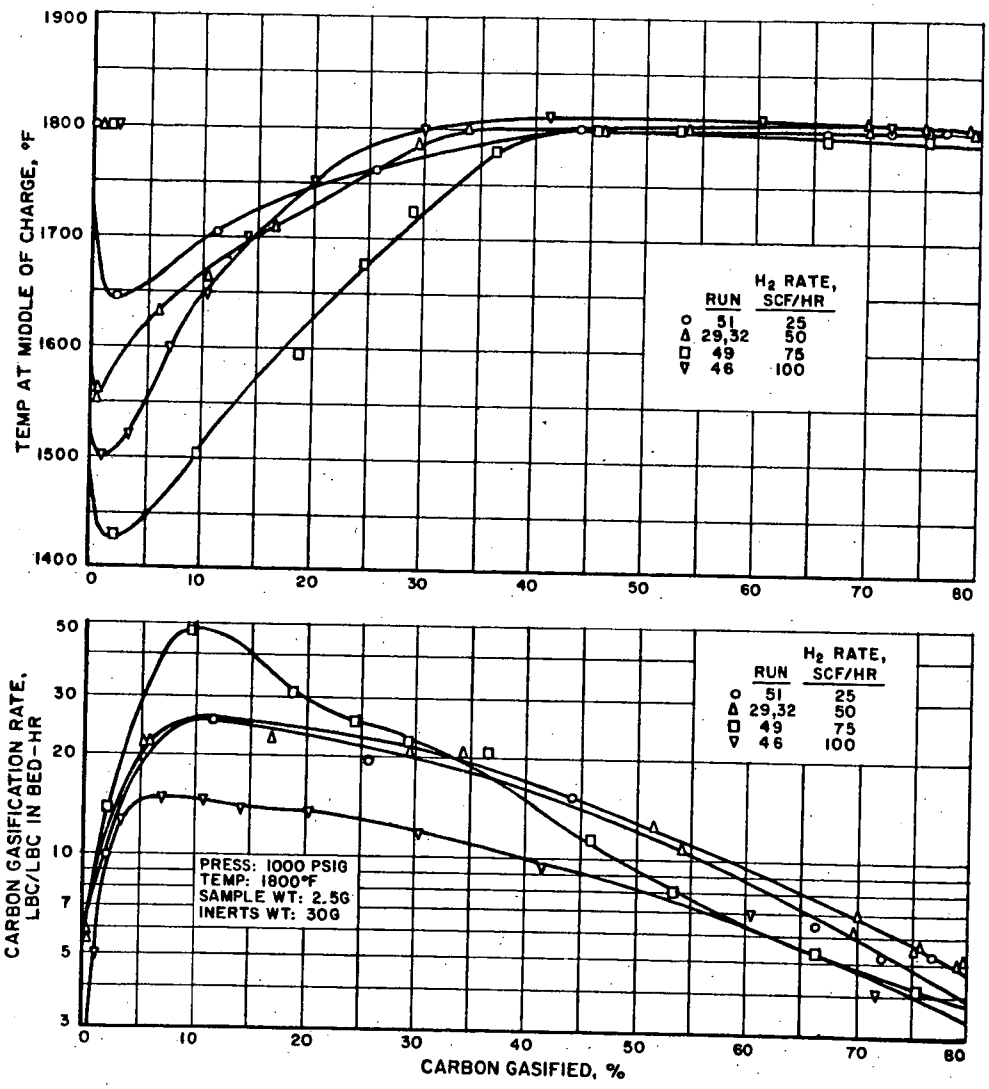

Fig 5. EFFECT OF HYDROGEN FEED RATE ON RATE OF HYDROGASIFICATION OF BITUMINOUS COAL CHAR AT 1800°F

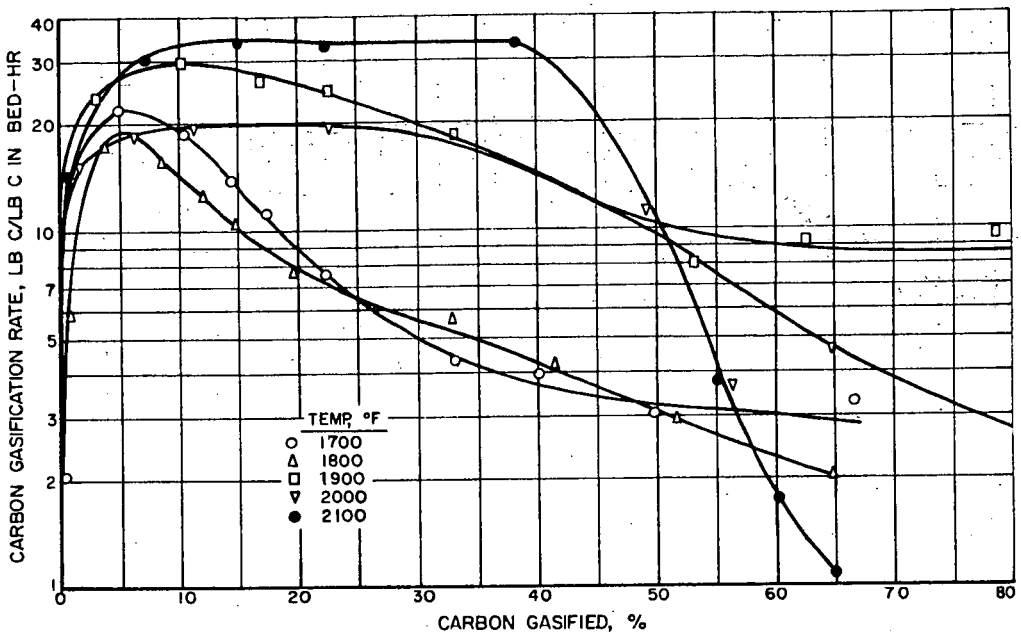

Fig. 6. EFFECT OF TEMPERATURE AND CARBON GASIFICATION ON GASIFICATION RATE WITH EQUIMOLAR STEAM-HYDROGEN MIXTURES

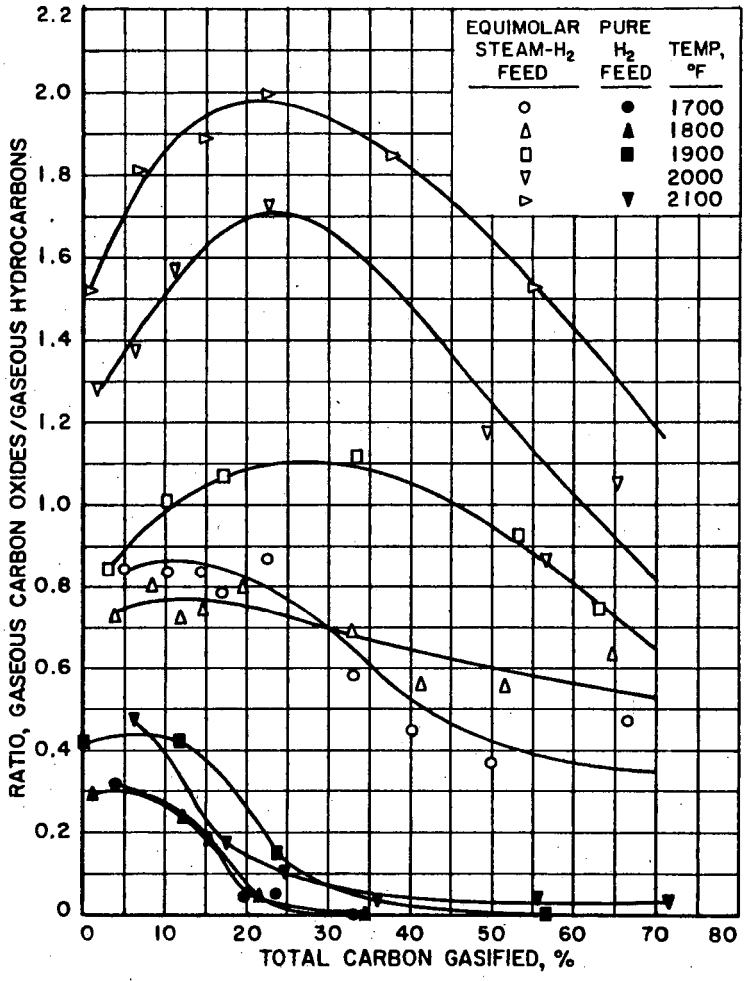

Fig. 7. EFFECT OF TEMPERATURE AND CONVERSION ON THE RELATIVE RATES OF FORMATION OF CARBON OXIDES AND HYDROCARBONS WITH EQUIMOLAR STEAM-HYDROGEN MIXTURES

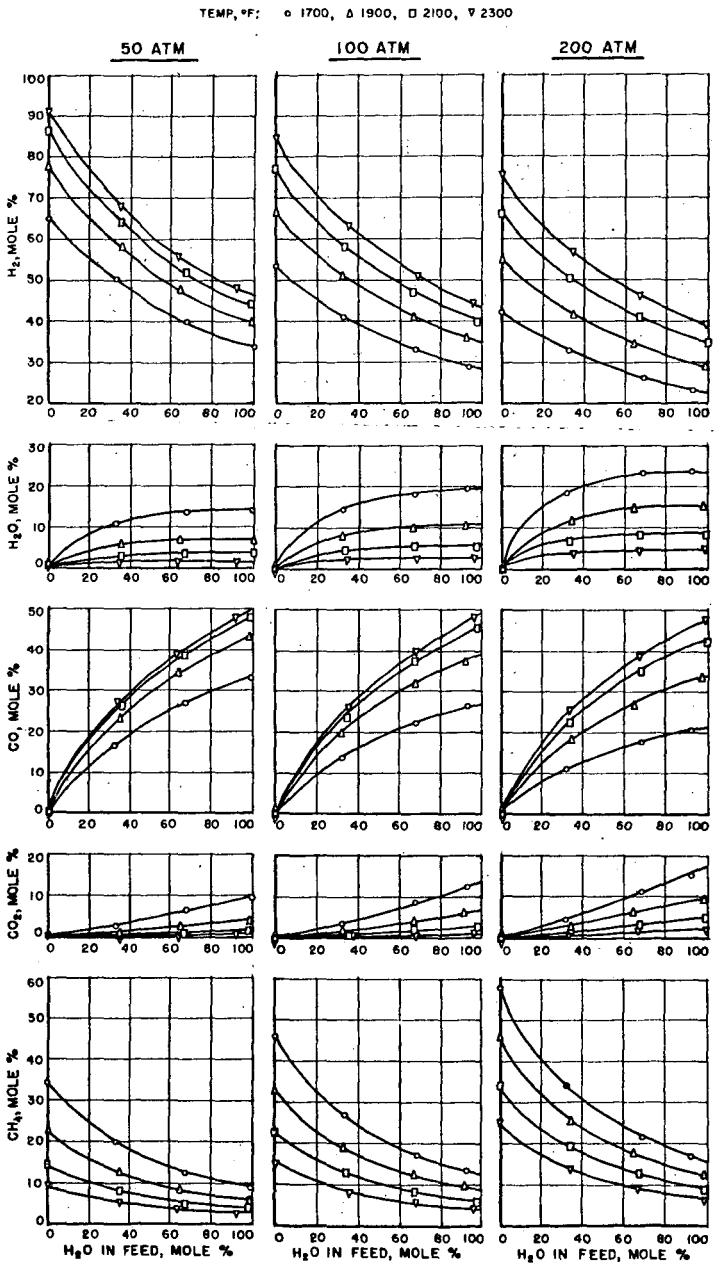

Fig. 8.-IDEAL GAS EQUILIBRIUM COMPOSITIONS FOR STEAM-HYDROGEN GASIFICATION OF CARBON AT HIGH TEMPERATURES AND PRESSURES

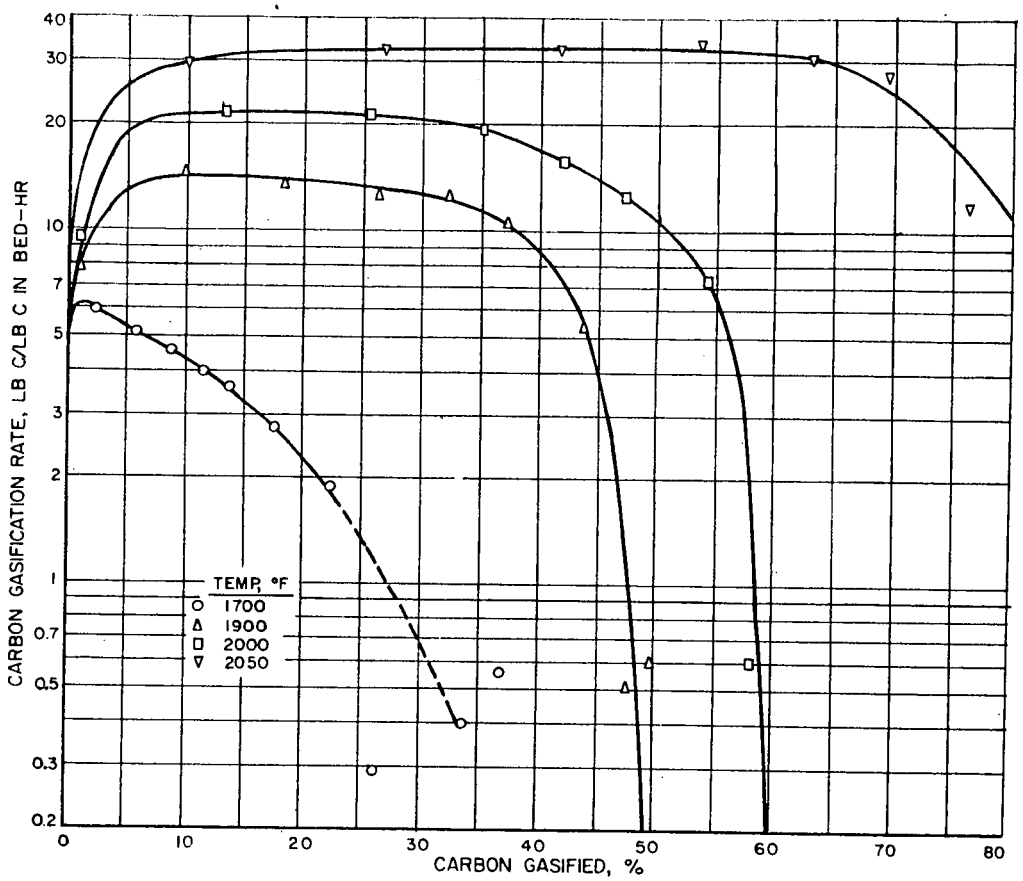

Fig 9 EFFECT OF CARBON GASIFICATION AND TEMPERATURE ON GASIFICATION RATE WITH STEAM

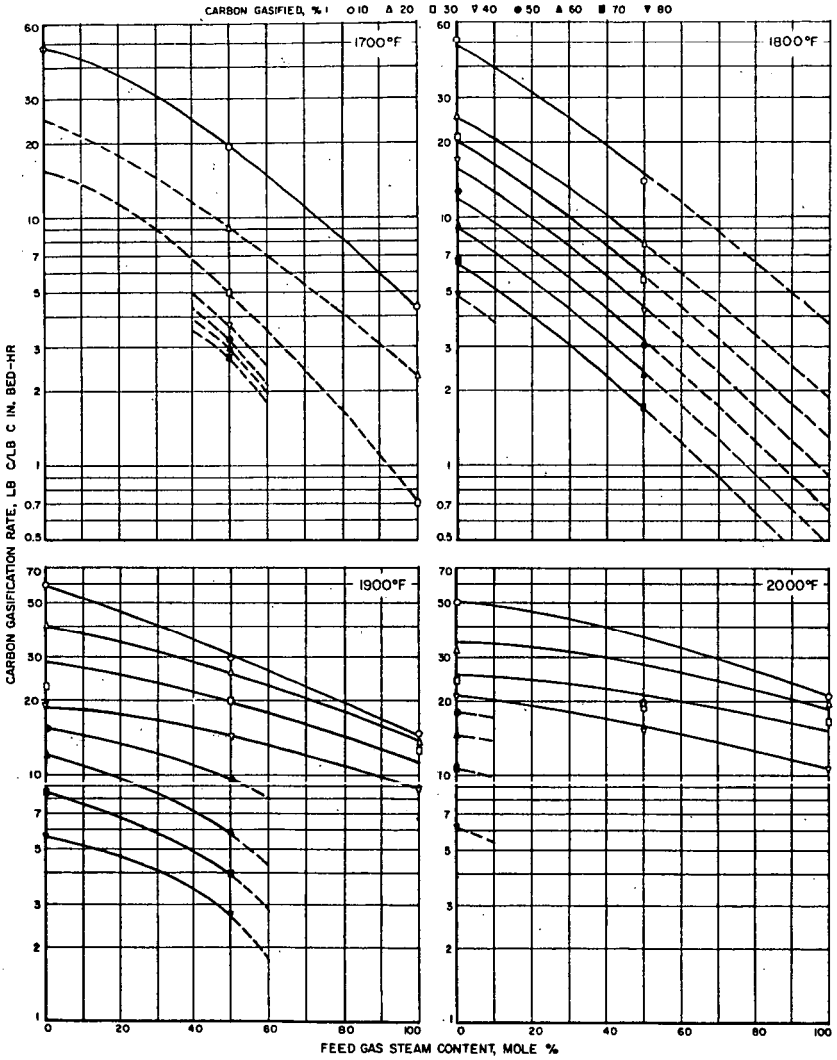

Fig. 10.-EFFECT OF FEED GAS STEAM CONTENT AND CONVERSION ON GASIFICATION RATE AT 1000 P.S.I.G.

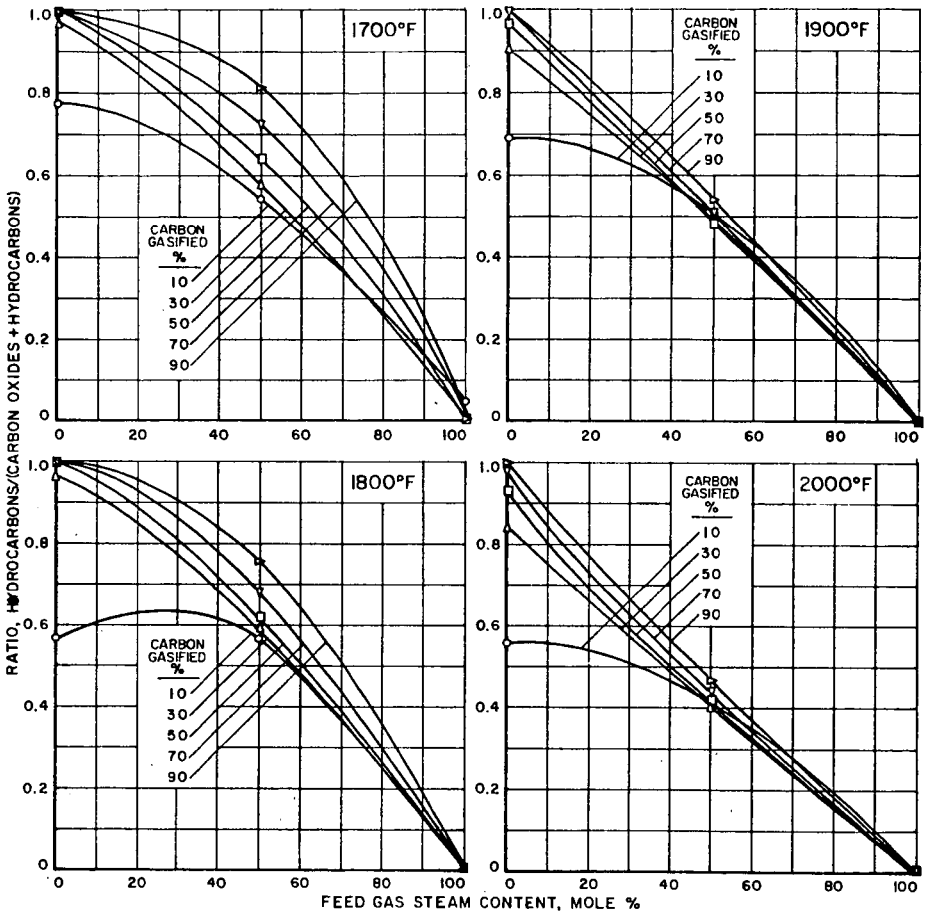

Fig 11 EFFECT OF FEED GAS STEAM CONTENT AND CONVERSION ON RATIO OF METHANE FORMATION TO CARBON OXIDES FORMATION AT 1000 P.S.I.G.

FOREIGN DEVELOPMENTS IN COAL GASIFICATION

by Harry Perry
Director of Coal Research, Bureau of Mines
U. S. Department of the Interior

INTRODUCTION

The manufacture of either producer, synthesis, or higher heating value gases from coal continues to attract worldwide attention even though large new reserves of natural gas have been discovered and production of gas from oil rather than coal appears to be more economic in many countries at present. Because proved reserves of coal are much larger than those of oil and gas, coal is expected ultimately to be the raw material used to supplement these more convenient energy forms. The timing, however, will depend on how rapidly new reserves of oil and gas are discovered, their price, and also on the success of research and development efforts on coal conversion processes.

Many factors influence the degree of interest in gasification research. For example, a review of the Soviet literature shows a sharp decline in research on coal gasification starting about 1959 and indicates the shift in emphasis to other fuels. In many countries, the reduction in the number of miners employed as a result of a decline in total coal production or because of greater productivity per man has caused serious economic dislocations and social problems. For this reason and because of a desire to use indigenous resources rather than imports, there is still a good deal of interest in the development of new processes for economically converting coal to either oil or gas. Either of these potential outlets promises large new markets for coal.

Conversion processes that make gas from coal can be classified best by the type of gas that is produced. Producer gas, enriched producer gas, water gas, enriched water gas, synthesis gas, and synthetic methane are the major types of products that are usually made. Processes are operated at either atmospheric or superatmospheric pressures. Coal, coke, and char can be gasified in fixed beds in fluidized beds, and by entrainment.

In the U.S. after World War II, interest in gasification was centered upon the production of synthesis gas for subsequent use in the manufacture of either liquid or gaseous fuels. Since most synthetic fuel processes use gas at elevated pressures, significant savings are possible if pressure gasification is used. Moreover, because the manufactured products would be needed first in the densely populated eastern portion of the U.S., processes were sought that could use the strongly coking coals that are found in the east.

Interest in producer gas and water gas declined rapidly as natural gas became available in those markets at relatively low cost. However, as gas prices have continued to rise steadily during the past 15 years, there has been a revival of interest in the manufacture of a clean hot producer gas from coal for industrial use. In the more distant future, supplementing natural gas reserves with methane made from coal appears to be most promising.

In most foreign countries gas of lower heating value than methane is distributed, and processes making such gases have been extensively investigated. Lurgi generators, which operate at high pressure and produce a considerable

percentage of methane in the synthesis gas, are particularly well suited for this type of market. However, in many foreign countries noncoking or weakly coking coals, which the Lurgi generators require, are usually readily available.

GASIFICATION WITH AIR AND STEAM

While the U.S. coal industry has indicated renewed interest[1/] in the development

1/ Garvey, James R. Report in Proceedings of National Coal Assoc. 44th Anniversary Meeting, Washington, D.C., June 6-8, 1961, pp. 59-68.

of lower cost processes for the manufacture of producer gas for industrial use, as yet no new research has been initiated. This same situation exists in many foreign countries. In Germany, the vortex producer[2/] developed by Ruhrgas is not

2/ Nistler, F. The Ruhrgas Vortex Coal Dust Producer. Coke and Gas, Vol. 19, No. 213, February 1957, pp. 54-57.

being operated, although a similar gas generator has been constructed in England at the Manvers Main Coke Works. At such installations, the manufactured producer gas is used to heat coke ovens, thus releasing the higher heating value coke-oven gas for distribution.

In Japan, research has been carried out at the Tokyo Institute of Technology[3/]

3/ Kensuki Kawashimo, and Kozo Katayama. Combustion of Coal by Gasification. Bulletin Japanese Soc. of Mech. Eng., Vol. 4, November 1961.

on developing novel methods of making producer gas to be used for combustion in boilers, gas turbines, or industrial furnaces. In early experiments, 12 nozzles were used to inject two-thirds of the air tangentially into a fixed-bed producer. The other one-third was introduced beneath the rotating grate to reduce the carbon content of the ash. These tests proved that high-ash low-quality coals could be used to manufacture a satisfactory producer gas.

In more recent experiments, the producer was enlarged from 800 to 1,350 mm. in diameter. In July 1963, a rectangular producer 1,400 by 2,800 mm. with a number of cylindrical, horizontal, rotating grates was placed in operation and is now under test.

At the Industrial Research Institute of Hokkaido,[4/] experiments have been

4/ Private correspondence, Rinzo Midorikawa, Director of Ind. Research, Institute of Hokkaido.

conducted on making producer gas from high-ash coals, lignite, and peat in a fixed bed. Coals with ash contents as high as 40 percent gave low thermal efficiencies, but lignites and peats were more easily converted and gave a gas of higher quality. Gas obtained from the drainage of methane from coal seams and containing up to 45 percent of air was converted to an oxygen-free gas in the producer, but the methane in the gas was decomposed in the process.

Although there has been a decline in interest in coal gasification in France because of the discovery of large deposits of natural gas, work on a fluidized-bed

process was pursued until recently.[5] Most of the tests used either lignite or

5/ Jequier, L., L. Longchambon, and G. Van De Putte. The Gasification of Coal Fines. J. Inst. Fuel, Vol. 33, No. 239, December 1960, pp. 584-591.

anthracite as fuel, although a few tests were made with bituminous coal. Temperatures had to be controlled closely to permit proper removal of the ash, but gasification of fines using a gasifier with specially designed bottom sections and carefully controlled injection of gases made this possible. As a result of this work, it was concluded that a large-scale plant could be built and operated successfully.

In Germany, increased capacity of water gas sets has been attained, and gases suitable for town gas distribution can be produced through oil carburetion during the down run period. This development will permit producers using coal and coke to compete effectively in some areas with gas produced from petroleum products alone.[6]

6/ Domann, Von Friedrich. Methods of Gas Production - The Effect of New Types of Gas, Reprinted from Internationale Zeitschrift fur Gaswarme (International Gas Heat Journal, Vol. 12, 1963, pp. 177-179.

In another modification of the water gas process, the generation of water gas from coal rather than coke has been developed in order to be able to use indigenous noncoking coals and avoid the use of more expensive coke.[7] In this process, the

7/ Domann, Von Friedrich and Hubert Schmitt. The Production of City Gas by Low-Temperature Carbonization of Coal in Tokyo andFreiburg (Breisgau)., Reprint from "Erdol und Kohl" Volume 12, 1959, pp. 883-90.

vessel above the gas generator is designed so that there is sufficient residence time for the coal to be carbonized before it reaches the gas generator.

GASIFICATION WITH OXYGEN-ENRICHED AIR AND STEAM

Starting in the mid-1950's, research in The Netherlands using oxygen-enriched air (50 percent oxygen) in fixed-bed gasifiers showed that such equipment could be operated using coke as the fuel and with the removal of ash as slag. These tests were continued until 1960, using oxygen concentrations as high as 90 percent because gases produced in this manner gave greater flexibility and were more economically attractive than either straight producer or water gas. Work on this process was discontinued with the recent discovery of large reserves of natural gas in The Netherlands.

The "bottom blown" gasifier requires only a relatively shallow fuel bed because of the more uniform distribution of the gasifying medium and the bottom flow characteristics of the fuel bed. However, the actual depth of bed required will depend on the rate of carbonization of the coal under the conditions in the gasifier.

Experimental work is still required to determine (1) the extent of the carry-over of fines and whether they can be recycled, and (2) the carbonization time of the coal in the gasifier. Large-scale experimental work under pressure is also needed to determine the heat losses in the water-cooled grates and the reduction in coal gas efficiency because of higher exit gas temperatures in the shallow fuel bed.

Badische Anilin and Soda Fabrik of Germany has developed a slagging gas producer operating at atmospheric pressure that can produce synthesis gas, using as a fuel either coke or a mixture of coke and hydrocarbons.[10/] The design

10/ Duftschmidt, F. and F. Markert. Large-Scale Slagging Producers of Gas for Chemical Syntheses (Entwicklung von grosstechnischen Abstichgeneratoren zur Synthesegas-Erzeugung) Chemie-Ing-Techn., Vol. 32, No. 12, 1960, pp. 806-811.

of the slagging section was reported to be particularly satisfactory, and little difficulty has been reported from failure of refractories or with removal of the slag. A bath of slag is maintained at the base of the generator and slag is tapped intermittently. Satisfactory removal of the ash requires the addition of a limestone flux. The reaction of limestone with the coke ash to give a free flowing slag takes place mainly in the slag bath so that good distribution of the limestone and adequate residence time of the slag bath are required for satisfactory operation. The carryover dust is recirculated and is injected into the gasifier in a stream of the gasification medium. Forty to fifty percent gasification of dust is accomplished in one reinjection. Table 1 shows typical results obtained in this gasifier.

At the Regional Research Laboratory at Hyderabad, India, interest in gasification is centered about the use of coals containing from 25 to 35 percent ash. A slagging fixed-bed gasifier with a coal rate of 30 to 40 pounds per hour has been erected with a shaft 6 inches in I.D. and a slagging section 12 to 14 inches in I.D.[11/] Four water-cooled tuyeres of 3/8 inch I.D. and 1/2 inch

11/ Some Aspects in the Design of Gasifier. Indian Chemical Engineer, July 1963.

diameter centrally located taphole have been provided. To date only preliminary experiments have been made using low-temperature coke as fuel and blast-furnace slag as a fluxing medium. These first experiments are being directed toward developing a satisfactory method of slag removal, and with a weight ratio of coke to slag of 7 to 3, satisfactory operations of from 45 minutes to 3 hours have been achieved.

Table 1.-Atmospheric pressure fixed-bed slagging gasification using coke

Material requirements[1/]	
Coke (87% C), pounds	27.8
Steam, pounds	18.9
Oxygen (90%), cu. ft.	240
Steam generated, pounds	10.8
Superheated steam, pounds	3.8
Gas analysis, volume percent	
CO_2	6
CO	62
H_2	31
N_2	1

1/ Per 1,000 cu. ft. CO +H_2

The Koppers Totzek process, which uses a wide range of solid and liquid fuels as feedstock, has been installed in a number of locations throughout the world.[12] However, no recent developments have been reported in oxygen gasification

12/ Osthaus, K. H., and T. W. Austen. Production of Gas from a Wide Range of Solid and Liquid Feedstocks by the Koppers Totzek Process. Gas World, Vol. 157, No. 4091, Jan. 12, 1963, pp. 98-103.

using entrained processes.

Improvements have also been reported[13] in the fluid-bed Winkler generator,

13/ Flesch, Von Wilhelm, and Gunter Velling. The Gasification of Coal in the Winkler-Generator. Erdol und Kohle, Vol. 15, No. 9, September 1962, pp. 710-713.

which is capable of gasifying both lignitic and bituminous coals. Modifications have been made in design to accommodate coking coals, and improvements in the generator are reported to give increased economies. By feeding a portion of the oxygen and steam into the upper part of the fluidized bed, it is possible to get high carbon conversions without slag formation.

Pressure Gasification

For many uses, synthesis gas is required at pressures of 30 atmospheres or more. Thus there has been a continuing interest in gasification processes operating at elevated pressures, since considerable savings are possible if the product gas is to be used at these pressures.

Because of limitations inherent in entrained and fluid-bed processes, the most economic method for producing synthesis gas from solid fuels at pressure appears to be fixed-bed operation removing the ash either dry or as a slag. Fixed-bed processes, however, require a sized fuel, and if coal is used, it must be noncoking or weakly coking. Dry ash removal requires an excess of steam and low throughput per unit volume of gasifier to keep the ash in a condition to be successfully handled. The removal of slag under pressure, however, introduces many difficult operating and design problems for which solutions are still being sought.

A number of Lurgi installations using dry ash removal have been installed in many countries. Operating results of the Westfield Lurgi Plant in Scotland, which is the most modern plant for which data are available, have recently been published[14] and are shown in Table 2.

14/ Ricketts, T. S. The Operation of the Westfield Lurgi Plant and High-Pressure Grid System. The Institution of Gas Engineers, Copyright Publication 633, May 1963, 21 pp.

A major improvement in Lurgi plant design has been accomplished recently in Germany by changing from water-cooled to steam-cooled grates, using the wet steam from the gasifier for this purpose, and by reducing the amount of steam to the gasifier. At Dorsten, the steam requirement was cut nearly in half, and the volume of gas produced could then by increased by 70 percent with only a 45-percent increase in oxygen consumption.

Table 2.-Operating results of Lurgi gasifier at Westfield

Material requirements 1/	
Coal, pounds	55.5
Steam, pounds	56.1
Oxygen, cu. ft.	238
Gas analysis, (crude), volume percent	
CO_2	24.6
C_nH_m	1.1
CO	24.6
H_2	39.8
CH_4	8.7
N_2	1.2

1/ Per 1,000 cu. ft. CO + H_2

Two other improvements in the Lurgi process have been introduced at Dorsten. In the first, the carbon monoxide in the crude gas is converted over a cobalt-molybdenum catalyst (by water gas shift) to carbon dioxide before the gas is purified. This results in a lower cost gas since no additional steam must be added as must be done in conventional carbon monoxide conversion where the excess steam is first removed from the raw gas and then added back before shift conversion. In the second improvement, air was added to the gasifying medium (this is satisfactory for certain types of gases in town use) and resulted in further improvement in plant operation. Steam decomposition was increased, thus reducing steam requirements, and because part of the oxygen was introduced as air, there was a substantial reduction in power requirements to produce oxygen.

In Germany experiments were conducted on pretreating the coal in the lock hopper of the coal feeding device to reduce the coking characteristics of the coals so that a wider range of coals could be used. The coal was treated with a mixture of carbon dioxide, nitrogen, and 1 percent O_2 at 200° to 250° C for 15 minutes; however, on the coals tested, little difference was noted in the operating results. These tests, along with others, indicated that for a given coal, coking problems were more severe in the smaller test generators than they are in the full-scale units. Because of the potential advantages of slagging operation, the most recent fixed-bed pressure gasification experimentation has used this type of ash removal. Research is underway on this method in the U.S., England, the U.S.S.R., and Germany.

The only recent report on gasification from the Soviet Union describes tests with a fixed-bed slagging gasifier operating at 5 atmospheres using anthracite as the fuel. These tests also involved refiring carryover dust and using up to 50 percent pulverized fuel.

In England, research on pressure gasification using a slagging fixed-bed gasifier has been conducted by the Gas Council at the Midlands Research Station and by the Ministry of Power at the B.C.U.R.A. Research Station at Leatherhead. This latter program was terminated in March 1962 after demonstrating that slagging operation under pressure could be accomplished. In addition, these experiments indicated probable methods for "scaling up" through the use of multiple tuyeres

and has shown the potentials for using coal rather than coke as a fuel.[15/]

15/ Masterman, S. O., and W . A . Peet. The Development of a Pressurized Slagging Fixed Bed Gasifier. Proc. of the Joint Conf. on Gasification (Institution of Gas Engineers and Institute of Fuel), Hastings, September 1962.

At the Midland Research Station, work is continuing on the slagging gasifier in a new pilot plant that was installed in 1962. The gasifier has a 3-foot I.D., operates at pressures up to 375 psi, and is designed to produce 5 million cubic feet per day of gas.

Until now the program has been aimed at the development of the hearth, slag tap, and slag discharge system. To avoid unnecessary experimental difficulties, graded coke has been used as a fuel, and the plant has been operated for as long as 90 hours at pressures of 300 psi and at 3 million cubic feet per day throughput. Slag is tapped intermittently and is quenched in water at the operating pressure. Experiments on the use of coal as a fuel were started in late November.

HYDROGASIFICATION OF COAL

Interest continues on the hydrogasification of coal, which was started at the Midland Research Station, but experimental work has been delayed because of the present emphasis in England on the use of petroleum feedstocks. For the type of gas distributed in England, the process selected[16/] for study

16/ Dent, F. J. Chemical Engineering in the Production of Town Gas by Pressure Gasification Processes. Proc. of the Joint Conf. on Gasification (Institution of Gas Engineers and Institute of Fuel), Hastings, September 1962.

involves a two-stage hydrogenation of coal in fluidized beds at 70 atmospheres pressure. The first stage will operate at 1,475° to 1,560° F. to hydrogenate the volatile matter at lower temperatures, which thermodynamically favor a higher heat content of the gas. Char will be recycled to enable use of all types of coals. The second stage will operate at 1,650° to 1,740° F. to take advantage of the faster reaction rates at the higher temperatures required for the less reactive char. The residue of the hydrogenation is gasified, using oxygen and steam in a fluidized bed. The residue from the gasifier is used for steam production.

In similar research in Australia, tests have been made on the hydrogenation of brown coal in fluidized beds at pressures of 300 to 600 psi and at temperatures between 930° and 1,740° F. Early tests using cocurrent flow have been reported,[17/]

17/ Birch, T . J., K. R . Hall, and R. W. Urie. Gasification of Brown Coal with Hydrogen in a Continuous Fluidized-Bed Reactor. J. Inst. Fuel, Vol. 33, No. 236, September 1960, pp. 422-435.

but the latest design uses countercurrent flow of reactants. The first experiments indicated that the reaction occurs in two stages with the first stage involving a rapid reaction of the oxygen-containing functional groups. The second stage involves a much slower reaction of the hydrogen with condensed carbon and required a much higher concentration of hydrogen and higher temperatures to get reasonable reaction rates.

Experiments with the countercurrent apparatus are still underway. To take advantage of the rapid hydrogenation at low temperatures during the initial period

and yet obtain the higher temperatures required for the second stage, the 20-foot reactor is divided by perforated plates into a number of separate fluidized beds operated is progressively changing temperatures.[18] Because of the difficulties

18/ Bennett, B. B. The Gasification of Latrobe Valley Brown Coal. Presented at Conf. on Gasification of Lignite and Inferior Fuels, Belgrade, Yugoslavia, September 16-18, 1963.

encountered with excessive devolatilization in the coal delivery tube, only chars have been used until now for extended runs. Comparison of these results with those in the cocurrent apparatus cannot be made as yet because of the use of char and other differences in operating conditions. Preliminary results using this apparatus are shown in Table 3.

Table 3.-Hydrogasification of Latrobe Valley Coal

Volatile matter in char, percent		18.0
Pressure, psi		600
Temperature, °F.		1,380
Effective reactor length, feet	4	6½
CH_4 content outlet, percent	17.3	27.2
Char gasified, percent	50.2	63.3

SPECIAL GASIFICATION PROCESSES

Using entrained gasification systems with fine coal, high carbon conversions can only be attained with high oxygen requirements. The Rummel[19] single-shaft

19/ Rummel, Roman. Gasification in a Slag Bath. Coke and Gas, Vol. 21, No. 247, December 1959, pp. 493-501, 520.

generator in which the oxygen-coal and steam are injected into a rotating slag bath is an apparatus designed to provide extra residence time to get more complete gasification at reduced gasifier volumes. Other potential advantages are its ability to use a high-ash coal, to operate with both coking and noncoking coals, and to use a larger sized feed. If air is used in place of oxygen, producer gas can be manufactured.

Another modification of the slag bath generator uses a double shaft instead of the single shaft, substitutes air for oxygen, and still produces a nitrogen-free mixture of carbon monoxide and hydrogen. The slag bath contained in the bottom of a circular shaft is divided into sections by two vertical dividing walls. On one side coal and steam are injected into the rotating slag bath, and the coal is devolatilized and partly gasified by the steam, using heat supplied by the molten slag. In the second section, the balance of the coal and some fresh fuel are burned to raise the temperature of the slag and to oxidize the slag constituents that were reduced in the gasification section.

An experimental program on the double-shaft generator is being carried out at the Bromly-by-Bow Works of the North Thames Gas Board to determine its feasibility and to predict the cost of making gas in a full scale plant. The plant was designed to have a capacity of 95,000 standard cubic feet per hour, and a gas composition of 3.9 percent CO_2, 45.2 percent CO, 50.5 percent H_2, and 0.4 percent H_2S (nitrogen-free basis) was expected.

In initial tests (June 1962) coal was fired into the combustion shaft with the separating curtains absent so that the slag could flow unimpeded from one chamber to another. The slag flowed easily at 2 feet per second with a mass flow of about 200 tons per hour. In subsequent tests coal was introduced into the gasification chamber but the seal between the two chambers was not used because even in its absence insufficient heat was transferred to the slag by the combustion of coal. In addition, the points of admission of the steam and coal in the gasification chamber were such that contact between the reactants was poor.

After suitable modifications, the heat transfer to slag was increased by raising the blast pressure from 18 to 100 inches of water gauge, and the slag circulation rate was increased to 500 tons per hour. Better contact between the coal and steam was obtained by admitting these reactants to the gasification chamber in a single tuyere submerged below the slag surface. After the seal between the two chambers was put into place, a gas output of 40,000 standard cubic feet per hour was obtained. Gas composition was:

	Percent
CO_2	8.5
CO	23.0
H_2	45.0
C_nH_m	0.3
CH_4	2.5
O_2	0.5
N_2	20.2

Overall efficiency was 20 percent (heating value of gas divided by the heating value of coal consumed), although the corresponding efficiency considering only process coal was 69 percent. Improvements in the tuyeres are being made that are expected to increase the efficiency to 30 to 35 percent.

An economic appraisal of the process is now underway and if it can be shown to be economically attractive, if 50-to 60-percent efficiency can be achieved, an attempt will be made to demonstrate that such an efficiency can be obtained by redesign of the gasifier.

SUMMARY

Although improvements have been made in many of the coal gasification processes that have been developed, the competition from new discoveries of natural gas and from oil gasification processes makes their widespread application difficult to attain both in the U.S. and abroad. Continued experimentation, however, is being carried out on the most promising processes, and additional reductions in the cost of manufacturing a suitable gas for distribution can be expected. While many of the foreign research programs in this field have direct application to U.S. conditions, because a lower heating value gas is being sought, there is some difference in emphasis between foreign and U.S. programs. Of special interest at present are the experimental projects on slagging fixed-bed pressure gasification and the direct hydrogasification of coal to a higher heating value gas.

SOME RESULTS FROM SLAGGING, FIXED-BED GASIFICATION OF LIGNITE AT PRESSURES TO 400 PSIG

G. H. Gronhovd, A. E. Harak, and M. M. Fegley

U. S. Department of the Interior, Bureau of Mines
Grand Forks Lignite Research Laboratory
Grand Forks, N. Dak.

INTRODUCTION

Gasification of coal with steam and oxygen to produce synthesis gas is one of the promising basic starting procedures for converting our vast coal reserves into the convenient fluid fuels, gas and oil. Perhaps the most attractive gasification method, from the standpoint of thermal efficiency, is the fixed-bed system with its inherent good heat exchange between the countercurrent flowing coal and hot gases. Fixed-bed gasification is limited to those fuels that do not agglomerate under the conditions existing in the gasifier shaft. Lignite, being a nonagglomerating fuel, is well suited for this process.

In 1958 the Bureau of Mines began development of a high-pressure, fixed-bed, slagging gasification pilot plant at Grand Forks, N. Dak. The objectives of the program were to develop a suitable pilot plant technique for slagging gasification of lignite and other noncaking fuels at pressures to 400 psig and to obtain process data as a function of operating pressure and other variables. It was hoped that the new process would show significant advantages over the conventional Lurgi pressure gasifier, which operates with dry ash removal. Some of the advantages predicted for slagging operation were increased capacity, increased thermal efficiency, reduced steam consumption, and reduced quantity of waste liquors. Other advantages of a slagging gasifier are its ability to use coals having low ash fusion temperatures and the absence of a mechanical grate, which can require considerable maintenance in a large commercial gasifier.

Slagging pressure gasification does, however, pose some formidable problems in refractory erosion and in methods of discharging molten slag from a pressure vessel.

The gasifier was originally equipped with a low-pressure bottom section, and the early development work was done at 80 psig. A bituminous coal char, Disco, was used as feed material for the initial tests because it was tar-free, and the char ash, when fluxed with blast-furnace slag, had very desirable flow characteristics. In general, the development procedure has been to establish a satisfactory slagging technique for a given design and pressure, using Disco char, and then, after developing necessary techniques, to switch to operation with lignite.

Based on the experience and data obtained at 80 psig, a new high-pressure bottom section was designed for the gasifier. This unit was installed in October 1962, and since then, the gasification pilot plant has been operated at pressures

---

[1] Trade names are used for identification only, and endorsement by the Bureau of Mines is not implied.

to 400 psig. Disco char was used for the first high-pressure tests, but in May 1963 a series of tests was started to demonstrate the operability of the gasifier at high pressures using North Dakota lignite. Since then, eight tests have been run at pressures from 200 to 400 psig, and this paper will be primarily concerned with the experiences and results from these tests.

DESCRIPTION OF THE PROCESS

A flowsheet of the slagging gasification pilot plant is presented in figure 1. The fuel, which is periodically charged to the coal lock, moves by gravity flow into the generator and is continuously gasified by an oxygen-steam mixture introduced through four water-cooled tuyeres at the bottom of the gasifier. Molten slag is formed at the hearth and flows through a central 1-inch-diameter taphole into a water quench bath. The slag-water slurry is periodically discharged from the slag lock.

The product gas leaving the gasifier and containing water vapor and tar is scrubbed in the spray cooler with recycled liquor that has been condensed out of the gas. The washed gas is then cooled to about 60° F in an indirect cooler before being sampled, metered, and flared.

Some cooled product gas is compressed and recycled through the coal lock to prevent steam and tar vapors from condensing on the cold fuel.

Gas from the high-temperature reaction zone can be drawn through the taphole to aid slag flow. This gas is cooled and metered in a separate circuit.

A cross-section view of the gasifier is presented in figure 2. The inside diameter of the unit is 16-5/8 inches, giving a fuel bed area of 1-1/2 square feet. An available maximum fuel bed depth of 15 feet provides heat exchange and gas residence times similar to those in a commercial Lurgi unit.

For additional details on equipment design and operating procedure, refer to the recent Bureau of Mines Report of Investigations 6085 (1).

FUELS AND FLUXES TESTED

North Dakota lignite as-mined usually contains from 35 to 40 percent moisture. Before being charged to the gasifier, this lignite is dried to 20 to 25 percent moisture in a Fleissner steam drier and then screened to 3/4 by 1/4 inch. A typical analysis of a dried lignite as charged to the gasifier is shown in table 1, along with an analysis of Disco char.

One of the most important criteria for a coal to be used in any slagging process is that the molten slag must have a sufficiently low viscosity to flow readily at the temperatures and atmospheres developed in the process. As an aid to predicting desirable fuel and flux combinations to be used in the slagging gasifier, viscosity determinations were made by an industrial laboratory on a number of prepared samples. Figure 3 shows viscosity-versus-temperature curves for Disco char ash, for lignite ash, and for these ashes fluxed with blast-furnace slag in the ratio of 3 pounds flux per pound of ash. Chemical compositions for the various materials are given in table 2.

The Disco ash, either alone or fluxed with blast-furnace slag, exhibited essentially Newtonian flow over the temperature range investigated, and the flux was very effective in reducing the slag viscosity.

TABLE 1. - Typical analysis of fuels gasified

	North Dakota lignite	Disco char
Proximate analysis, percent:		
Moisture	22.4	2.5
Volatile matter	31.4	19.2
Fixed carbon	39.8	67.8
Ash	6.4	10.5
Ultimate analysis, percent:		
Hydrogen	5.9	3.6
Carbon	52.4	72.0
Nitrogen	0.9	1.6
Oxygen	34.0	10.4
Sulfur	0.4	1.9
Ash	6.4	10.5
Heating value, Btu/lb	8,610	12,100
Ash fusibility temperature, °F:		
Initial deformation	2,100	2,130
Softening	2,135	2,190
Fluid	2,170	2,500

TABLE 2. - Typical chemical analysis of various fuel ashes and fluxes

	Lignite ash	Lignite clinker	Disco char ash	Blast furnace slag
Analysis, percent:				
SiO_2	33.0	41.8	48.0	36.3
Al_2O_3	13.5	17.1	23.0	11.8
Fe_2O_3	7.3	8.0	18.5	3.9
TiO_2	0.6	0.8	1.0	0.3
CaO	14.5	16.9	3.3	36.6
MgO	4.4	4.4	1.0	9.0
Na_2O	12.1	8.5	0.3	0.4
K_2O	1.0	0.9	1.9	0.3
SO_3	13.8	2.6	2.7	0.9
Mn_3O_4	--	--	--	0.5
Ash fusibility, °F:				
Initial deformation	1,910	2,020	2,050	2,440
Softening	2,050	2,050	2,140	2,480
Fluid	2,140	2,140	2,430	2,520

The lignite ash had relatively low viscosity in the fluid range but exhibited a sharp deviation from Newtonian flow at about 2,000° F. This point at which the viscosity increases rapidly with a small drop in temperature is called the "Temperature of critical viscosity." The addition of blast-furnace slag reduced the slag tappability of the lignite ash by increasing the "temperature of critical viscosity" by about 350° F.

The laboratory-determined ash viscosities are helpful in assessing suitability of fuel-flux combinations for slagging gasification, and we have had some success in correlating these data with actual performance in the gasifier. However, the laboratory conditions where the sample is slowly heated and allowed to come to equilibrium at each temperature are quite different from conditions in the gasifier where the slag upon formation flows rapidly to the taphole and may not react completely with the flux material. Also, the atmosphere surrounding the slag in the gasifier may be quite different from the atmosphere in the laboratory test.

In our small gasifier it is sometimes necessary to add fluxing material with certain fuels to reduce the slag viscosity, and it is usually desirable to increase the quantity of slag flowing through the taphole and thus reduce heat loss per pound of slag flowing.

GASIFICATION OF NORTH DAKOTA LIGNITE

In some of the early lignite tests, blast-furnace slag was tried as a fluxing material, but, as predicted from the laboratory viscosity data, reliable slagging operation could not be obtained. Various methods for improving the lignite slag flow were tried, but the most successful procedure has been to add sized combustion clinkers from a local powerplant to the lignite charge. By this method the chemical composition of the ash is not appreciably changed, and the slag flow can be increased to any desired rate. The ratio of clinkers to lignite for the tests to date has ranged from 30 to 10 pounds per 100 pounds of lignite, depending upon the gasification rate. The average slag flow rates have generally been from 150 to 200 pounds per hour.

The operability of the gasifier on lignite at pressures to 400 psig was generally satisfactory, although in some tests difficulties in maintaining slag flow were encountered after 5 to 10 hours of slagging operation. As will be discussed later in the report, this problem seems to be related to iron segregation on the hearth.

Contrary to expectations, no trouble has been experienced in carrying tar vapors out of the gasifier despite the low gas offtake temperatures, often less than 300° F.

TEST RESULTS

The gas production rate is determined by the oxygen-steam input rates, and during this series of eight tests, oxygen rates used were from 4,000 to 6,500 cubic feet per hour. The oxygen-steam molar ratio was maintained at approximately 0.9 for all tests. Because of limitations on gas cooling and metering equipment, the maximum capacity was limited to 6,500 cubic feet per hour oxygen rate.

Typical results from gasification of lignite at 400 psig and 6,000 cubic feet per hour oxygen input are given in table 3. For comparison, results from a Disco char test at the same pressure and oxygen rate are also given. The gas production rate is about 29,000 cubic feet per hour, or 19,300 cubic feet per square foot per hour, for both tests. The lignite feed rate is 1,442 pounds per hour; 934 pounds per hour is the rate for Disco. The gas analysis for the lignite test shows higher CH_4 and CO_2 as a result of increased pyrolysis gas from this fuel. The concentration of sulfur compounds in the product gases are approximately proportional to the total sulfur input in the fuel.

Table 4 is a typical material balance for a lignite test at 400 psig, and table 5 is a heat balance for the same test. The heat loss to the slag is 1.3 percent, and the other unaccounted for losses are 4.0 percent of the total input heat.

TABLE 3. - Typical results from gasification at 400 psig

	Fuel	
	Steam-dried lignite	Disco char
Oxygen rate.....scf/hr[1/]	6,000	6,000
Oxygen/steam ratio .....mole/mole	0.9	0.8
Fuel rate.....lb/hr	1,442	934
Fuel rate (maf).....lb/hr	987	792
Flux ratio.....lb/100 lb fuel	10	15
Total gas rate.....scf/hr	29,000	29,100
Specific gas rate.....scf/ft^2/hr	19,300	19,400
Slag discharge rate.....lb/hr	214	231
Material requirements per Mft^3 crude gas:		
Oxygen.....ft^3	207	206
Steam.....lb	10.9	12.2
Fuel (maf).....lb	34.0	27.2
Material requirements per Mft^3 ($CO+H_2$):		
Oxygen.....ft^3	245	227
Steam.....lb	12.9	13.5
Fuel (maf).....lb	40.2	30.0
Cold gas efficiency.....percent[2/]	84.5	89.5
Operational efficiency.....do..[3/]	91.0	89.5
Average gas offtake temperature.....°F	508	880
Steam decomposition.....percent[4/]	-	83.4
Crude gas analysis:[5/]		
CO_2.....do..	7.5	3.3
Illuminants.....do..	0.4	0.1
O_2.....do..	0.1	0.2
H_2.....do..	28.4	29.7
CO.....do..	56.2	61.2
C_2H_6.....do..	0.5	0.0
CH_4.....do..	6.9	5.5
Heating value.....Btu/ft^3	354	345
H_2S.....grains/100 ft^3	107	284
Organic sulfur.....grains/100 ft^3	20	73

1/ All gas volumes at 30 in. Hg and 60° F.

2/ Cold gas efficiency = $\frac{\text{potential heat in gas}}{\text{potential heat in fuel}} \times 100.$

3/ Operational efficiency = $\frac{\text{potential heat of gas + potential heat of tar}}{\text{potential heat in fuel}} \times 100.$

4/ Steam decomposition = $\frac{H_2 \text{ in gas + tar} - H_2 \text{ in mf fuel}}{H_2 \text{ in steam}} \times 100.$

5/ Gas analysis is calculated to nitrogen-free basis to correct for inert gas added to the system, and gas production rates are given on this basis.

TABLE 4. - Typical material balance from gasification of lignite at 400 psig

	Pounds per hour	Percent
Material in:		
Steam	316	13.1
Oxygen	507	21.0
Fuel	1,442	59.9
Flux	144	6.0
Total	2,409	100.0
Material out:		
Product gas	1,701	70.6
Slag	214	8.9
Condensate + tar	495	20.5
Unaccounted for	-1	0.0
Total	2,409	100.0

TABLE 5. - Typical heat balance from gasification of lignite at 400 psig

	M Btu per hour	Percent
Heat in:		
Fuel	12,153	96.4
Steam	401	3.2
Oxygen	54	0.4
Total	12,608	100.0
Heat out:		
Product gas:		
Potential	10,273	81.5
Sensible	270	2.1
Slag	166	1.3
Water vapor	620	4.9
Tar (potential)	781	6.2
Unaccounted for losses	498	4.0
Total	12,608	100.0

Figure 4 shows the variation in gas analysis with operating pressures when gasifying lignite at pressures from 80 to 400 psig. The CO and H_2 concentrations decrease slightly with pressure, and the CO_2 and CH_4 concentrations increase slightly.

LIGNITE TAR

In a fixed-bed gasifier of this type, the moisture and pyrolysis products of the fuel are carried out of the gasifier with the product gas. These tar and water vapors are condensed in the spray washer by direct contact with cooled recycled liquor. The tar is discharged from the spray washer in the form of a tar-water emulsion that usually contains from 40 to 50 percent water. The specific gravity of the tar is very close to unity, and no satisfactory method of breaking this

emulsion has been found. Commercial Lurgi plants are also plagued with this problem (2). The tar recovery has varied considerably during the test program, usually ranging from 10 to 20 gallons of moisture-free tar per ton of moisture- and ash-free lignite. The variations in yield are believed to be caused, to a large extent, by the tar separation and recovery problems.

Table 6 shows data on lignite tar obtained at operating pressures from 80 to 400 psig. In general, there appears to be little difference between the various tars.

TABLE 6. - Properties of tars and tar fractions from the pressure gasification of North Dakota lignite

Run number	51	P-15	P-16	P-20
Pressure, psig	80	200	300	400
Moisture, weight-percent:				
Distillation to cracking	51.6	52.2	55.0	42.1
Primary distillation, weight-percent of dry tar:				
Distillate	82.6	74.8	79.6	76.4
Pitch	11.8	19.6	15.5	18.3
Loss	5.6	5.6	4.9	5.3
Temperature of decomposition, °C	300	310	300	332
Composition of distillate, weight-percent:				
Tar acids	44.0	39.0	39.2	36.9
Tar bases	1.2	0.4	0.4	0.5
Neutral oil	54.8	60.6	60.4	62.6
Distillate, Hempel distillation, weight-percent:				
To 95° C	4.2	6.6	5.5	2.7
95-105	0.9	0.9	0.1	0.5
105-170	3.7	1.9	1.9	5.5
170-185	4.3	2.7	6.2	4.5
185-200	7.5	6.0	6.6	10.9
200-210	5.1	7.0	6.2	6.3
210-235	12.7	14.6	10.0	11.3
235-270	13.9	10.3	13.9	10.2
270-decomposition	30.9	40.5	39.2	39.7
Pitch	13.8	6.7	7.7	7.0
Loss	3.0	2.8	2.7	1.4
Temperature of decomposition, °C	360	370	382	376
Tar recovery, gal tar per ton maf coal	21.0	8.7	13.8	10.8
Specific gravity, 25/25 °C	1.0208	1.0570	1.0423	1.0453
Ultimate analysis, percent:				
Carbon	83.8	83.2	82.9	83.3
Hydrogen	9.1	8.4	8.6	8.4
Nitrogen	-	1.0	0.9	1.0
Oxygen	-	6.7	6.9	6.6
Sulfur	-	0.7	0.7	0.7

SIZE DEGRADATION IN THE FUEL BED

As the lignite passes down through the drying and carbonizing zones in the gasifier, significant size reduction occurs. Additional fines are probably produced in the turbulent zones of the raceways in front of each tuyère. Figure 5 shows screen analyses of the material charged to the gasifier and of the material in the upper and lower portions of the bed after a test using either lignite or Disco char. The lignite-clinker mixture as charged contains about 66 percent plus 1/2-inch material and about 2 percent minus 1/8 inch. Screen analysis of the lower 3 feet of the fuel bed at the conclusion of a test showed 4.4 percent of the plus 1/2-inch material and 54.4 percent of the minus 1/8-inch material. The deep fuel bed tends to filter out this fine material, and no fuel bed carryover has been noted at 400 psig with gasification rates as high as 20,000 cubic feet per square foot per hour. As shown, the size degradation in the Disco char tests were much less than for lignite.

Because of the greater amount of fines when gasifying lignite and the resultant greater pressure drop for a given gasification rate, it is expected that the maximum capacity will be less for lignite than for Disco char.

EFFECT OF COAL CHARGE CYCLE

During the high-capacity tests at 400 psig, the fuel flux feed rate was about 1,570 pounds per hour, or about 1,000 pounds per square foot per hour. This rate required charging the coal lock every 45 minutes. The charging operation usually required about 11 minutes, and since no fuel was being fed to the shaft during this time, the fuel bed level dropped an estimated 4 to 5 inches per minute, or a total of about 4 feet. This fluctuation in fuel bed height has a great effect on the gas offtake temperature and some effect on the gas composition. As shown in figure 6, the gas offtake temperature is 300° to 400° F during the time that coal is being fed to the shaft, but when the coal lock becomes empty, this temperature quickly rises to 1,500° to 1,600° F. The bed temperature 10 feet above the hearth is also plotted in figure 6 and shows no effect of the charge cycle but remains constant at about 2,300° F.

The CO_2 in the product gas is continuously monitored by an infrared analyzer, and these data are also plotted in figure 6. The CO_2 drops sharply during the charging period by as much as 5 percent.

The drop in fuel bed height during charging could ultimately limit the maximum capacity of the gasifier because the remaining fuel bed will contain a greater percentage of fines and will thus fluidize more easily. This problem of fuel bed height variation could be solved by adding another coal lock to the gasifier, either in series or parallel with the present unit. To do this now would require extensive modifications to the gasifier and supporting structure, and this change is not presently being considered.

SLAG FLOW PROBLEMS

As was stated earlier, some of the tests in this series proceeded smoothly for 5 to 10 hours of slagging operation, and then sudden freezing of material in the taphole caused premature shutdown. In most of these instances, several pounds of iron agglomerates were found on the hearth bottom during cleanout, and solidified iron streams indicated flow toward or inside of the taphole. It appears that the lignite slag itself is very fluid and flows well until the iron pools become large enough and start flowing toward the taphole.

Indications are that most of the metallic iron produced flows uniformly through the taphole with the slag. For example, in one test it was estimated that each coal-clinker charge contained the equivalent of about 9.5 pounds of iron. Analysis of the slag collected per charge showed 2.2 pounds of magnetic material, which would indicate that about 25 percent of the iron is being reduced. Since a coal-clinker charge produces about 2.2 pounds of iron per 45 minutes and the troublesome iron agglomerate of several pounds does not occur until after 5 to 10 hours of operation, it follows that most of the iron produced flows uniformly through the taphole with the slag. The phenomenon causing the iron agglomerates on the hearth bottom and the resultant flow problems are not understood but are currently being studied. The separated iron may have a higher melting temperature than the lignite slag, and the intimate contact between the hearth bottom and the iron may be responsible for the iron freezing before discharge.

COMPARISON OF RESULTS WITH COMMERCIAL LURGI

Detailed results from the new Westfield Lurgi gasification plant in Scotland have recently been published (3, 4), and in table 7 the preliminary high-pressure results from the experimental slagging gasifier are compared with those from the dry-ash Lurgi plant.

The Westfield plant uses a bituminous coal; however, on an as-charged basis, the volatile matter and fixed carbon contents of this fuel are about the same as for the steam-dried lignite.

Ricketts states that gas production rates of 11,000 cubic feet of crude gas per square foot per hour have been obtained at Westfield and indicates that even higher rates may be possible. This compares with a rate of 19,300 cubic feet per square foot per hour which has presently been obtained with the slagging gasifier. We believe this rate will be increased substantially in future tests. On the basis of ($CO+H_2$), the slagging gasifier rate per square foot is about 2.4 times that of the conventional Lurgi because of the much higher CO and lower CO_2 in the product gas from the slagging operation.

The material requirements per 1,000 cubic feet ($CO+H_2$) for the two processes are also given in table 7. The maf fuel requirements are 40.2 pounds for the slagging gasifier vs 47.4 pounds for the Lurgi. The oxygen requirements are 245 cubic feet vs 267 cubic feet for the Lurgi. The largest difference is in the steam requirements; the slagging gasifier uses only 12.9 pounds, compared with 67.4 pounds for the dry ash unit. The average gas offtake temperature for the Westfield gasifier is about 900° to 1,000° F, compared with 500° F for the slagging gasifier.

SUMMARY

Slagging gasification of North Dakota lignite at pressures to 400 psig has been demonstrated in a beginning series of eight tests at high pressure. Performance of the gasification pilot plant during these tests was generally good, although taphole plugging limited some tests to about 5 to 10 hours of slagging operation. This taphole freezing problem appears to be directly related to iron segregation and agglomeration on the hearth and constitutes the most serious impediment to extended operation of the gasifier at the present time. No flux was used with the lignite, and, neglecting the iron segregation, the slag was very fluid and flowed nicely through the taphole, indicating the suitability of lignite for a slagging process.

TABLE 7. - Comparison of results from slagging gasifier and commercial Lurgi plant

	Slagging gasifier	Westfield Lurgi plant
Operating pressure, psig	400	355
Fuel gasified	Steam-dried lignite	Bituminous
Fuel analysis, proximate, percent		
Moisture	22.4	16.0
Ash	6.4	14.3
Volatile matter	31.4	28.5
Fixed carbon	39.8	41.2
Gas production rate:		
Crude gas, $ft^3/ft^2/hr$	19,300	11,000
$(CO+H_2)$, $ft^3/ft^2/hr$	16,300	6,970
Gas analysis, percent:		
CO_2	7.5	26.1
O_2	0.1	-
N_2	-	0.8
CO	56.2	26.0
H_2	28.4	37.4
CH_4	6.9	9.1
C_2H_6	0.5	-
CnHm	0.4	0.6
Heating value, Btu/ft^3	354	310
Material requirements per Mft^3 $(CO+H_2)$:		
Fuel, lb:		
As-charged	58.8	68.0
Moisture- and ash-free	40.2	47.4
Fixed carbon	22.4	28.0
Steam, lb	12.9	67.4
Oxygen, ft^3	245	267
Average gas offtake temperature, °F	500	900-1,000
Cold gas efficiency, 1/ percent	84.5	81.0

1/ Cold gas efficiency = $\frac{\text{Potential heat in product gas}}{\text{Potential heat in the coal}} \times 100$

Considerable process data were obtained from the lignite tests at various pressures to 400 psig. The gas composition, tar composition, and material requirements per unit synthesis gas showed only small variation with operating pressure.

The maximum gas production rate during this series was limited to about 20,000 cubic feet per square foot per hour because of limitations on gas metering and cooling equipment. However, at this rate and at 400 psig, there was no indication of fuel bed carryover. It is expected that considerably higher rates will be obtained in future tests.

Comparison of results with those of the Westfield dry-ash Lurgi plant shows favorable material requirements of the slagging gasifier per unit of synthesis gas, and production rates per square foot are more than double those from the Lurgi plant.

Because of the drop in fuel bed height while coal is being charged to the gasifier, the gas offtake temperature increases from 300° to 1,600° F and the CO_2 in the product gas decreases by about 5 percent. This fluctuation is undesirable and could be avoided either by using double lock-hoppers for the coal feed or by several other possible modifications of the fuel-charging system.

No trouble has been experienced in carrying tar vapors out of the gasifier despite the generally low gas offtake temperatures. Difficulties in tar-water emulsion separation are blamed for inconsistent results in tar yields per ton of lignite, which range from 10 to 20 gallons of moisture-free tar per ton of moisture- and ash-free lignite.

Size degradation in the shaft is quite severe when using lignite, and over 50 percent of the material in the lower part of the shaft is minus 1/8 inch. The deep fuel bed acts as an efficient filter to prevent dust carryover; however, the additional pressure drop caused by the fine material should cause hangup of the fuel bed at lower gas production rates with lignite than with Disco char.

The hearth design as developed for this small pilot gasifier would not be suitable for scale-up for a commercial unit. The life expectancy of the refractory taphole is less than 50 hours, and some type of water-cooled hearth and taphole is envisioned for a large gasifier. In addition, some means of heating the taphole during periods of low load or temporary shutdown would probably be required. The British investigators have made significant progress in the development of these items (5, 6).

The pilot plant is now being modified to permit higher capacity operation, and tests will be continued in order to determine maximum capacity and other process data as a function of operating pressure and other variables.

REFERENCES

1. Gronhovd, G. H., A. E. Harak, W. R. Kube, and W. H. Oppelt, Design and Initial Operation of a Slagging, Fixed-Bed, Pressure Gasification Pilot Plant. BuMines Rept. of Inv. 6085, 50 (1962).

2. Smith, B. E., and F. G. Westbrook, Tar Separation Problems at Morwell Lurgi Plant. Coke and Gas, 487-491 (Dec. 1961).

3. Ricketts, T. S., and D. C. Elgin, The Gasification of Solid Fuels in the Gas Industry. Proc. Joint Conf. on Gasification Processes, Inst. Gas Engineers and Inst. Fuel, Hastings, England, 10 pp. (Sept. 1962).

4. Ricketts, T. S., The Operation of the Westfield Lurgi Plant and the High-Pressure Grid System. Inst. Gas Engineers Communication 633, 21. (presented at 100th Annual General Meeting, London, May 14-17, 1963).

5. Masterman, S., and W. A. Peet, The Development of a Pressurized Slagging Fixed-Bed Gasifier. Proc. Joint Conf. on Gasification Processes, Inst. Gas Engineers and Inst. Fuel, Hastings, England, 10 pp (Sept. 1962).

6. Hoy, H. R., A. G. Roberts, and D. M. Wilkins, Some Investigations Into the Gasification of Solid Fuel in a Slagging Fixed-Bed Gasifier. Proc. Joint Conf. on Gasification Processes, Inst. Gas Engineers and Inst. Fuel, Hastings, England, 12 pp (Sept. 1962).

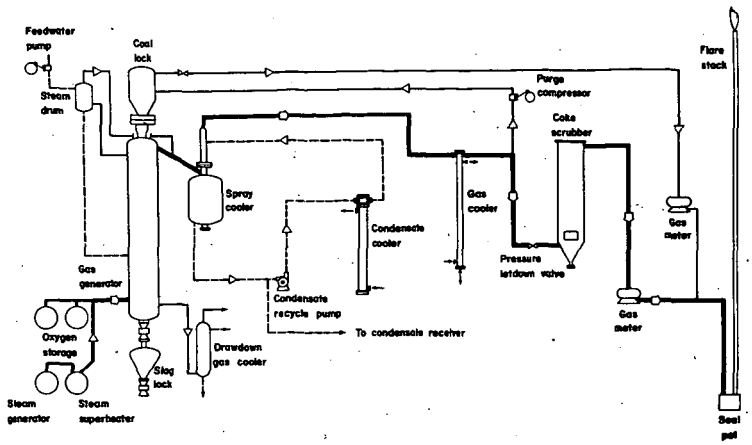

Fig. 1 Process flow diagram for pressure gasification pilot plant.

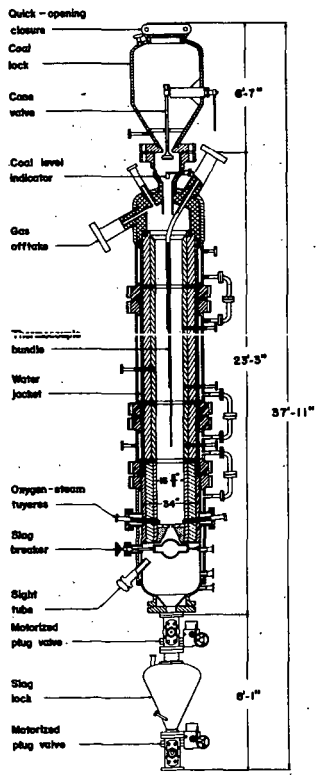

Fig. 2 Cross section of pressure gasifier.

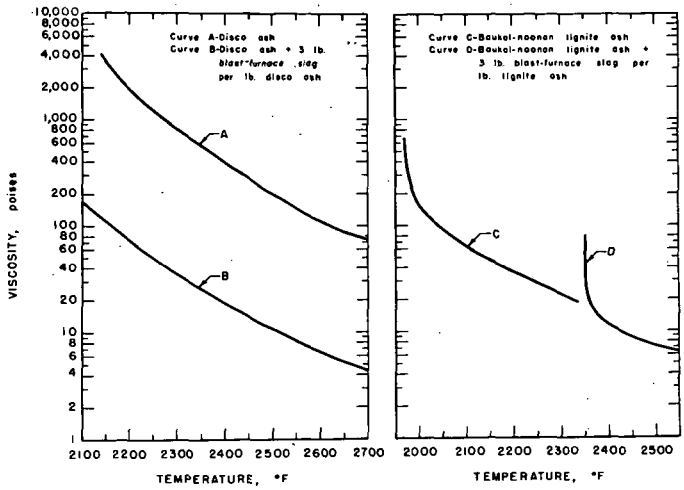

Fig. 3 Measured viscosity-temperature relationships for various coal ashes and for mixture of coal ashes and flux.

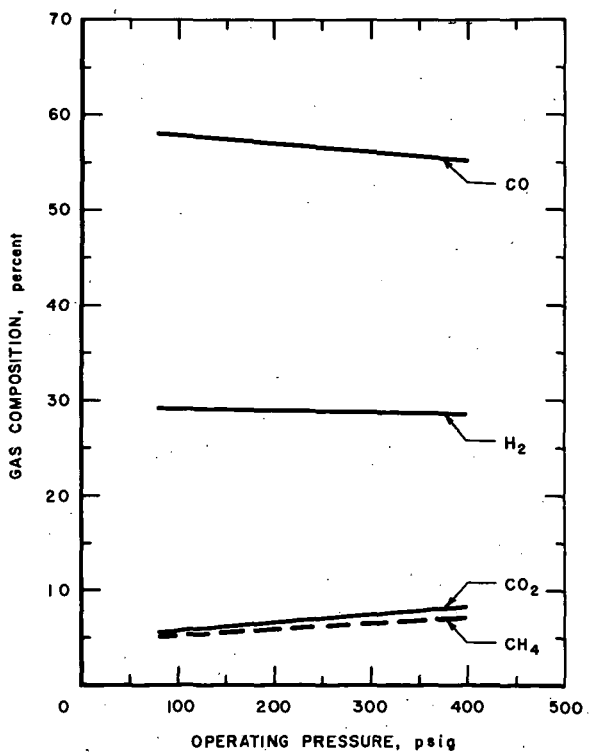

Fig. 4 Gas analysis versus operating pressure using North Dakota lignite.

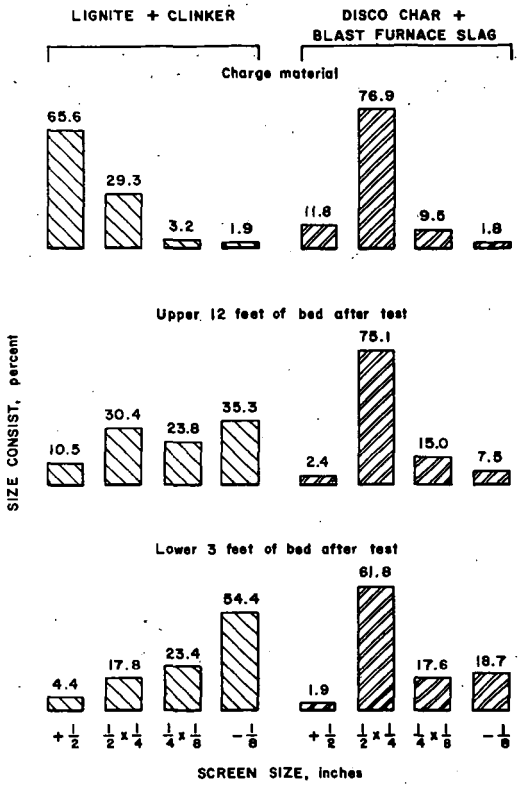

Fig. 5 Typical screen analysis of material fed to gasifier and fuel bed removed from gasifier after test.

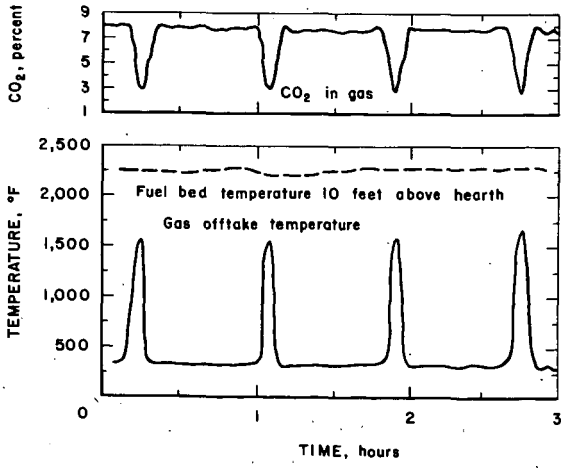

Fig. 6 Gas offtake temperature, fuel bed temperature, and CO_2 in product gas as influenced by the coal charge cycle.

Development of Catalysts and Reactor Systems for Methanation

J. H. Field, J. J. Demeter, A. J. Forney, and D. Bienstock
U. S. Bureau of Mines, 4800 Forbes Avenue,
Pittsburgh, Pennsylvania 15213

INTRODUCTION

The continued increase in the consumption of natural gas, the slowly declining reserves-to-consumption ratio, and the slow but steady increase in the price of natural gas have extended the interest in production of high-Btu gas from coal. Estimates of the time when supplemental gas will be required range from about 10 to 25 years, depending on the estimated rise in consumption and ultimate reserves (4).[1/] Despite record production, reserves of natural gas are still increasing slowly. For example, while U.S. production increased to 13.75 trillion cubic feet in 1962, the reserves at the end of 1962 were 285.3 trillion cubic feet, an increase of 8 trillion cubic feet for the year, with gas well completions at an all time high at 5,848 (5). Importation of gas from Canada and Mexico and possibly of liquefied methane by tanker are other factors that will affect the need for supplemental gas. Nevertheless, synthetic pipeline gas from coal can insure a long-time domestic source of gas from an abundant raw material.

Research is continuing on the principal methods of producing high-Btu gas by coal hydrogenation, $C + 2H_2 \rightarrow CH_4$, and catalytic methanation of synthesis gas, $3H_2 + CO \rightarrow CH_4 + H_2O$. The synthesis gas is obtained by gasifying coal with steam. Direct hydrogenation has a higher possible thermal efficiency and requires only about half as much gas as methanation--1,500 to 2,000 cubic feet of hydrogen as compared with 3,000 to 4,000 cubic feet of synthesis gas per 1,000 cubic feet of methane. The 1,500-cubic-foot value is achieved by utilizing some of the hydrogen in the coal and converting only part of the carbon. The lower requirement of 3,000 cubic feet of synthesis gas for catalytic methanation can be realized when a gasification process is employed that yields a gas containing about 10 percent methane.

Despite the inherent advantage of hydrogenation over catalytic methanation, there are two reasons justifying continued development of the catalytic method. First, catalytic methanation, being a gas phase reaction conducted at mild conditions of about 300° to 350° C and 20 to 30 atmospheres, is much simpler to operate and technical feasibility is apparent. However,

---

1/ Underlined numbers in parentheses indicate items in the bibliography at the end of this paper.

process improvements are needed to improve the economics of catalytic methanation and its continued development is warranted. Additionally, catalytic methanation may be necessary in conjunction with direct hydrogenation to increase the heating value of the gas by converting the carbon oxides and residual hydrogen to methane.

In the past 20 years catalytic methanation has been investigated in fixed-bed and fluidized reactors. The principal objectives have been to develop reactor systems that permit effective removal of the exothermic heat of reaction in order to provide adequate temperature control and maintain a long catalyst life. Important contributions in catalytic methanation have been made in the past 20 years by Dent (2), Dirksen and Linden (3), Schlesinger, Demeter, and Greyson (6, 7) and Wainwright (8), and their coworkers. Our group at the Bureau of Mines has reported previously the development of a hot-gas-recycle system (1). This paper covers further methanation studies using hot-gas recycle and bench-scale tests of a newer reactor system, the tube-wall reactor, in which the wall of the tube is coated with catalyst.

EQUIPMENT AND EXPERIMENTAL RESULTS

In the hot-gas-recycle system, the temperature is controlled by recycling several volumes of tail gas to the reactor inlet per volume of feed gas. Low resistance to gas flow across the bed is necessary to keep the pressure drop low and to avoid the high compression cost of gas recycle. Earlier work using two reactors in series has been reported (1). A simplified flowsheet of the system is shown in figure 1. The bulk of the synthesis gas was converted over steel lathe turnings as catalyst in the first reactor; the remainder was converted over nickel catalyst in a second reactor. This system was tested in 3- and 12-inch-diameter reactors.

Recently, catalyst prepared by flame spraying a thin coat of Raney nickel on metal plates has been tested, figure 2, using $3H_2+1CO$ synthesis gas or the product gas from a reactor using steel turnings. This gas contains hydrogen, carbon monoxide, carbon dioxide, methane, and C_2 to C_5 hydrocarbons, and is similar to the product gas from hydrogenation except that it is somewhat higher in carbon oxides. It is, however, essentially sulfur-free. As shown in table 1 (column 2), the sprayed nickel after extraction and activation is highly effective for reacting product gas to increase the heating value. Most of the carbon oxides are hydrogenated, and the C_2 to C_5 hydrocarbons are hydrocracked to methane. The inlet and outlet reactor temperatures in the test shown were 300° and 338° C and the gas recycle ratio was 8 to 1.

In the tests using $3H_2+1CO$ gas with sprayed catalyst in a single reactor, gas with a heating value of 900 Btu per cubic foot has been produced. Typical results are shown in table 1 (column 1). Rather limited conditions have been tried to date. By modifying the gas throughput, temperatures, and gas recycle ratio, increased gas conversion and heating value can be obtained.

Recently most of the emphasis in methanation has been given to studies of a tube-wall reactor. The reactor, shown in figure 3, consists of two concentric pipes; the inner is made of 3/4-inch pipe or 1-1/8-inch tubing, and the outer is made of 1-1/2-inch stainless steel pipe. The outer surface of a 6-inch length of the inner tube is coated with a layer of catalyst about 0.02 inch thick, and the synthesis gas passes over the catalyst in the annulus of about 0.15 to 0.18 inch between the tubes. A concentric tube arrangement is used because the catalyst is applied by flame spraying and the inner wall of a small diameter pipe cannot be coated by this technique. The heat of reaction generated on the tube surface during methanation is transferred effectively to Dowtherm located within the center tube. The outer tube of stainless steel is not a methanation catalyst at the operating temperatures employed. Temperature measurements along the catalyst surface are made with a sliding thermocouple positioned in a well located in the annulus.

Tubes sprayed with Raney nickel are activated by immersing them in a 2-percent solution of sodium hydroxide at 30° to 95° C until 60 to 85 percent of the aluminum in the coating is converted to $NaAlO_2$ or Al_2O_3. The tube is washed thoroughly to remove excess alkali.

After a pretreatment with hydrogen, synthesis follows with $3H_2+1CO$ gas, usually at an hourly space velocity of 7,000 based on the annular volume. Gas recycle is seldom used because it is not required for heat removal or temperature control. Synthesis is continued until the heating value of the product gas is less than 900 Btu per cubic foot (CO_2- and N_2-free). The catalyst coating must be activated and pretreated in a prescribed manner to obtain a long catalyst life. Several tests were made in which the conversion declined rapidly within 100 hours or less of synthesis because the catalyst spalled and dropped off the tube surface. X-ray analysis showed that the spalled material was largely nickel carbide. In other tests at similar operating conditions, the catalyst remained intact and active, and nickel carbide was not present. It is believed that alkali remaining from the activation promoted the reaction

$$3Ni + CO + H_2 \rightarrow Ni_3C + H_2O.$$

This problem was overcome by prolonged rinsing of the catalyst following the activation.

TABLE 1.- Experiments using sprayed Raney nickel catalyst

	Experiment 30	Experiment 29
Metal base	Carbon steel	Stainless steel
Feed gas	$3H_2+1CO$	1/
Space velocity	1,500	5,800
Recycle ratio, recycle-to-fresh	26:1	8:1
Reactor temperature, °C		
Top, inlet	242	300
Bottom, outlet	284	338
Conversion, pct		
H_2	92.3	---
CO	95.6	---2/
H_2+CO	93.1	98.0 2/
Heating value of product gas, Btu/cu ft 3/	907	943
Product gas composition, vol-pct		
H_2	22.6	7.5
CO	4.3	0.8
CO_2	0.2	2.1
CH_4	65.3	87.2
C_2H_6	4.6	1.0
C_3-C_5	2.6	0.6
N_2	0.4	0.8

1/

H_2	56.7 pct
CO	4.0
CO_2	8.7
CH_4	23.6
C_2H_6	3.5
C_3-C_5	2.4
N_2	1.1
	100.0 pct

2/ Overall conversion of H_2+CO in synthesis gas.
3/ Volumes of dry gas at 60° F and 30 inches Hg.

Following the water rinse and drying, a hydrogen pretreatment has been found desirable for maximum catalyst activity. As shown in table 2, while the catalyst had considerable activity without hydrogen treatment (experiment 46), for most of the time on stream the heating value was lower than for comparable experiments. The gas conversion decreased from 97.4 to 95.4 percent relatively quickly in experiment 46, whereas in the other experiments in which the catalyst had been pretreated with hydrogen, the conversion remained near the initial level for several weeks. The heating value of the product gas changes appreciably with small changes of the conversion at these high conversion levels. Thus for experiment 46 it had declined to 905 Btu per cubic foot at 300 hours, while in experiments 43 and 44 it was about 950 Btu per cubic foot. The maximum prolonged high activity was obtained in experiment 44 where the catalyst was pretreated at 300° C and 100 psig for 20 hours and at 300 psig for 0.1 hour.

In experiments 19, 39, and 41 the effect of varying the thickness of the catalyst layer was studied. Data for these tests are given in table 3. Synthesis could not be sustained on the 0.009-inch layer used in experiment 19, and the desired heating value of the product gas could be obtained for only 8 hours. In tests 39 and 41, where the catalyst thicknesses were 0.019 and 0.057 inch, respectively, no difference in conversion and catalyst life was observed. It was possible to renew the activity of the thicker coating used in experiment 41 by scraping the fouled surface and repeating the caustic treatment of the new surface. However, it is not likely that the ultimate life of the 0.057-inch layer would be three times that of the 0.019-inch layer to compensate for the additional amount of catalyst applied.

Plots of the heating value of the product gas with time on stream for typical tests are shown in figure 4. The product contains 80 to 85 percent CH_4 and the balance H_2, CO_2, and CO as shown in table 4. The maximum operating time to date with the prescribed minimum heating value of 900 is slightly more than 1,200 hours. The production of high-Btu gas within this period amounted to 180,000 cubic feet per pound of catalyst, giving a low catalyst cost of under 1 cent per 1,000 cubic feet based on a cost of $1.50 per pound for the applied and treated catalyst.

Temperature control has been excellent in the tube-wall reactor. Figure 5 shows temperature profiles along the catalyst surface as indicated from the readings of the movable thermocouple during an early and later period of operation. The temperature peak indicating the area where the bulk of the reaction occurs is located initially about 1 inch below the gas inlet, and then moves down the tube with time on stream. A possible explanation for this occurrence is that the surface gradually becomes deactivated because traces of sulfur in the synthesis gas react with the nickel. Analyses of the coating indicate some localized accumulation of sulfur.

TABLE 2.- Variation of hydrogen pretreatment[1]

Expt. No.	Hydrogen pretreatment		Time on synthesis, hr. 20	300	500	Synthesis life, hr.[2]
43	20 hr. at 25 psig, 350° C; 0.3 hr. at 300 psig, 350° C	H_2+CO conversion, pct.	98.1	97.5	95.2[3]	479
		Heating value, Btu/cu ft[4]	964	952	898	
44	20 hr. at 100 psig, 300° C; 0.1 hr. at 300 psig, 300° C	H_2+CO conversion, pct.	97.7	97.7	97.4	1,200
		Heating value, Btu/cu ft	953	956	949	
46	No pretreatment	H_2+CO conversion, pct.	97.4	95.4	95.2	730
		Heating value, Btu/cu ft	949	905	901	

1/ Catalyst coating about 0.02 inch; 12.4 gram catalyst activated; activated with 2 percent NaOH solution and water washed 24 hours to remove excess alkali.
2/ Hours at 7,000 hourly space velocity with the heating value of the product at least 900 Btu/cubic foot.
3/ At 479 hours.
4/ Volumes of dry gas at 60° F and 30 inches Hg.

TABLE 3.- Variation of thickness of catalyst coating

Expt. No.	Thickness catalyst layer, in.	Catalyst activated, gram		Time on synthesis, hr. 20	300	500	Synthesis life, hr.[1]
19	0.009	6.7	H_2+CO conversion, pct.	--	--	--	8
			Heating value, Btu/cu ft[2]	--	--	--	
39	.019	12.0	H_2+CO conversion, pct.	98.2	97.4	95.7	650
			Heating value, Btu/cu ft	967	949	912	
41	.057	12.1	H_2+CO conversion, pct.	98.0	97.3	96.4	678
				957	944	926	

1/ Hours at 7,000 hourly space velocity with the heating value of the product at least 900 Btu per cubic foot.
2/ Volumes of dry gas at 60° F and 30 inches Hg.

TABLE 4.- Operating and yield data, tube-wall reactor, experiment 44

Catalyst age, hr.	263	1,107
Hourly space velocity of feed gas	7,000	7,000
Average catalyst temperature, °C	363	366
Maximum catalyst temperature, °C	390	390
Location of maximum temperature, inches from top	1	2.3
H_2 conversion, pct.	97.0	95.2
CO conversion, pct.	100	98.8
H_2+CO conversion, pct.	97.8	96.1
Product gas analysis, vol pct.		
H_2	7.7	12.0
CO	0	1.0
CO_2	5.2	5.6
CH_4	85.2	80.1
C_2H_6	0.1	0.4
N_2	1.8	0.9
Heating value of product gas (CO_2- and N_2-free), Btu/cu. ft.[1/]	957	920

1/ Volumes of dry gas at 60° F and 30 inches Hg.

The effectiveness of heat removal in the tube-wall reactor can be shown from the heat transfer coefficient. Based on the estimated heat release and the differential between the average temperature of the tube surface and that of the boiling Dowtherm of 30° F, an overall heat transfer coefficient of 250 Btu per hour-square foot-° F has been calculated for the reactor. This high value indicates that convective heat transfer is of little significance and that the heat is evolved at the catalyst surface and is removed through the tube wall to the boiling Dowtherm.

CONCLUSIONS

Progress has been made in developing reactor systems for methanation that provide effective heat transfer and excellent temperature control. Raney nickel sprayed on plates or tube surfaces and extracted with alkali has proved to be an active and durable catalyst. The nickel is thoroughly utilized by being applied in a thin layer. The life of the catalyst has been sufficient to attain a low catalyst cost per unit of product gas. This is an important objective because the catalyst is the most expensive item in the methanation step regardless of the type of reactor. Because either $3H_2$+1CO synthesis gas or partially converted gas can be reacted, product gas from hydrogenation of coal can be upgraded in heating value.

A tubular reactor with a catalyst coating on the wall shows promise for methanation. Potentially the tube-wall reactor has advantages of need for little or no gas recycle, efficient catalyst utilization, low pressure drop and power consumption, and the combined function of reactor and heat recovery in one vessel. Low capital and operating costs for the methanation step can result from these features. Thus far, only a small tube has been used, and further investigation will be made in a larger reactor. For full-scale operatinn the reactor is visualized as a common multipass tube and shell heat exchanger with the tubes coated on their outer surface and the gas passing across the baffled tubes. Six reactors, each comprised of a 10-foot-diameter shell containing 2-inch tubes on 3-3/8-inch centers and 30 feet long, would be ample for a 90-million-cubic-foot-per-day methanation plant.

BIBLIOGRAPHY

1. Bienstock, D., J.H. Field, A.J. Forney, and R.J. Demski. Pilot Plant Development of the Hot-Gas-Recycle Process for the Synthesis of High-Btu Gas. BuMines Rept. of Inv. 5841, 1961, 27 pp.

2. Dent, F.J., L.A. Moignard, A.H. Eastwood, W.H. Blackburn, and D. Hebden. Joint Research Committee, A. 49th Report, The Synthesis of Methane from Carbon Monoxide and Hydrogen. Gas Times, v. 46, Jan. 5, 1946, pp. 29-33.

3. Dirksen, H.A., and H.R. Linden. Pipeline Gas by Methanation of Synthesis Gas Over Raney Nickel Catalyst. Ind. and Eng. Chem., v. 52, 1960, pp. 584-489.

4. Elliott, M. A. The Future of Piped Energy. American Gas Journal, v. 189, No. 6, 1962, pp. 34-39.

5. _____. Natural Gas Had Best Year Ever. Oil and Gas Journal, v. 61, No. 4, 1963, pp. 168-169.

6. Greyson, M., J.J. Demeter, M.D. Schlesinger, G.E. Johnson, J. Jonakin, and J.W. Myers. Synthesis of Methane. BuMines Rept. of Inv. 5137, 1955, 50 pp.

7. Schlesinger, M.D., J.J. Demeter, and M. Greyson. Catalyst for Producing Methane From Hydrogen and Carbon Monoxide. Ind. and Eng. Chem., v. 48, 1956, pp. 68-70.

8. Wainwright, H.W., G.C. Egleson, and C.M. Brock. Laboratory-Scale Investigation of Catalytic Conversion of Synthesis Gas to Methane. BuMines Rept. of Inv. 5046, 1954, 10 pp.

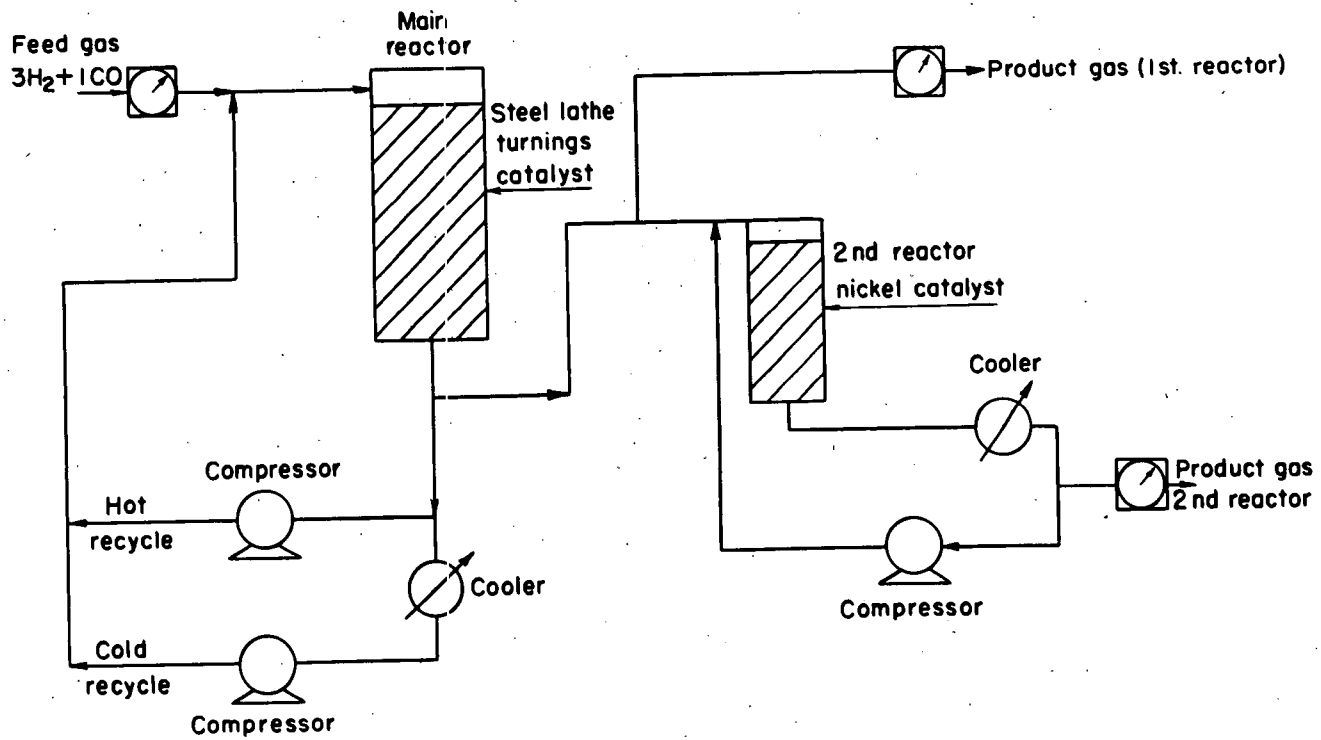

Figure 1. - Flowsheet of hot-gas-recycle process.

L-7523 4-18-62

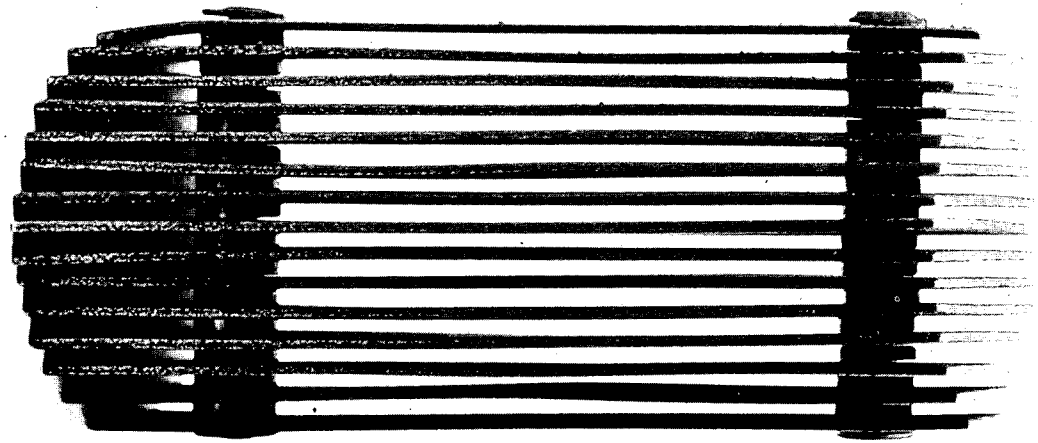

Scale, inches

Figure 2.- Catalyst prepared by flame spraying a thin coat of Raney nickel on metal plates.

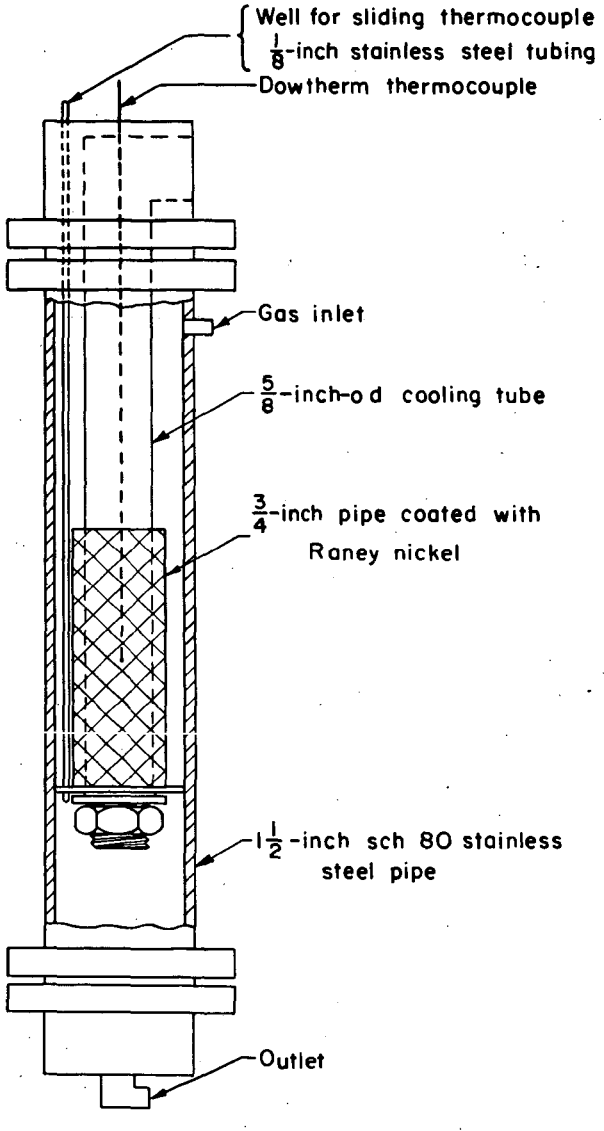

Figure 3.- Reactor for testing Raney nickel in catalyst coated tubes.

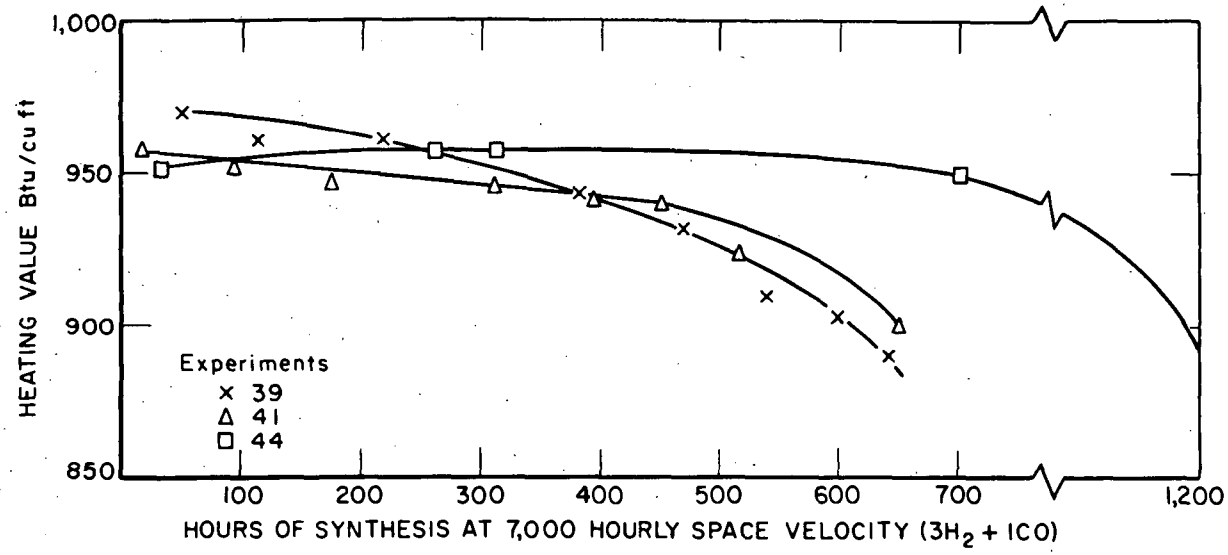

9-6-63 L-8294

Figure 4.- Tube-wall reactor: Heating value changes with time of operation.

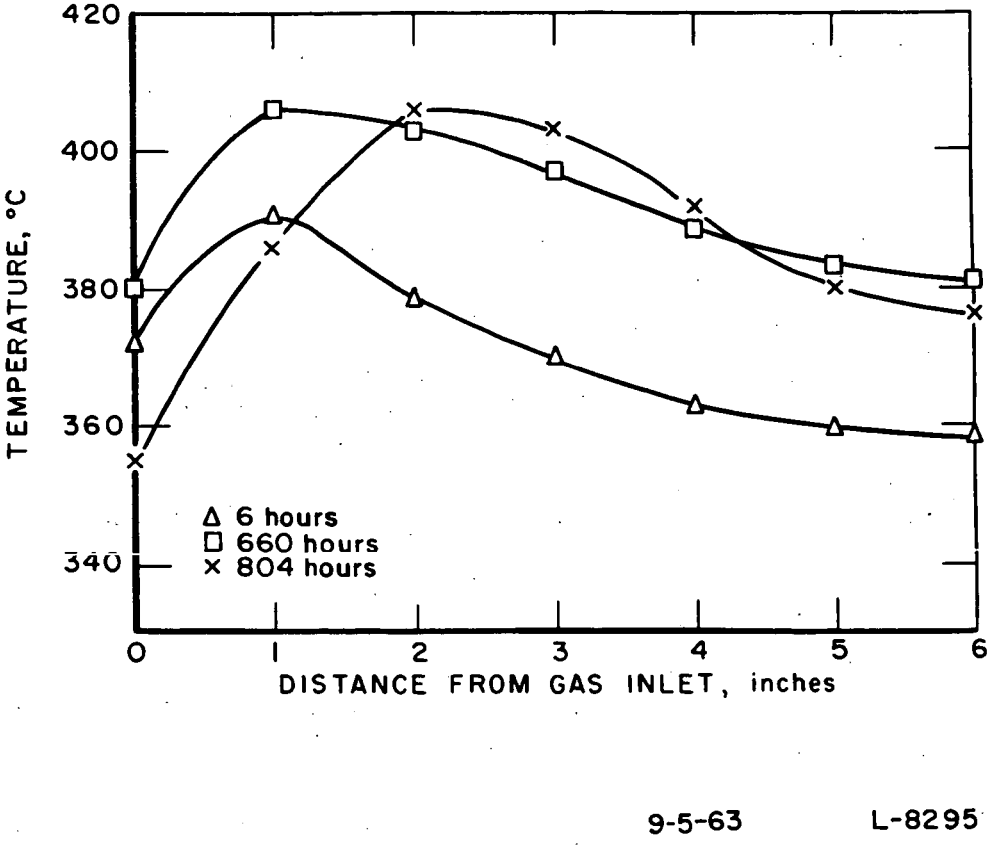

Figure 5.- Temperature profile, tube-wall reactor.

Evaluation of Processes and Costs of Separating Mixtures of Hydrogen and Methane

W. P. Haynes, J. W. Mulvihill, S. Katell, and J. H. Field
U. S. Bureau of Mines, 4800 Forbes Avenue,
Pittsburgh, Pennsylvania 15213

INTRODUCTION

In the hydrogenation of coal at pressures of 60 to 400 atmospheres to produce synthetic fuel gas, the product contains 5 to 80 percent methane, with the balance principally hydrogen (7, 20).[1/] Small quantities of carbon oxides, sulfur compounds, higher molecular weight hydrocarbons including aromatics, and water vapor constitute the remainder of the gas. By separating the hydrogen from the methane and increasing the methane content of the product to about 90 percent, the heating value can be increased to 900 Btu per cu ft. A further benefit of separation is that the hydrogen is made available for recycle to the hydrogenation reactor (36).

The objectives of this paper are to determine whether separation is economically feasible by existing techniques and to determine the effect of the methane concentration on the cost of separation. This latter information is valuable for guiding the direction of research on hydrogasification, because some operating techniques inherently produce gases of low methane content.

Five types of processes are applicable for separating mixtures of methane and hydrogen as follows:

1. Adsorption by solid agents (4, 6, 15, 17, 18, 25, 35):
   a. Activated carbon.
   b. Molecular sieves, silica gel, and activated alumina.
   c. Fuller's earth (hydrous Al-Mg-silicate).

2. Absorption by liquids (16, 31):
   a. High molecular weight oils--gas oil.
   b. Low molecular weight hydrocarbons--propane and butane (at low temperature).

3. Diffusion (2, 13, 21, 22, 26, 28, 32, 34):
   a. Metallic membranes and tubes:
      (1) Palladium and palladium-silver.
      (2) Nickel.
   b. Plastic membranes:
      (1) Polyvinyl acetate.
      (2) Polystyrene.
      (3) Ethyl cellulose.

1/ Underlined numbers in parentheses indicate items in the bibliography at the end of this paper.

c. Mechanical means:
   (1) Perforated plates and screens.
   (2) Centrifugal devices.
d. Thermal diffusion.

4. Refrigeration and liquefaction of methane (1, 12, 19, 23):
   a. Principally compression-expansion systems:
      (1) Joule-Thompson effect.
      (2) Expansion engines.
   b. Cascade type using auxiliary refrigerants:
      (1) Vapor recompression system.
      (2) Expansion engines.

5. Formation of methane hydrate (29).

For treating the large quantities of gas for a 90 million cu ft per day plant, adsorption, absorption, and liquefaction have been selected as being most practical. Diffusional systems were ruled out because low gas throughput is inherent, requiring a tremendous number of multiple units of high capital cost. The formation of methane hydrate was eliminated because published information indicated that the space and initial refrigeration requirements were several times greater than for liquefaction processes (29).

Adsorption with active carbon was selected over molecular sieves because the adsorptive capacity of carbon is considerably greater at high partial pressures of methane (15, 18, 25, 35). Moreover, the cost of the activated carbon is less than one-half that of sieves. A moving-bed adsorption operation was arbitrarily selected for this study instead of a fixed-bed system. However, fixed-bed adsorption accompanied by regeneration by pressure letdown offers a very promising method of separation according to costs reported for purifying hydrogen (8).

With regard to liquid absorption, although methane is highly soluble in liquid propane and butane, gas oil was chosen as solvent over liquid propane and butane because it can be used at ambient temperature (16). The lower molecular weight materials operate at low temperatures requiring some refrigeration. Finally a cascade system was chosen for separation by liquefaction because its thermodynamic efficiency is greater than compression-expansion systems (1). Higher capital costs were anticipated for a cascade system, however.

Plant capacity was set at 90 million std cu ft per day of high-Btu gas containing about 90 percent methane. Cases 1 through 3, respectively, designate the methane content of the feed gas at 5, 20, and 50 percent. The feed gas, obtained from raw hydrogasification product gas after the removal of most of the carbon dioxide and hydrogen sulfide, is assumed to have the following composition:

	Case 1	Case 2	Case 3
CH_4	5.0	20.0	50.0
H_2	94.25	77.78	44.84
C_2H_6	0.05	0.2	0.5
CO	.2	.8	2.0
CO_2	.2	.2	0.2
N_2	.2	.8	2.0
C_6H_6	.04	.16	0.4
H_2O	.06	.06	.06
H_2S (trace)	.0016	.0016	.0016

At these concentrations, the effects of the contaminants (gases exclusive of methane and hydrogen) are unknown with respect to the adsorptive capacity of charcoal, and are considered negligible in oil absorption. The design assumptions, therefore, neglect the presence of contaminants in the moving-bed adsorption plant and in the case of the oil absorption plant arbitrarily assign ethane, carbon dioxide, benzene, water, and hydrogen sulfide contaminants to the methane product stream, and carbon monoxide and nitrogen contaminants to the hydrogen byproduct stream. In the case of the liquefaction process, prepurification of the feed gas is mandatory and is considered in this evaluation. Inlet and outlet conditions for all separation schemes were held nearly constant at a pressure level of about 1,500 psia and at ambient temperatures.

The estimate of the working capital comprises a 30- to 60-day supply of makeup material, 3 months payroll overhead, 3 months operating supplies, and 4 months indirect cost, fixed charges, spare parts, and miscellaneous expenses. Basic rates for operating costs were:

Electricity	$0.008	per kwhr
Cooling water	.01	per 1,000 gal
Direct labor:		
Operating labor	$2.75	per man-hr
Supervision	15	percent of operating labor
Plant maintenance:		
Labor	$6,000	per man-yr
Supervision	20	percent of maintenance labor
Material	50	percent of maintenance labor
Payroll overhead	18.5	percent of payroll
Operating supplies	20	percent of plant maintenance
Indirect cost	50	percent of labor
Fixed costs:		
Taxes and insurance	2	percent of total plant cost
Depreciation	5	percent of total plant cost and interest during construction

Cost rates for items such as steam and raw material vary and are presented for each process.

MOVING-BED CHARCOAL ADSORPTION PROCESS

Commercial-scale moving-bed charcoal adsorbers have been used in the separation of light hydrocarbon gases from refinery gas and, in special tests (5),

have demonstrated the feasibility of separating methane-hydrogen mixtures. The distinctive feature of the process is its use of a moving bed of activated carbon for the selective adsorption of gases and vapors.

Data by Frolich and White (15) on the adsorption of mixtures of methane and hydrogen on activated charcoal at pressures ranging up to 140 atmospheres show that methane is selectively adsorbed with virtual exclusion of hydrogen. A flowsheet of the separation of methane-hydrogen mixtures by the moving-bed charcoal adsorption process at essentially 1,500 psi is shown in figure 1. Feed gas enters the downward-flowing bed of activated carbon, about 12 to 30 Tyler mesh size, at the adsorption zone where the methane is adsorbed and carried down into the rectification zone. The methane-free hydrogen flows upward and leaves the adsorber at the top of the adsorption zone. Part of the byproduct hydrogen continues upward through the cooling zone to dry and cool the incoming carbon. Much cooling of the carbon is done by desorption of residual water vapor. Cooling water tubes provide additional cooling. Hot hydrogen from the cooling zone is cooled and dehumidified in a cooler-condenser.

Activated carbon containing adsorbed methane flows downward by gravity from the adsorption zone into the rectification zone where a reflux stream of methane desorbs the small quantity of hydrogen left on the carbon. The activated carbon then flows to the stripping zone where methane is stripped from the carbon by steam at 650° F. A Dowtherm heating system provides additional heat to the stripping zone.

The activated carbon, saturated with water vapor but stripped of methane and hydrogen, is returned to the top of the adsorber column by a gas lift conveying system. A small stream of carbon is stripped with 800° F steam to remove heavy hydrocarbons and maintain a high methane capacity.

The methane and steam flow from the adsorber column to a cooler-condenser where the methane is cooled and the steam is condensed. The methane is then blended with untreated feed gas to give the final product containing 90 percent methane and 10 percent hydrogen.

The size of an adsorber column is 5 ft ID by 81 ft high, with 6-1/2-in wall thickness. The number of columns required is 57, 14, and 6 for cases 1 through 3, respectively.

In the design of the process, published isotherm data (18) for methane adsorbed on activated carbon was extrapolated to estimate the methane adsorbed at high partial pressures. From comments by Kehde et al (24), carbon attrition rate was assumed to be 0.005 percent of the rate of carbon recirculation. Additional unit costs were:

Fuel	$0.25 per million Btu
Steam--1,510 psig, 800° F	.35 per thousand lb
Steam--1,510 psig, 650° F	.29 per thousand lb
Steam--1,485 psig, 600° F	.27 per thousand lb
Activated carbon	.40 per lb

A breakdown of the capital investment costs and operating costs for the moving-bed adsorption process is shown, respectively, in tables 1 and 2. The

TABLE 1.- Total estimated capital requirements, moving-bed charcoal adsorption process

Item	Case 1, 5 percent methane		Case 2, 20 percent methane		Case 3, 50 percent methane	
	Dollars	Percent	Dollars	Percent	Dollars	Percent
Installed equipment	36,363,600	77.5	11,153,500	76.9	5,650,700	76.9
Plant facilities	3,636,400	7.7	1,115,400	7.7	565,100	7.7
Plant utilities	4,800,000	10.2	1,472,300	10.2	745,900	10.1
Total construction	44,800,000	95.4	13,741,200	94.8	6,961,700	94.7
Initial requirements	903,800	1.9	238,500	1.6	102,000	1.4
Total plant cost (insurance and tax bases)	45,703,800	97.3	13,979,700	96.4	7,063,700	96.1
Interest during construction	914,100	2.0	279,600	1.9	141,300	1.9
Subtotal for depreciation	46,617,900	99.3	14,259,300	98.3	7,205,000	98.0
Working capital	332,100	.7	240,700	1.7	145,000	2.0
Total investment	46,950,000	100.0	14,500,000	100.0	7,350,000	100.0

TABLE 2.- Estimated annual operating costs, moving-bed charcoal adsorption process

	Case 1, 5 percent methane		Case 2, 20 percent methane		Case 3, 50 percent methane	
	Dollars	Percent	Dollars	Percent	Dollars	Percent
Direct cost:						
Raw materials and utilities	2,696,900	38.0	1,176,000	41.3	809,000	44.9
Direct labor	332,500	4.7	193,900	6.8	138,600	7.7
Plant maintenance	306,000	4.3	183,600	6.4	132,600	7.4
Payroll overhead	101,500	1.4	59,800	2.1	43,000	2.4
Operating supplies	61,200	0.9	36,700	1.3	26,500	1.5
Total direct cost	3,498,100	49.3	1,650,000	57.9	1,149,700	63.9
Indirect cost	349,900	4.9	207,100	7.3	148,900	8.3
Fixed cost:						
Taxes and insurance	914,100	12.9	279,600	9.8	141,300	7.8
Depreciation	2,330,900	32.9	713,000	25.0	360,300	20.0
Total operating cost	7,093,000	100.0	2,849,700	100.0	1,800,200	100.0
Operating cost per thousand scf of product gas	0.239		0.096		0.061	

adsorber columns were the highest cost equipment items with their installed costs amounting to 71, 62, and 55 percent of total installed equipment costs for cases 1 through 3, respectively; the cost of steam, the highest direct cost item, respectively amounts to 23, 25, and 27 percent of total operating cost.

OIL ABSORPTION PROCESS

The oil absorption process uses an oil enrichment step patented by Davis (10) because existing solvents are not selective enough to get the desired separation by conventional absorption-stripping techniques. By the enrichment step, methane-rich oil can be further enriched with methane to insure getting a methane concentration of more than 90 percent in the flashed and stripped product gases. A flowsheet of the oil absorption process is shown in figure 2 for case 1.

Feed gas enters the bottom of the primary absorber, countercurrent to the lean oil passing downward through the tray column. Absorption occurs at 100° F with a total system pressure of 1,500 psia. Effluent gas from the primary absorber, which is mainly hydrogen, is combined with effluent hydrogen from a secondary absorber. Enriched oil from the primary absorber enters a secondary absorber at a suitable point for further enrichment with methane.

The secondary absorber selectively strips hydrogen from--and adds methane to--the incoming methane-enriched oil by forcing absorption of additional methane-rich gas entering at the bottom. Lean oil also enters the top of the secondary absorber to remove residual methane from the liberated hydrogen. The methane-rich oil leaves the bottom of the secondary absorber and passes through an oil turbine where approximately 46 percent of the theoretical expansion work is recovered by pressure letdown of the liquid and expansion of dissolved gases. Rich oil from the turbine enters a flash drum at 100° F and 15 psia. Flashed methane is removed and recompressed to 1,500 psia. Some of this gas is sent to the secondary absorber. The remainder combines with methane-rich gas from the stripping column to form the high-Btu product gas.

Rich oil leaving the flash drum is heated to 240° F prior to entering the top of the stripping column where the oil is stripped of absorbed gases by steam. Lean oil from the stripping column is recirculated through a heat exchanger and a cooler and is finally pumped to both absorbers. When the methane concentration in the feed gas is increased from 20 percent to 50 percent, as in going from case 2 to case 3, the flash drum pressure and the oil feed to the secondary absorber are appropriately modified to take advantage of the reduced need for oil enrichment.

A 200 molecular-weight oil was selected as the absorbent. Data of Dean and Tooke (11) and of Sage and Lacey (30) were used for estimating values of K for the solubility of hydrogen and methane, respectively.

The inside diameter and the wall thickness of both the primary and secondary absorbers were 7.5 ft and 6.5 in., respectively. In case 1 the

TABLE 3. Total estimated capital requirements, oil absorption process

Item	Case 1, 5 percent methane		Case 2, 20 percent methane		Case 3, 50 percent methane	
	Dollars	Percent	Dollars	Percent	Dollars	Percent
Installed equipment	318,434,700	78.4	113,647,600	78.1	29,167,500	78.4
Plant facilities	31,843,500	7.8	11,364,800	7.8	2,916,800	7.8
Plant utilities	42,033,400	10.4	15,001,500	10.3	3,850,100	10.4
Total construction	392,311,600	96.6	140,013,900	96.2	35,934,400	96.6
Initial chemical requirements	2,724,400	0.7	1,580,400	1.1	240,000	0.6
Total plant cost (insurance and tax bases)	395,036,000	97.3	141,594,300	97.3	36,174,400	97.2
Interest during construction	7,900,700	1.9	2,831,900	2.0	723,500	1.9
Subtotal for depreciation	402,936,700	99.2	144,426,200	99.3	36,897,900	99.1
Working capital	3,340,300	0.8	1,073,800	0.7	318,100	0.9
Total investment	406,277,000	100.0	145,500,000	100.0	37,216,000	100.0

TABLE 4.- Estimated annual operating costs, oil absorption process

	Case 1, 5 percent methane		Case 2, 20 percent methane		Case 3, 50 percent methane	
	Dollars	Percent	Dollars	Percent	Dollars	Percent
Direct cost:						
Raw materials and utilities	18,598,200	36.3	10,343,500	48.0	2,596,200	46.3
Direct labor	1,108,100	2.2	277,000	1.3	110,900	2.0
Plant maintenance	1,428,000	2.8	357,000	1.7	132,600	2.3
Payroll overhead	391,500	0.8	97,900	0.5	37,800	0.7
Operating supplies	285,600	0.5	71,400	0.3	26,500	0.5
Total direct cost	21,811,400	42.6	11,146,800	51.8	2,904,000	51.8
Indirect cost	1,410,900	2.7	352,700	1.6	135,000	2.4
Fixed cost:						
Taxes and insurance	7,900,700	15.4	2,831,900	13.1	723,500	12.9
Depreciation	20,146,800	39.3	7,221,300	33.5	1,844,900	32.8
Total operating cost	51,269,800	100.0	21,552,700	100.0	5,607,400	100.0
Operating cost per thousand scf of product gas	1.726		.726		.189	

reabsorption section of the secondary absorber had an inside diameter of 3.3 ft and a wall thickness of 3 in. With overall plate efficiencies taken at 20 to 40 percent, absorber heights ranged from 5 to 110 ft. The estimated number of absorbers was as follows:

Case	Percent methane in feed	Primary absorber	Secondary absorber
1	5	191	239
2	20	48	139
3	50	17	6

Capital and operating costs of the oil absorption process are shown in tables 3 and 4, respectively. Of the installed equipment cost, absorber costs were the highest and amounted to 65, 43, and 34 percent of the installed equipment cost for cases 1 through 3, respectively. Heat exchangers were usually the next highest cost equipment. Power costs constituted the largest single operating cost aside from the fixed cost. For cases 1 through 3, power costs were, respectively, 34, 45, and 44 percent of total operating costs.

CASCADE LIQUEFACTION PROCESS

The cascade liquefaction process uses a series of auxiliary refrigerants in its approach to the temperature of liquefaction of the product methane. To prevent the accumulation of frozen solids in the liquefaction step, the feed gas must undergo three prepurification steps prior to liquefaction. A simplified flowsheet of the overall liquefaction is shown in figure 3. Only cases 2 and 3, 20 and 50 percent methane in feed gas, are considered. Scrubbing the feed gas with monoethanolamine-diethylene glycol solution lowers carbon dioxide to 50 ppm, hydrogen sulfide by 80 percent, and water vapor to 0.03 mole-percent. Adsorption with activated charcoal removes benzene (9). Adsorption with molecular sieves lowers the water vapor content to a dewpoint of -100° F. Finally, in the liquefaction step, only methane and traces of other hydrocarbon are liquefied. Some hydrogen physically dissolves in the liquefied gas because liquefaction occurs at a pressure of about 1,400 psia.

The complex cascade liquefaction step is illustrated by the flowsheet for case 2 presented in figure 4. With slight modifications, the flow scheme is essentially the same as that proposed by Keesom (23). In this scheme, the three refrigerants--ammonia, ethylene, and methane--are arranged so that evaporation of the higher boiling refrigerant produces liquefaction of the next lower boiling refrigerant. Thus ammonia liquefies the ethylene in evaporator V_1, ethylene liquefies methane refrigerant in evaporator V_2, and methane refrigerant liquefies methane product in evaporator V_3. A gas phase product of approximately 90 percent methane at about 1,400 psia is obtained by reevaporating the liquefied product gas through heat exchange with incoming feed gas at exchangers E_6, E_5, E_7, and evaporator V_4.

Some of the published data used in the design include the enthalpy of methane (14), enthalpy of hydrogen (33), and the solubility of hydrogen in methane (3). The unit cost of steam was $0.32 and $0.153 per thousand pounds, at the respective pressures of 184 and 25 psia.

Capital costs and operating costs are presented in tables 5 and 6 for methane-hydrogen separation by the cascade liquefaction process. As shown in table 5, the cost of prepurification equipment is small compared to the cost of the equipment in the cascade liquefaction step. Evaporators and heat exchangers in the liquefaction section comprise well over half of the total installed equipment costs. The largest direct cost item, electric power, amounts to 32 and 33 percent of total operating costs for cases 2 and 3. Practically all of this power is used in the compression of refrigerants.

TABLE 5.- Total estimated capital requirements, cascade liquefaction process

	Case 2, 20 pct methane		Case 3, 50 pct methane	
Unit	Dollars	Percent	Dollars	Percent
Amine-glycol	793,300	1.8	431,400	1.6
Activated carbon	1,122,900	2.5	597,900	2.3
Molecular sieves	307,100	.7	195,800	.7
Liquefaction	32,603,100	73.4	19,390,900	73.8
Total installed equipment	34,826,400	78.4	20,616,000	78.4
Plant facilities	3,482,600	7.8	2,061,600	7.9
Plant utilities	4,597,100	10.4	2,721,300	10.4
Total construction	42,906,100	96.6	25,398,900	96.7
Initial adsorbent requirements	48,000	.1	24,600	.1
Total plant cost (insurance and tax bases)	42,954,100	96.7	25,423,500	96.8
Interest during construction	859,100	2.0	508,500	1.9
Subtotal for depreciation	43,813,200	98.7	25,932,000	98.7
Working capital	586,800	1.3	345,000	1.3
Total investment	44,400,000	100.0	26,277,000	100.0

TABLE 6.- Estimated annual operating costs, cascade liquefaction process

	Case 2, 20 pct methane		Case 3, 50 pct methane	
	Dollars	Percent	Dollars	Percent
Direct cost:				
Raw materials and utilities	2,168,100	34.0	1,298,400	34.2
Direct labor	277,000	4.3	166,200	4.4
Plant maintenance	357,000	5.6	214,200	5.6
Payroll overhead	97,900	1.5	58,700	1.5
Operating supplies	71,400	1.1	42,800	1.1
Total direct cost	2,971,400	46.5	1,780,300	46.8
Indirect cost	352,700	5.5	211,600	5.6
Fixed cost				
Taxes and insurance	859,100	13.5	508,500	13.4
Depreciation	2,190,700	34.5	1,296,600	34.2
Total operating cost	6,373,900	100.0	3,797,000	100.0
Benzene credit per thousand scf of product gas	.035		.009	
Operating cost per thousand scf of product gas	.215		.128	

DISCUSSION

The economic merit of the three processes considered decreases in the following order: Moving-bed charcoal adsorption, cascade liquefaction, and oil absorption. As shown in figures 5 and 6, respectively, the operating costs and capital costs are lowest for the moving-bed charcoal adsorption process at all levels of feed gas composition.

With total operating costs for the overall hydrogasification process estimated to range from \$0.70 to \$0.85 per M cu ft of high-Btu product gas, operating costs for the oil absorption process, as shown in figure 5, are impractically high at the 5- and 20-percent methane feed levels, while operating cost for the cascade liquefaction process shows some merit at \$0.13 per M cu ft of product for 50 percent methane in the feed gas. However, charcoal adsorption in a moving bed is the most economic method of separation and is of practical interest at methane feed concentrations as low as 20 percent. As shown also in figure 5, unit operating costs of all three separating processes decline as the percent methane in the feed gas increases from 5 to 50 percent. These costs tend to level out as the percent methane in the feed gas approaches 50 percent.

The relationship of the capital investment costs of the three processes, as shown by figure 6, parallels that of the operating costs. Compared to a total investment cost of \$70 to \$100 million for a complete hydrogasification plant producing 90 million std cu ft per day of high-Btu pipeline gas, capital investments ranging from \$26 to \$40 million for the cascade liquefaction and the oil absorption processes are far too high for practical consideration. However, capital costs for the charcoal adsorber process are attractive, amounting to less than \$15 million at feed gas concentrations of 20 percent

methane and higher. The ability of the moving-bed charcoal adsorption process to deliver both hydrogen and methane streams at pressure without additional recompression is of great value to any high pressure process requiring a separating step with recycle of either gas at high pressure.

Should the impurities in the feed gas significantly lower the efficiency of the moving-bed charcoal adsorption process, the maximum penalty inflictable upon the operating cost is between $0.04 and $0.03 per M cu ft of product gas for cases 2 and 3, respectively, based upon the prepurification costs in the liquefaction process. Even in this instance the relative standings of the processes are not changed. However, the assumptions made in this estimate regarding the adsorptivity of activated carbon in the presence of possible contaminants and the overall loss of carbon should be substantiated experimentally to verify the validity of this estimate.

In spite of the fact that the cascade liquefaction process is thermodynamically more efficient than other liquefaction processes, the recovery of methane from methane-hydrogen mixtures by the cascade liquefaction process was not found to be as economic as recovery by a liquefaction process proposed by Mann and Pryor (27) that utilizes Joule-Thompson cooling. Operating costs for the Mann and Pryor liquefaction process for 98 percent hydrogen in the recycle stream were $0.13 and $0.07 per M cu ft of product for the 20- and 50-percent methane cases, respectively; whereas, the corresponding operating costs for cascade liquefaction are $0.22 and $0.13 per M cu ft of product. These differences in operating costs are primarily due to the capital costs of the cascade liquefaction being over four times those estimated for the process of Mann and Pryor. Operating costs of the process of Mann and Pryor are nearly as low as those estimated for the moving-bed charcoal adsorption process. When the product gas is to be stored cryogenically before use, instead of being transmitted immediately by pipeline, separation and storage by a liquefaction process employing Joule-Thompson cooling may be superior to separation by moving-bed charcoal adsorption followed by cryogenic storage of product gas.

At present, the prospects of the oil scrubbing process being greatly improved are poor. Major obstacles to its improvement are; the lack of a solvent with high capacity and selectivity for methane and the need to recompress the flashed methane product from essentially atmospheric pressure to pipeline pressure.

BIBLIOGRAPHY

1. Barber, N. R., and G G. Haselden. The Liquefaction of Naturally Occurring Methane. Trans. Inst. Chem. Eng., v. 35, 1957, pp. 77-86.

2. Benedict, M., and A. Boas. Separation of Gas Mixtures by Mass Diffusion. Chem. Eng. Prog., v. 47, No. 3, 1951, pp. 111-122.

3. Benham, A. L., and D L. Katz. Vapor-Liquid Equilibria for Hydrogen-Light Hydrocarbon Systems at Low Temperatures. A I. Ch. E. J., v. 3, No. 1, March 1957, pp. 33-36.

4. Berg, C. Hypersorption--A Process for Separation of Light Gases. Gas, v. 47, No. 52, January 1947, pp. 32-37.

5. Berg, C., R. G. Fairfield, D. H. Imhoff, and H. J. Multer. Hypersorption. Oil and Gas J., v. 47, No. 52, April 23, 1949, pp. 95, 97, 130, 132, and 135.

6. Campbell, M. Larry, and Lawrence N. Canjar. Adsorption of Methane from Hydrogen on Fixed Beds of Silica Gel. A. I. Ch. E. J., v. 8, No. 4, Sept. 1962, pp. 540-542.

7. Channabasappa, K. C., and H. R. Linden. Fluid-Bed Pretreatment of Bituminous Coals and Lignite, Direct Hydrogenation of Chars to Pipe-line Gas. Ind. Eng. Chem., v. 50, No. 4, April 1958, pp. 637-644.

8. Chemical Week. Sifting Gases the Heatless Way. v. 93, No. 2, July 13, 1963, pp. 65-66.

9. Coolidge, A. S. Adsorption of Vapors by Charcoal. J. Am. Chem. Soc., v. 46, No. 3, March 1924, pp. 596-627.

10. Davis, W. H. Absorptive Separation of Methane and Hydrogen. U. S. Patent 2,689,624, Sept. 21, 1954.

11. Dean, M. R., and J W. Tooke. Vapor-Liquid Equilibria in Three Hydrogen-Paraffin Systems. Ind. Eng. Chem., v. 38, No. 4, April 1946, pp. 389-393.

12. DeLury, J. Liquefaction: New Gas Market. Chem. Eng., v. 66, No. 25, Dec. 14, 1959, pp. 165-168.

13. DeRosset, A. J. Processing Industrial Gas Streams at High Pressures. Diffusion of Hydrogen Through Palladium Membranes. I. E. Chem., v. 52, No. 6, June 1960, pp. 525-528.

14. Elliott Company. Elliott Multistage Centrifugal Compressors. Bulletin P-11, 1962, Jeannette, Pa., 57 pp.

15. Frolich, Per K., and A. White. Adsorption of Methane and Hydrogen on Charcoal at High Pressure. Ind. and Eng. Chem., v. 22, No. 10, October 1930, pp. 1058-1060.

16. Frolich, Per K., E. J. Tauch, J. J. Hogan, and A. A. Peer. Solubilities of Gases in Liquids at High Pressure. Ind. and Eng. Chem., v. 23, No. 5, May 1931, pp. 548-550.

17. Granquist, W. T., F. A. Mitch, and C. H. Edwards. Adsorption of Normal Saturated Hydrocarbons on Fuller's Earth. Ind. and Eng. Chem., v. 46, No. 2, Feb. 1954, pp. 358-362.

18. Grant, R. J., M. Manes, and S. B. Smith. Adsorption of Normal Paraffins and Sulfur Compounds on Activated Carbon. A. I. Ch. E. J., v. 8, No. 3, July 1962, pp. 403-406.

19. Harper, E. A. Kerosine as Absorber Oil--How Good? Petrol. Refinery, v. 38, No. 5, May 1959, pp. 144-146.

20. Hiteshue, R. W., R. B. Anderson, and S. Friedman. Hydrogenation of Coal and Chars. Ind. and Eng. Chem., v. 52, No. 7, July 1960, pp. 577-579.

21. Hobbis, L. C. W., and E. R. Harrison. Use of Nickel Diffusion Tubes for the Purification of Hydrogen. Rev. Sci. Instr., v. 27, No. 4, April 1956, p. 238.

22. Hunter, J. B. Silver-Palladium Films for Separation and Purification of Hydrogen. U. S. Patent 2,773,561, Dec. 11, 1956.

23. Keesom, M. Sur L'Économie du Procédé à Cascade pour la Liquefaction des Gaz. (The Economy of the Cascade Process for the Liquefaction of Gases.) Leiden Comm. Suppl., No. 76A, 1933, pp. 1-20.

24. Kehde, Howard, R. G. Fairfield, J. C. Frank, and Leonard W. Zahnstecher. Ethylene Recovery Commercial Hypersorption Operation. Chem. Eng. Prog., v. 44, No. 8, 1948, pp. 575-582.

25. Lederman, Peter B., and Brymer Williams. (University of Michigan.) Adsorption of Nitrogen-Methane on Molecular Sieves. Presented at A. I. Ch. E. meeting, Los Angeles, Calif., Feb. 1962, 11 pp.

26. Maier, C. G. Mechanical Concentration of Gases. BuMines Bulletin 431, 1941, 148 pp.

27. Mann, L. R., and J. A. Pryor. Cryogenic Separation and Purification of Methane and Hydrogen. (Manuscript presented at 1963 A.I.Ch.E. meeting in New Orleans.) Air Products and Chemicals, Inc., Allentown, Pa., Jan. 31, 1963, 9 pp.

28. Meares, P. (Univ. Old Aberdeen, Scot.), Diffusion of Gases in Poly (Vinyl Acetate) in Relation to the 2nd-Order Transition. Trans. Faraday Soc., v. 53, 1957, pp. 101-106.

29. Parent, J. D. The Storage of Natural Gas as Hydrate. Inst. of Gas Tech. Research Bulletin, No. 1, Chicago, Ill., Jan. 1948, 40 pp.

30. Sage, B. H., and W. N. Lacey. Phase Equilibria in Hydrocarbon Systems. Ind. Eng. Chem., v. 30, No. 11, Nov. 1938, pp. 1296-1304.

31. Salvi, G., and A. Fiumara. The Solubility of Methane in Propane and Butane. Riv. Combust. (Italy), v. 14, Nov. 1960, pp. 822-836.

32. Schmahl, N. G., and J. Schewe. The Thermal Separation of Gas Mixtures. II. Thermal Diffusion. Z. Elektrochem., v. 46, 1940, pp. 203-212.

33. Scott, R. B. Cryogenic Engineering (1st ed.). D. Van Nostrand Co., Inc., Princeton, N. J., 1959, pp. 294-297.

34. Steiner, W., and S. W. Weller. Fractionator of Gaseous Mixtures by Means of Permeable Nonporous Membranes. U. S. Patent 2,597,907, May 27, 1952.

35. Szepesy, L., and V. Illes. Adsorption of Gases and Gas Mixtures. II. Acta. Chim. Hung., v. 35, No. 1, 1963, pp. 53-59.

36. von Fredersdorff, C. G. Process for Coal Hydrogasification. Ind. and Eng. Chem., v. 52, No. 7, July 1960, pp. 595-598.

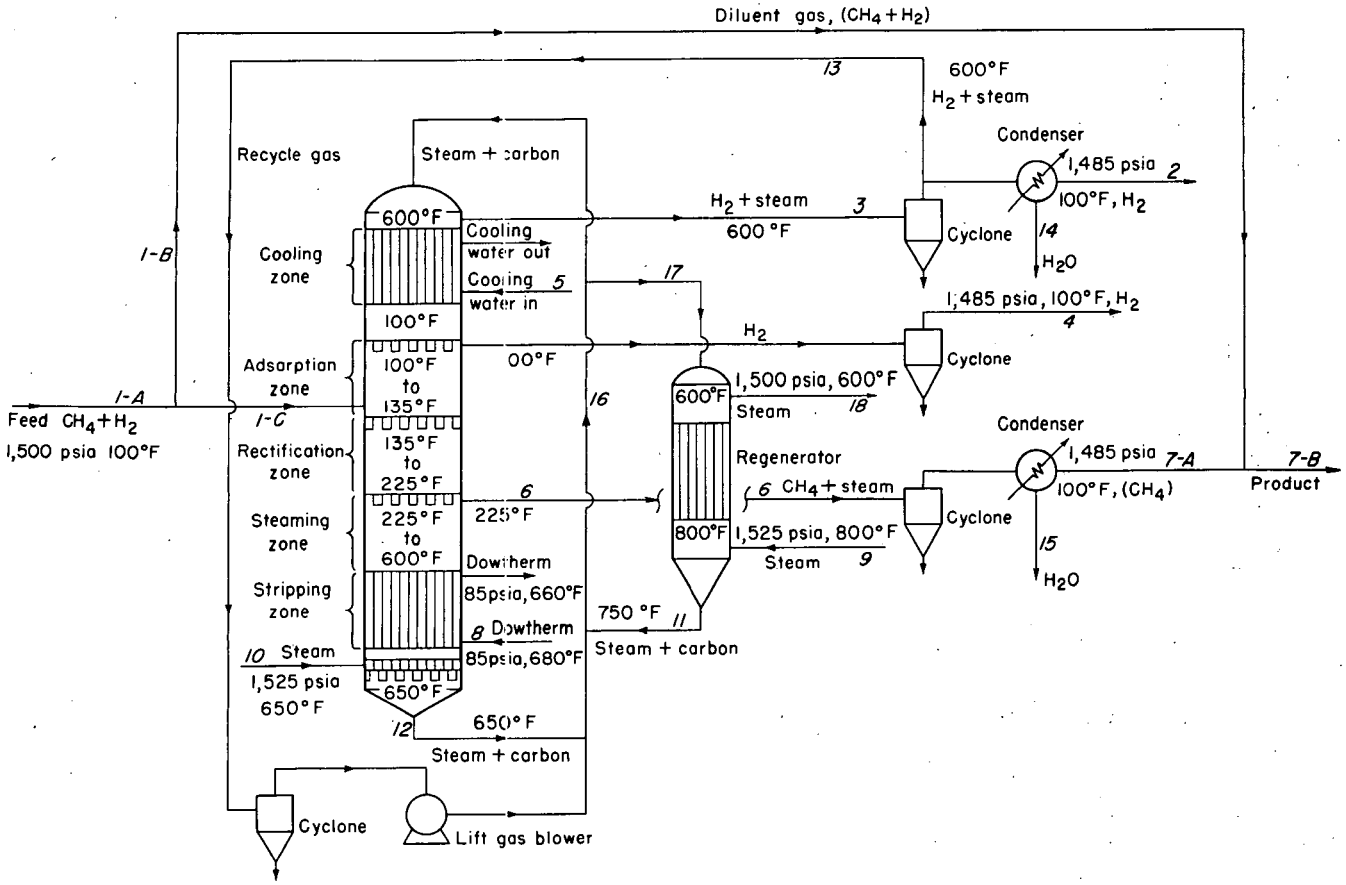

Figure 1.—Moving-bed charcoal adsorption process.

8-13-63 L-8258

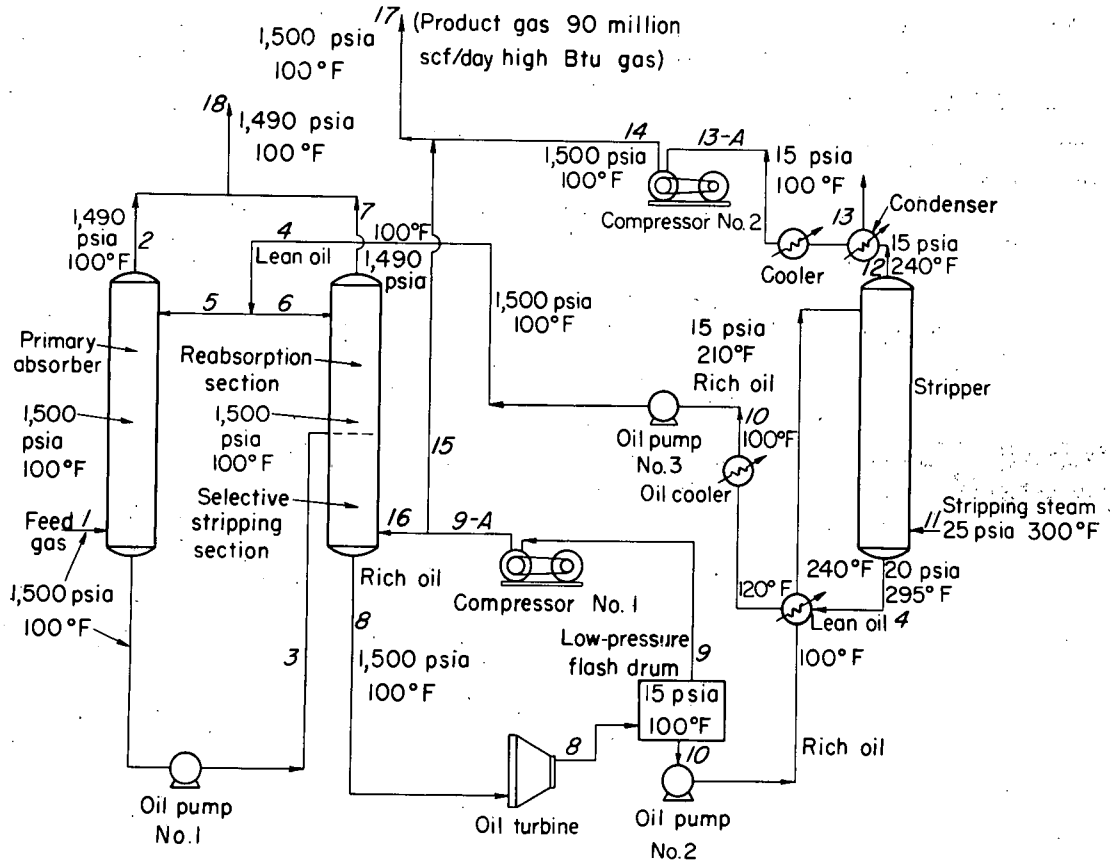

Figure 2.-Oil absorption process case 1.

8-13-63 L-8259

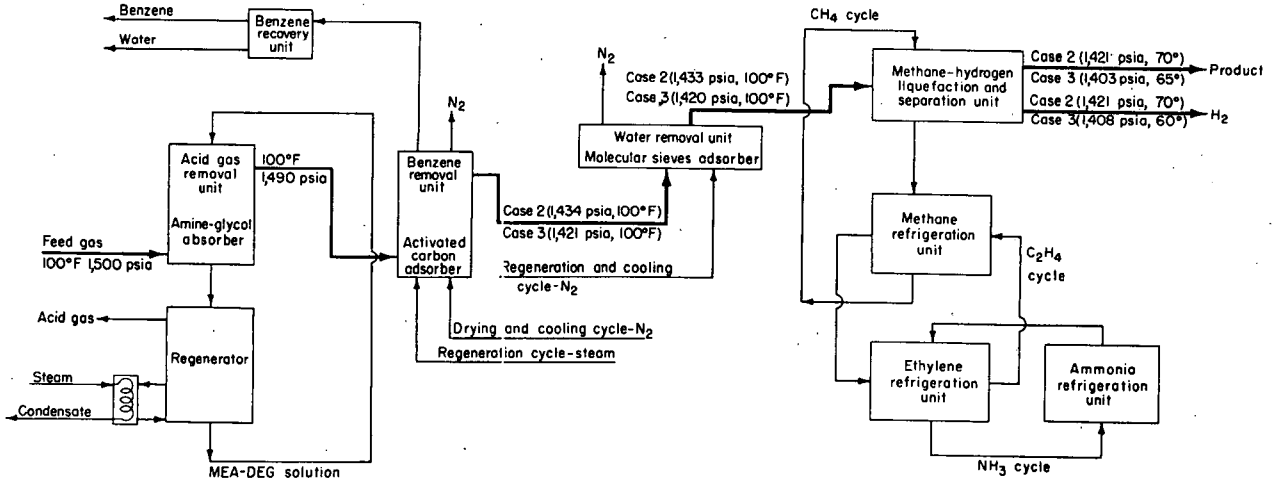

Figure 3—Overall process flowsheet, cascade liquefaction.

7-27-63 L-8262

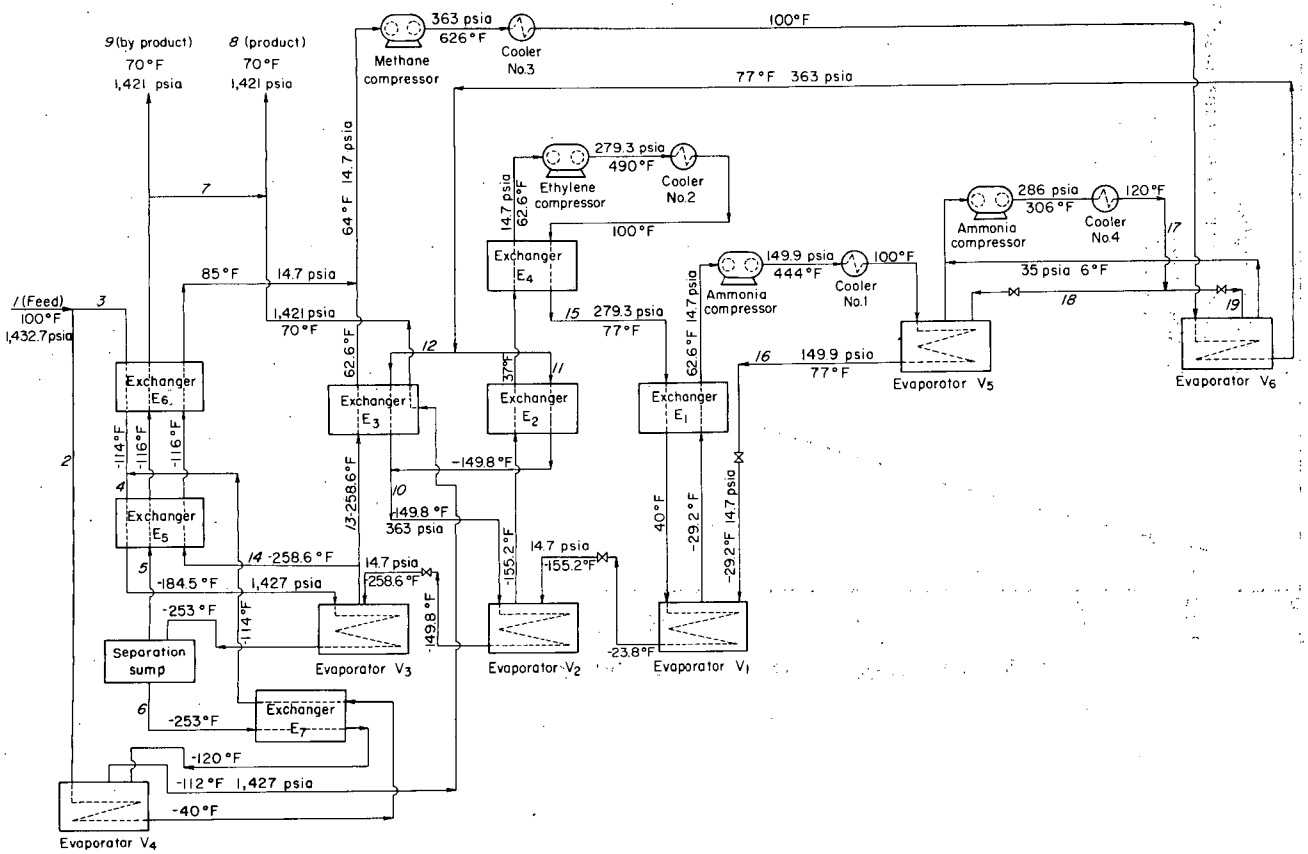

Figure 4.-Cascade liquefaction-case 2.

8-13-63 L-8266

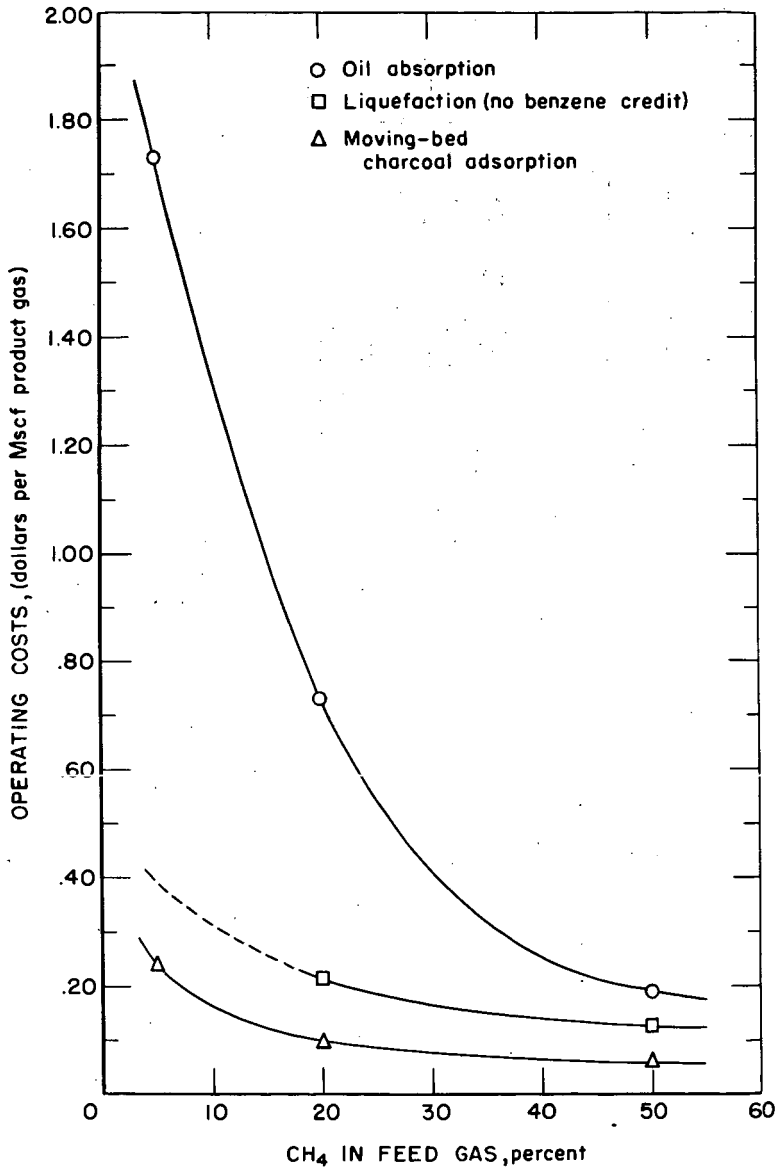

Figure 5.-Methone feed gos composition versus operoting cost.

L-8268 8-2-63

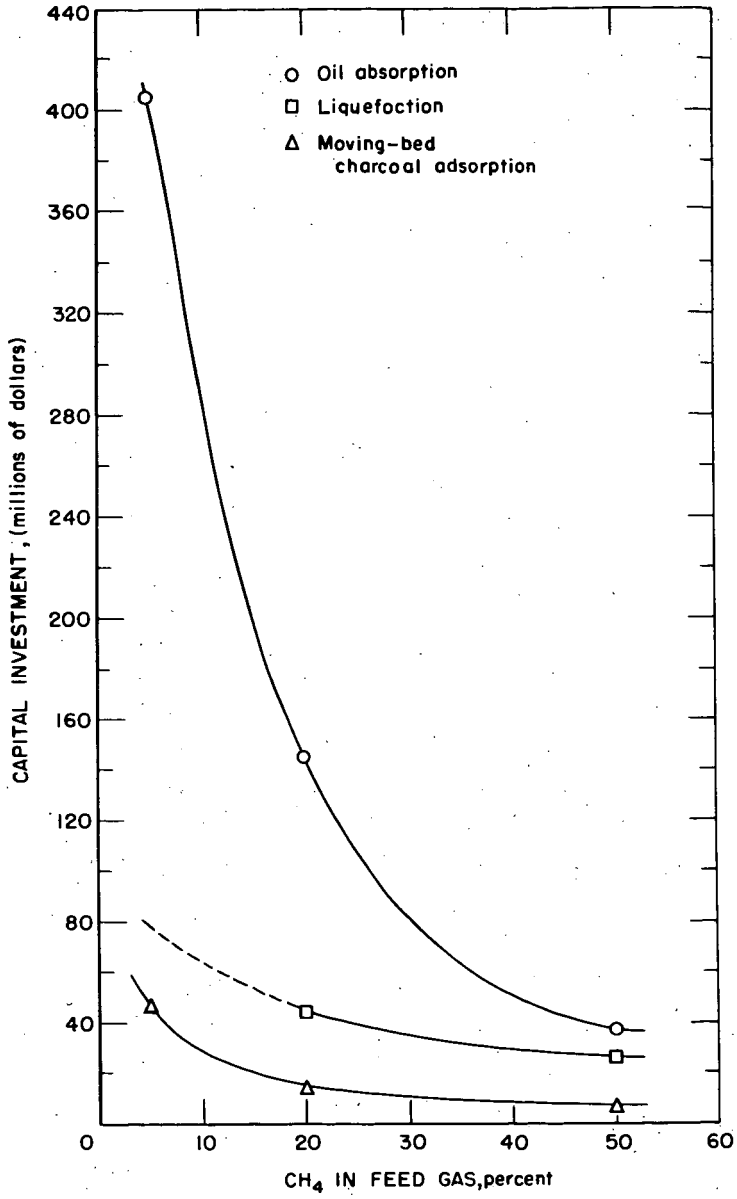

Figure 6.-Methane feed gas composition versus capital investment.

L-8269 8-2-63

PETROLEUM RESIDUALS IN PREBAKED CARBON ANODE BINDERS

By

M. B. Dell

Alcoa Research Laboratories
New Kensington, Pa.

INTRODUCTION

In the Hall-Heroult Process for producing aluminum, alumina dissolved in molten cryolite at 950-1000°C is electrolyzed using a carbon lined cell as cathode and baked carbon as anode. Anodes are made by mixing about 18 per cent binder with 82 per cent carefully sized calcined petroleum coke and molding a green block, which is subsequently baked at 1100° in an inert atmosphere to coke the binder.

During electrolysis the anode in slowly consumed. Carbon consumption is caused by: (1) combination of carbon with the oxygen released at the anode, (2) further combination of carbon with CO_2 initially formed, (3) air-burning of the exposed top of the anode, and (4) disintegration caused by particles of petroleum coke falling into the bath if the binder coke is more reactive than the petroleum coke. All but the first are strongly affected by the reactivity of the carbon anode, and this in turn is dependent on the quality of the coke formed by the binder.

Numerous tests have been proposed for characterizing binders. They have been reviewed comprehensively by Thomas[3] and somewhat more critically by Weiler[4]. It is generally agreed that the binder should meet a softening point requirement for ease of processing, must have a low ash content to prevent contamination of the bath and also to avoid catalyzing carbon reactivity, and should be low in sulfur because of corrosion problems. In addition, high aromaticity[1] is desirable to form a less reactive anode with good electrical conductivity. Coke-oven pitch derived from coal is very aromatic and meets all these requirements. It is the binder used almost exclusively in the United States. We have now found that certain less-aromatic materials, such as those derived from petroleum, can be blended with coke-oven pitch to produce anodes equivalent in all significant properties to conventional anodes.

ANALYTICAL PROCEDURES

Softening Point

Cube-in-air method. Barrett Test No. D-7, Allied Chemical and Dye Corporation, New York, New York.

Reactivity

Sodium sulfate reactivity is the loss in weight on immersing a 1-in. cylinder of carbon 0.5-in. long for 30 minutes in sodium sulphate at 980°C. Carbon is oxidized by molten sodium sulphate[2]. A reference carbon containing a standard binder is always run with this test for comparison. Both results are reported here since for some of the earlier tests the procedure was modified slightly.

Infrared Index of Aromaticity

This is taken as the ratio of the aliphatic transmittance at 3.4 microns

Infrared Index of Aromaticity

divided by the aromatic transmittance at 3.3 microns as previously described[1].

Miscibility Test

This test measures the compatibility of a binder with coke-oven tar. A 1:1 mixture of the binder under test and coke-oven tar is heated about 30 degrees above the softening point. A small droplet is transferred to a warm glass microscope slide on a hot plate and covered with a cover glass. While still warm, slight pressure is applied to the cover glass to reduce the film thickness so that it will transmit light. When viewed under the microscope at 200X, absence of flocculation of the C-I particles normally present in coke-oven pitch indicates compatibility of the binder.

RESULTS AND DISCUSSION

A typical analysis of coke-oven pitch binder for prebaked electrodes is given in Table I. The softening point corresponds to about 215-233°F ring-and-ball.

TABLE I

TYPICAL PROPERTIES OF COKE-OVEN PITCH BINDERS FOR PREBAKED ANODES

Softening point, cube-in air	105-115
Sulfur, %	0.5
Ash, %	0.1
Infrared index	1.3

For carbon anodes made with unblended binders, the reactivity increased with decreasing aromaticity of the binder as measured by infrared index (Figure I). On the basis of infrared index binders may be divided somewhat arbitrarily into three aromaticity classes: high (>1.2), intermediate (0.6 to 1.2) and low (<0.6).

High Aromaticity Binders

Coke-oven pitch is about the only member of this class. In prebaked anodes almost any high-temperature, coke-oven pitch can produce a good anode.

Intermediate Aromaticity Binders

Pitches derived from vertical retort tars or oil-gas tar, and petroleum residuals from high temperature cracking processes fall in this class.

Low Aromaticity Binders

Among these are pitches derived from low-temperature coal tar, solvent extracts of petroleum and most petroleum residuals.

In general low and intermediate aromaticity binders do not produce good anodes and are not used alone in carbon anodes. In the United States a very minor amount of oil-gas pitch is used in 50:50 blends with coke-oven pitch.

Low Aromaticity Binders

In a search for low cost binders derived from petroleum, several residuals were found which unexpectedly produced good anodes in blends. Typical laboratory results are presented in Table II, and similar good results have been obtained in plant operation for several of these binders.

All intermediate aromaticity binders tested produced good anodes when blended with coke-oven pitch. These results were not unexpected since blends of oil-gas pitch have been used for some time in anodes. Recently residuals produced in petroleum processing by high-temperature cracking have become available. Those having intermediate aromaticity (A and B in Table II) should find application blended in anode binders. None of the petroleum residuals tested had aromaticities as high as coke-oven pitches.

Certain low aromaticity binders when blended with coke-oven pitch produced good binders. These included a petroleum residual (C - Table II) produced by propane deasphalting of an Ordovician crude and a pitch (D) derived from low-temperature lignite tar. Other low aromaticity binders, such as air-blown asphalt (E in Table II), produced poor binders. The only laboratory test which differentiated among these binders was the miscibility test. Those blends in which the C-I particles were flocculated produced poor binders (E and F in Figure 2). If the C-I particles remained uniformly dispersed (A and C in Figure 2) the blend produced good anodes.

While some of these binders did produce good anodes, their true coking values were lower than that of coke-oven pitch (Table II). This did not seem to affect their utility, but their economic value was lowered since less carbon would be available for reaction with oxygen produced at the anode in smelting cells.

CONCLUSION

High aromaticity binders can be used alone to produce good anodes. Intermediate aromaticity binders blended with coke-oven pitch produced good anodes. In blends low aromaticity binders which were miscible with coke-oven pitch produced good anodes.

REFERENCES

1. Dell, M.B., FUEL 38, 183 (1959)

2. Fotiev, A.A., Zh. Prikl. Khim. 35, 2402-9 (1962)

3. Thomas, B.E.A., Gas World, Coking Supplement 51-66 (April 2, 1960)

4. Weiler, J.F., "Chemistry of Coal Utilization", Lowry, H.H. - ed. Supplementary volume, John Wiley & Sons, Inc., New York, 1963 P. 627

TABLE II

BINDER BLENDS IN LABORATORY PREBAKED ANODES

Binder	Source	IR Index	Coke-Oven Pitch in Blend, %	Binder %	Actual Coking Value, %	Anode Properties Resistivity ohm-in.	Anode Properties Reactivity %
A	Pet. therm. Process	1.07	50	18.5	52.7	0.0024	11.9
Reference	Coke-oven pitch		100	17.5	64.2	0.0023	22.6
B	Pet. therm. Process	0.78	60	17.5	55.9	0.0021	33.6
Reference	Coke-oven pitch		100	17.5	68.8	0.0022	57.0
C	Pet. propane deasphalt.	0.3	50	17.5	49.7	0.0023	30.1
Reference	Coke-oven pitch		100	17.5	63.4	0.0026	46.8
D	Lig., low-temp. carb.	0.14	60	18.5	-	0.0026	6.7
Reference	Coke-oven pitch	1.36	100	18.5	-	0.0025	5.6
E	Pet. air-blown	0.11	50	18.5	-	0.0035	9.3
Reference	Coke-oven pitch	1.32	100	18.5	-	0.0022	4.5

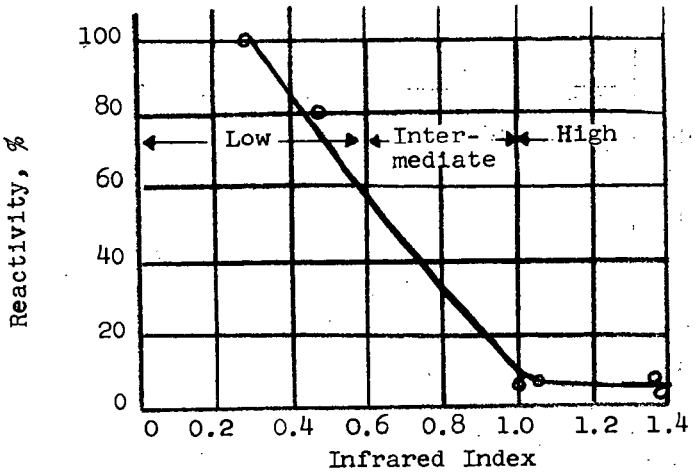

Reactivity of
Laboratory Prebaked Anodes

Figure 1

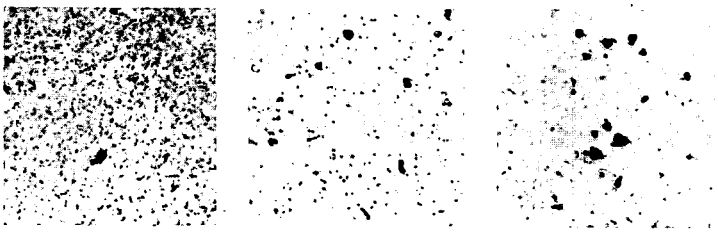

100% Coke 50% - C 50% - A

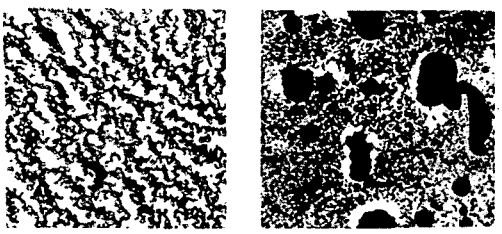

50% - F 50% - E

Miscibility Test Micrographs of Coke Oven
Pitch Blends (Transmitted Light, 200X)

Figure 2

Aspects of the Reactivity of Porous Carbons with Carbon Dioxide

J. H. Blake (a), G. R. Bopp (b), J. F. Jones (c), M. G. Miller (c), W. Tambo (d)

(a) Chemical Engineering Department, University of Colorado

(b) Present address, Chemical Engineering Department, Stanford University

(c) FMC Corp., Chemical Research and Development Center

(d) Present address, Cabot Corp., Boston, Massachusetts

I. Introduction

This work was undertaken in order to develop a simple and effective test that would compare the reactivities of granular carbons. The carbons studied were samples of formed metallurgical coke and of calcined coal char made from subbituminous coal in the process developed by FMC Corp., and demonstrated in a semi works plant at Kemmerer, Wyoming (1). This coke is permeated by a system of very fine pores, it has a highly amorphous solid structure, and it is very reactive compared to byproduct or beehive cokes. The reactivity is believed to be an important property of cokes used as reducing agents.

As a second objective, some knowledge of the influence of rather mild thermal treatment on the reactivity of these cokes was sought.

Carbon dioxide was selected as the oxidizing agent for the reactivity tests, since its reaction with carbon is not complicated by secondary effects such as the water gas shift. The reaction was followed by measuring the weight of carbon as a function of time, and this procedure proved to be both simple and precise.

While the variables affecting the results of the test were studied in a semi-empirical manner, certain interesting information regarding the kinetic behavior of these carbons as they underwent reaction did result, and this work is presented with the hope of providing a lead toward a better picture of what happens on the surface of carbon during reaction.

II. Experimental Details

A. Reactivity Measurements

The apparatus shown in Figure 1 consisted of an impervious silica tube 2.54 cm. I D mounted vertically in a tube furnace. Carbon dioxide flowed upward through the tube at controlled rates which ranged from 2870 cc per minute (STP) to 4730 cc per minute. The samples of granular carbon to be evaluated were suspended in a sample holder from an analytical balance mounted above the reaction tube. The sample holder was a No. 2 Gooch crucible cut off where the outside diameter was 23 millimeters so that clearance between the crucible and the reaction tube averaged 1.2 mm. The perforations in the bottom of the crucible were each .7 mm Diam. Holes were cut in the sides of the crucible with a diamond saw so that a bale of quartz fiber which hooked on to another long quartz fiber attached the sample holder to the balance.

Nearly all of the reactivity measurements were made at 900°C and the temperature was controlled automatically by the thermocouple mounted about 1 cm below the sample. At 900°C, the rates of reaction of most of these samples were in a range that was convenient to follow.

A loose fitting cover on top of the reaction tube with a small hole for the quartz fiber prevented air from diffusing down to the sample yet permitted the CO_2 to escape.

The dynamic force or upward drag on the sample basket was about 50 milligrams at the highest gas velocity used, and it was steady as long as gas velocity and temperature were kept constant.

To make a reactivity measurement the carbon particles were screened, usually to -16 +20 USS mesh, dried overnight in a desicator and a sample of either 200 or 500 milligrams was weighed into the sample holder. With the apparatus at reaction temperature and thoroughly purged with nitrogen, the sample holder was quickly lowered into place, hung from the balance, and the cover placed on top of the reaction tube.

The sample was then allowed to heat in a stream of nitrogen until it came to a constant weight, which usually happened within ten minutes, but for most runs a 20 minute devolatilization period was used. At the end of this time the weight was observed, the carbon dioxide was turned on and its flow adjusted to give a superficial velocity of either 15.6 or 9.45 centimeters per second (STP) in the reaction tube. The weight was again measured as soon as possible after turning on the CO_2 and thereafter at frequent intervals during the course of the reaction. At the end of the run the system was purged with nitrogen, and the sample was removed and allowed to cool to room temperature. The empty sample holder was then placed back in the furnace and weighed in a stream of nitrogen at reaction temperature. Reactivities are reported as percent of the sample reacting per hour, based on the total weight (including ash) of carbon at the end of the devolatilization period.

For most of the work the lower gas velocity, 9.45 cm/sec, was used because it gave somewhat more reproducible results. At this velocity, the Reynolds Number in the annular space past the sample is 900, so that flow is laminar.

B. Fluidized Reactor

The apparatus to react carbon with steam in a fluidized bed consisted of an impervious silica tube 2.54 cm I D mounted vertically in a furnace. The heated section of the tube was 45 cm long, and it contained refractory packing to a depth of 25 cm to preheat the steam. A perforated porcelain plate pinched into a constricted section of the tube lay on top of the packing and served as a grid. A thermocouple in a fine quartz well was immersed in the bed from the top, and it operated a controller which acted to maintain a constant temperature in the bed.

The rate of steam flow was controlled by manual adjustment of the current to a heating mantle enclosing a two liter flask. The flask was filled to a level well above the windings in the mantle.

To begin a run, the empty reaction tube was weighed, then mounted in the furnace, brought up to temperature, and the steam flow was adjusted to the proper rate. The weighed carbon sample (20 grams) was then poured into the tube, and a plug of glass wool was inserted into the top. By proper manipulation of the heater, the bed temperature reached the desired value (usually 750°C) within 5 minutes.

Coarse carbons, -6 +10 USS mesh, were used for this work. At a superficial steam velocity of 25 cm/sec under reaction conditions, particles in the bed moved

about continuously. Thus each particle should have been exposed to the same conditions. The beds were about 5 cm deep.

C. Surface Area Measurements

A Perkin-Elmer-Shell Sorptometer (Model 212) was used to measure pore surfaces. Samples were degassed in the apparatus at 600°C under .1 mm Hg for 30 minutes.

Isotherms for adsorption of nitrogen at 78°K were obtained by a flow technique which is rapid, but which may not allow sufficient time for equilibrium to be attained in very fine pores. Thus the surface areas reported here may be somewhat low.

D. Particle Density and Pore Volumes

Particle densities or volumes were measured by displacement of Hg at 10 psig in an American Instrument Co. Porosimeter. Pressures to 5000 psi enabled pore volume distributions to be determined down to pore diameters of 350A.

E. Helium Densities

Helium density was measured in a Beckman purgeable gas pycnometer, after degassing in the apparatus at room temperature and .1 mm Hg twice for about 10 minutes each time, and breaking the vacuum with He in each case.

F. Heat Treatment of the Samples

To study the effect of heat treatment on reactivity the carbons were soaked for various periods of time in a muffle furnace kept at either 1000°C or 1100°C. During this soaking, whole briquets were contained in glazed porcelain crucibles with calcined coal packed around them and with covers on the crucibles.

III. Samples

Two samples of FMC Coke briquets and one sample of calcined coal char were studied in this work.

The coke briquets were made in pilot scale equipment by first calcining the ground coal in a series of fluidized retorts, then briquetting the devolatilized coal or calcinate with a binder made by air blowing the tar distilled from the coal. The green briquets were then cured in the presence of air to polymerize the binder, and were finally coked or baked at about 900°C.

One sample of coke was made from Elkol Coal, a sub-bituminous coal mined near Kemmerer, Wyoming. The other coke was from another sub-bituminous coal mined near Helper, Utah.

For the samples used here, coke briquets were crushed and screened to the desired size.

The sample of calcinate was made from Elkol Coal and was produced by FMC Corp's demonstration plant at Kemmerer, Wyoming. The pulverized coal was first dried at 150°C, then carbonized at 450°C, and finally calcined at 800°C in a series of fluidized retorts.

Properties of these carbons are given in Table I.

TABLE I

Properties of Samples

		Elkol Coke	Helper Coke	Elkol Calcinate**
Ultimate Analysis Wt. %	C	89.8	86.6	89.6
	H	1.0	1.0	1.3
	N	1.0	1.2	1.2
	S	.6	.3	.4
	O (by diff.)	1.7	2.6	1.7
	Ash	5.9	8.3	5.8
Volatile matter %		2.0%	2.0%	4.5%
Surface area (m^2/gm) BET-Nitrogen		240*	170	190
Apparent density by Hg displacement (gm/cc)		.94	.96	.94
Helium density (gm/cc)				1.98
Crushing strength of cylinders 1-1/4"D x 3/4"		3400#	3400#	

*190 m^2/gm is a typical surface area for the coke produced by the large-scale plant at Kemmerer.

**The Elkol Coke used here was not made from this sample of calcinate.

IV. Results

A. Effects of Procedure

Several of the possible variables of this apparatus were studied to determine their effects on the reactivity measurements and to establish a standard procedure. The Elkol coke was used for this aspect of the work.

The numerical rates or reactivities reported in this section are based on the overall slope of the weight versus time curve between the times of 30 and 160 minutes where the slope was fairly constant. In the first few minutes of reaction, rates were somewhat higher than the slope in this interval, and the possible significance of this higher initial rate is discussed in a later section.

Table II shows the effects of sample size, devolatilization time, gas velocity, and particle size on the measured values of reactivity. In brief, increasing the sample size from 200 to 500 milligrams decreased the reactivity about 20%; longer devolatilization times (40 compared to 20 minutes) decreased the reactivity roughly 10%; and decreasing the gas velocity from 15.6 to 9.45 centimeters per second lowered the reactivity about 20%. Particle size between -6+10 and -28+32 mesh had no appreciable effect. (These screen sizes cover a five fold range of average particle size, from 2.5 down to .5 millimeters.)

TABLE II

Variables Affecting Reaction Rate*

Particle Size	Heating time min.	Sample Wt. mg.	Gas Velocity cm/sec	Reaction Rate %/hr
-16+20	20	200	15.6	25.6
				25.1
				26.4
		500		20.1
				21.4
				20.2
	40	200		24.1
				24.1
		500		18.3
				18.4
	20		9.45	17.6
			9.15	17.2
- 6+10			9.45	17.8
				17.7
				18.2
-16+20				17.6
-28+32				17.8
				17.9

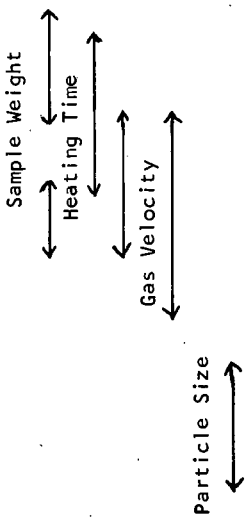

*(Elkol Coke)

The procedure adopted as standard used the -16+20 mesh size range, a heating time of 20 minutes, 500 mg. of sample and a gas velocity of 9.45 cm/sec. Reproducibility under these conditions was good, as can be seen from Table II.

The reactivity was reproduced with several different sample baskets made as described above, but having slightly different wall clearances. Thus the dimensions of the sample holder are not critical.

B. Effects of Carbon Monoxide

It is well known that CO and H_2 retard the reaction between CO_2 and carbon (2,3). With the sample sizes and flows of CO_2 that were used here, the average concentration of CO generated in the reactivity apparatus was usually between .1 and .2% (i.e. moles CO produced/unit time divided by moles of CO_2 fed/unit time). For the most reactive sample, the composition of CO in the effluent gas was about .45%.

Several runs with CO added to the CO_2 fed to the reactor (total flow kept constant) showed the rate to be lowered about 20% with 3.7% CO in the gas. This is about what Ergun's data (4) would predict and it shows that the CO generated by reaction should have a very minor influence on the measured values of reactivity.

C. Heat Treatment

Figures 2, 3, 4, and 5 show how the weights of carbon samples changed with time during reactivity determinations. Note that zero time has been shifted for most of the data on Figures 3, 4, and 5 so that several runs can conveniently be compared on a single plot.

From these plots, two results are apparent. First, as would be expected, a more severe heat treatment causes a given carbon to react more slowly.

Secondly, the heat treatment causes the rate of reaction to become more nearly constant, during a particular run. In Figure 2, for example, a sample of Helper coke which had been soaked at 1000°C for 16 hours reacted at very nearly a constant rate until more than 56% of the carbon had been consumed. The least-squares slope of this line to 56% burn off gives a reactivity of 38.1%/hr with 95% confidence limits of ±.51%/hr. The other sample in Figure 2 was soaked for 27 hours at 1000°C and it reacted to 57% burnoff at a constant rate of 24.7 ±.28%/hr. The 95% confidence limits give a quantitative idea of how nearly constant these reaction rates were.

D. Effect of Temperature

Except for two runs at 850°C all of the reactivities reported here were measured at 900°C. The two runs at 850° with Elkol coke gave reactivities of 6.5 and 7.1% per hour and when compared with 17.8% per hour at 900°C the apparent overall activation energies were 58.3 and 56.0 K cal per mole, respectively.

E. Variation of Pore Surface with Burnoff

Pore surface areas and particle densities were determined for 500 mg samples of Elkol calcinate which had reacted with CO_2 for various lengths of time in the reactivity apparatus. The first part of Table III shows these data. This carbon had been heated only to 800°C before undergoing reaction, so that the rate of reaction decreased continuously with burnoff, as was the case for the "un-heat-treated" carbon in Figure 5.

The specific surface of the carbon increased more or less continuously with burnoff, but when the surface area was based on 1 gram of original sample, before reaction (Column 6), it went through a maximum at about 35% burnoff. The data, plotted in Figure 6, show that the surface of a sample rises rapidly to a maximum and then falls off as carbon is consumed. Probably, during the initial stages of reaction, additional pore surface is very quickly made available by erosion of constrictions, and perhaps by enlargement of very fine pores. However, during the later part of the reaction, beyond 35 to 40% burnoff, pore surface is destroyed more rapidly than it is created, most likely by consumption of walls separating fine pores.

It is conceivable that the actual surface accessible to the carbon dioxide or steam at reaction conditions differs greatly from that measured by adsorption of nitrogen at 78°K. However, it is hard to imagine that the pore surface available to the reactant gas can do anything but increase during the first 10 to 20% of burnoff. During this part of the reaction, the rate either remains essentially constant, or decreases gradually.

Thus during the course of reaction of a particular sample of carbon there seems to be no correlation between reaction rate and pore surface area.

The percent internal reaction from the last column in Table III gives the weight loss calculated from the particle densities, which assumes that all reaction takes place on the internal pore surface. The difference between this figure and the actual weight

TABLE III

Variation of Pore Surface with Burnoff

Time Reacted Min.	Overall Wt. Loss %	Particle Density gm/cc	Overall Rate %/hr	Specific Surface m^2/gm	Surface* Per Gm. Starting Material m^2/gm	Internal** Reaction %
		Calcined Elkol Coal -20+30 Mesh Reacted with CO_2 in Reactivity Apparatus at 900°C				
0	0	.935		190	190	
15	5.7	.934	20.7	453	430	
30	10.0	-	20.0	592	534	
45	13.9	.815	18.5	642	552	12.8
60	18.2	.765	18.2	760	622	18.2
75	21.8	.721	17.4	790	616	22.9
90	25.9	.737	17.3	930	689	21.2
105	27.4	.681	15.7	975	707	27.1
120	32.0	.686	16.0	982	668	26.6
135	34.8	.655	13.9	1165	770	30.0
150	40.7	.639	16.2	1180	700	31.7
165	41.2	.605	15.0	1229	721	35.3
180	44.1	.625	14.7	1158	646	33.1
210	44.5	.618	12.7	1108	615	33.8
240	58.9	.530	14.7	1501	616	43.3
270	60.2	.510	13.4	1581	625	45.5
300	63.1	.549	12.6	1426	526	41.3
		Calcined Elkol Coal -6+10 Mesh Reacted with Steam in Fluid Bed at 750°C				
0	0	.965		139	139	
30	8.0	.908	16.0	560	515	5.9
45	13.0	.873	17.4	559	485	9.5
60	20.0	.817	20.0	743	596	15.2
75	23.5	.835	18.8	801	612	13.5
75	21.5	.767	17.2	798	628	20.5
90	26.5	.702	17.7	792	583	27.1
90	28.5	.760	19.0	784	561	21.1
105	34.5	.649	19.7	942	619	32.7
105	32.5	.711	18.6	899	608	26.1
105	33.5	.731	19.2	830	552	24.1
120	35.0	.693	17.5	911	592	28.1
120	37.5	.678	18.8	712	445	29.7
135	43.5	.579	19.3	893	504	40.0
135	43.0	.645	19.1	933	532	33.1
150	48.0	.586	19.2	911	475	39.2
150	45.0	.588	18.0	968	532	39.0
165	51.2	.615	18.6	907	442	36.2
165	49.9	.494	18.1	1100	551	38.8
180	55.5	.527	18.5	964	429	35.4
180	52.0	.567	17.3	1064	511	41.3
180	56.6	.589	18.9	945	409	39.0
180	51.5	.552	17.2	942	457	42.8

* (Specific Surface)(100 - % wt. loss)/100

** 1 - (part. density)/(initial part. density)

loss represents carbon consumed on the outsides of the particles. Although the data are somewhat erratic, roughly 85% of the reaction took place on the interal surface up to 40% burnoff.

The second set of data in Table III refers to -6+10 mesh Elkol calcinate reacted with steam at 750°C in the fluidized bed. Here, at a lower temperature, the rate of reaction of "un-heat-treated carbon" is very nearly constant at 18.2%/hr with 95% confidence limits of ±1.0%/hr. (These measurements are less precise.) In this case also, the pore surface increases to a maximum at about 30% weight loss, and then decreases. Since there is some attrition in the fluid bed, particularly at high burnoff, the amount of internal reaction is quite a bit less than that indicated by the actual weight loss.

V. Discussion

A. Variables affecting reactivity

Several observations indicate that mass transfer is not a major factor limiting the rate of reaction in this work. First, the fact that a five fold range of particle sizes had no apparent influence argues that diffusion within the pores of the particles and diffusion from the voids in the sample bed to the surface of the particles did not cause a significant concentration gradient, and that therefore, the concentrations of carbon dioxide and carbon monoxide in the voids between particles must be essentially the same as at the pore surfaces where reaction takes place.

Second, the overall activation energy of 56 to 58 K cal is too large for diffusion to the particles to control the rate, even though this activation energy was determined between only two temperatures, and most of the data pertain to the higher temperature

Another factor which suggests that external or film diffusion does not govern the rate is that the observed rates of reaction varied from 70% per hour to 4% per hour depending only upon the characteristics of the carbon. Thus, over this range of reactivities any effects on the diffusion rate to and from the particles by the geometry of the apparatus or the pattern of gas flow should have been unchanged.

Although diffusion of gas either to the particles or within their pores does not appear to strongly affect the rate of reaction here, its effect may not be negligible, particularly at the higher rates. If film diffusion, pore diffusion, and chemical reaction at the pore surface are regarded as three resistances to reaction arranged in series, lowering one resistance, as when the pore surface becomes more reactive, increases the relative significance of the others.

The importance of pore diffusion is undoubtedly affected by the pore structure. If a carbon is very dense, and has only very fine pores, its permeability to the reactant gas may very well be so low that reaction only takes place near the external surface of the particles. Thus the pore structure (permeability as well as pore surface area) might very well influence measured values of reactivity in this apparatus.

A further, and most likely the predominant, physical factor influencing the values of these reaction rates is that the samples were probably not isothermal. At a rate of 20% per hour, the endothermic reaction of carbon dioxide requires about 360 calories per hour for a 1/2 gram of carbon. Assuming that this heat is transferred principally by radiation, the surface of the sample was probably 2° to 4°C less than the measured temperature inside the reaction tube. With an activation energy of 58 K cal such a difference in temperature would lower the rate by a factor of 4 to 8%. This cooling effect would be more pronounced with the larger samples and at the lower gas

velocities. Therefore, the actual sample temperature and thus the measured reaction rate would be somewhat lower for larger samples and lower gas flows, as was observed.

The net result of all of these factors is that while this procedure does indicate significant differences in reactivity among various samples of carbon, the measured values are somewhat compressed. At the higher rates of reaction the combined retarding effects of diffusion, carbon monoxide, and a somewhat lowered sample temperature give a measured value of the reactivity which is less than would be the case if the sample were reacting under the same actual conditions as one with a lower reactivity. At the lower rates of reaction these inhibiting influences are not so large since concentration differences between the sample and the main stream of the gas are less, as are temperature differences. Thus these differing values of reactivity must be interpreted as occurring under conditions of reaction which are not exactly similar and where the higher rates have taken place under "slower" conditions so that the true differences in reactivity are actually somewhat greater than those reported here.

B. Concentration Gradient Inside Particles

Since, with the Elkol Coke, variation of particle size from about 2.5 to .5 mm did not influence the measured reactivity, one might conclude that reaction occurred entirely within Zone I (5) - that is uniformly throughout the particles, with a negligible radial gradient in the concentration of CO_2.

However, the particle densities reported in Table III for Elkol calcinate show the percent of internal reaction to be consistently less than the overall weight loss, which suggests that reaction is not uniform throughout the particle.

In the case of Elkol calcinate, macro-pore volume measurements by displacement of Hg up to 5000 psi show a porosity of 28% in pores larger than 350A in diam. About two-thirds of this porosity is in pore sizes between 3000 and 30,000A. If these large pores are regarded as arteries which conduct gas to cells where the pores are much finer (the mean diameter of the pores less than 350A diam. is 25 to 30A), it should be possible to estimate whether a significant radial concentration gradient occurs in these pores.

From density profiles of carbon rods exposed to CO_2 for various times at several temperatures, Walker and co-workers (6,7) concluded that the dimensionless group $\left(\frac{R}{C_R\ Deff}\right)\left(\frac{dn}{dt}\right)$ is a measure of whether reaction occurs uniformly throughout the particle in Zone I, or Zone II where the CO_2 is all consumed before it can diffuse to the center of a particle. Here R is the particle radius; C_R the reactant concentration in the main stream; dn/dt the overall reaction rate per unit particle external surface; and Deff the effective diffusion coefficient of CO_2 within the particle, all these terms being in consistent units. Deff equals $D\epsilon/\gamma$, where D is the diffusion coefficient in a single cylindrical pore; γ, the tortuosity factor (estimated at 20); and ϵ the fraction of the external particle surface covered with pore openings - estimated to be 1/3 the volume porosity for pores 3000 to 30,000 A in diam.

Assuming spherical particles, a first order reaction, and no inhibition by products, if $(R/C_R\ Deff)(dn/dt)$ is less than .03, reaction should be in Zone I; if greater than 6.0, the conditions of Zone II apply.

Using data from Table III and 3000 A for "large" pore diameters, estimates of this dimensionless group vary from .8 to 2.4, which indicates that while reaction occurs throughout a particle, it does so to a greater extent close to the external surface -- that is, the condition is between Zones I and II.

A question remains concerning the "cells" of fine pores surrounded by the network of large arterial channels. If the dimensionless group $\left(\frac{R}{C_R\ Deff}\right)\left(\frac{dn}{dt}\right)$ is set equal

to .03, which is its maximum value if the conditions of Zone I (uniform reaction) apply, the equality can be solved for R, the maximum particle or "cell"radius for uniform reaction. Estimating values for C_R, Deff (Knudsen diffusion occurs in pores 25A diameter) and dn/dt (a function of R), and solving for R gives a value of .014 cm for the calcinate used in the first part of Table III. This gives a "cell" diameter which is about half a particle diameter. Since a "cell" of this size must surely be permeated by the large pores, it is the concentration gradients in the large arterial pores which must be responsible for non-uniform reaction.

C. The Constant Rate of Reaction

Figures 2, 3, 4, and 5 show that for heat treated carbons, the weight-time plot during a considerable portion of reaction is very close to a straight line.

The fact that the kinetic order of carbon can be zero after 1 or 2% burnoff has often been observed before (8,9). The carbons discussed here were all exposed to some CO_2 or steam at 800°-900°C in their preparation, so this initial burnoff undoubtedly occurred prior to these reactivity measurements.

It is of particular interest to note that while the reaction rate is either constant or slowly decreasing, the pore surface first rises rapidly, and then decreases. The data for Elkol Calcinate of Table III are plotted in Figure 6.

Forty years ago, Chaney and co-workers established that the pore surface as manifested by adsorptive capacity for vapors first rises to a maximum and then falls off as a given sample of carbon undergoes activation (10).

Thus there is apparently no relation between a carbon's pore surface area and its rate of reaction with CO_2 or steam as a particular sample undergoes reaction. Even though pores may be available to the reacting gas at 750°-900°C which are not coated by nitrogen at low temperature in the surface area determinations, the extent of pore surface and its accessibility must certainly increase during the first 10 to 20% of reaction.

With the available surface changing as it does, the constancy of the reaction rate of these stabilized carbons is particularly striking. The explanation of a constant "porosity profile", which might well apply under conditions of Zone II (6) does not seem to apply here, where reaction is occurring throughout the particles.

In the reaction mechanism set forth by Ergun (11) an oxygen atom adsorbed on the carbon surface goes off as carbon monoxide and leaves behind either one, two or no active sites on the carbon. In the present case a single active site must be left behind on the stabilized carbon to give a rate of reaction so nearly constant. This constant rate is strong evidence that for a carbon stabilized by heat treatment, reaction of a molecule of CO_2 or H_2O with an active site on the solid to give an adsorbed atom of oxygen, and the subsequent evaporation of CO from this site must preserve or replace the active site somehow. Thus when one active site reacts, another is regenerated in its place, so that the number of active sites remains virtually the same as reaction proceeds.

This picture is a reasonable one. A reactive site probably involves an atom on an edge or a corner having one or more high energy bonds (12); when this atom is removed one of its neighbors would very likely be left similarly situated.

Studies of electron spin resonance have shown that carbons which have been heated to over 800°C have very few unpaired electrons (at room temperature) so that the active site is probably not a surface free radical. Harker and co-workers (13) believe that in impure carbons, surface sites involving hydrogen or metallic impurities contribute more to the reactivity than do unpaired electrons. Perhaps the hydrogen and metal contents are sufficiently stable in carbon at 900°C after treatment at 1000° or 1100° so

that the number of atoms of each remains constant during a large part of the reaction. It seems unlikely, however, that the hydrogen content would remain so precisely constant during oxidation by CO_2, so a constant level of catalytic metallic impurities during the reaction appears to be a possibility for explaining the constant rates. This explanation would demand that a "stable" active site be associated or coupled with such an impurity, and it is certainly reasonable that a carbon atom on the edge of a graphitic crystallite might exchange electrons with a metallic atom contacting the same crystallite.

D. Effect of Thermal Treatment

Amorphous carbons usually (but not always) become less reactive upon heat treatment. The loss in reactivity with heat treatment shown in Figure 7 is therefore to be expected. The fact that reactivity plotted vs. time of heat treatment gives very roughly a straight line on log log coordinates as in Figure 7, shows that heat treatment decreases the reactivity quite rapidly at first and very much more slowly as the time of treatment is extended. The thermal soaking would be expected to permit local rearrangements or recrystalization of the carbon to anneal points of strain or perhaps to allow edge carbon atoms to orient themselves into a graphitic structure. Less reactive sites or perhaps isolated dislocations could be expected to stabilize themselves more slowly. At 1000° or 1100°C graphitization of an amorphous carbon hardly proceeds at all, and x-ray diffraction patterns of some of these heat treated carbons did not differ significantly from those of the "unsoaked" coke. Thus, while no gross recrystalization occurred in these heat treatments, it is logical to expect that very local rearrangements may have stabilized the carbon.

Figure 5 shows that the rate of reaction of the untreated or unheated Elkol coke falls off within 2½ hours to about the same rate as coke which had been heat treated at 1000° for seven hours. This decrease in rate of the untreated sample is too much to explain by the effect of the thermal treatment alone. Neither will reaction of binder carbon in the briquetted coke at a faster rate than carbon from the particles explain this decrease, since the calcined coal particles follow practically the same reaction paths as the coke. (See Table III.)

If active sites are regenerated during reaction they must migrate around the surface of the carbon so that occasionally an adjacent carbon atom might already be active and therefore both active sites might not be regenerated on reaction. However, while this factor could very well be appreciable in the later stages of reaction it apparently is not of importance in the heat treated samples and therefor it is hard to see why it might be significant in the untreated cases.

One possible explanation for the decrease in rate with unstabilized carbon could be that there are several types of reactive sites, some of which are much less stable and more reactive than others. This concept actually is highly likely and has often been cited. These more reactive sites would be those more readily annealed by the heat treating process and if they are not always regenerated on reaction but instead are replaced by less active sites, the rapid loss in reactivity of the untreated sample could be explained. Thus the heat treated samples would probably contain not only fewer reactive sites but also sites which are of a lower and more uniform order of reactivity and which are apparently regenerated in kind by gasification.

As another possibility, stable sites might be those associated with metallic impurities, while less stable, non-regenerated sites might be those solid defects that are readily healed by annealing.

VI. Summary

The principal finding of this work is that a carbon stabilized by suitable thermal treatment reacts with carbon dioxide at very nearly a constant rate during the consump-

tion of a major portion of the sample. This occurs under conditions where the overall rate of reaction is largely governed by the chemical step.

This constant reaction rate strongly suggests that every time a reactive atom of carbon leaves the solid state as carbon monoxide, another carbon atom is made reactive. Thus, during the course of oxidation the chemical state of the carbon surface remains constant even though the physical state (shape and surface area) changes.

With the unstable carbons the reaction rate falls off faster during reaction than during heat treatment alone. Therefore the chemical state of these carbons must change during the course of reaction. A possible hypothesis suggests that when a highly reactive site is removed from the solid matrix, it leaves behind a less reactive site so that the carbon stabilizes as reaction proceeds.

It is a pleasure to acknowledge that this work was supported by FMC Corporation, and to thank J. Work, R. T. Joseph, J. A. Robertson, and C. H. Hopkins of FMC for many helpful suggestions.

BIBLIOGRAPHY

(1) Coking Western Coals, Coal Age, pg. 90, (December 1963); Chemical Wk (17 Jan 1960).

(2) Ergun, S., Kinetics of reactions of CO_2 and steam with Coke, USBM Bull. 598, (1962).

(3) Walker, P. L., Rusinko, F., Austin, L. G., Gas reactions of carbon. Adv. in Catalysis XI, pg. 143, (1959).

(4) Ref. (2) pg. 9.

(5) Ref. (3) pg. 165.

(6) Ref. (3) pg. 178.

(7) Kawahata, M., Walker, P. L., Mode of Porosity Development in Activated Anthracite. Proc. 5th Carbon Conf., Vol. 2, pg. 261, (1962).

(8) Ref. (3) pg. 161.

(9) Walker, P. L., Foresti, R. J., Wright, C. D., Surface area studies of carbon, Ind. Eng. Chem. 45, 1703, (1953).

(10) Chaney, N. K., Ray, A. B., St. John, A., Properties of Active Carbon, Ind. Eng. Chem. 15, 1244, (1923).

(11) Ref. (2) pg. 13.

(12) Bradshaw, W., Oxidation of Graphite and Various types of carbon. 6th Biennial Conf. on Carbon.

(13) Harker, H., Jackson, C., Gallagher, J. T., Horsely, J. T., Reactivity of Carbon and Graphite: Role of unpaired electrons. 6th Biennial Conf. on Carbon.

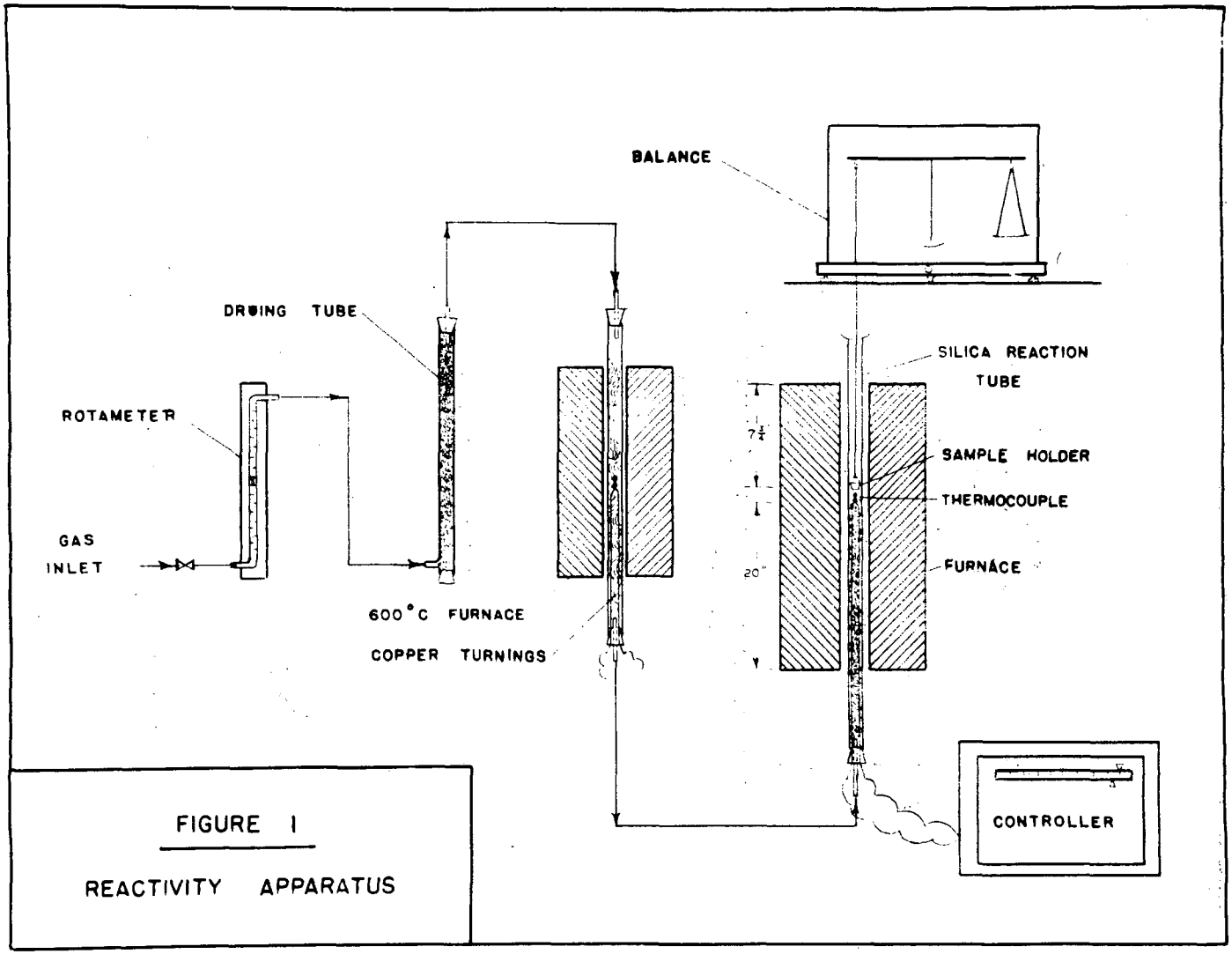

FIGURE 1

REACTIVITY APPARATUS

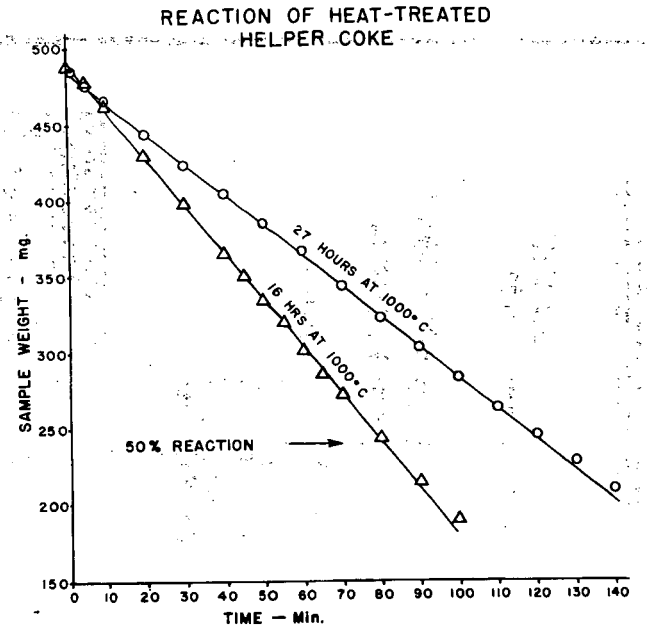
REACTION OF HEAT-TREATED
HELPER COKE
SAMPLE WEIGHT - mg.
500
450
400
350
300
250
200
150
0 10 20 30 40 50 60 70 80 90 100 110 120 130 140
TIME — Min.
27 HOURS AT 1000° C
16 HRS AT 1000° C
50% REACTION

FIG. 2

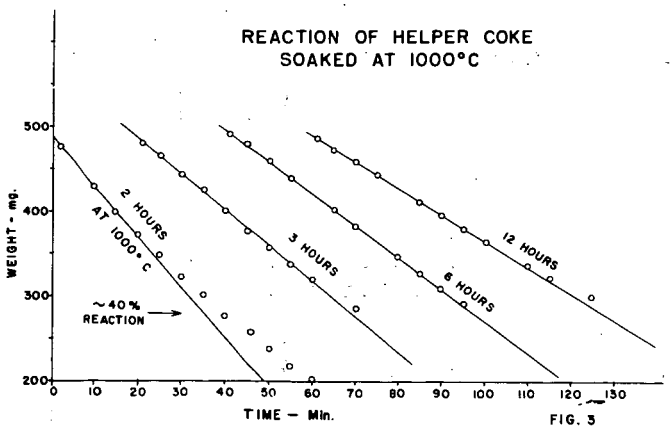
REACTION OF HELPER COKE
SOAKED AT 1000°C
WEIGHT - mg.
500
400
300
200
0 10 20 30 40 50 60 70 80 90 100 110 120 130
TIME — Min.
2 HOURS AT 1000° C
~40% REACTION
3 HOURS
6 HOURS
12 HOURS

FIG. 3

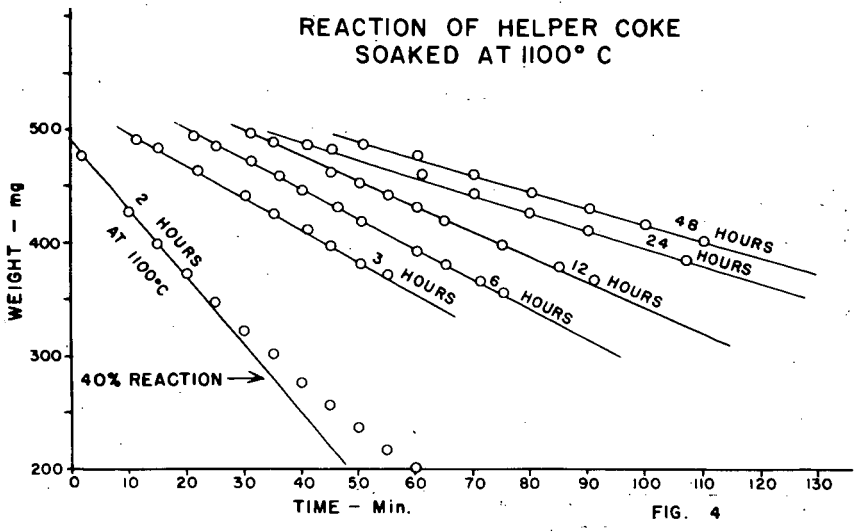
REACTION OF HELPER COKE
SOAKED AT 1100° C
WEIGHT - mg
500
400
300
200
0
10
20
30
40
50
60
70
80
90
100
110
120
130
TIME - Min.
2 HOURS AT 1100°C
3 HOURS
6 HOURS
12 HOURS
24 HOURS
48 HOURS
40% REACTION

FIG. 4

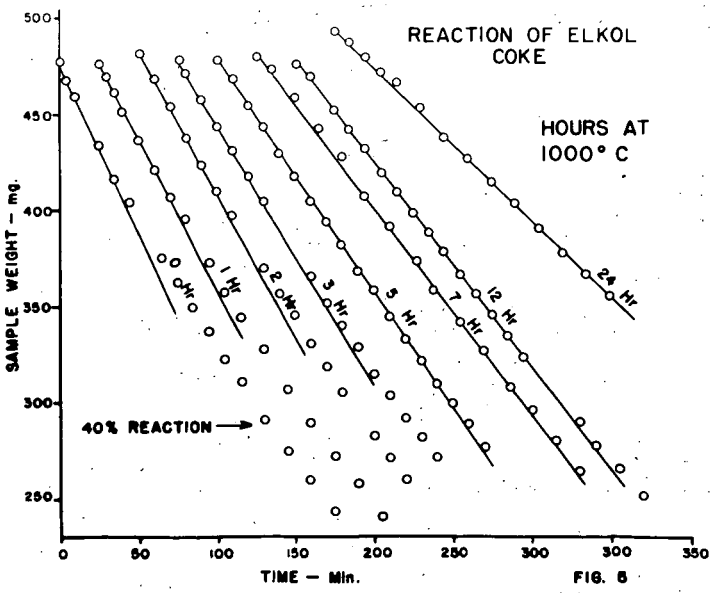
REACTION OF ELKOL COKE
HOURS AT 1000° C
SAMPLE WEIGHT - mg.
500
450
400
350
300
250
0
50
100
150
200
250
300
350
TIME - Min.
1 Hr.
2 Hrs.
3 Hr.
5 Hr.
7 Hr.
12 Hr.
24 Hr.
40% REACTION

FIG. 5

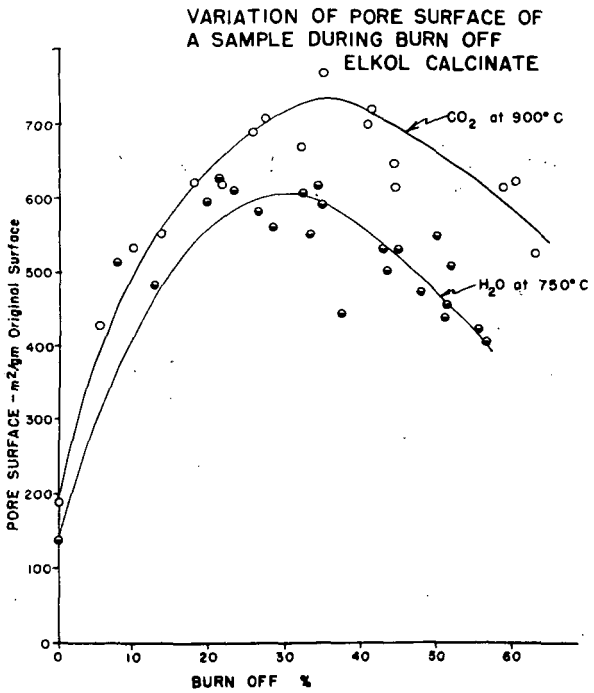
VARIATION OF PORE SURFACE OF
A SAMPLE DURING BURN OFF
ELKOL CALCINATE
CO_2 at 900° C
H_2O at 750° C
PORE SURFACE - m2/gm Original Surface
BURN OFF %
0
100
200
300
400
500
600
700
10
20
30
40
50
60

FIG. 6

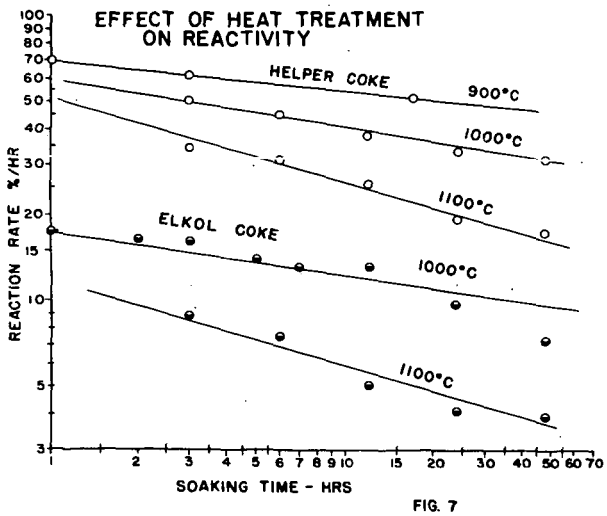
EFFECT OF HEAT TREATMENT
ON REACTIVITY
HELPER COKE
900°C
1000°C
1100°C
ELKOL COKE
1000°C
1100°C
REACTION RATE %/HR
SOAKING TIME - HRS
100
90
80
70
60
50
40
30
20
15
10
5
3
1
2
3
4
5
6
7
8
9
10
15
20
30
40
50
60
70

FIG. 7

EFFECT OF INHIBITORS ON FLAMMABILITY OF HEPTANE-AIR MIXTURES

H. Landesman and J. E. Basinski

National Engineering Science Company, Pasadena, Calif.

A large scale investigation of the effect of inhibitors on flammabilities of heptane-air mixtures has been reported by workers at Purdue University (2)(3). The technique involves measuring upward flame propagation at various n-heptane inhibitor-air percentages in a standard 4 ft. long, 2 in. diameter tube and plotting the percentages of extinguishant versus heptane percentages where mixtures are nonflammable. A curve such as shown in Fig. 1 is obtained.

With better inhibitors than that shown in Fig. 1, a peak in the flammability curve will be obtained at a lower percentage of inhibitor than the 6 mol. percent of Fig. 1. This peak percentage may be translated to weight percentages of inhibitor producing nonflammability of heptane-air mixtures and comparisons on a weight basis also can be obtained. These data have been found to follow fairly closely the extinguishment capability of the materials on actual test heptane or gasoline fires (3), though there is controversy over the extrapolation of data to potential fire extinguishing performance (4).

It was necessary to obtain a pre-fire test screening of extinguishants for hydrocarbon fires which would be stable at 550°F and have low vapor pressures at that temperature. This screening was accomplished by means of the combustion tube apparatus mentioned before. Since high concentrations of low vapor pressure inhibitors could not be maintained in the vapor phase with heptane-air mixtures in a conventional ambient temperature flammability limit combustion tube (5), it was necessary to design a heated combustion tube in which the flame propagation could still be observed. Visibility was necessary for evaluation of the inhibitory effects of the candidate extinguishant.

Experiments were carried out at sub-atmospheric pressures to prevent explosions or excessive pressures in the tube. Relative inhibitory effects have been found to be essentially independent of pressures down to about 200 mm (2).

The system is diagrammed in Fig. 2 and photographs are shown in Figs. 3 and 4. The gas containing sections of the apparatus are heated to 200°C to prevent condensation of the inhibitor. The glass combustion tube is heated by a baked on transparent conductive coating, while the metal inlet system and the pressure gauge are heated by electrical tapes.

The lower end of the combustion tube is closed by a metal flange, which is joined to the tube by a kovar-glass seal. The removable half of the flange has a glass feed-through insulator for the tungsten ignition wire (Fig. 4). This entire flange assembly and lower end of the tube is submerged in the 200°C silicone oil bath to insure the gases reaching a uniform temperature.

Partial pressures of the inhibitor and the heptane are measured directly with a Kern-Springham glass spiral manometer with attached mirror. Rotation of the spiral deflects the mirror and the deflection is measured on the scale.

The spiral deflection was calibrated to read pressures up to 50 mm against an external mercury manometer which was read with a cathetometer. Total pressure of the combined inhibitor-heptane-air mixtures was 300 mm.

For the larger air pressures, the manometer is used as a null indicator. The desired air pressure is introduced to the outside of the glass spiral, then balanced with pre-heated air on the system side. The gases are mixed by a sliding perforated disc, which is driven by an external magnet. After twenty minutes of mixing, the disc was brought to the top of the tube and the mixture sparked. If ignition, as evidenced by flame propagation to the top of the tube, did not occur, mixing was continued another five minutes and the mixture sparked again. It was found that the rich limit for heptane-air increased to 8.75 percent heptane at 203°C and 300 mm total pressure compared to 6.9 percent at approximately ambient temperature and 300 mm pressure (2). The lean limit did not change. A few comparison points were made in this work at 203°C with the same inhibitors used in the Purdue work at ambient temperatures. It was found that peak percentages for sym-dibromotetrafluoroethane and for trifluorobromomethane increased about 10 - 12 percent with the temperature increase. However, since experimental conditions, including mixing times and methods of mixing, are considerably different, the comparison has little meaning. It was found during this work that changes in these variables led to large differences in observed flammability.

In Figs. 5, 6, 7 and 8 are shown flammability plots for the inhibitors evaluated. The curves exhibit a variety of shapes and peaks occurring at various heptane-air-inhibitor ratios. The significance of this is not known. The peaks of the curves are of interest since these represent a comparison of the individual molecules' effectiveness as flame inhibitors. In Table I are presented data obtained on peak inhibition percentages and the weight this volume percentage represents in 100 liters of a heptane-inhibitor-air mixture. These data are taken from peaks of the curves previously shown.

The Purdue University work previously referenced contained a study of the effectiveness of 56 compounds as flame inhibitors, in a combustion tube at room temperature. This study includes many halogenated hydrocarbons, however, since their tube was not heated, they were unable to test the less volatile materials. Two major correlations emerge from their work, the first is a confirmation of work of earlier investigators who found that hydrocarbons containing iodine are better extinguishants than those containing bromine, which in turn, are better than the aliphatic chlorides. The Purdue group also found that hydrocarbon compounds containing only fluorine were very poor extinguishants. The second major correlation was the observation that as the molecular weight increases the extinguishing ability also increases, i.e., the peak percentage decreases. This relation, however, is not invariable and it is not possible to determine the extinguishing ability of a molecule from its molecular weight alone.

This study was carried out at a temperature of 203°C, thus, it was possible to determine the peak percentages of some higher molecular weight halogenated hydrocarbons. Figure No. 9 is a plot of the peak percentages from all the Purdue data plus those determined in this work as a function of molecular weight. The situation is quite complex, however, the chlorine containing compounds appear to form a rough series.

The general curvature of this line suggests that a straight line might occur if peak percentage were plotted against the inverse molecular weight. As can be seen from Figs. 10 - 14, this is the case. For a given series of halogenated hydrocarbons, the general trend is quite well marked, despite the wide variation in structures. There are two possible explanations that might clarify this relationship between peak percentage and inverse molecular weight. The first would be a purely physical process in which the extinguishant molecule acts as a "third body" to promote free radical recombinations. The alternate possibility would be to reason that the inverse molecular weight was related to some chemical property, such as bond energy, which was the actual cause of the effectiveness of the extinguishant. At the moment, we are investigating various parameters in an attempt to discover a rational correlation and explanation of the relation of extinguishant ability to the physical properties and chemical structures of the halogenated hydrocarbons.

References

1. This work was supported by the Federal Aviation Agency under U.S. Air Force Aeronautical Systems Division Administration on Contract AF33(657)-8937.
2. McBee, E. T., et al, ATI114, 903 Report on USA Contract W-44-009. ENG-507.
3. Malcolm, James E., National Fire Protection Quarterly, October 1954.
4. Engibous, E. L. and Torkelson, T. R., WADC-TR-59-463, p. 9.
5. Coward, H. F. and Jones, G. W., Bureau of Mines, Bulletin 503.

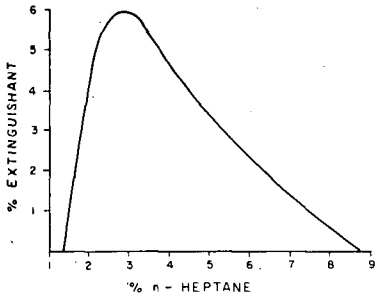

FIGURE 1

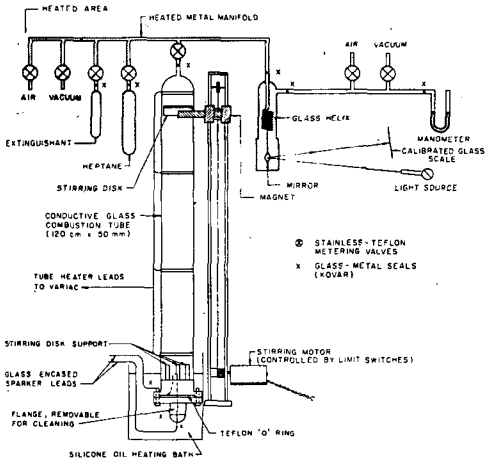

FIGURE 2
COMBUSTION TUBE FOR FLAMMABILITY LIMIT STUDIES (DIAGRAM)

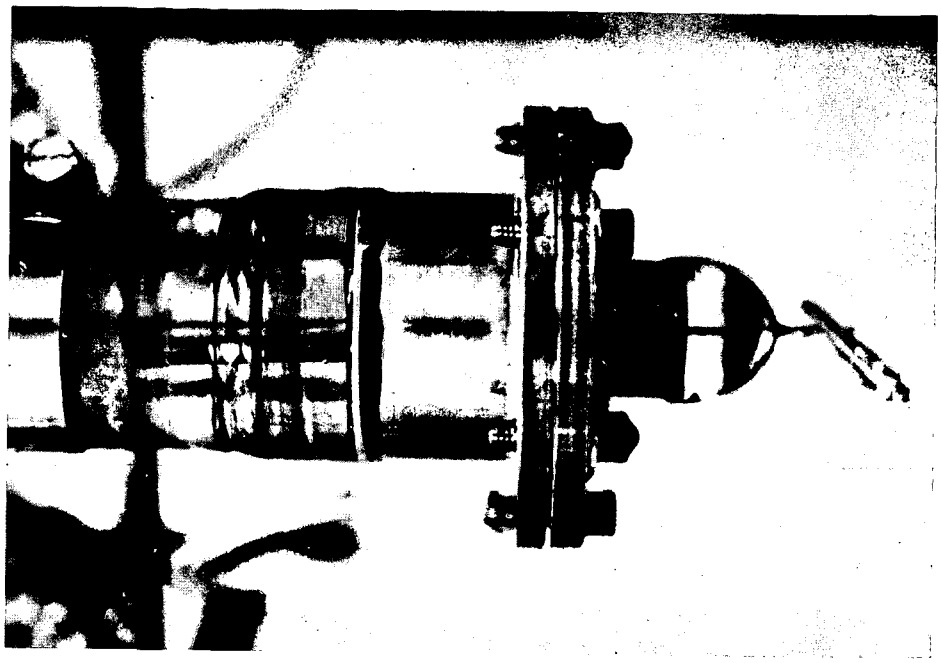

FIGURE 4 FLANGE DETAIL

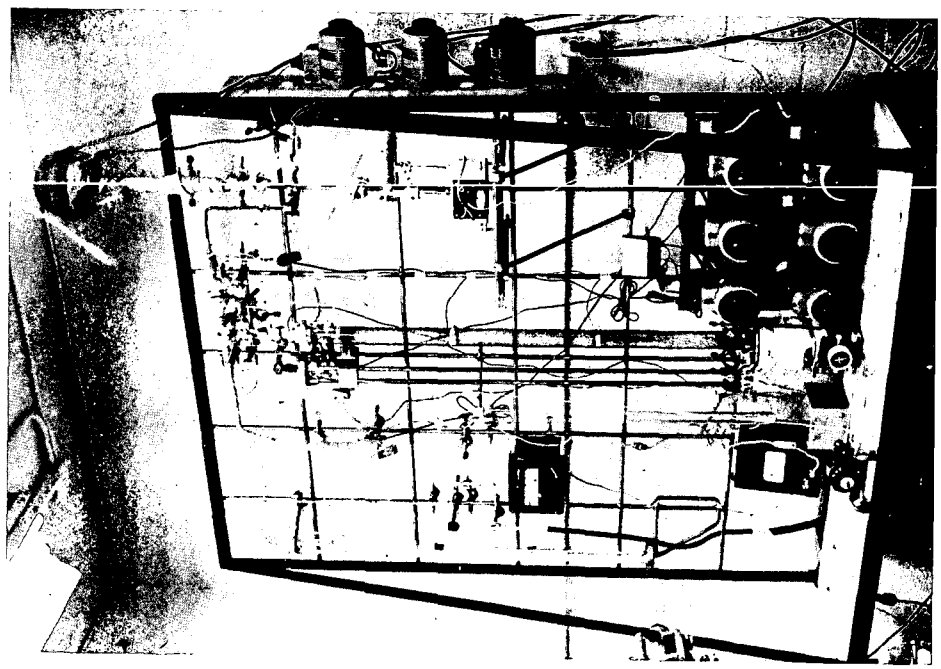

FIGURE 3 COMBUSTION TUBE

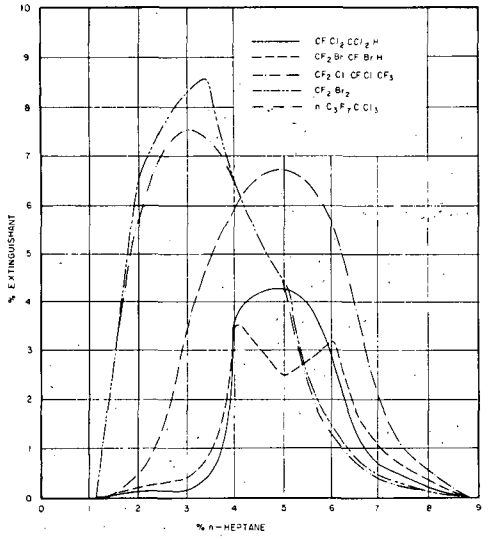

FIGURE 5
EFFECT OF CANDIDATE EXTINGUISHANTS ON FLAMMABILITY OF n - HEPTANE - AIR MIXTURES

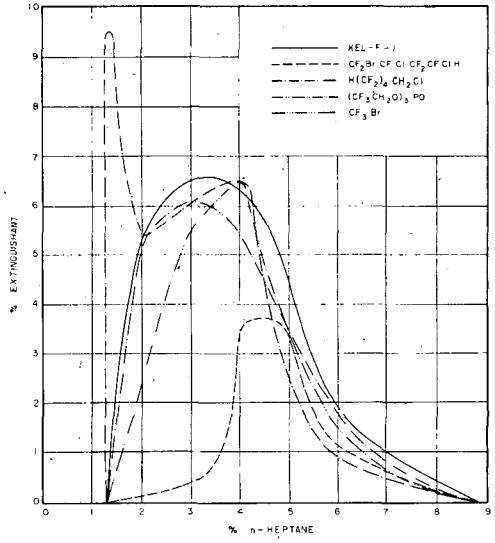

FIGURE 6
EFFECT OF CANDIDATE EXTINGUISHANTS ON FLAMMABILITY OF n - HEPTANE - AIR MIXTURES

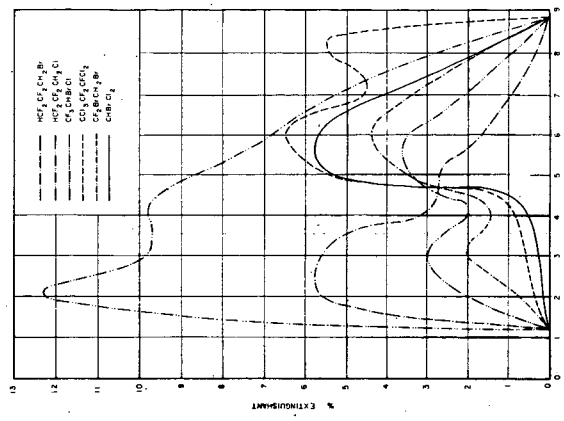

FIGURE 8
EFFECT OF CANDIDATE EXTINGUISHANTS ON
FLAMMABILITY OF n - HEPTANE - AIR MIXTURES

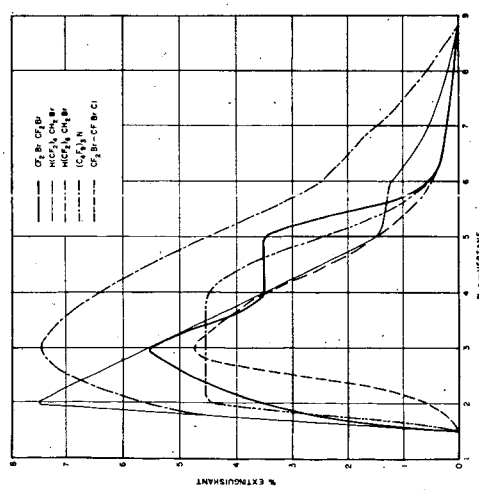

FIGURE 7
EFFECT OF CANDIDATE EXTINGUISHANTS ON FLAMMABILITY
OF n - HEPTANE - AIR MIXTURES

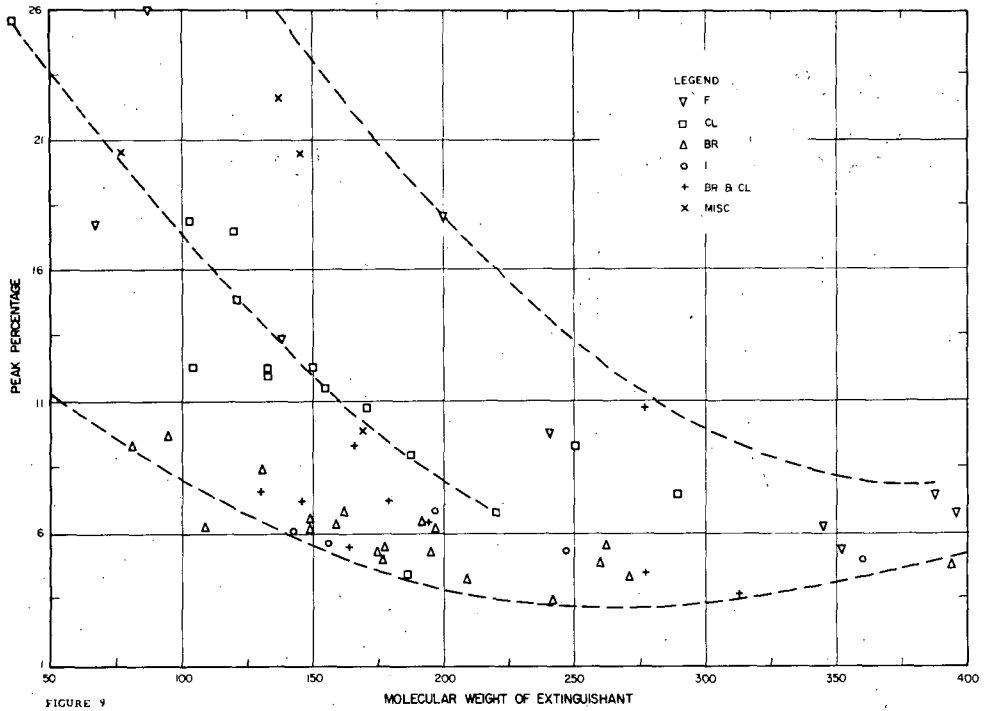

FIGURE 9

PEAK PERCENTAGE OF EXTINGUISHANT TO RENDER HEPTANE-AIR MIXTURE NON-FLAMMABLE AS A FUNCTION OF EXTINGUISHANT MOLECULAR WEIGHT

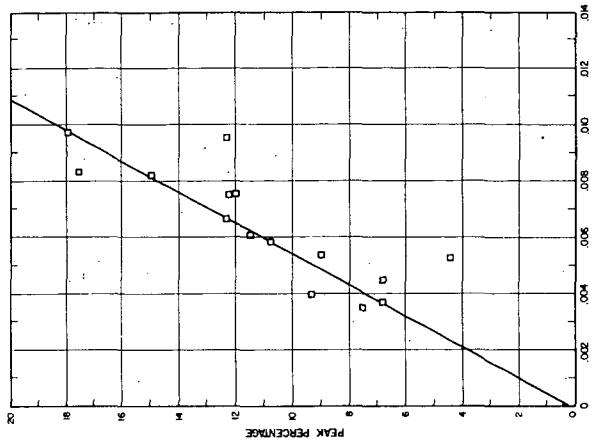

FIGURE 11
PEAK PERCENTAGE OF CHLORINE CONTAINING EXTINGUISHANTS AS A FUNCTION OF $\frac{1}{mw}$

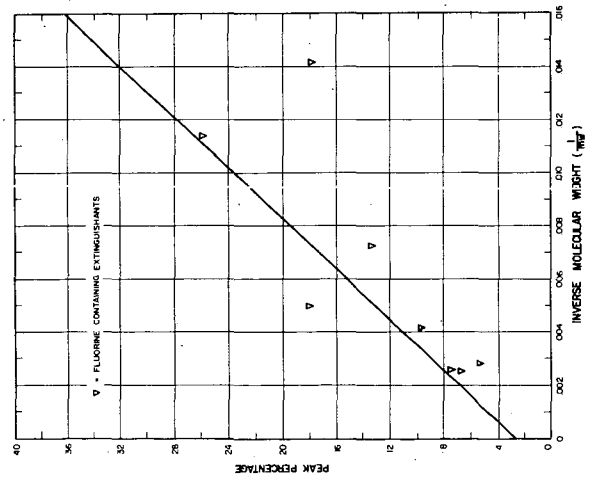

FIGURE 10
PEAK PERCENTAGE OF FLUORINE CONTAINING COMPOUNDS AS A FUNCTION OF INVERSE MOLECULAR WEIGHT

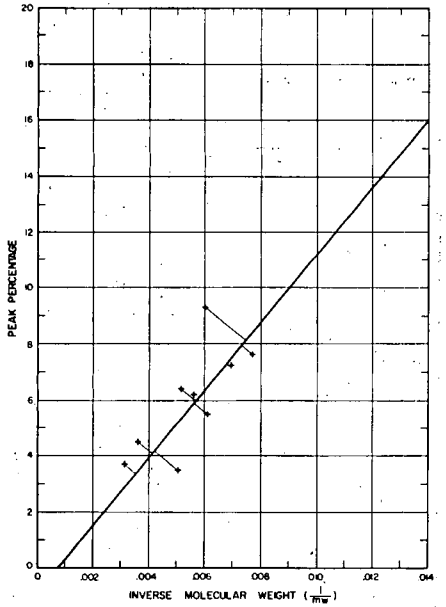

FIGURE 12
PEAK PERCENTAGES OF COMPOUNDS CONTAINING BOTH CHLORINE AND BROMINE AS A FUNCTION OF INVERSE MOLECULAR WEIGHT

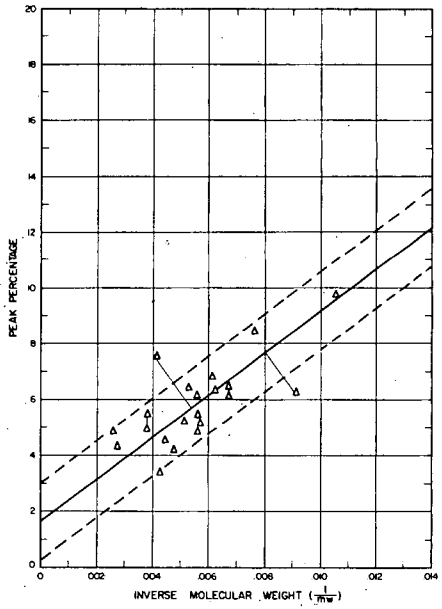

FIGURE 13
PEAK PERCENTAGE OF BROMINE CONTAINING EXTINGUISHANTS AS A FUNCTION OF 1/mw

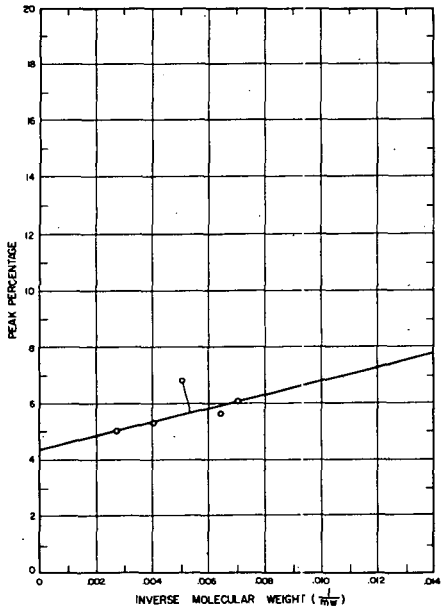

FIGURE 14
PEAK PERCENTAGE OF IODINE CONTAINING EXTINGUISHANTS AS A FUNCTION OF 1 / mw

TABLE I

EFFECT OF INHIBITORS ON HEPTANE-AIR FLAMMABILITY

Total Pressure 300 mm, Temperature 398°F

	MW	Peak %	Wgt. at Peak %	Rank Wgt. Basis	Rank Vol. Basis
$CF_2CHBrCl$	197.5	3.5	30.7	1	2
$CFCl_2CHCl_2$	186	4.4	36.6	2	4
$CF_3BrCHBrF$	242	3.4	36.8	3	1
$CHBrCl_2$	164	5.5	40.3	4	9
$CBrF_3$	149	6.5	43.2	5	13
$CH_2BrCBrF_2$	224	4.5	45.0	6	5
$CHF_2CF_2CH_2Br$	195	5.2	45.3	7	8
$CBrF_2CClFCF_2CHClF$	314	3.7	51.8	8	3
$CBrF_2CBrClF$	276.5	4.5	55.5	9	6
$CBrF_2CBrF_2$	260	5.5	65.8	10	10
$CClF_2CClFCF_3$	221	6.8	67	11	14
$CCl_3CF_2CCl_2F$	270.5	6.8	78.5	12	15
$CHF_2CF_2CH_2Cl$	150.5	12.3	82.6	13	20
$CHF_2(CF_2)_5CH_2Br$	395	4.75	83.6	14	7
$CF_3CF_2CF_2CCl_3$	287.5	7.5	96.5	15	16
$(CF_3CH_2O)_3PO$	344	6.3	96.7	16	11
$CHF_2(CF_2)CH_2Br$	295	7.5	99.0	17	17
$CHF_2(CF_2)_3CH_2Cl$	250.5	9.3	104.2	18	19
KEL-F-1 chloro-fluoroolefin polymer	500 av.	6.5	145.0	19	12
$(CF_3(CF_2)_3)_3N$	671	7.5	219.0	20	18

Ignition Characteristics of Colorado Oil Shale

V. Dean Allred and L. S. Merrill, Jr.

Marathon Oil Company, Littleton, Colorado

Introduction

Spontaneous ignition is usually characterized by an abrupt (exponential) increase in temperature and results when the rate of heat production in exothermic reaction exceeds the rate of heat dissipation to the surrounding media. Ordinarily the term spontaneous ignition temperature is applied to those systems being oxidized by air. However, in this paper the term applies to systems using oxygen enriched or partially depleted gas streams.

In a practical application it is important to know the ignition characteristics of oil shale in developing an understanding of processes for recovering oil from oil shales. This is particularly true when using the countercurrent or reverse combustion in situ recovery or the parallel flow retorting process (1, 2).

The countercurrent combustion process is one in which the combustion or oxidation zone moves against the flow of the injected gas stream. Figure 1 shows a schematic representation of such a process. To be practical, the combustion zone must progressively move toward the source of the oxidant injection at such a rate that only a minimum amount of fuel is consumed and the useful products produced in an oxygen free atmosphere. The process is somewhat unconventional but has been demonstrated in the laboratory as a means of producing oil from oil shale.

One way of explaining why the process works is as follows: As ignition of a given particle takes place, it is accompanied by an exponential temperature rise which in turn causes a rapid increase in combustion (oxidation) rate. This effectively removes the oxygen from the surrounding gas stream, so no further oxidation takes place at this point. However, heat has been transferred to the surrounding particles as well as the gas stream. One effect is that particles immediately upstream are continuously being heated to their ignition temperature and the process repeats itself with the combustion zone effectively progressing against the gas flow. Another effect is that the oxygen has been efficiently removed from the gas downstream from the combustion zone. This provides an inert hot gas in which the hydrocarbon components are effectively distilled from the solids.

Experimental

In this investigation the ignition temperatures were determined in a flow-type system so that conditions would be somewhat comparable to the retorting process. The experimental arrangement is given in Figure 2.

The basic unit of equipment was a small Inconel block furnace containing two one-half inch sample holes. One hole contained the sample and the other was filled with an inert reference material. Alternate junctions of twelve chromel-alumel thermocouples were located in the two holes to form a sensitive thermopile detector.

Since ignition is characterized by a rapid temperature rise, the differential thermopile was used in most experiments to detect the temperature at which combustion

occurred. However, advantage was also taken of the fact that ignition is also accompanied by the simultaneous release of carbon dioxide. In the latter case, the gas stream was continually monitored as a function of temperature with a differential thermal conductivity cell. Both techniques proved equally effective.

Determinations were made in air and in gas mixtures of oxygen and nitrogen over a pressure range from atmospheric to 1000 psig. The gas mixtures contained six, thirteen, twenty-one, and fifty-five percent by volume of oxygen.

In a typical experiment, about two grams of -40 to 60 mesh oil shale was placed in the sample hole. A similar sized sample of previously pyrolyzed oil shale was placed in the reference cell. The oxidant containing gas passed at the same rate through the shale and the reference material at the pressure of the experiment. The block was heated at a uniform rate of about 40°F/minute. Temperature and differential temperature were recorded by use of either a two-pen or an x-y recorder. In the alternate detection system the off-gas was taken from the cells, passed through drying tubes to remove water vapor, and then to the reference and sample sides, respectively, of a thermal conductivity detector. This signal was then continuously recorded as a function of the sample temperature.

Experimental Results

Ignition temperatures as a function of oxygen partial pressure for data covering several oxygen concentrations in the gas stream are tabulated in Table I and shown in Figure 3. (Note: These data are plotted with the square root of the oxygen partial pressure as a coordinate so that the scale could be expanded on the low pressure end and still extrapolated to zero. Plotting the square root has no other significance). From the curve shown in Figure 3 it is readily observed that the ignition temperature is relatively independent of total pressure, but strongly dependent on the oxygen concentration.

Other data have shown that lower rates of supplying the oxygen has little or no effect on the ignition temperature as long as excess oxygen is present for the combustion reaction.

One interesting set of data are shown in Figure 4. Of particular interest are the characteristics of the ignition temperatures at pressures below 100 psig where two temperature peaks were noted. The first peak showed a temperature rise but did not result in ignition.

These same data are plotted as a function of oxygen partial pressure in Figure 5, which shows the nature of the transition region clearly. It is thought that this transition region is associated with the well known "cool flame" oxidation phenomena observed for ignition of many hydrocarbons as a function of pressure. For example, Figure 6 shows these oil shale data, together with ignition curves, for n-octane, i-octane, and propane (3, 4). Naturally one would not expect the data to coincide with these particular hydrocarbons, but the similarity of the shape of the curves and the temperature range is striking. One possible interpretation of this behavior is that the shale ignition is associated with gas phase combustion of hydrocarbons being distilled out of the oil shale.

Discussion

The question arises why oil shales ignite at such low temperatures when destructive distillation of the shale oil does not occur until temperatures in excess of 700°F are reached.

This question can possibly be answered by considering the fact that Colorado oil shale has from one to three percent by weight (about ten percent of total

TABLE I

Gas Composition Volume %	Total Pressure (psi)	*Oxygen Partial Pressure (psi)	Ignition Temperature (°F)
(Air)	125	24	450
(21% O_2)	162	34	435
	212	44	435
	587	123	385
	954	203	365
	22.2	4.7	545
	32.2	6.8	540
	32.2	6.8	535
	52.2	11.0	500
	72.2	15.1	475
	26.2	5.5	530
	92.2	19.4	465
	112.0	23.6	455
	212.0	44.5	425
(55% O_2)	22.2	12.2	455
(45% N_2)	112	61.7	400
	210	116	375
	512	281	354
	812	446	340
(13% O_2)	22.2	2.9	580
(87% N_2)	44.2	5.7	560
	60.2	7.8	500
	110	14.4	495
	167	21.8	453
	594	77.3	395
(6% O_2)	22.2	1.3	586
(94% N_2)	39.2	2.4	565
	62.2	3.7	535
	112	6.7	506
	277	16.6	435
	860	51.6	405

*Data taken at gas flow rate of 1350 standard cubic feet per square foot of cross sectional area per hour.

organic matter) of benzene soluble components in it. As shown in Figure 7, about the same weight fraction of oil shale is volatile between 360°F and 700°F when analyzed by thermogravimetric (TGA) techniques. These data indicate that volatiles start being evolved in an appreciable amount at about 360°F, which was about the same as the lowest self ignition temperature observed. Further, this preliminary evolution reaches a maximum at about 600°F, which is about the normal ignition temperature in air at atmospheric pressure.

Based on these data, it seems very likely that ignition is associated with the evolution of hydrocarbon vapors from the oil shale in the temperature range 360°-700°F.

Summary

The self ignition temperature of Colorado oil shale has been determined to vary with oxygen concentration from about 630°F at atmospheric conditions to 360°F at high (about 500 psi) oxygen partial pressure.

The ignition temperature is shown to correspond closely to temperature range during which organic vapors evolve prior to the onset of destructive distillation of the kerogen in the shale.

Literature Cited

1. Allred, V. D., and Nielson, G. I., Countercurrent Combustion - A Process for Retorting Oil Shale. Preprint No. 9, AIChE 48th National Meeting, Denver, Colorado.

2. Allred, V. D., U. S. Patent 3,001,775 (September 26, 1961) assigned to Marathon Oil Company.

3. Affens, W. A., Johnson, J. E., and Carhart, H. W., Ignition Studies Part V., NRL Report 5437 (January 27, 1960).

4. Maccormac, M., and Townsend, D. T. A., The Spontaneous Ignition Under Pressure of Typical Knocking and No-Knocking Fuels: Heptane, Octane, Iso-octane, etc. J. Chem. Soc. 143 (1940).

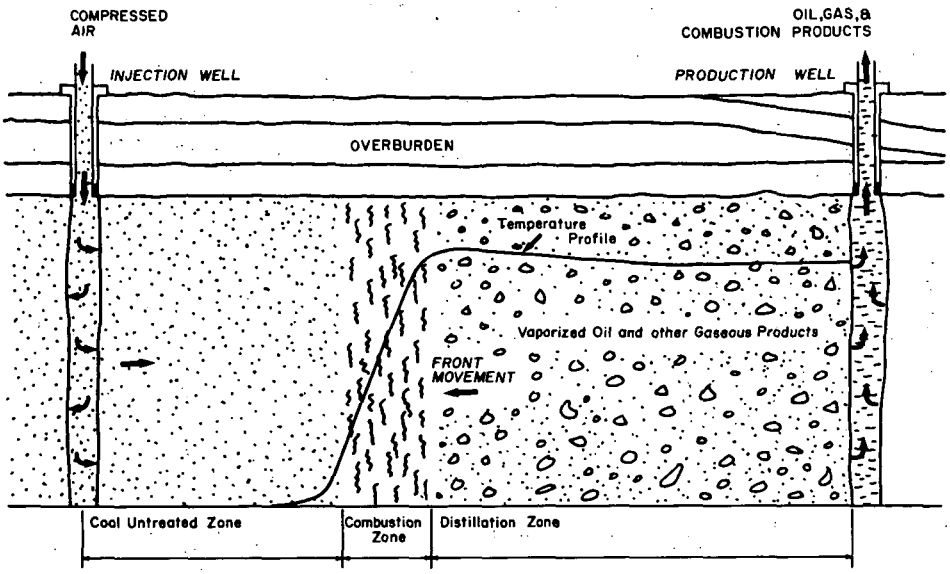

Figure 1. The Countercurrent Combustion In Situ Process for Recovering Hydrocarbons.

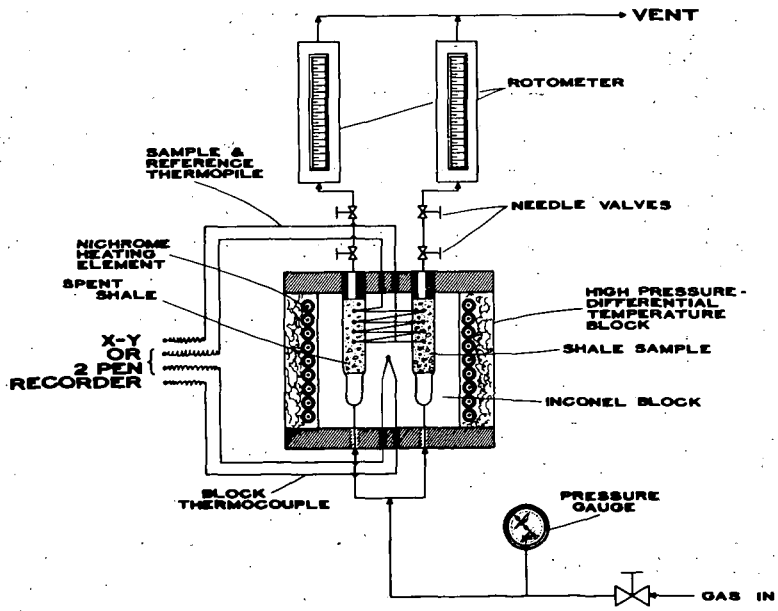

Figure 2. High Pressure Differential Analysis Equipment for Determining Spontaneous Ignition Temperature of Oil Shale.

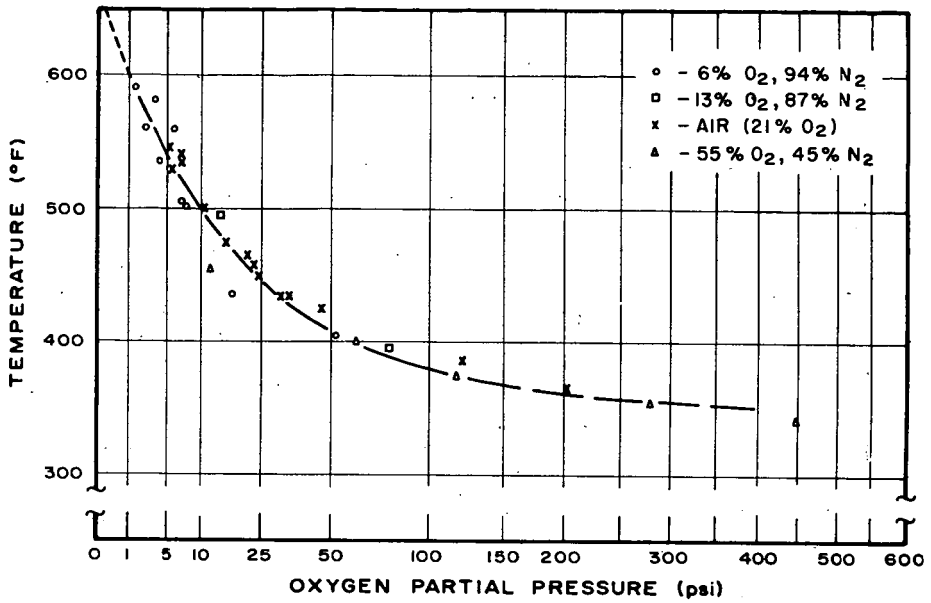

Figure 3. Ignition Temperature of Colorado Oil Shale as a Function of Oxygen Partial Pressure.

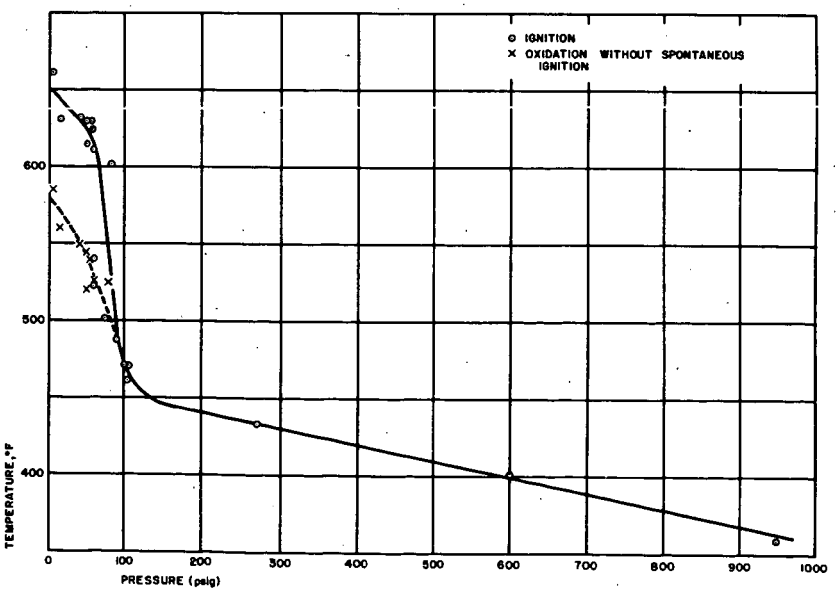

Figure 4. Spontaneous Ignition Temperature of Colorado Oil Shale as a Function of Pressure.

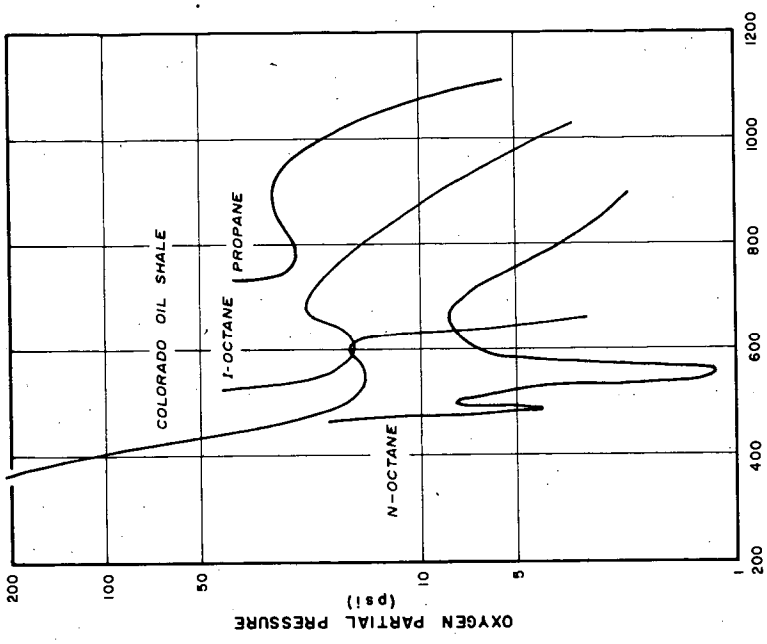

Figure 6. Spontaneous Ignition Curves for Selected Hydrocarbons.

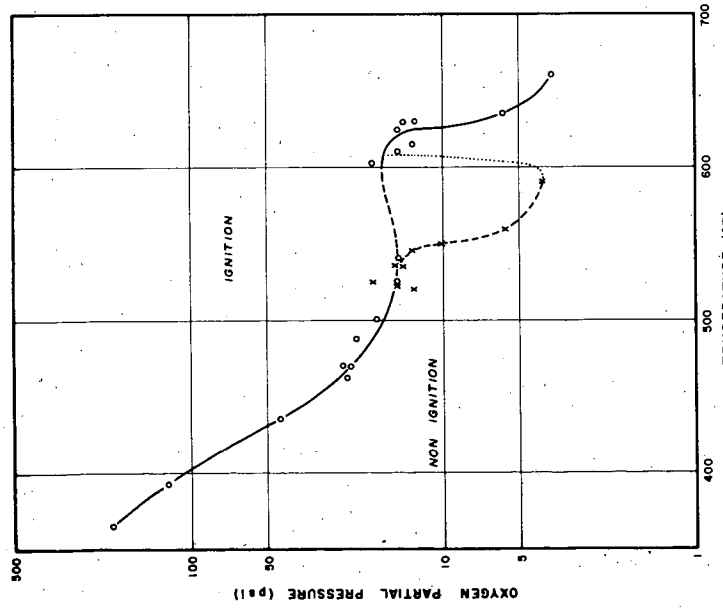

Figure 5. Spontaneous Ignition Curve for Colorado Oil Shale.

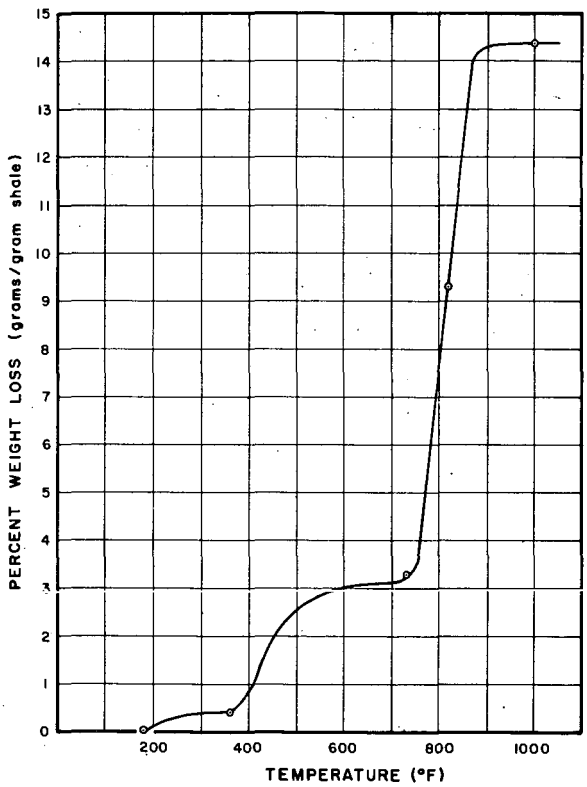

Figure 7. TGA of Colorado Oil Shale.

Production of Alcohols from Olefins in Low Temperature Coal Tars

Bernard D. Blaustein, Sol J. Metlin, and Irving Wender

Pittsburgh Coal Research Center, Bureau of Mines
U. S. Department of the Interior
4800 Forbes Avenue, Pittsburgh 13, Pennsylvania

ABSTRACT

Olefins constitute as much as one-half the neutral oil obtained by low-temperature carbonization of low-rank coals. It is difficult to separate these olefins from other materials in the tar fractions. However, without a prior separation, a large fraction of these olefins can be converted to mixtures of primary alcohols by hydroformylation with H_2 + CO in the presence of dicobalt octacarbonyl as a catalyst (oxo reaction). Several neutral oils were so treated and the alcohols separated via their borate esters. The highest yields of alcohols (25 percent by weight of starting material) were obtained from the neutral oil of a lignite tar. The carbon number distribution of the alcohols was determined by mass-spectrometric analysis of the trimethylsilyl ethers. C_9- to C_{27}-alcohols were produced; an unusually high concentration of C_{20}-alcohols appeared in the products from lower rank coals. Nuclear magnetic resonance spectra of the alcohol mixtures showed that an "average" molecule contains from 1 to 3 branched methyl groups. By using $C^{14}O$, and assuming that each olefin will react with one CO, the percentage of olefins originally in the tar can be determined from the radioactivity of the product. An advantage of this analytical method is that no separation of the olefins, or their oxo product, need be made. By this procedure, the neutral oil from the lignite tar was shown to contain about 50 percent olefins.

INTRODUCTION

The high olefinic content of tars derived from low temperature carbonization of lower rank coals is of interest as a source of commercially valuable chemicals. However, there is no good way of separating these olefins from the other materials present in the tar fractions. The oxo (or hydroformylation) reaction offers a promising way to convert the olefins in the tar, without prior separation, to alcohols that are of potential commercial value as detergent and plasticizer intermediates. The oxo synthesis (1) is the reaction of an olefin with H_2 + CO (synthesis gas) in the presence of dicobalt octacarbonyl, $Co_2(CO)_8$, as the catalyst to yield a mixture of primary alcohols.

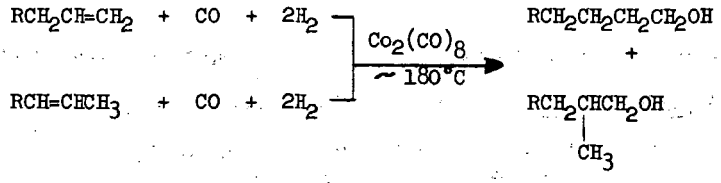

The reaction takes place predominantly at the terminal double bond.

The advantages of using this reaction to convert olefins to useful products are (a) the olefins need not be separated from the tar fractions to undergo reaction, (b) the reaction is not poisoned by sulfur compounds or any of the other substances in low-temperature tar, (c) conversion of the olefins is high, (d) during the oxo reaction, any internal olefinic bonds migrate to the terminal position so that all olefins react as if they were alpha olefins; all the olefins in the tar, terminal and internal, are thus utilized to make alcohols, and (e) the oxo reaction is quite versatile and can be successfully carried out under a wide range of conditions: gas pressures of 50-400 atm, and reaction temperatures of 50-200°C.; $Co_2(CO)_8$ can be used either in the preformed state, or can be formed during the reaction from a variety of cobalt salts.

EXPERIMENTAL

Samples of Rockdale lignite tar were obtained from the Texas Power and Light Company. They had separated the whole lignite tar into "methanol solubles" and "hexane solubles." The hexane solubles were further separated by distillation into two fractions, the hexane solubles foreruns (HSF) and the hexane solubles distillate (HSD). The total hexane solubles constitute 66 percent of the primary tar; the HSF 7 percent, the HSD 46 percent, and the residue from the distillation of the hexane solubles 13 percent. About 98 percent of the HSF boils below 235°C., and 89 percent of the HSD boils up to 355°C. The composition of these fractions is given in table 1.

Both fractions contain approximately 50 percent olefins, of which about half are alpha olefins (2-4). Phenolic compounds and other constituents are also present in both fractions. Since these phenols would interfere with our analytical procedure for determining alcohol yield, they were removed by chromatographing the fractions on alumina with petroleum ether as the eluting solvent. About 20 percent by weight of the starting material was removed in this way during the preparation of a "phenol-free" lignite tar fraction.

TABLE 1.-Approximate composition of low-temperature tar fractions, volume percent

Type of constituent	Hexane solubles foreruns Rockdale lignite tar	Hexane solubles distillate Rockdale lignite tar	Nugget tar distillate	Kentucky high-splint tar distillate
Caustic solubles	6-8	10-15	44	31
Acid solubles	2-4	1-3	3	7
Neutral oil	88-92	80-90	53	62
Paraffins	13-15	15-20	22	34
Olefins	40-55	40-50	20	21
Alpha-olefins	17-20	17-20		
Aromatics	30-47	35-45	37	45
Oxygenates			21	

Nugget tar, formed by the low-temperature carbonization of a hvcb-suba Wyoming coal, was also investigated. A sample of this tar was distilled under vacuum to 170°C/3mm (est. bp 320°C/760mm). The distillate, including a small amount of water phase, amounted to 42.1 percent of the whole tar. Repeated chromatography finally yielded a phenol-free neutral oil amounting to 37.9 percent of the distillate. A neutral oil derived from the low-temperature carbonization of a Kentucky hvab (high splint) coal was chromatographed on alumina to eliminate the phenols shown to be present by infrared spectral analysis. Recovery of phenol-free neutral oil was 86.8 percent.

The alcohols were separated from the oxo products by conversion to their borate esters (5-8). The borate esters formed from the alcohols are sufficiently high-boiling that the non-esterified material can be distilled away from the esters. The esters are hydrolyzed to regenerate the alcohols, which are then separated and vacuum distilled, resulting in an alcohol fraction of high purity.

$$3ROH + H_3BO_3 = (RO)_3B + 3\ H_2O$$

$$3\ ROH + (C_4H_9O)_3B = (RO)_3B + 3\ C_4H_9OH \qquad (1)$$

$$(RO)_3B + 3\ H_2O = 3\ ROH + H_3BO_3 \qquad (2)$$

In a typical run, 50 grams of chromatographed (phenol-free) HSF, 4 grams of $Co_2(CO)_8$ and 3500 psi 1:1 synthesis gas were charged into a rocking Aminco autoclave, heated to 180-190°C. and kept there for five hours. The product was treated with tri-n-butylborate (equation 1), the non-esterified material was distilled off, the borate esters were hydrolyzed

(equation 2), and the alcohols were vacuum distilled. The product was an almost water-white alcohol fraction in 25 percent yield, based on the weight of starting material. The alcohol content was confirmed by infrared spectral analysis, the only impurity detected being a small amount of a carbonyl compound. To determine the carbon number distribution of the alcohols formed, the trimethylsilyl ethers of the alcohols were analyzed by mass spectrometry (9). The results are shown in figure 1.

The chromatographed (phenol-free) HSD was subjected to the same reactions and subsequent procedures for alcohol recovery. The alcohol yield was also 25 percent by weight of the starting material; the carbon number distribution data is given in figure 2. The phenol-free neutral oil from the Nugget tar distillate was subjected to the oxo reaction and the same alcohol recovery procedures as those previously described for the Rockdale tar. An alcohol yield of 13 percent was realized. The alcohols were converted to their trimethylsilyl ethers and analyzed by mass spectrometric analysis. The results are shown in figure 3. The phenol-free neutral oil from the Kentucky hvab coal was reacted under oxo conditions. The subsequent recovery of alcohol was 7.5 percent. The product, water-white in color, was converted to trimethylsilyl ethers and submitted for mass spectrometric analysis. The results are shown in figure 4.

NMR spectra were obtained on all the alcohol mixtures produced from the tar fractions. These results will be considered in the Discussion section of this paper.

Under oxo conditions, it can be assumed that each molecule of olefin will react with one molecule of CO. Further reaction under oxo conditions will produce alcohols, aldehydes, esters, and other oxygenated products. If $C^{14}O$ is incorporated into the synthesis gas, the product will be radioactive. A determination of the amount of radioactivity in the product can then be used to calculate the concentration of olefins present originally in the tar fraction. Several runs of this type were made, both on known mixtures, and on the low-temperature tar fractions. The results obtained are discussed below.

RESULTS AND DISCUSSION

Carbon Number Distribution of Alcohols Produced

Figure 1 shows the distribution of the alcohols produced from the HSF fraction of the lignite tar. The carbon number range shown is C_{10}-C_{15}, the maximum concentration is at C_{12}, and the average carbon number is 12.2. Not shown on the graph are minor concentrations of C_9 and C_{16}-C_{20} alcohols. This mixture is composed of alcohols of the carbon number

range now used for plasticizer and detergent production. A higher boiling fraction of these alcohols ranged from C_9 to C_{24}, with an average carbon number of 16.2. Figure 2 shows the distribution of the alcohols produced from the HSD fraction of the lignite tar. The carbon number range shown is C_{13}-C_{22}, the largest percentage is at C_{20}, and the average carbon number is 17.8. There are also traces of C_{11}-C_{12} and C_{23}-C_{27} alcohols.

Figure 3 shows the distribution of alcohols produced from the neutral oil from the Negget tar distillate. The carbon numbers range from C_{11}-C_{23}, the largest concentration is at C_{15}, and the average carbon number is 16.3. Trace amounts, not shown, are also present at C_{24} and C_{25}. Figure 4 shows the distribution of the higher boiling alcohols produced from the neutral oil from the Kentucky hvab coal. The carbon numbers range from C_{13}-C_{23}, the greatest concentrations are at C_{16} and C_{17}, and the average carbon number is 17.2. Trace amounts, not shown, were also present at C_{24}. A lower boiling fraction of these alcohols ranged from C_{10} to C_{22}, with an average carbon number of 14.1.

In the alcohol mixtures produced from the lower rank lignite and hvcb-suba coals, there are anomalously high concentrations of C_{20} alcohols. (See figures 2 and 3.) This did not appear in the alcohols from the hvab coal (figure 4). Gas-chromatographic methods, and other separation techniques, will be used to obtain highly concentrated samples of either the C_{20} alcohols and/or their precursors, the C_{19} olefins from the lignite tar. If identification of either the alcohols or olefins can be made, it may point out interesting differences between the low-temperature carbonization tars produced from low and medium rank coals. It is conceivable that the C_{19} olefin present in such high concentration in the tars from the lower rank coals is some isomer of pristene (2,6,10,14-tetramethylpentadecene), since the saturated paraffin, pristane, recently has been isolated from a low-temperature brown coal tar (10), and was shown to be present in abnormally high concentrations in two petroleums (11).

NMR Spectra of Alcohol Mixtures

The NMR spectra of these alcohol mixtures were run on a Varian HR-60 instrument. Data were obtained for the number of H atoms on the C atom bonded to the OH group (that is, if the alcohol is a primary alcohol), and the number of H atoms present in methyl groups. This latter quantity gives a measure of the branching of the carbon chain.

For the HSF alcohols, there were 1.8 H atoms on C bonded to OH, and 1.8 methyl groups/molecule; HSD, 1.9 H, 3.4 methyl; Nugget, 2.3 H, 3.0 methyl; and Kentucky, 1.9 H, 2.6 methyl. Within the accuracy of the method, all

of the alcohols appear to be primary, as expected from the nature of the oxo reaction. In general, the number of branched methyl groups increases with the average carbon number of the alcohol mixture. As a comparison with some other, more highly branched, commercially-produced oxo alcohols, C_{13}-alcohols made from triisobutylene would have at least 6 methyl groups/molecule; those made from tetrapropylene would have at least 4 methyl groups/molecule; and C_{17}-alcohols made from tetraisobutylene would have at least 8 methyl groups/molecule.

Determination of Olefin Content of Mixtures by Using $C^{14}O$

If a mixture containing olefins is reacted with H_2 + $C^{14}O$, to a good approximation, each molecule of olefin will react with one molecule of CO, and therefore each olefin will be "tagged" with radioactivity. This will be true whether the olefin ends up as an alcohol, aldehyde, ester, ether, etc. The only exception is when the olefin hydrogenates to form the paraffin, and this is an important reaction under oxo conditions only for highly branched olefins, or compounds such as indene.

By measuring the radioactivity of the total oxo product obtained from each olefin-containing fraction relative to the radioactivity of the residual CO in equilibrium with the bomb contents at the end of the run, the initial olefin content of the mixture can be determined. In each 100 molecules of the olefin-containing mixture, where x molecules are olefinic, and Y is the average carbon number of the mixture;

$$\frac{x}{100\ Y + x}\ \text{(radioactivity of gas in bomb at end of run)} = \text{(radioactivity of product)}.$$

Table 2 gives the results obtained by this procedure. Agreement between

TABLE 2.-Determination of olefin content of mixtures by using $C^{14}O$

Mixture	Assumed average carbon number	Olefin Content, mole percent Known	Found
Decene-1 + 1-methylnaphthalene	10.0	47 50	52 56
Decene-1 + dodecene-1 + limonene + 4-methylcyclohexene-1 + 1-methylnaphthalene	9.5	55	53
HSF	12.4	1/ 40-55	55, 48
HSD	16.8	1/ 40-50	53, 42

1/ See table 1.

known and found values is satisfactory. Further work is being done on the other tar fractions, and on improving the accuracy of this analytical procedure.

ACKNOWLEDGMENTS

The authors wish to thank R. A. Friedel and A. G. Sharkey, Jr., for the spectrometric analyses; and P. Pantages for his technical assistance. The Nugget tar sample was obtained from Willis Beckering, U. S. Bureau of Mines, Grand Forks, North Dakota. The tar sample from the Kentucky hvab (high splint) coal was obtained from Bruce Naugle, U. S. Bureau of Mines, Pittsburgh, Pa.

REFERENCES

1. Wender, I., H. W. Sternberg, and M. Orchin. The Oxo Reaction. Ch. 2 in Catalysis, v. 5, ed. by P. H. Emmett, Reinhold Pub. Corp., New York, N. Y., 1957.

2. Aluminum Co. of America and Texas Power & Light Co. On Stream Prototype Solvent Extraction Plant for Lignite Tar. Texas Power & Light Co., P. O. Box 6331, Dallas 22, Texas.

3. Batchelder, H. R., R. B. Filbert, Jr., and W. H. Mink. Processing Low Temperature Lignite Tar. Ind. and Eng. Chem., v. 52, 1960, pp. 131-136.

4. Kahler, E. J., D. C. Rowlands, J. Brewer, W. H. Powell and W. C. Ellis. Characterization of Components in Low-temperature Lignite Tar. J. Chem. and Eng. Data, v. 5, 1960, pp. 94-97.

5. Alekseeva, K. A., D. M. Rudkovskii, M. I. Ryskin, and A. G. Trifel. Preparation of High Molecular Weight Alcohols from the Products of Catalytic Coking by the Oxo Synthesis Method. Khim. i. Tekhnol. Topliv i Masel, v. 4, No. 5, 1959, pp. 14-18. Translation by Associated Technical Services, Inc., East Orange, N. J.

6. Rottig, W. Separation of Aliphatic Alcohols from Hydrocarbon-Alcohol Mixtures. U. S. Patent 2,746,984, May 22, 1956.

7. Société belge de l'azote et des products chimiques du Marly, S. A. Continuous Separation of Higher Fatty Alcohols from Mixtures Containing Hydrocarbons. Belgian Patent 541,333, March 15, 1956; Chem. Abs., v. 54, 1960, 16877e.

8. Washburn, R. M., E. Levens, C. F. Albright, and F. A. Billig. Preparation, Properties, and Uses of Borate Esters. Chap. in Metal-Organic Compounds, Adv. in Chemistry Series, v. 23, Am. Chem. Soc., Washington, D. C., 1959, pp. 129-157.

9. Zahn, C., A. G. Sharkey, Jr., and I. Wender. Determination of Alcohols by Their Trimethylsilyl Ethers. BuMines Rept. of Inv. 5976, 1962, 33 pp.

10. Kochloefl, K., P. Schneider, R. Rericha, M. Horák and V. Bazant. Isoprenoid-skeleton hydrocarbons in low-temperature brown coal tar. Chem. and Ind. (London), April 27, 1963, p. 692.

11. Bendoraitis, J. G., B. L. Brown, and L. S. Hepner. Isoprenoid hydrocarbons in petroleum - Isolation of 2,6,10,14-tetramethylpentadecane by high temperature gas-liquid chromatography. Anal. Chem., v. 34, 1962, pp. 49-53.

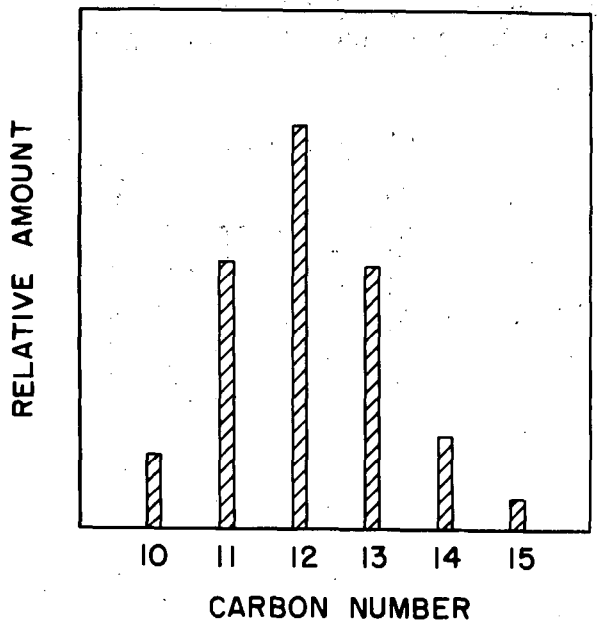

Figure 1.- Distribution of alcohols produced from hexane solubles foreruns fraction of Rockdale lignite tar.

L-8036 4-19-63

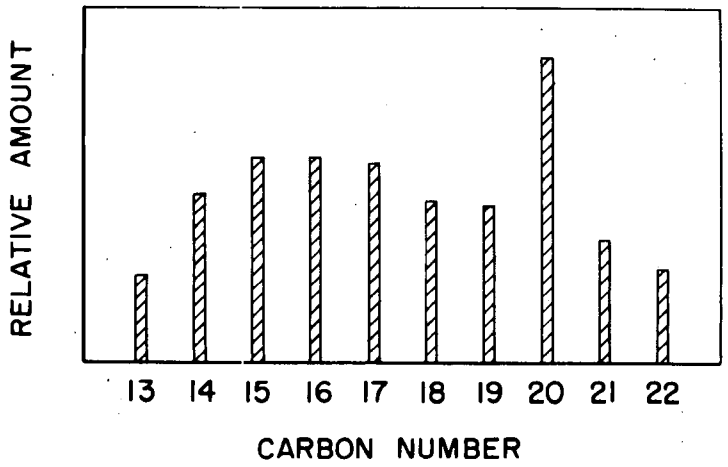

Figure 2.-Distribution of alcohols produced from hexane solubles distillate fraction of Rockdale lignite tar.

L-8037 4-19-63

11-6-63 L-8363

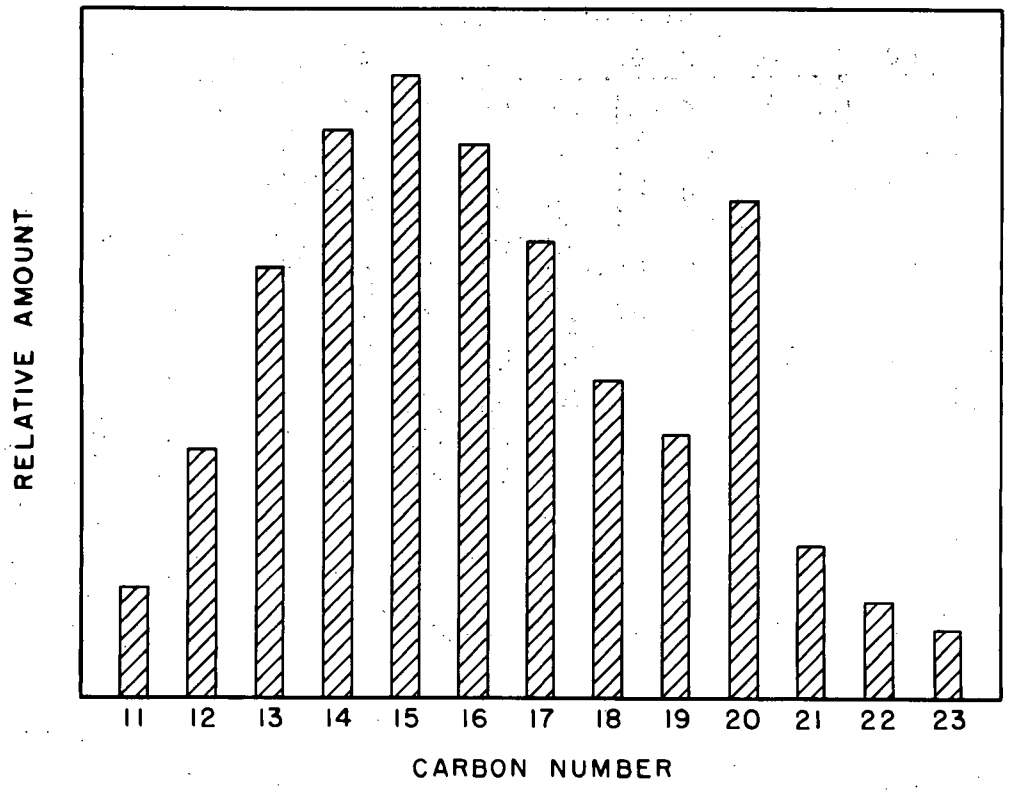

Figure 3. — Distribution of alcohols from nugget tar neutral oil produced from a Wyoming hvcb-suba coal.

11-6-63 L-8362

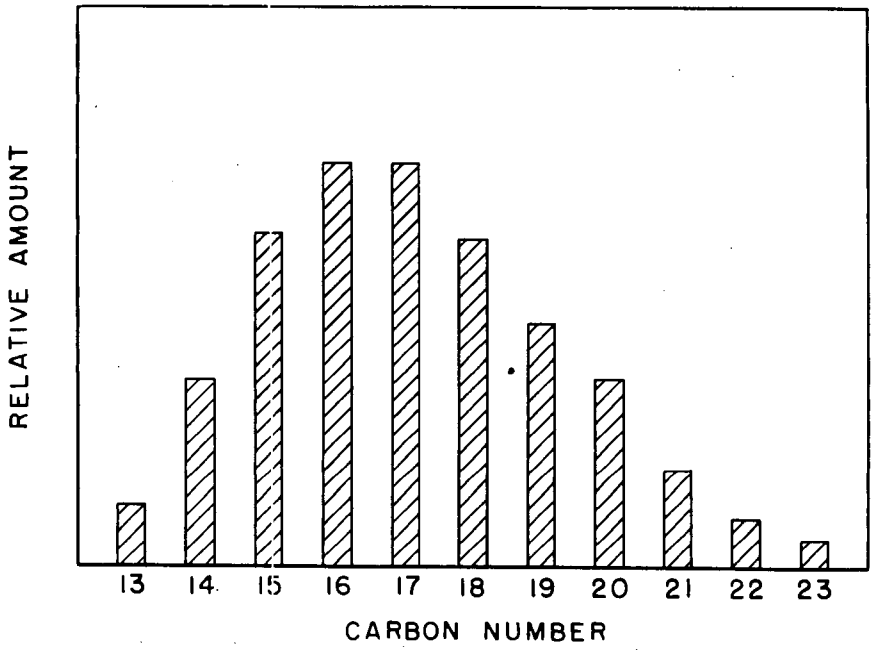

Figure 4.- Distribution of alcohols from a low-temperature tar neutral oil produced from a Kentucky hvab (high splint) coal.

Isolation of Porphyrins From Shale Oil and Oil Shale

J. R. Morandi and H. B. Jensen

Bureau of Mines, U.S. Department of the Interior
Laramie, Wyo.

INTRODUCTION

Oil shale is a laminated rock of sedimentary origin that ranges from gray to dark brown to almost black. It owes its color to carbonaceous matter called "kerogen" which is derived from plant and animal remains (1). Kerogen is largely insoluble in common organic solvents, but when heated to about 900°F it yields shale oil. This shale oil resembles petroleum in that it is composed of hydrocarbons and sulfur-, nitrogen-, and oxygen-derivatives of hydrocarbons.

The discovery of porphyrins in petroleum and oil shale by Treibs (12, 13) in 1934 gave direct evidence for the organic origin of petroleum and oil shales. In 1953 Groennings (5) published a method for extracting and spectrophotometrically determining porphyrins in petroleums. Groennings' procedure stimulated the work on the analysis of porphyrins in natural products. In 1954 Moore and Dunning (8) extracted Green River oil shale with various solvents and obtained a number of extracts that contained porphyrin-metal complexes. They concluded that the majority of the porphyrin exists in the shale as an iron-porphyrin complex. Although these researchers have reported the occurrence of porphyrins in oil shale, no one has reported their presence in shale oil. The present work was undertaken to determine if porphyrins were able to survive the retorting step and if so, what changes were brought about by retorting.

It was found in this investigation that:

(1) Porphyrins are present in shale oil so they survive the retorting step.

(2) Retorting changes the porphyrins from phyllo to etio type, and their average molecular weight is lowered. This lowering of the molecular weight is partially accounted for by decarboxylation.

(3) Porphyrins present in shale oil are shown to be a complex mixture of predominantly etio type with an average of nine methylene substituents on the porphine ring. The absorption spectrum of the purest porphyrin prepared was nearly identical to the spectrum of a synthesized etio-type porphyrin.

EXPERIMENTAL WORK

Method of Extracting Porphyrins

Groennings' method (5) for the extraction of porphyrins was used with two modifications: (1) To reduce loss of porphyrins to the organic phase, a 20 percent

hydrochloric acid solution was used instead of the recommended 7 percent solution, and (2) to minimize decomposition of the porphyrin by contact with halogenated solvents (2) the final transfer of the porphyrins was made into benzene instead of into chloroform.

Source of Materials Studied

The oil shale studied was from the Mahogany Ledge of the Green River formation near Rifle, Colo. The shale contained 35 weight percent organic matter and assayed 64.3 gallons of oil per ton by the Modified Fischer assay method (10). Because the shale contained approximately 10 percent by weight of CO_2 as mineral carbonates, it was pretreated with 4 percent hydrochloric acid and air-dried prior to the porphyrin extraction step.

The crude shale oil was produced in an internally fired retort. The feed shale for this retort was also from the Mahogany Ledge of the Green River formation and averaged about 30 gallons of oil per ton. Selected properties of the oil, using the Bureau of Mines shale-oil assay method (11), were specific gravity, 0.950; weight percent nitrogen, 2.11; weight percent sulfur, 0.88; and a distillation analysis of 4.6 volume percent naphtha, 14.3 volume percent light distillate, 26.7 volume percent heavy distillate, and 54.3 volume percent residuum.

Spectral Procedures

The absorption spectra from 450 to 650 mu of all porphyrin extracts, concentrates, and reference compounds were obtained in benzene solution. The method of Dunning (2) was used for correcting for background absorption in determining the type and quantity of porphyrins. The spectral reference compounds used in this research were mesoporphyrin IX dimethylester and etioporphyrin I.

Low-ionizing-voltage and high-ionizing-voltage mass spectra were obtained on selected extracts and concentrates. When a nickel complex of a porphyrin sample was introduced into the mass spectrometer, the spectrum obtained was of the nickel complex. The introduction of uncomplexed porphyrins resulted in the spectrum of the indium chloride complex of the porphyrins.1/ In both cases the mass spectra will be discussed as the spectra of the uncomplexed porphyrins.

Extraction and Concentration of Porphyrins From Shale Oil

Small-Scale Extraction

A 100-gram sample of the crude shale oil was extracted using the modified Groennings' method. This extract was purified by chromatographing it on a column containing 100 grams of activated alumina. Benzene was used to prewet the alumina and as the initial eluent. Benzene elution was continued until the solvent was almost colorless. Spectral examination of the benzene showed that no prophyrins were

1/ The indium chloride in the instrument resulted from the reaction of indium used for the valves in the sample introduction system and chlorine from chlorinated solvents used in other mass spectral projects.

removed. The porphyrin band was removed from the column using 1,2-dichloroethane, and elution with this solvent was continued until no porphyrins were discernible in the eluent. Visible absorption spectra were obtained on the extract before and after the chromatographic step. Low- and high-voltage mass spectra were obtained on the chromatographically purified extract.

Large-Scale Extraction

To obtain enough porphyrin extract for a characterization study, 2,300 grams of crude shale oil was extracted by the modified Groennings' method. The extract was chromatographed on 1,000 grams of activated alumina. Benzene was used to prewet the column and to elute the colored impurities, as was done on the small-scale experiment. The porphyrins were slowly eluted, using first recycled benzene and then mixtures of benzene and 1,2-dichloroethane. Twenty fractions were collected using benzene and 11 using benzene containing increasing quantities of 1,2-dichloroethane. Visible absorption spectra were obtained on all fractions, and mass spectra were obtained on selected fractions.

Countercurrent extraction was used as an additional separation on several of the fractions from the large-scale chromatographic separation. In each case, cyclohexane and 0.25 N hydrochloric acid were used as the immiscible solvents and 100 transfers were made. Absorption data were used to determine the distribution of porphyrins in the 100 tubes. Each time the separation was into four areas with concentration maxima occurring near tubes 33, 55, 75, and 95. The porphyrins in the tubes in each of the concentration areas were combined, and mass and absorption spectra were obtained on the recovered porphyrins.

Extraction of Porphyrins From Oil Shale

A sample of the hydrochloric acid leached shale, containing 105 grams of organic matter, was placed in a glass bomb, and 300 ml of benzene was added as a dispersant. The modified Groennings' extraction procedure was used to extract the porphyrins, except that the bomb was shaken continuously during the extraction. Visible absorption and mass spectra were obtained on the resulting extract.

RESULTS AND DISCUSSION

Porphyrin is the term applied to a class of compounds in which four pyrrole rings are united by bridge carbons to form a conjugated, macrocyclic structure, known as porphine. Figure 1 shows the numbering system that will be used in this paper for the porphine ring (9). This conjugated ring system is heat stable and can be halogenated, nitrated, or sublimed without destroying the macrocyclic structure (4).

Porphyrins, dissolved in organic solvents, have a typical, four-banded absorption spectrum in the visible region between 450 and 650 mu. They have been classified into etio, phyllo, and rhodo types according to the height of the individual peaks relative to one another (3). Representative spectra of each of these three types are shown in figure 2. The four bands or peaks are numbered I, II, III, and IV starting from the long-wavelength end of the spectrum. In general, the height of the peaks increases toward the shorter wavelengths.

Porphyrins that have methyl, ethyl, vinyl, propionic acid, or hydrogen in positions 2, 3, 7, 8, 12, 13, 17, and 18 (see figure 1) around the porphine ring

give the etio-type spectrum. This etio-type spectrum, which is characteristic of blood-pigment porphyrins, has four peaks, which become progressively higher proceeding from the longer to the shorter wavelengths. The shale-oil extracts and concentrates gave etio-type spectra.

The phyllo-type spectrum, which is typical of the chlorophyll porphyrins, has peak II larger than III. This type of spectrum has been attributed either to the presence of an isocyclic ring between one of the pyrrole rings and the adjacent bridge carbon atom or to an alkyl group on one of the bridge carbon atoms. The oil-shale extracts gave phyllo-type spectra.

The rhodo-type spectrum has been observed in compounds having a carbonyl group attached to one of the pyrrole rings and has the number III peak as the strongest of the four main peaks. The rhodo-type spectrum was not observed for any of the oil-shale or shale-oil extracts.

The porphyrins in the extract from oil shale were characterized by the use of absorption and mass spectra. The absorption spectrum of this oil-shale extract is shown in figure 3. This spectrum is characteristic of phyllo-type porphyrin, which has peak II higher than peak III.

The low-voltage mass spectrum showed porphyrins with molecular weights from 462 to 536. The ions in this spectrum were in the three following homologous series: (1) The alkyl-substituted porphine series, (2) the series two mass units greater than the porphine series, and (3) the series two mass units less than the porphine series. Figure 4 shows the distribution of intensities of the ions for the series occurring at two mass units greater than the porphine series. The average molecular weight of the porphyrins in this series (as calculated from this distribution) is 508. More than half of the total ions in the low-voltage spectrum were in this series, and the data presented in figure 4 represent the three series.

In the high-voltage spectrum of the oil-shale extract there was a series of ions 44 mass units less than the parent ions. This series of ions was shown to be a fragment ion series corresponding to the loss of CO_2 from the porphyrins.

These characterization data show the following facts about the oil-shale porphyrins:

(1) Oil-shale porphyrins are composed of at least three homologous series of compounds with no fewer than six different compounds in each series.

(2) The majority of these compounds have a phyllo-type spectrum.

(3) Some of these porphyrins have carboxyl substituents.

(4) The average molecular weight of 508 for the oil-shale porphyrins can be accounted for by 1 carboxyl and 11 methylene substituents on the porphine ring.

Before the porphyrins from the small-scale extraction of shale oil could be characterized, it was necessary to remove some of the impurities carried along by Groennings' extraction. This was done by chromatographing on alumina, and the absorption spectra of the porphyrin extract before and after chromatography are shown in figure 5. Improvement in the purity of the porphyrins by the chromatographic step is shown by the smaller background absorption in the chromatographed concentrate. The shale-oil extract both before and after chromatographing gave an etio-type spectrum, whereas the oil-shale extract showed a phyllo-type spectrum.

In the low-voltage mass spectrum of the shale-oil extract, more than 90 percent of the parent ions were in the alkyl-substituted porphine series. Figure 6 shows the distribution of the ions in this series with molecular weight range from 366 to 492. The abscissa scale shows both m/e of the ions (molecular weights) and the number of methylene substituents necessary on the porphine ring to have this molecular weight. The average molecular weight of the porphyrins in shale oil (as calculated from this distribution) is 436, or the equivalent of nine methylene substituents on the porphine ring.

In the high-voltage spectrum of the shale-oil extract, there was no evidence of a fragment ion series 44 mass units less than the parent ions. This indicates that there are no carboxyl groups present in shale-oil porphyrins.

These characterization data show that shale-oil porphyrins are predominantly alkyl-substituted porphines with 4 to 13 methylene groups per molecule. Because the absorption spectrum of this extract is of the etio type, these alkyl substituents are on the eight pyrrole carbons in the porphine ring.

Comparison of the character of the porphyrins from oil shale with the character of the porphyrins from shale oil indicates the changes that porphyrins undergo during retorting. These changes are as follows:

(1) The molecular weight is lowered an average of 72 mass units. In part, this is explained by decarboxylation. The decrease in average molecular weight is equivalent to the loss of one carboxyl and two methylene groups per molecule.

(2) The phyllo-type character is changed to an etio-type character. The reaction necessary to bring about this change in spectral type is the removal of substituents from the bridge carbons on the porphine ring. This could also contribute to the lowering of the molecular weight of the porphyrins.

Further characterization of the porphyrins in shale oil was accomplished by examining the fractions from the chromatographic separation of the large-scale shale-oil extraction. The absorption spectra of the first 25 fractions from this chromatographic separation were of the etio type, and these fractions contained 70 percent of the total porphyrins recovered. Beginning with the 26th fraction, the height of peak II relative to peak III became increasingly greater. This indicated that some phyllo-type porphyrins were being eluted with the 1,2-dichloroethane. This presence of a phyllo-type porphyrin in the shale-oil extract is an indication that a part of the porphyrins is relatively unchanged during retorting.

A benzene-eluted fraction was used to demonstrate further the character of the etio-type porphyrins in shale oil. A nickel complex of the 15th fraction was prepared, and low- and high-voltage mass spectra of this complex were obtained. The peak heights in these spectra were corrected for isotope contribution. Figure 7a is the resulting low-voltage spectrum, and figure 7b is the resulting high-voltage spectrum. Each of the figures shows the corrected peaks only in the molecular weight region of the porphyrins.

The low-voltage mass spectrum has only ions in the porphine series. The number of substituents on the porphine ring is from 3 to 12 methylene groups with an average of 7 methylene substituents per molecule. The greater abundance of odd-numbered substituents over even-numbered is unexplained; this distribution is not evident in the low-voltage spectrum of the total shale-oil concentrate (see figure 5).

Hood (6) and Mead (7) have reported the mass spectral cracking pattern for metal complexes of etioporphyrin, and they concluded that the main fragmentation process is the loss of methyl groups. The peaks shown in figure 7b at one mass unit less than the porphine series could be due to the loss of methyl groups and indicate the presence of methyl or ethyl substituents on the porphine ring of shale-oil porphyrins.

The high-voltage spectrum of this fraction shows the presence of singly charged ions at every m/e from the molecular weight of the porphyrins to the doubly charged parent ions.2/ Both Hood and Mead have shown that in the mass spectrum of etioporphyrin I the porphyrin skeleton remains intact because no singly charged ions occur between the molecular weight of the porphyrin skeleton and the doubly charged parent ions. The conclusion, therefore, is that the fraction shows the presence of impurities. Because the low-voltage spectrum of this fraction showed no molecular ions other than porphyrins, the impurity is probably nonaromatic.

Countercurrent extraction was used to further purify the porphyrin concentrates. Fraction 14 from the large-scale chromatographic separation was countercurrent extracted and separated into four concentrates. Judging by the comparison of specific extinction coefficients, one of these concentrates was the purest porphyrin concentrate prepared in this work. That the impurity was still present can be seen by comparing the molar extinction coefficient (2) for this fraction which was 1.8×10^3 in benzene, with that for etioporphyrin I, which was 6.2×10^3 in benzene. This impurity, however, has low absorption in the visible region. This is illustrated by the good agreement of the visible spectrum of this concentrate with the spectrum of a synthesized etio-type porphyrin as shown in figure 8.

The low-voltage mass spectrum of the porphyrin concentrates from countercurrent extraction showed a series of molecular ions in the porphine series. One of the concentrates had parent ions occurring at molecular weights corresponding to four to eight methylene substituents on the porphine ring. Of the total parent ions present in the mass spectrum of this concentrate, 25 percent showed the presence of four methylene substituents, and 65 percent showed the presence of five methylene substituents.

CONCLUSION

This work has demonstrated that the skeleton of the porphyrin molecules in oil shale is capable of surviving retorting temperatures. However, the substituent groups on the skeleton are changed. As expected, reduction in average molecular weight is the most obvious change. Partial explanation of this reduction was demonstrated to be decarboxylation. Another change that can be inferred to take place is the removal of substituents responsible for the phyllo character of the oil-shale porphyrins. This could result either from the destruction of an isocyclic ring or from the removal of substituents from a bridge-carbon atom.

The porphyrins present in shale oil were shown to be a complex mixture of predominantly etio type. The absorption spectrum of the purest porphyrin prepared was nearly identical to the spectrum of a synthesized etio-type porphyrin. The porphyrins in shale oil have an average molecular weight equivalent to the porphine ring with nine carbon atoms of methylene substituents. The total number of carbon substituents ranged from 4 to 13.

2/ This was true for all extracts and concentrates prepared in this work.

ACKNOWLEDGMENTS

The work upon which this report is based was done under a cooperative agreement between the Bureau of Mines, U.S. Department of the Interior, and the University of Wyoming.

The authors wish to thank Dr. J. G. Erdman, Mellon Institute, for the samples of etioporphyrin I and mesoporphyrin IX dimethylester used in this research.

REFERENCES

(1) Belser, Carl. Green River Oil-Shale Reserves of Northwestern Colorado. BuMines Rept. of Inv. 4769, 1951, 13 pp.

(2) Dunning, H. N., J. W. Moore, and A. T. Meyers. Properties of Porphyrins in Petroleum. Ind. and Eng. Chem., v. 46, September 1954, pp. 2001-2007.

(3) Fischer, H., and H. Orth. Die Chemie des Pyrroles (The Chemistry of the Pyrroles). Akademische Verlagsgesellschaft M.B.H., Leipzig, 1937; Edwards Bros., Inc., Ann Arbor, Mich., v. 2, pt. 1, 1943, pp. 579-587.

(4) Goldstein, Jack M. Instrumental Studies of Porphyrin Compounds Obtained From Pyrrole Aldehyde Condensation. Ph. D. Dissertation, Univ. of Pennsylvania, 1959, 192 pp.

(5) Groennings, Sigurd. Quantitative Determination of the Porphyrin Aggregate in Petroleum. Anal. Chem., v. 25, No. 6, June 1953, pp. 938-941.

(6) Hood, A., E. G. Carlson, and M. J. O'Neal. Petroleum Oil Analysis. Ch. in The Encyclopedia of Spectroscopy, ed. by George W. Clark. Reinhold Publishing Corp., New York, N.Y., 1960, pp. 613-625.

(7) Mead, W. L., and A. J. Wilde. Mass Spectrum of Vanadyl Etioporphyrin I. Chem. and Ind., August 19, 1961, pp. 1315-1316.

(8) Moore, J. W., and H. N. Dunning. Interfacial Activities and Porphyrin Contents of Oil-Shale Extracts. Ind. and Eng. Chem., v. 47, July 1955, 1440 pp.

(9) Patterson, Austin M., Leonard T. Capell, and Donald F. Walker. The Ring Index. McGregor and Werner, Inc., 1960.

(10) Stanfield, K. E., and I. C. Frost. Method of Assaying Oil Shales by a Modified Fischer Retort. BuMines Rept. of Inv. 4477, 1949, 13 pp.

(11) Stevens, R. F., G. U. Dinneen, and John S. Ball. Analysis of Crude Shale Oil. BuMines Rept. of Inv. 4898, 1952, 20 pp.

(12) Treibs, A., Uber das Vorkommen von Chlorophyllderivaten en eines Olschiefer aus der oberen Triss (Occurrence of Chlorophyll Derivatives in an Oil Shale From the Upper Triassic). Ann. Chem. Liebigs, v. 509, 1934, pp. 103-114.

(13) _____. (Chlorophyll and Hemin Derivatives in Bituminous Rock, Petroleums, Coals, and Phosphate Rock.) Ann. Chem. Liebigs, v. 517, 1935, pp. 172-196.

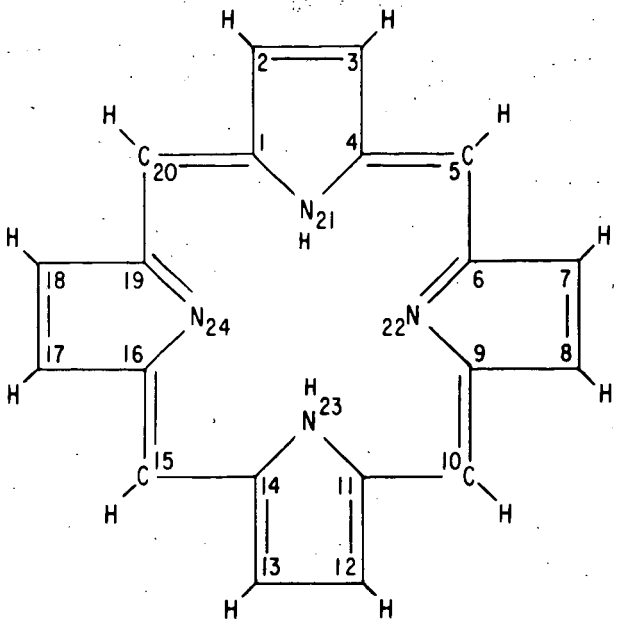

FIGURE 1.-Numbering system for the Porphine Ring

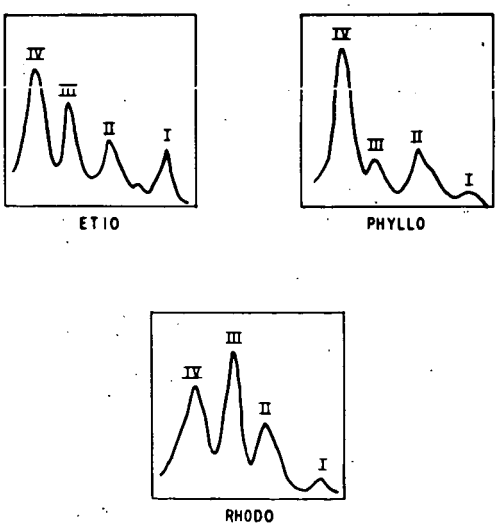

FIGURE 2.-Types of Porphyrin Spectra.

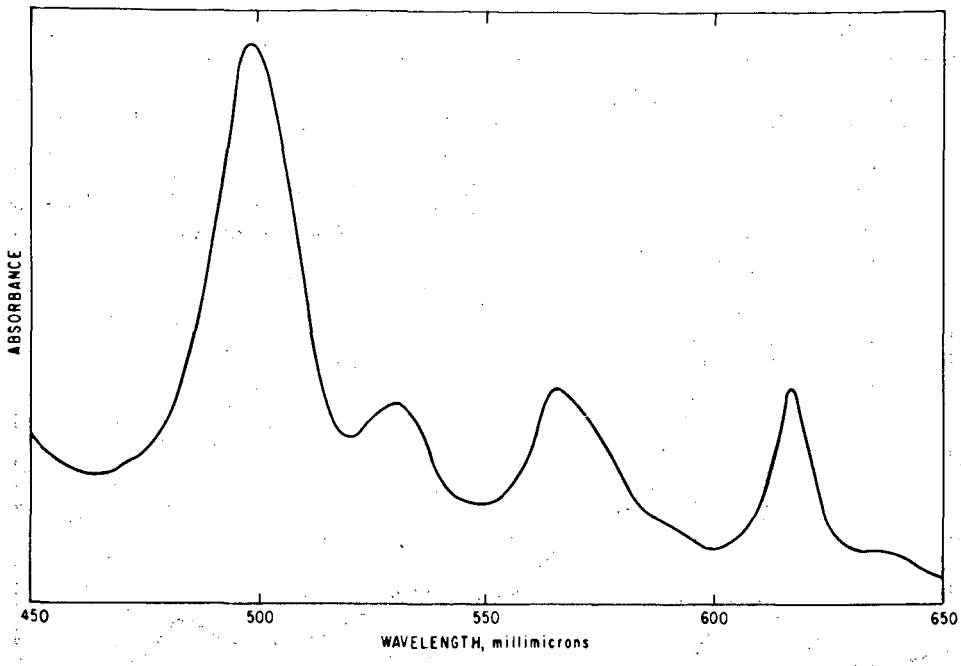

FIGURE 3.-Spectrum of oil-shale extract

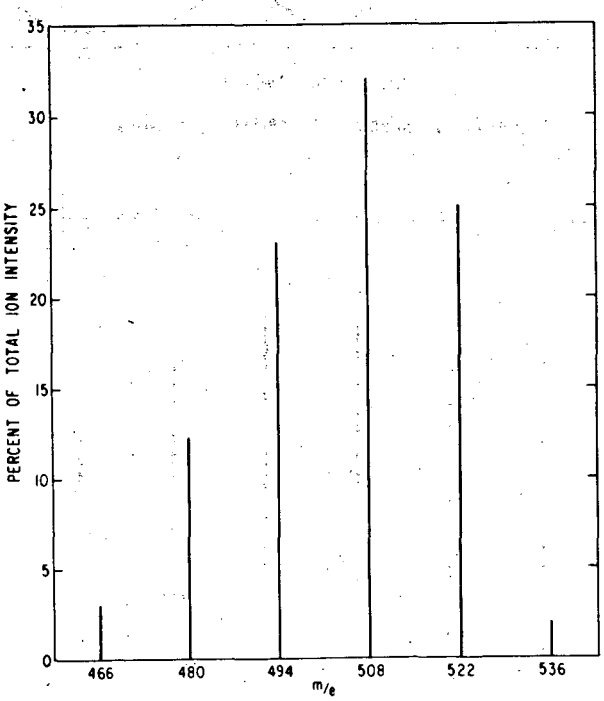

FIGURE 4-Distributions of ion intensities for oil-shale porphyrins

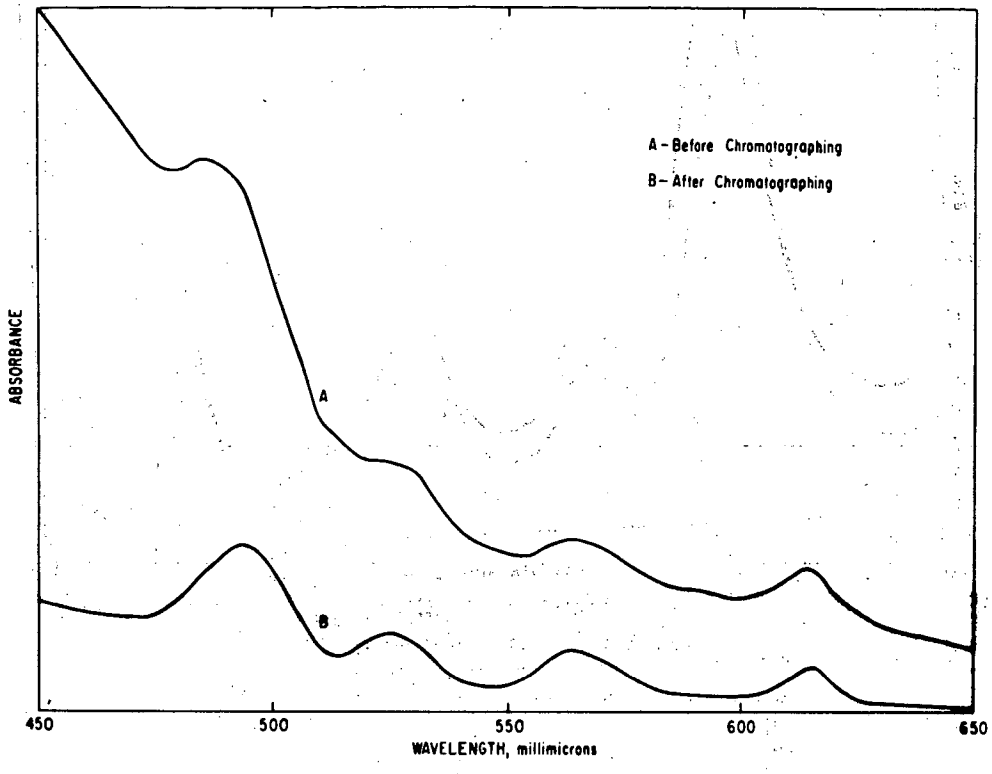

FIGURE 5.- Spectra of shale-oil porphyrins

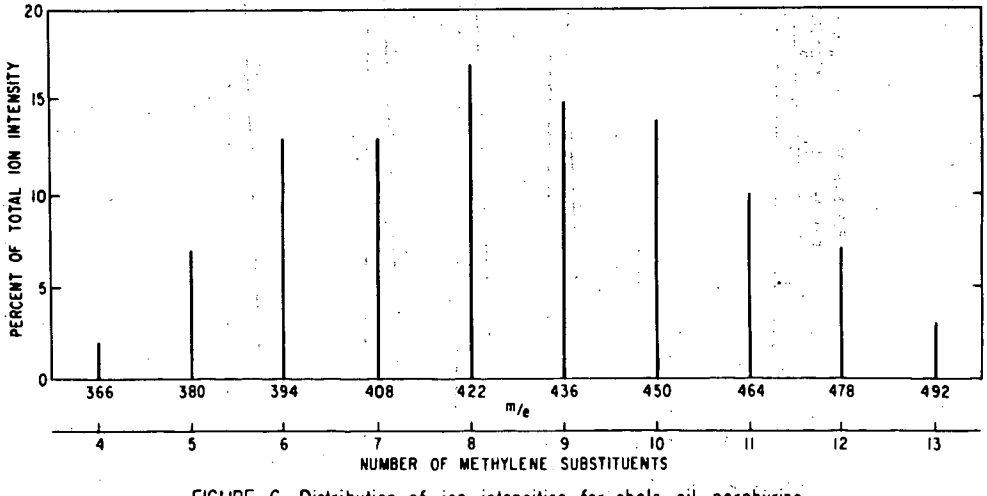

FIGURE 6.-Distribution of ion intensities for shale-oil porphyrins

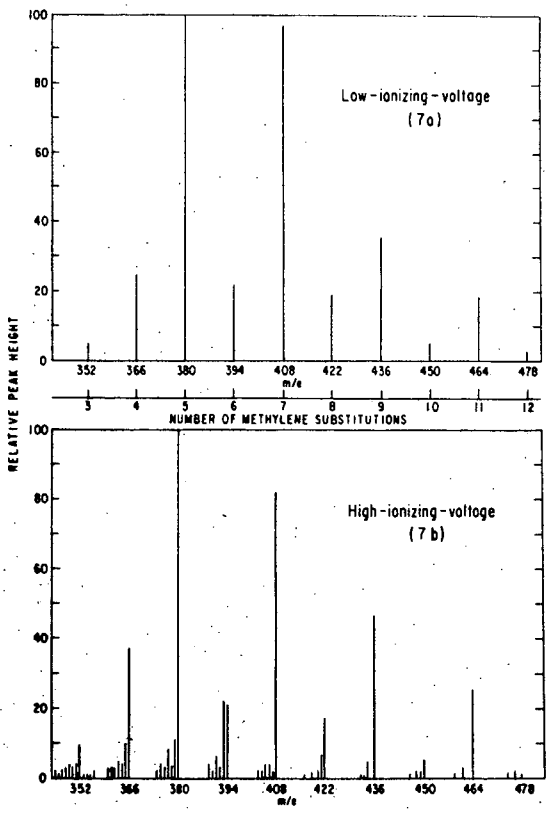

FIGURE 7-Mass Spectra of Fraction 15.

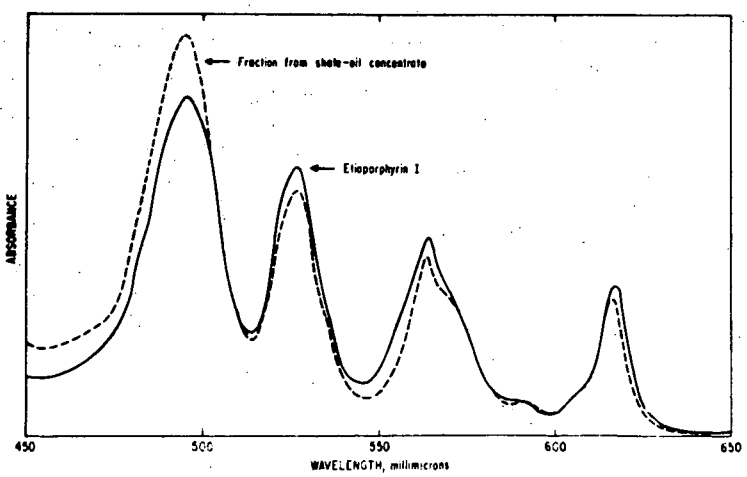

FIGURE 8-Comparison of spectra